Performance of Hemp-Fibre Reinforced Polypropylene Composite Materials

A thesis submitted in partial fulfilment of the requirements for the degree of

Doctor of Philosophy in Materials and Process Engineering

by

Gareth Beckermann

THE UNIVERSITY OF
WAIKATO
Te Whare Wānanga o Waikato

December, 2007

Be ye strong therefore, and let not your hands be weak: for your work shall be rewarded.

2 Chronicles 15:7

Abstract

Increasing worldwide environmental awareness is encouraging scientific research into the development of cheaper, more environmentally friendly and more sustainable construction and packaging materials. Natural fibre reinforced thermoplastic composites are strong, stiff, lightweight and recyclable, and have the potential to meet this need. Industrial hemp fibre is amongst the strongest of the natural fibres available, and possesses a similar specific stiffness to E-glass, but with additional benefits such as low cost and low production energy requirements.

The favourable mechanical properties of hemp, however, have yet to be transferred successfully to thermoplastic-matrix composite materials. The aim of this thesis was to achieve a greater understanding of the various parameters that contribute to composite strength and stiffness, and to manipulate these parameters in order to produce an improved hemp fibre reinforced polypropylene composite material.

Hemp fibre was alkali treated at elevated temperatures in a small pressure vessel with either a solution of 10wt% NaOH or 5wt% NaOH / 2wt% Na_2SO_3. Single fibre tensile tests were performed on treated and untreated fibres, and it was found that the NaOH/Na_2SO_3 treatment produced the strongest and stiffest fibres with a good level of fibre separation. Lignin tests revealed that both alkali treatments were effective in the removal of lignin from hemp fibre, and XRD analysis showed that both alkali treatments resulted in increases in the hemp fibre crystallinity index. TGA and DTA analysis showed that the alkali fibre treatments improved the thermal stability of the treated hemp fibre when compared to the untreated fibre.

Alkali treated hemp fibre, polypropylene and a maleic anhydride modified polypropylene (MAPP) coupling agent were compounded in a twin-screw extruder, and injection moulded into composite tensile test specimens. A range of

composites with different fibre and MAPP contents were produced and tested. Tensile tests revealed that the optimum composite consisted of polypropylene with 40wt% NaOH/Na_2SO_3 treated hemp fibre and 4wt% MAPP, and had a tensile strength of 50.5 MPa and a Young's modulus of 5.31 GPa, respectively.

The effect of MAPP on the fibre/matrix interface of NaOH/Na_2SO_3 treated hemp fibre/polypropylene composites was assessed by means of the single fibre fragmentation test. A composite consisting of NaOH/Na_2SO_3 treated fibres in a matrix of 4wt% MAPP and polypropylene was found to have a critical fibre length of 0.83mm and an interfacial shear strength of 16.1 MPa. The effects of MAPP on the composite fracture mechanisms were evaluated by means of SEM microscopy. TGA and DTA analysis showed that untreated hemp fibre composites and NaOH/Na_2SO_3 treated hemp fibre composites, each with a matrix of 4% MAPP and polypropylene, were less thermally stable than the polypropylene matrix alone.

The Bowyer-Bader model was used to model the strength of an injection moulded composite with a normal fibre length distribution, consisting of 40wt% NaOH/Na_2SO_3 treated fibre, 4% MAPP and polypropylene. A theoretical composite tensile strength of 149 MPa was obtained from the model, based on the assumption that all the fibres were axially aligned in the composite.

Composites with long, axially aligned fibres were produced using a novel solution mixing technique, where the polymer matrix and MAPP coupling agent were dissolved in a solvent and then precipitated inside an aligned fibre mat. Significant improvements in tensile strength and Young's modulus were achieved for solution mixed composites compared to composites produced by means of extrusion and injection moulding. The strongest solution mixed composite had a tensile strength of 84.7 MPa, and consisted of 56wt% NaOH/Na_2SO_3 treated fibre, 4% MAPP and polypropylene; and the stiffest injection moulded composite had a Young's modulus of 16.0 GPa, and consisted of 63wt% NaOH/Na_2SO_3 treated fibre, 4% MAPP and polypropylene.

Acknowledgements

I have many people to thank for the assistance and support that I have gained throughout the duration of my study.

First and foremost, I would like to thank my family for all that they have given me throughout my lifetime. I would like to give special thanks to my parents, Colin and Fay Beckermann, who have always supported me in what I've done, and who have given me the opportunities that have led me to where I am today. Their valiant attempts to understand my work are highly commendable. I would also like to give thanks to my brothers, Justin and Alistair, who have provided many laughs and good times along the way.

I would like to thank my main academic supervisor, Dr. Kim Pickering, who has tirelessly assisted me with every step of my research, and who was never short of good advice and direction when it was needed most. I would also like to offer thanks to my two co-supervisors, Dr. Johan Verbeek and Prof. Alan Langdon, and my industrial supervisor, Nic Foreman.

I would like to thank the Foundation for Research Science and Technology in New Zealand for their financial assistance through a Bright Future Top Achiever Doctoral Scholarship.

I would also like to thank the Dept. of Engineering technicians who provided the technical assistance for my research, especially Yuanji Zhang, Paul Ewart, Indar Singh and Helen Turner.

And finally, I would like to say thank-you to the other composites group members, especially Dalour, Saiful, Moyeen, Paul, Carmen and Nick for their constant encouragement and valuable contributions to my research.

Table of Contents

Abstract ..... *i*

Acknowledgements ..... *iii*

Table of Contents ..... *iv*

List of Figures ..... *ix*

List of Tables ..... *xiv*

Symbols and Abbreviations ..... *xv*

Symbols ..... **xv**

Abbreviations ..... **xvi**

Chapter 1: Introduction *1*

1.1 Overview of Composite Materials **1**

1.2 Natural Fibre Reinforced Thermoplastic Composites **4**

1.3 Opportunities For Natural Fibre Composites **8**

1.4 Research Objectives **11**

Chapter 2: Literature Review *12*

2.1 Natural Fibres **12**

2.2 Comparisons of Natural Cellulose Fibres **13**

2.3 Industrial Hemp Fibre **15**

2.3.1 Hemp Plant Morphology 16

2.3.2 Bast Fibre Morphology 19

2.3.3 Factors Affecting Fibre Properties 20

2.3.4 Hemp Growing Conditions 21

2.3.5 Hemp Harvesting 21

2.4 Hemp Fibre Constituents **21**

2.4.1 Cellulose 22

2.4.2 Lignin 24

2.4.3 Hemicelluloses 25
2.4.4 Pectins 25

2.5 Thermoplastic Matrices 26

2.6 Issues Regarding the Use of Natural Cellulose Fibres in Composites 28

2.6.1 Interfacial Bonding 29
2.6.2 Thermal Stability 32
2.6.3 Moisture Absorption 33
2.6.4 Fibre Separation and Dispersion 33
2.6.5 Biodegradability 35
2.6.6 Fibre Aspect Ratio 35
2.6.7 Fibre Orientation 36
2.6.8 Fibre Tensile Strength, Young's Modulus and Volume Fraction . 39

2.7 Fibre and Matrix Treatments 40

2.7.1 Biological Treatments 41
2.7.2 Physical Treatments 44
2.7.3 Chemical Treatments 45

2.8 Processing of Fibre Reinforced Thermoplastic Composites 52

2.8.1 Melt Mixing 52
2.8.2 Extrusion Compounding 53
2.8.3 Injection Moulding 54
2.8.4 Compression Moulding 56
2.8.5 Solution Mixing 56
2.8.6 Solution Mixing of Oriented Fibre Composites 58

2.9 Composite Interfacial Shear Strength 59

2.9.1 The Single Fibre Fragmentation Test 60
2.9.2 The Single Fibre Pullout Test 62
2.9.3 The Micro-Debond Test 63
2.9.4 The Single Fibre Compression Test 64
2.9.5 Advantages and Limitations of IFSS Test Methods 66

2.10 Composite Strength Predictions 69

2.10.1 Rule of Mixtures Model (Parallel Model) 70

2.10.2 Inverse Rule of Mixtures Model (Series Model) 71
2.10.3 Hirsch Model..... 72
2.10.4 Halpin-Tsai Model 72
2.10.5 Modified Halpin-Tsai Equation 73
2.10.6 Modified Rule of Mixtures (Kelly-Tyson Model) 74
2.10.7 Bowyer-Bader Model..... 76
2.10.8 Problems and Limitations Associated with Strength Prediction Models..... 77

2.11 X-Ray Diffraction Analysis 79

2.12 Thermal Analysis 80
2.12.1 Thermal Oxidative Degradation of Polypropylene..... 81
2.12.2 Thermal Oxidative Degradation of Hemp..... 84

Chapter 3: Materials and Methods..... 86

3.1 Experimental Overview..... 86

3.2 Fibre Modification and Evaluation 87
3.2.1 Alkali Solution Preparation..... 87
3.2.2 Fibre Processing..... 88
3.2.3 Lignin Measurement 91
3.2.4 Single Fibre Tensile Testing 92
3.2.5 Compliance and Young's Modulus Determination..... 94
3.2.6 X-Ray Diffraction Analysis of Fibres..... 96

3.3 Fabrication and Evaluation of Composites 96
3.3.1 Composite Extrusion and Injection Moulding..... 96
3.3.2 Solution Mixing of Composites 99
3.3.3 Composite Tensile Testing..... 103
3.3.4 Fibre Extraction and Length Analysis 104
3.3.5 Single Fibre Fragmentation Testing..... 105
3.3.6 Microscopic Analysis of Fibres and Composites..... 107
3.3.7 Thermal Analysis 108

Chapter 4: Results and Discussion *109*

4.1 Fibre Evaluation **109**

4.1.1 The Effects of Alkali Treatment on Diameter, Tensile Strength and Young's Modulus of Fibres 109

4.1.2 Lignin Content of Fibres 111

4.1.3 Fibre Separation 112

4.1.4 Microscopic Evaluation of Untreated and Alkali Treated Fibres 115

4.1.5 Determination of Fibre Crystallinity Index by Means of X-Ray Diffraction 118

4.2 Evaluation of Extruded and Injection Moulded Composites **121**

4.2.1 The Effects of Injection Moulder Processing Conditions on Composite Mechanical Properties 121

4.2.2 The Effects of Fibre Content on Composite Mechanical Properties 124

4.2.3 The Effects of Fibre Treatment and MAPP Content on Composite Mechanical Properties 126

4.2.4 Fibre Length Analysis and the Effects of Fibre Length on Composite Properties 139

4.2.5 Fibre Orientations of Injection Moulded Composites 143

4.3 Evaluation of Solution Mixed Composites **149**

4.3.1 Comparisons Between Short Randomly Oriented Fibre Composites Produced by Extrusion/Injection Moulding and Solution Mixing Methods 149

4.3.2 Long Oriented Fibre Composites Produced by Solution Mixing 153

4.4 Composite Modelling **157**

4.4.1 Determination of Critical Fibre Length 157

4.4.2 Fibre Strength Prediction at the Critical Fibre Length 161

4.4.3 Interfacial Shear Strength Determination 163

4.4.4 Composite Tensile Strength Predictions 165

4.5 Thermal Analysis of Fibres and Composites **175**

Chapter 5: Conclusions ***183***

5.1 Alkali Fibre Treatments **183**

5.2 Extruded and Injection Moulded Composites **184**

5.3 Solution Mixed Composites **185**

5.4 Composite Modelling **186**

Chapter 6: Recommendations for Future Work ***187***

References ***190***

Appendix ***201***

List of Figures

Figure 1.1 CO_2 emissions per ton of composite, and reduction in emissions by substituting glass fibres with hemp fibres 9
Figure 2.1 Industrial hemp plants 16
Figure 2.2 Cross section of a hemp stem 17
Figure 2.3 Schematic of a hemp stem cross section 17
Figure 2.4 Fibre with primary and secondary walls 19
Figure 2.5 Scanning Electron Micrograph (SEM) of a fractured hemp fibre showing mesofibrils and microfibrils 20
Figure 2.6 The molecular structure and arrangement of cellulose 23
Figure 2.7 Schematic representation of the crystallite structure of cellulose 23
Figure 2.8 Microfibril surface 24
Figure 2.9 Cell wall polymers responsible for the properties of lignocellulosics in order of importance 26
Figure 2.10 Schematic of mechanical interlocking 30
Figure 2.11 Schematic of electrostatic bonding 31
Figure 2.12 Schematic of chemical bonding, ... 31
Figure 2.13 Schematic of reaction bonding involving polymers 32
Figure 2.14 Schematic of interdiffusion bonding 32
Figure 2.15 Fibre alignment as a result of extrusion..... 37
Figure 2.16 Fountain flow experienced during injection moulding 38
Figure 2.17 Theoretical relationship between tensile strength and fibre volume fraction for short-fibre reinforced composites. 40
Figure 2.18 Retted hemp stem. 42
Figure 2.19 Reaction mechanisms of MAPP with the surface of a lignocellulosic fibre. 49
Figure 2.20 Schematic of possible PP molecular entanglements with the longer chains of MAPP. 49
Figure 2.21 The extrusion compounding process 53
Figure 2.22 Basic operations of the injection moulding cycle: 55
Figure 2.23 Schematic of the single fibre fragmentation test. 60

Figure 2.24 Schematic of the single fibre pullout test. 62
Figure 2.25 A typical force-displacement curve obtained from a single fibre pullout test. 63
Figure 2.26 Schematic of the micro-debond test. 64
Figure 2.27 Schematic of single fibre compression test. 65
Figure 2.28 Schematic representation of the Parallel Model. 71
Figure 2.29 Schematic representation of the Series Model. 71
Figure 2.30 Schematic representation of the Hirsch Model. 72
Figure 2.31 Schematic of the X-ray diffraction method. 80
Figure 3.1 Schematic of a pulp digester. 88
Figure 3.2 Lab-scale pulp digester. 89
Figure 3.3 Digester cook schedule for NaOH treatment. 90
Figure 3.4 Digester cook schedule for $NaOH/Na_2SO_3$ treatment. 90
Figure 3.5 Pulp and paper fibre washer. 91
Figure 3.6 Single fibre mounting. 92
Figure 3.7 Instron-4204 tensile testing machine. 93
Figure 3.8 System compliance of the tensile testing system based on data obtained from E-glass fibres. 95
Figure 3.9 Stack of carded hemp fibre mats. 100
Figure 3.10 Solution mixing apparatus 102
Figure 3.11 Solution mixed hemp fibre mat containing loosely bound polypropylene precipitates. 102
Figure 3.12 Solution mixed and hot pressed hemp fibre composite. 103
Figure 3.13 Fabrication of single fibre fragmentation test specimens. 106
Figure 3.14 SDT 2960 Simultaneous DTA-TGA analyser. 108
Figure 4.1 Granulated hemp fibre showing colour differences. 111
Figure 4.2 Relationship between lignin content and fibre diameter of untreated and alkali treated hemp fibres. 112
Figure 4.3 Scanning Electron Micrograph (SEM) of untreated hemp fibres showing poor fibre separation. 113
Figure 4.4 Scanning Electron Micrograph (SEM) of NaOH treated hemp fibres showing good fibre separation. 114
Figure 4.5 Scanning Electron Micrograph (SEM) of $NaOH/Na_2SO_3$ treated hemp fibres showing good fibre separation. 114

Figure 4.6 Scanning Electron Micrograph (SEM) of untreated hemp fibre surface. 115
Figure 4.7 Scanning Electron Micrograph (SEM) of NaOH treated hemp fibre surface..... 116
Figure 4.8 Scanning Electron Micrograph (SEM) of NaOH/Na_2SO_3 treated hemp fibre surface..... 117
Figure 4.9 X-ray diffraction profiles of untreated and alkali treated hemp fibre.120
Figure 4.10 Effects of injection moulder processing conditions on the tensile strength of composites containing 40wt% NaOH treated hemp fibre..... 123
Figure 4.11 Effects of injection moulder processing conditions on the Young's modulus of composites containing 40wt% NaOH treated hemp fibre..... 123
Figure 4.12 Effects of fibre content on the tensile strength of composites containing NaOH treated NZ hemp fibre..... 125
Figure 4.13 Effects of fibre content on the Young's modulus of composites containing NaOH treated NZ hemp fibre..... 125
Figure 4.14 Effects of fibre treatment and MAPP content on the tensile strength of composites containing 40wt% hemp fibre..... 128
Figure 4.15 Effects of fibre treatment and MAPP content on the Young's modulus of composites containing 40wt% hemp fibre..... 128
Figure 4.16 Scanning Electron Micrograph (SEM) of the fracture surface of an extruded and injection moulded composite [40wt% untreated hemp fibre, PP and 0wt% MAPP]. 130
Figure 4.17 Scanning Electron Micrograph (SEM) of the fracture surface of an extruded and injection moulded composite [40wt% untreated hemp fibre, PP and 4wt% MAPP]. 131
Figure 4.18 Scanning Electron Micrograph (SEM) of the fracture surface of an extruded and injection moulded composite [40wt% NaOH treated hemp fibre, PP and 0wt% MAPP]. 132
Figure 4.19 Scanning Electron Micrograph (SEM) of the fracture surface of an extruded and injection moulded composite [40wt% NaOH treated hemp fibre, PP and 4wt% MAPP]. 133
Figure 4.20 Scanning Electron Micrograph (SEM) of the fracture surface of an extruded and injection moulded composite [40wt% NaOH/Na_2SO_3 treated hemp fibre, PP and 0wt% MAPP]..... 134

Figure 4.21 Scanning Electron Micrograph (SEM) of the fracture surface of an extruded and injection moulded composite [40wt% $NaOH/Na_2SO_3$ treated hemp fibre, PP and 4wt% MAPP]..... 135
Figure 4.22 Scanning Electron Micrograph (SEM) of a $NaOH/Na_2SO_3$ treated hemp fibre extracted from a composite containing PP and 0wt% MAPP. . 137
Figure 4.23 Scanning Electron Micrograph (SEM) of a $NaOH/Na_2SO_3$ treated hemp fibre extracted from a composite containing PP and 4wt% MAPP. . 138
Figure 4.24 Fibre distribution for short fibre length composites. 141
Figure 4.25 Fibre distribution for normal fibre length composites. 141
Figure 4.26 Fibre distribution for long fibre length composites. 142
Figure 4.27 Optical micrograph of extracted hemp fibres showing composite processing induced damage. 143
Figure 4.28 Schematic of a composite test specimen showing the cross-sectional view. 144
Figure 4.29 Macroscopic view of a test specimen cross-section showing a distinct core layer and two skin layers 144
Figure 4.30 Schematic of a composite test specimen showing a cut-away plan view. 145
Figure 4.31 Macroscopic plan view of a test specimen with half the thickness removed, showing a distinct core layer and two skin layers. 145
Figure 4.32 Optical micrograph showing the cross-sectional view of a composite specimen. 146
Figure 4.33 Optical micrograph showing a plan view of a specimen with the top half removed (core layer). 147
Figure 4.34 Optical micrograph showing a plan view of a specimen with the top quarter removed 147
Figure 4.35 Optical micrograph showing a specimen surface plan view 148
Figure 4.36 Micrograph showing fibre breaks after the fragmentation test. 158
Figure 4.37 Fragment L/D values for treated hemp fibre with a polypropylene/4% MAPP matrix. 159
Figure 4.38 Theoretical fibre fragment aspect ratio distribution 160
Figure 4.39 Fragment L/D values for treated hemp fibres with a polypropylene/4% MAPP matrix (anomalies removed). 161

Figure 4.40 Mean fibre tensile strength plotted against gauge length for $NaOH/Na_2SO_3$ treated hemp fibres. 163
Figure 4.41 Fragment lengths of treated hemp fibres with a polypropylene/4% MAPP matrix presented as a Weibull distribution..... 164
Figure 4.42 Linear build-up of stress inside a fibre. 167
Figure 4.43 Stress-Strain curve for polypropylene, showing the stress of the matrix at the failure strain of the composite..... 168
Figure 4.44 Kelly-Tyson prediction of composite tensile strength vs. fibre length for composites with fibre contents of 40wt% and perfect fibre alignment. 169
Figure 4.45 Scanning Electron Micrograph (SEM) of the fracture surface of an extruded and injection moulded composite [40wt% $NaOH/Na_2SO_3$ treated hemp fibre, PP and 4wt% MAPP]..... 151
Figure 4.46 Scanning Electron Micrograph (SEM) of the fracture surface of a solution mixed and injection moulded composite [40wt% $NaOH/Na_2SO_3$ treated hemp fibre, PP and 4wt% MAPP]..... 152
Figure 4.47 Tensile strength of solution mixed and hot pressed composites containing $NaOH/Na_2SO_3$ treated hemp fibre..... 154
Figure 4.48 Young's modulus of solution mixed and hot pressed composites containing $NaOH/Na_2SO_3$ treated hemp fibre. 154
Figure 4.49 Scanning Electron Micrograph (SEM) of the fracture surface of a solution mixed and hot pressed composite [40wt% $NaOH/Na_2SO_3$ treated hemp fibre, PP and 4wt% MAPP]..... 155
Figure 4.50 TGA and DTA curves for alkali treated and untreated hemp fibre. 177
Figure 4.51 TGA and DTA curves for polypropylene, the composite containing untreated hemp and the composite containing alkali treated hemp. 178
Figure 4.52 TGA and DTA curves for polypropylene, untreated hemp fibre and the composite containing untreated hemp. 179
Figure 4.53 TGA and DTA curves for polypropylene, alkali treated hemp fibre and the composite containing alkali treated hemp..... 180
Figure 4.54 Effect of injection moulder temperature settings on the tensile strength of composites containing 40wt% NaOH treated hemp fibre and 3wt% MAPP. 182

List of Tables

Table 1.1 Comparison of thermoplastic and thermoset matrices. 2
Table 1.2 Properties of natural fibres in relation to those of E-glass 5
Table 1.3 Comparison of fibre reinforced polypropylene composites 5
Table 1.4 Overall energy schedule for hemp fibre mat thermoplastic composites and glass fibre mat thermoplastic composites..... 6
Table 1.5 Length of fibres after processing 7
Table 1.6 Use of natural fibres for serial parts in the automotive industry 10
Table 2.1 Commercially important fibre sources..... 13
Table 2.2 Natural plant fibre costs 14
Table 2.3 Hemp bast fibre comparisons..... 18
Table 2.4 Summary of hemp stalk composition 18
Table 2.5 Chemical constituents of hemp 22
Table 2.6 Physical properties of various polymers. 27
Table 2.7 Solubility parameters of polymers and solvents. 57
Table 4.1 Mechanical properties of untreated and alkali treated fibres.. 109
Table 4.2 Lignin content of untreated and alkali treated fibres. 111
Table 4.3 Crystallinity index of untreated and alkali treated hemp fibre..... 119
Table 4.4 Mechanical properties of injection moulded composites reinforced with fibres separated by length 139
Table 4.5 Tensile strength and Young's modulus of randomly oriented fibre reinforced composites prepared by solution mixing/injection moulding and extrusion/injection moulding..... 150
Table 4.6 Tensile strength and Young's modulus of extruded/injection moulded composites containing non-degraded fibres and degraded hemp fibres 157

Symbols and Abbreviations

Symbols

α	Shape parameter of the Weibull distribution
β	Scale parameter of the Weibull distribution
Γ	Standard gamma function
δ	Solubility parameter ($cal^{1/2}\ cm^{-3/2}$)
ε_c	Composite failure strain (%)
ε_m	Matrix strain (%)
ζ	Empirically fitted measurement of reinforcement geometry
η	Relative strength of the fibre and matrix
ρ	Density (g/cm^3)
ρ_f	Fibre density (g/cm^3)
ρ_m	Matrix density (g/cm^3)
σ_{adj}	Adjusted compressive stress (MPa)
σ_{app}	Applied stress (MPa)
σ_c	Composite strength (MPa)
σ_f	Mean fibre tensile strength (MPa)
σ_{fc}	Fibre tensile strength at the critical fibre length (MPa)
σ_m	Matrix stress or tensile strength (MPa)
τ	Interfacial shear strength (MPa)
τ_m	Shear strength of the matrix (MPa)
τ_{max}	Maximum interface shear stress (MPa)
φ_{max}	Maximum fibre packing fraction
A	Average fibre cross sectional area (m^2)
C	True compliance (mm/N)
C_a	Apparent compliance (mm/N)
C_s	System compliance (mm/N)
D	Fibre diameter (μm)
E_f	Fibre Young's modulus (GPa)
F	Applied force (N)
F_d	Critical force at which debonding occurs (N)
F_f	Frictional force between the fibre and the matrix (N)
F_{max}	Peak force (N)
I_{002}	Maximum intensity of diffraction of the (002) lattice peak
I_{am}	Intensity of diffraction of the amorphous material
I_c	Fibre crystallinity index (%)
K_1	Fibre orientation factor
K_2	Fibre length factor
k	Global stiffness constant
L	Average fibre length (mm)

L_{ave}	Mean fragment length (mm)
L_{ave}/D	Arithmetic mean aspect ratio
L_c	Critical fibre length (mm)
L_c/D	Critical aspect ratio
L_e	Embedded fibre length (mm)
L_i	Sub-critical fibre lengths (mm)
L_j	Super-critical fibre lengths (mm)
P_d	Mean debonding load (N)
P_f	Probability of failure
r	Fibre radius (μm)
V_{crit}	Critical fibre volume fraction
V_f	Fibre volume fraction
V_i	Volume fraction of the sub-critical fibre lengths
V_j	Volume fraction of the super-critical fibre lengths
V_m	Matrix volume fraction
W_{24h}	Water absorption over a 24-hour period (wt%)
W_f	Fibre weight fraction
x	Fibre efficiency factor

Abbreviations

DTA	Differential thermal analysis
GMT	Glass fibre mat thermoplastic composite
GPa	Gigapascal
HDPE	High-density polyethylene
HMT	Hemp fibre mat thermoplastic composite
IFSS	Interfacial shear strength
KPa	Kilopascal
LDPE	Low-density polyethylene
MA	Maleic anhydride
MAPP	Maleic anhydride modified polypropylene
MPa	Megapascal
M.T	Melting temperature
NaOH	Sodium hydroxide
Na_2SO_3	Sodium sulphite
OH	Hydroxyl groups
PMC	Polymer matrix composite
PMPPIC	Polymethylenepolyphenyl isocyanate
PP	Polypropylene
PVC	Polyvinylchloride
SEM	Scanning electron microscope
SFFT	Single fibre fragmentation test
SFPT	Single fibre pullout test
TGA	Thermogravimetric analysis
THC	Tetrahydrocannabinol
T.S	Tensile strength

Chapter 1: Introduction

1.1 Overview of Composite Materials

Fibre-reinforced composites are strong, stiff and lightweight materials that consist of strong, stiff, but commonly brittle fibres that are encapsulated in a softer, more ductile matrix material. The matrix transmits applied loads to the reinforcing fibres within the composite, resulting in a material with improved mechanical properties compared to the un-reinforced matrix material.

Many composites used today are at the leading edge of materials technology, enabling their use in advanced applications such as aircraft and aerospace structures. The idea of using composite materials, however, is not a new or recent one but has been around for thousands of years. The Ancient Egyptians used chopped straw to reinforce mud bricks; and Mongol warriors used a composite consisting of bullock tendon, horn, bamboo strips, silk and pine resin to produce high-performance archery bows.

Since the early 1960s, there has been an increase in the demand for stronger, stiffer and more lightweight materials for use in the aerospace, transportation and construction industries. High performance demands on engineering materials have led to the extensive research and development of new and improved materials, such as composites. Composite materials used for structural purposes often have low densities, resulting in high stiffness to weight and high strength to weight ratios when compared to traditional engineering materials. In addition, the high fatigue strength to weight ratio and fatigue damage tolerance of many composites also makes them an attractive option.

As a result, composite materials are rapidly being utilised in industries that have traditionally used metals, and are now at the forefront of research and development in many related areas.

Composite materials can be grouped into five major categories, which include ceramic matrix composites, metal matrix composites, intermetallic matrix composites, carbon-carbon composites and polymer matrix composites (PMCs). The focus of this research is on the development of PMCs.

A PMC can consist of either a thermoplastic or thermoset matrix, which is used to bind the reinforcing fibres together, as well as to transfer applied stresses from the composite to the fibres. Thermosets are plastics that cannot be melted once cured, and include resins such as epoxies, polyesters and phenolics. Thermoplastics, on the other hand, are plastics that can be repeatedly melted, thus enabling them to be recycled. Commonly used thermoplastics include polyethylene, polypropylene and polyvinyl chloride (PVC). Both thermoset and thermoplastic polymers have advantages and disadvantages when used as composite matrices, as can be seen in Table 1.1

Table 1.1 Comparison of thermoplastic and thermoset matrices.

Thermoplastic Advantages	Thermoplastic Disadvantages
• Unlimited shelf life • Easy to handle (no tackiness) • Recyclable • Easy to repair by welding and solvent bonding • Post formable • Tough	• Prone to creep • Poor melt flow characteristics • Thermoplastics need to be heated above the melting point to sufficiently wet the fibres

Thermoset Advantages	Thermoset Disadvantages
• Low resin viscosity • Good fibre wetting • Excellent thermal stability once polymerised • Chemically resistant • Creep resistant	• Brittle • Non-recyclable via standard techniques • Not post-formable

The reinforcing fibres in PMCs can be either short or continuous, with continuous-fibre reinforcement providing the best mechanical properties in the direction of fibre alignment. Continuous fibre composites are primarily reinforced with high performance carbon or aramid (e.g. Kevlar™) fibres. These composites are often utilised in applications such as aircraft components, where the exceptional fibre properties can be fully exploited. Some commonly used continuous-fibre composite processing methods include compression moulding, hand lay-up, filament winding and pultrusion. Such materials, however, cannot always be adapted to mass production and are often limited to simple shaped items.

Short fibre composites, on the other hand, are primarily reinforced with chopped fibres such as glass, graphite and cellulose fibres. These types of composites are cheaper and easier to fabricate, and are well established in many applications where medium to low strengths and stiffnesses are required. Compared to continuous fibre composites, short fibre composites can easily be processed in a similar manner to the matrix. For short fibre composites with a thermoplastic matrix, it is thus possible to mass-produce complex-shaped moulded products by means of extrusion, injection moulding and compression moulding.

Composite mechanical properties are strongly influenced by the mechanical properties and distribution of the fibres and matrix, as well as the efficiency of stress transfer between the two components. Mechanical properties such as strength and stiffness are of great importance when designing composite products and can be predicted for short-fibre composites with varying degrees of accuracy by means of mathematical prediction models, which are discussed in detail in Chapter 2. The mechanical properties of short fibre composites are far more difficult to predict than continuous fibre composites. This is due to the complexities of determining parameters such as fibre dispersion, orientation and geometry (aspect ratio) of the fibres within the composite, fibre and matrix volume fractions and the interfacial shear strength between the fibres and matrix.

1.2 Natural Fibre Reinforced Thermoplastic Composites

High performance carbon and aramid (such as Kevlar™) fibres are the most commonly used reinforcements for composites where exceptional strength, high stiffness and low density are required. They are, however, prohibitively expensive for use in more general applications, therefore cheaper alternatives such as glass fibre are more commonly used in industry. Glass fibres have many benefits, including low cost and relative ease of manufacture, as well as possessing moderate strength and stiffness to weight ratios. However, they also have many disadvantages. They tend to be abrasive, thus making them dangerous to work with as well as increasing the wear on processing machinery. More importantly, glass fibres could present a health risk to those working with them. The biggest problem with glass and other synthetic fibres is that they are difficult to dispose of at the end of their lifetimes. Glass fibre reinforced composites cannot be incinerated as the residues tend to cause furnace damage, and there are problems associated with the recycling of glass fibre reinforced thermoplastics due to fibre breakages that occur during reprocessing operations. The only method of disposal is to discard the waste in landfills, which is becoming more costly in many countries with the introduction of landfill taxes.

Government regulations and a growing environmental awareness throughout the world have encouraged the development and utilisation of materials compatible with the environment. Natural fibres, especially hemp and flax, have become increasingly suitable alternatives to glass fibre and have the potential to be used in cheaper, more sustainable and more environmentally friendly composite materials. The properties of natural fibres in relation to those of E-glass can be seen in Table 1.2.

Table 1.2 Properties of natural fibres in relation to those of E-glass [1, 2].

	Fibres								
Properties	**E-glass**	**Hemp**	**Jute**	**Ramie**	**Coir**	**Sisal**	**Flax**	**Cotton**	**Kenaf**
Density, g/cm3	2.55	1.48	1.46	1.5	1.25	1.33	1.4	1.51	-
Tensile strength, MPa	2400	550-900	600-1100	500	220	600-700	800-1500	400	930
Young's modulus, GPa	69	50-70	10-30	44	6	38	60-80	12	-
Specific stiffness, MN.m/kg	27	34-47	7-21	29	5	29	43-57	8	-
Elongation at failure, (%)	3	1.6	1.8	2	15-25	2-3	1.2-1.6	3-10	-
Moisture absorption, (%)	-	8	12	12-17	10	11	7	8-25	-

Natural fibres are cheap, abundant and renewable, and can be produced at low cost in many parts of the developing world. They are strong and stiff, and due to their low densities, have the potential to produce composites with similar specific properties to those of E-glass. Table 1.3 shows a comparison between glass fibre, recycled newspaper and kenaf fibre reinforced polypropylene composites. Hemp fibre is generally stronger than kenaf fibre, so the use of hemp in a polypropylene matrix instead of kenaf would most likely result in a stronger composite material.

Table 1.3 Comparison of fibre reinforced polypropylene composites [3].

	Fibre Type			
Property	**None**	**Kenaf**	**Recycled Newspaper Fibre**	**E-Glass**
Fibre content, wt%	0	50	40	40
Young's Modulus, GPa	1.7	8.3	4.4	9
Specific stiffness (MN.m/kg)	1. 9	7.8	4.5	7.3
Tensile strength, MPa	33	65	53	110
Specific Strength (kN.m/kg)	37	61	54	89
Elongation at break, %	>10	2.2	-	32.5
Flexural strength, GPa	41	98	80	131
Flexural modulus, GPa	1.4	7.3	3.9	6.2
Notched Izod impact, J/m	24	32	21	107
Specific gravity, (g/cm^3)	0.9	1.07	0.98	1.23
Water absorption, % in 24h	0.02	1.05	0.95	0.06
Mould (linear) shrinkage, cm/cm	0.028	0.003	-	0.004

Unlike synthetic fibres, natural fibres require very little energy to produce, and because they possess high calorific values, can be incinerated at the end of their lifetimes for energy recovery. It has been estimated that hemp fibre reinforced polypropylene composites consisting of 65wt% fibre would consume only 30,800 MJ/ton of composite in processing energy, as opposed to 81,890 MJ/ton for glass fibre reinforced polypropylene composites consisting of 30wt% fibre (Table 1.4) [4]. It can also be seen in Table 1.4 that far less energy is required for hemp fibre cultivation than for glass fibre production, and hemp fibre composites produce more energy during incineration than their glass fibre counterparts.

Table 1.4 Overall energy schedule for hemp fibre mat thermoplastic (HMT) composites and glass fibre mat thermoplastic (GMT) composites [4].

Quantity (1 metric ton)	**HMT (65% fibre)**	**Energy (MJ)**	**GMT (30% fibre)**	**Energy (MJ)**
(a) Materials				
	Hemp cultivation	1340	Glass fibre production	14 500
	PP production	35 350	PP production	70 700
	Total	36 690	Total	85 200
(b) Production				
	Composite	11 200	Composite	11 200
(c) Incineration				
PP *incineration*				
	Energy required	117	Energy required	234
	Energy released	-7630	Energy released	-15 260
Hemp fibre incineration			*Glass fibre incineration*	
	Energy required	1108	Energy required	516
	Energy released	-10 650		
	Net	-17 055	Net	-14 510
(d) Balance				
	Gross energy required	49 115	Gross energy required	97 150
	Energy released	-18 222	Energy released	-15 260
	Net energy required	30 800	Net energy required	81 890

* The average fibre content in glass fibre plastics (auto sector) is taken as 30%, although in commercial grades it varies from 22% to 40%.

All plant-derived fibres utilise carbon dioxide when they are grown and can be considered CO_2 neutral, meaning that they can be burned at the end of their lifetime without additional CO_2 being released into the atmosphere [5]. Glass fibres, on the other hand, are not CO_2 neutral and require the burning of fossil fuels to provide the energy needed for production. The burning of fossil fuel based products releases enormous amounts of CO_2 into the atmosphere, and this phenomenon is believed to be the main cause of the greenhouse effect and the climatic changes that are being observed in the world today [1].

Natural fibre reinforced thermoplastic composites, unlike their glass counterparts, do not splinter during fracture [6], therefore making them suitable for crash-absorbing applications where safety is of concern. One of the most distinct advantages of using natural fibres in reinforced thermoplastic composites is the fact that the fibres are incredibly durable, and can be recycled several times with little reduction in strength and stiffness [7, 8]. Synthetic fibres on the other hand, tend to fracture with further processing and recycling, resulting in significant fibre length reductions (Table 1.5).

Table 1.5 Length of fibres after processing [9].

		Before Processing		After Processing	
Fibre	**Fibre diameter (μm)**	**Length (mm)**	**L/D**	**Length (mm)**	**L/D**
Glass	13	6.35	488	0.22	17
Carbon	8	6.35	794	0.18	22
Cellulose	12	2.0	167	1.20	100
Aramid	12	6.35	529	1.33	111
Nylon	25	6.35	254	4.51	180

* All fibres except cellulose fibres were chopped to 6.35mm before being dispersed in an elastomer (NR or NBR) on a mill, then separated by solvent extraction.

Natural fibres, however, display large variations in fibre properties from plant to plant, such as strength, stiffness, fibre length and cross sectional area. These variations can ultimately lead to difficulties in composite design and performance predictions. Natural fibres are also thermally unstable compared to most synthetic fibres, and are limited to processing and working temperatures of 200^{o}C. Another

major drawback when using natural fibres is the fact that they are hydrophilic (absorb water) and polar in nature, whereas common thermoplastic matrices such as polypropylene are hydrophobic (do not absorb water) and non-polar. Natural fibres used in thermoplastic matrices are therefore dimensionally unstable and display poor fibre-matrix interfacial bonding, which results in poor composite mechanical properties. It is therefore necessary to modify the fibres, the matrix or both to produce a composite with improved mechanical properties. Much work still needs to be done in this area to enable natural fibre reinforced thermoplastic composites to compete with glass fibre composites in terms of strength and stiffness.

1.3 Opportunities For Natural Fibre Composites

Several billion tons of fillers and reinforcements are used annually in the plastics industry, and there is a huge potential market for recyclable, energy efficient and more environmentally friendly composite materials.

One of the largest potential users of natural fibre composites is the automotive industry. Faced with the pressures of producing fuel-efficient and low polluting vehicles, the automotive industry has adopted the use of fibre reinforced plastic composites to reduce the weight of its products. Unfortunately, the production and use of composites is energy intensive and polluting, and glass, carbon, and aramid fibre reinforced thermoset composites are difficult to dispose of and can seldom be recycled. The use of a thermoplastic matrix presents an opportunity to produce recyclable composites, but such composites require the use of durable natural fibres for reinforcement as opposed to brittle synthetic fibres. Natural fibre composites also have distinct environmental advantages over competing materials. They can be incinerated to recycle thermal energy, and because natural fibres are considered CO_2 neutral, the only additional CO_2 emitted into the atmosphere from incineration would come from the combustion of the thermoplastic matrix.

Recent government regulations are encouraging the development and use of natural fibres in the automotive industry. In July 2002, The European Union Council of Ministers approved the EU end-of-life vehicle directive, which is expected to have a huge impact on the materials and processing methods used to produce motor vehicles in the future. The directive states that from 2015 onwards, all new vehicles should be 85% reusable and recyclable by weight, 10% can be used for energy recovery and only 5% can be disposed of in landfills [10, 11]. However, the automotive industry may be compelled to use other lightweight and recyclable materials such as foamed aluminium or composites made of only one petrochemical plastic (matrix and fibres made of the same plastic).

Many countries around the world have committed themselves to the Kyoto protocol, whereby a reduction in greenhouse gas emissions (mostly CO_2) must be reduced to levels below that of 1990 between the years 2008 and 2012. Pervaiz *et al*. [4] showed that, by converting the net energy consumed during composite production into CO_2 emissions, 3 tons CO_2 per ton of product could be saved by utilising hemp fibre instead of glass fibre in composite materials (Figure 1.1).

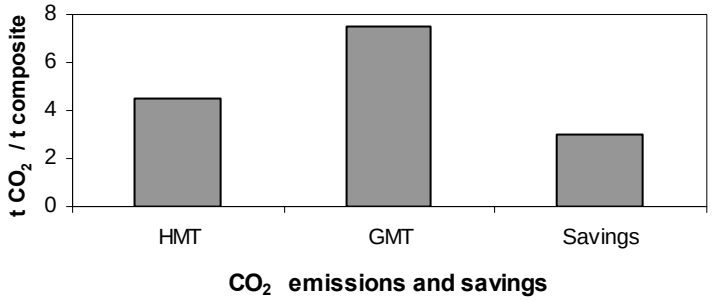

Figure 1.1 CO_2 emissions per ton of composite, and reduction in emissions by substituting glass fibres with hemp fibres [4].

At present, approximately 30,000 tons of natural fibre is used annually in the European Union automotive industry. Most major European motor vehicle manufacturers are now incorporating natural fibre reinforced composite components into their vehicles. The use of natural fibre composites for serial parts in the automotive industry can be seen in Table 1.6.

Table 1.6 Use of natural fibres for serial parts in the automotive industry (1997-2001) [10].

Manufacturers/Customers	Model/Application (dependant on model)
Audi	TT, A2, A3, A4 Avant (1997), A4 Variant (1997), A6, A8 (1997), Roadster, Coupe Seat back, side and back door panels, parcel tray, boot lining, rear flap lining, rear storage panel, spare tyre lining
BMW	3,5 and 7 Series and others Door inserts/door panels, headliner panel, boot lining, seat back
Citroen	C4 (2001) Door inserts
Daimler Chrysler	A-Klasse, C-Klasse, E-Klasse, S-Klasse Door inserts, Windshield/dashboard, business table, column cover
Fiat	Punto, Brava, Marea, Alfa Romeo 146, 156, Sportwagon
Ford	Mondeo CD 162 (1997), Cougar (1998), Mondeo (2000), Focus Door inserts, B-column cover, Parcel tray, in the future also motor protection (cover undershield)
MAN	Bus (1997) Headliner panel
Mitsubishi	Miscellaneous models (since 1997)
Nissan	Miscellaneous models
Opel	Astra, Vectra, Zafira Headliner panel, door inserts, column cover, instrument panel, rear shelf panel
Peugeot	New model 406
Renault	Clio, Twingo
Rover	Rover 2000 and others Insulation, rear storage panel
Saab	Coupe (1998) Door inserts
SEAT	Door inserts, seat backs
Toyota	Miscellaneous models
Volkswagen	Golf A4, Golf 4 Variant (1998), Passat Variant, BoraDoor inserts, seat backs, rear flap lining, parcel tray
Volvo	C70, V70, Coupe (1998) Door inserts, Parcel tray

Currently used natural fibre composites are mainly compression moulded parts, consisting of non-woven natural fibres in a thermoset or thermoplastic matrix [11]. Typical applications include door inserts, hat racks, pillar cover panels and boot linings.

The use of natural fibre composites is not, however, limited only to the automotive industry. At least 20 manufacturers are currently producing wood-fibre reinforced thermoplastic decking for the American markets [12]. Window and door profile manufacturers form another large industrial segment that uses wood-fibre reinforced polymers [6]. Other natural fibre composite applications

that have been reported include walls, flooring, louvers, and indoor and outdoor furniture [12, 13].

Unfortunately, the current generation of natural fibre reinforced thermoplastic composites do not offer sufficient mechanical properties to warrant their use in more demanding structural and load bearing applications. It is therefore necessary to improve the strength and stiffness of these composites, as well as confronting issues such water absorption and thermal instability before they can be used to their full extent in industry

1.4 Research Objectives

The aim of this thesis was to achieve a greater understanding of the various parameters that contribute to composite strength and stiffness, and to manipulate these parameters in order to produce an improved hemp fibre reinforced polypropylene composite material.

The research objectives are summarised as follows:

- To gain an understanding of natural fibre reinforced polymer composites, and to gain an insight into work previously done by other researchers in this particular area.
- To improve the strength, separation, crystallinity and removal of hydrophilic and thermally unstable hemp fibre constituents by means of chemical fibre treatments.
- To optimise composite processing methods to improve composite mechanical properties.
- To enhance the strength and stiffness of composites by improving, optimising and evaluating the fibre-matrix interfacial adhesion, fibre orientation, fibre length distribution and fibre volume fraction.
- To evaluate the performance of hemp fibre reinforced polypropylene composites produced in this study by comparing experimentally obtained composite strengths with theoretical composite strengths obtained by means of mathematical modelling.

Chapter 2: Literature Review

2.1 Natural Fibres

Natural organic fibres can be derived from either animal or plant sources. The majority of useful natural textile fibres are plant derived, with the exceptions of wool and silk. All plant fibres are composed of cellulose, whereas fibres of animal origin consist of proteins. Natural cellulose fibres tend to be stronger and stiffer than their animal counterparts, and are therefore more suitable for use in composite materials. Depending on the origin of the fibre, cellulose fibres can be classified into the following categories:

- Grasses and reeds: These fibres are found in the stems of monocotyledonous plants such as bamboo and sugar cane.
- Leaf fibres: These fibres run lengthwise through the leaves of most monocotyledonous plants such as sisal, henequen and abaca.
- Bast Fibres: These fibres are situated in the inner bark (phloem) of the stems of dicotyledonous plants. Common examples are jute, flax, hemp and kenaf.
- Seed and fruit hairs: These are fibres that come from seed hairs and flosses, which are primarily represented by cotton and coconut.
- Wood fibres: These fibres are found in the xylem of angiosperm (hardwood) and gymnosperm (softwood) trees. Examples are pine, maple and spruce.

2.2 Comparisons of Natural Cellulose Fibres

For centuries, cellulose fibres have been used in the manufacture of various products such as rope, string, clothing, carpets and other decorative products. Wood fibres are the most abundantly used cellulose fibres due to their extensive use in the pulp and paper industries, although the use of other fibre types is increasing (Table 2.1).

Table 2.1 Commercially important fibre sources [14, 15].

Fibre Source	Species	World Production (10^3 tonnes)	Origin
Wood	(>10,000 species)	1,750,000	Stem
Cotton lint	*Gossypium sp*.	18,450	Fruit
Bamboo	(>1250 species)	10,000	Stem
Jute	*Corchorus sp.*	2,300	Stem
Kenaf	*Hibiscus Cannabinus*	970	Stem
Flax	*Linum Usitatissimum*	830	Stem
Sisal	*Agave Sisilana*	378	Leaf
Roselle	*Hibiscus Sabdariffa*	250	Stem
Hemp	*Cannabis Sativa*	214	Stem
Coir	*Cocos Nucifera*	100	Fruit
Ramie	*Boehmeria Nivea*	100	Stem
Abaca	*Musa Textiles*	70	Leaf
Sunn hemp	*Crorolaria Juncea*	70	Stem

There are several physical properties that are important in selecting suitable cellulose fibres for use in composites. Fibre dimensions, defects, variability, crystallinity and structure are some of the most important properties that must be considered [16]. Mechanical properties are even more important when selecting a suitable fibre for composite reinforcement. To produce a strong composite material, it is important to utilise strong reinforcing fibres. However, fibre strength is not the only contributing factor to composite strength, as good bonding

between the fibres and matrix, good fibre orientation and good fibre dispersion are also required.

The cost of the cellulose fibres is also a factor that could influence fibre selection. Fibre prices tend to fluctuate considerably and are dependent on a number of factors, such as supply and demand, quality and exchange rates [15]. A comparison of the relative costs of a number of fibres can be seen in Table 2.2. The costs of bulk cellulose fibres are considerably lower than those of glass and carbon, but cellulose fibres require further processing to get them into a form where they can be used in composites. Despite this, cellulose fibres still appear to be a cheaper option when compared to synthetic fibres.

Table 2.2 Natural plant fibre costs [17].

Fibre Type	Price $US/Kg
Jute	0.3 - 0.7
Hemp	0.5 - 1.5
Flax	0.4 - 0.8
Sisal	0.4 - 1
Wood	0.2 - 0.4
Glass	1.5 – 3.2
Carbon	10 - 200

From the information provided in Table 1.2 in Chapter 1, it can be seen that the strongest cellulose fibres are hemp, jute and flax, with hemp and flax having the highest values for Young's modulus. Hemp and flax fibres also have high aspect ratios (length/width), which is a desirable attribute for fibres to be used as composite reinforcement.

The most suitable cellulose fibres for use in composite materials are therefore hemp and flax. Flax is more widely accessible and slightly cheaper than hemp due to its widespread use in the textiles industry. Hemp, however, has the potential for much higher fibre yields that could result in lower costs with improvements in cultivation techniques [6]. Hemp, compared to flax, also has the

advantage of being extremely disease and pest resistant, and can be planted at high densities to prevent weeds from growing between the plants. Pesticides and herbicides are therefore not required in the cultivation of hemp, and this provides a distinct advantage over flax in many countries where restrictions on herbicide use is prevalent [18].

2.3 Industrial Hemp Fibre

Industrial hemp fibre (*Cannabis Sativa* L.) has been widely used in many civilizations, and it is estimated that the earliest use of hemp was over 6000 years ago. Hemp fibres have long been valued for their high strength and long fibre lengths, and have been used extensively in the fabrication of ropes and sails, as well as for paper and textiles. In the middle of the 19th century, hemp cultivation decreased with competition from other natural fibres (cotton, sisal, jute) and synthetic fibres, as well as with the disappearance of traditional sailing ship navies. Due to its relationship with marijuana, industrial hemp was banned in many countries with the introduction of stricter drug laws [19]. In New Zealand, hemp cultivation was banned in the late 1930's, and this law was only amended in 2001 when nine growers were issued licenses to trial a crop of hemp for industrial use.

The essential difference between industrial hemp and marijuana is the amount of THC (Tetrahydrocannabinol) present within the plant. THC is a psychoactive chemical thought to have a range of detrimental effects of human beings, including a lowering of blood pressure, induced euphoria and long term degeneration of brain activity. There is ongoing debate as to whether the narcotic hemp plant is actually a different variety of plant, or actually the industrial variety bred to produce high levels of THC. An industrial hemp plant will naturally attain a THC content of 0.6%, and it is generally accepted that a content of 2% is required to have a noticeable effect on the human body.

2.3.1 Hemp Plant Morphology

Industrial hemp is part of the Mulberry genus and is a fast growing annual plant. It can grow up to five metres in height, and can reach between six and sixty millimetres in diameter, depending on the plantation density. Hemp plants have a well-developed primary root system with numerous branched secondary roots. Industrial hemp is naturally dioecious, meaning that it has separate male and female plants with different growth characteristics. The male plants tend to be taller and slenderer with few leaves surrounding the flowers, while female plants are shorter and stockier with many leaves at each terminal inflorescence, as can be seen in Figure 2.1.

Figure 2.1 Industrial hemp plants: a) Male and b) Female.

The cross-sectional structure of a hemp stalk can be seen in Figure 2.2 and Figure 2.3. The hemp stem consists of a woody core (xylem) with a hollow pith,

surrounded by an outer layer of bark consisting of cambium, bast fibre (phloem), cortex and epidermis [20, 21]. The woody core, called the hurd, is responsible for providing stiffness to the hemp stem, and the bast fibre in the bark provides tensile and flexural strength. An epidermis situated on the outside of the stem gives protection from parasites. The bast section of the stem represents about one third of the total stem volume, while the hurd represents about two thirds.

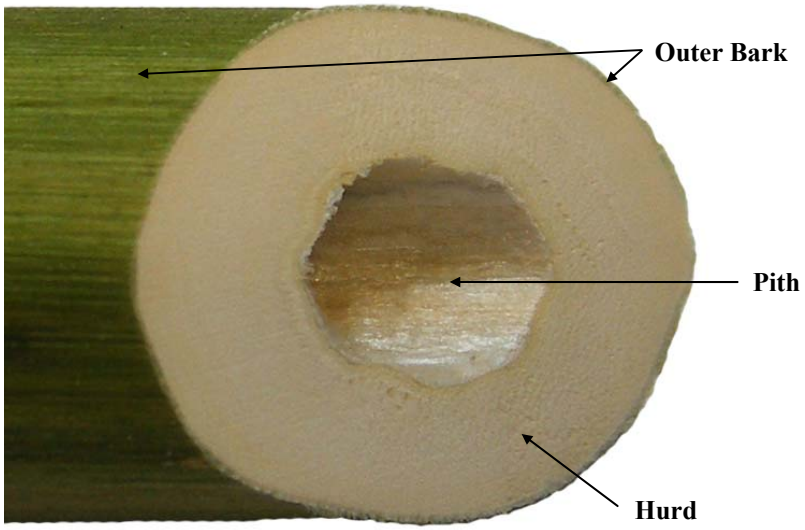

Figure 2.2 Cross section of a hemp stem.

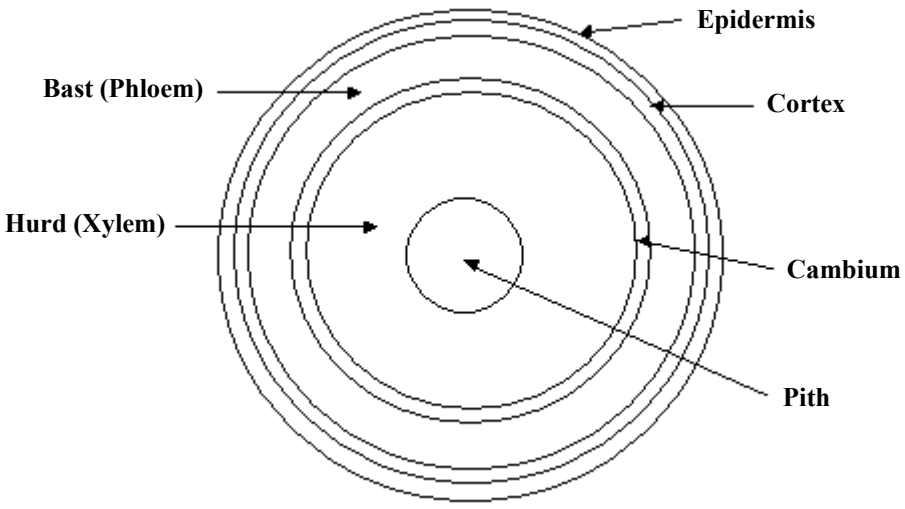

Figure 2.3 Schematic of a hemp stem cross section (not to scale).

The bast fibres are long, stiff and strong, and are suitable for use in textiles, ropes and composites. They are found in the inner and outer bark layers of the stem, and can be further categorised into primary or secondary bast fibres. Both are virtually solid in cross section, although a small lumen (void) is often present. The larger primary bast fibres are usually found nearer the epidermis, while the smaller secondary fibres dominate the inner regions of the bark. A comparison between the primary and secondary bast fibres can be seen in Figure 2.3.

Table 2.3 Hemp bast fibre comparisons.

	Secondary Bast Fibre	Primary Bast Fibre
Diameter (μm)	18-20	28-38
Length (mm)	18-25	25-40
Tensile Strength (MPa)	< 300	< 1000
Cellulose (wt%)	32-50	55-85

Elementary bast fibres overlap over a considerable length and are bonded together by an interface known as the middle lamella, which consists mainly of lignin, pectins and hemicelluloses [22]. These groups of joined fibres are known collectively as fibre bundles, and are responsible for making up the bark tissue.

The hurd fibres are situated in the woody core of the hemp stalk, and are very thin-walled and short compared to bast fibres. They have large lumens, high lignin and low cellulose contents compared to bast fibres, and they are weak and brittle. As a result, they are not suitable for use in composite materials, but can be used in the papermaking industry as a filler material. A comparison between the bast and hurd fibres can be seen in Table 2.4.

Table 2.4 Summary of hemp stalk composition [20, 23].

Type Of Fibre	Fibre Length (mm)	Fibre Width (μm)
Bast	5-55 (ave 25)	15-40 (ave 22)
Hurd	0.2 - 0.6	10-30

2.3.2 Bast Fibre Morphology

Elementary bast fibres, along with all lignocellulosic fibres, can actually be considered as composites themselves as they consist of helically wound cellulose microfibrils in an amorphous matrix of lignin and hemicellulose. Each fibre consists of many microfibrils that run along the length of the fibre (Figure 2.4 and Figure 2.5).

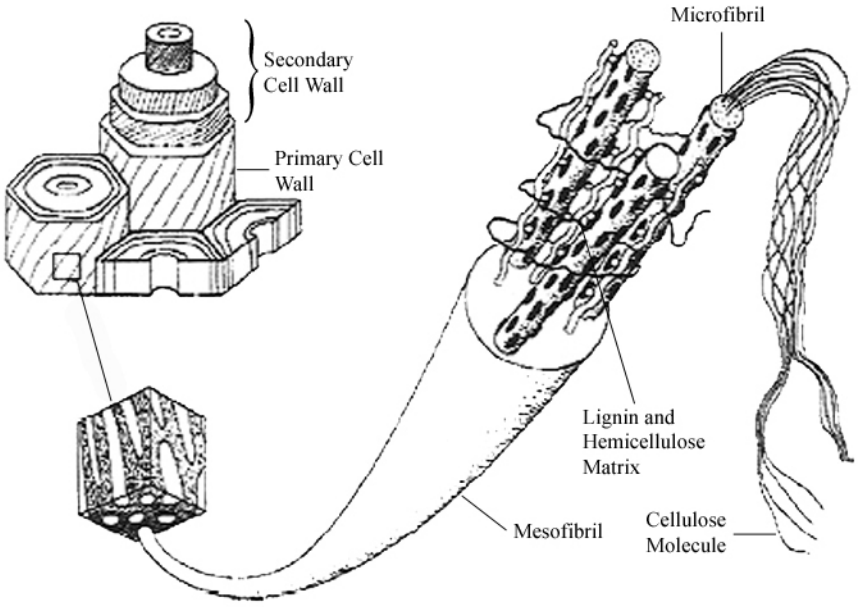

Figure 2.4 Fibre with primary and secondary walls. Cellulose molecules are united to form microfibrils, which in turn compose mesofibrils [24].

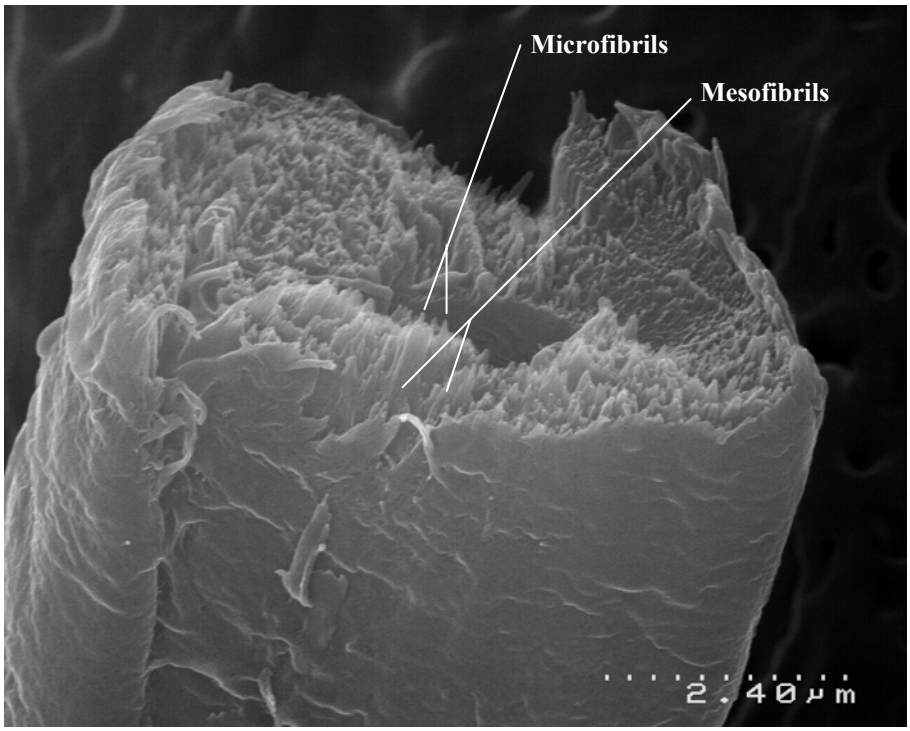

Figure 2.5 Scanning Electron Micrograph (SEM) of a fractured hemp fibre showing mesofibrils and microfibrils.

The fibre wall, or cell wall, is divided into two distinct parts, namely the primary cell wall and the secondary cell wall. The primary cell wall is relatively thin, about 0.2 μm, and consists of pectin, some lignin and cellulose. The secondary cell wall makes up most of the fibre diameter, and consists of oriented, highly crystalline microfibrils and amorphous lignin and hemicellulose. The microfibrils are packed together in a fibrillar structure, the mesofibrils, with the microfibrils oriented spirally at approximately 10^{o} to the fibre axis. The mesofibrils are presumably glued together by a hemicellulose and lignin rich phase [2, 25].

2.3.3 Factors Affecting Fibre Properties

The mechanical properties of single fibres are strongly influenced by many factors, particularly chemical composition and internal fibre structure, which differ between different parts of a plant as well as different plants. The most efficient cellulose fibres are those with a high cellulose content coupled with a low microfibril angle in the range of 7-12^{o} to the fibre axis. Other factors that

may affect the fibre properties are maturity, separating processes, microscopic and molecular defects such as pits and nodes, soil type and weather conditions under which they were grown. The highly oriented crystalline structure of cellulose makes the fibres stiff and strong in tension, but also sensitive towards kink band formation under compressive loading. The presence of kink bands significantly reduces fibre strength in compression and in tension [2].

2.3.4 Hemp Growing Conditions

Hemp is a hardy plant, and grows well in a moderately cool climate. The plant prefers well-drained soils that are high in organic matter, with a neutral or slightly alkaline pH. Clay soils are not suitable, as they restrict the rate of nutrient uptake. Hemp plants are not considered drought tolerant, and will attain an optimum growth rate with an annual rainfall of 750mm. The plant is fast growing, sometimes exceeding a growth rate of one inch per day, and therefore an abundance of water is crucial over the first 30-40 growth days. To achieve maximum fibre production, industrial hemp should be planted in a tight formation [26].

2.3.5 Hemp Harvesting

Hemp is an annual plant, and has five stages in its lifecycle: germination, growth, flowering, seed formation and death. As the plant goes through these growth stages, the chemical composition and fibre properties of the plant tissues change [16]. Harvesting of hemp for high quality fibre is normally done when 50% of the seeds resist compression [27], or when one third of the anthers on the male plants are shedding pollen. If harvested earlier, the fibre is softer and finer, but also weaker and less dense.

2.4 Hemp Fibre Constituents

The chemical composition of hemp varies according to the variety, the area of production and the maturation of the plant. Hemp fibres are mainly composed of cellulose, hemicelluloses, lignin and pectins, although the quantities of each are

different in bast and hurd fibres (Table 2.5). Bast fibres contain higher cellulose contents, and are therefore stronger than hurd fibres. Hurd fibres also contain high levels of lignin, which is undesirable for fibres that are to be used in composite materials.

Table 2.5 Chemical constituents of hemp (% w/w) [20].

	Cellulose	Hemicelluloses	Pectins	Lignin	Wax + fat	Ash	Proteins
Bast Fibre	55	16	18	4	1	4	2
Hurd Fibre	48	12	6	28	1	2	3

2.4.1 Cellulose

The long, thin crystalline microfibrils that dominate the secondary cell walls of lignocellulose fibres are made of cellulose, and are responsible for providing tensile strength to the fibres. Cellulose is a linear polymer consisting of D-anhydroglucose units joined together by β-1,4-glycosidic linkages [14]. The anhydroglucose units do not lie exactly in plane, but assume a chair conformation, with successive glucose residues rotated through an angle of 180^{o} (Figure 2.6).

Cellulose may either be crystalline or amorphous (non-crystalline), and native cellulose is usually composed of crystalline segments alternating with regions of amorphous cellulose [28] (Figure 2.7). Most plant-derived cellulose is highly crystalline and may contain as much as 80% crystalline cellulose [16].

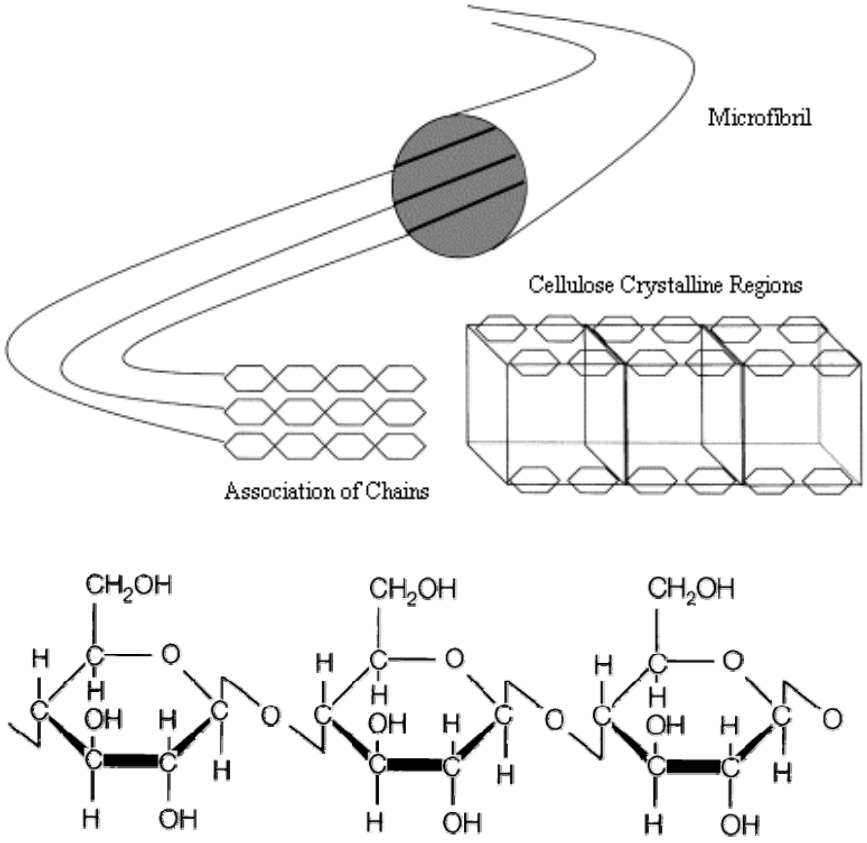

Figure 2.6 The molecular structure and arrangement of cellulose [29].

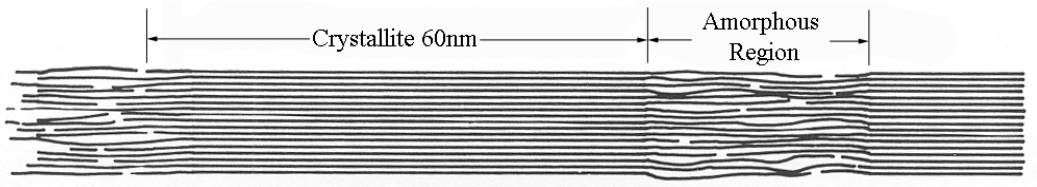

Figure 2.7 Schematic representation of the crystallite structure of cellulose [28].

The rigidity and strength of cellulose and lignocellulose based materials is a result of hydrogen bonding, both between chains and within chains [30]. The amorphous cellulose regions have fewer inter-chain hydrogen bonds, thus exposing reactive inter-chain hydroxyl groups (OH) for bonding with water molecules. Amorphous cellulose can therefore be considered hydrophilic due to its tendency to bond with water. Crystalline cellulose on the other hand is closely packed, and very few accessible inter-chain OH groups are available for bonding with water. As a result, crystalline cellulose is far less hydrophilic than amorphous

cellulose. Crystalline microfibrils consist of tightly packed cellulose chains with accessible hydroxyl groups present on the surface of the structure (Figure 2.8). Only the very strongest acids and alkalis can penetrate and modify the crystalline lattice of cellulose.

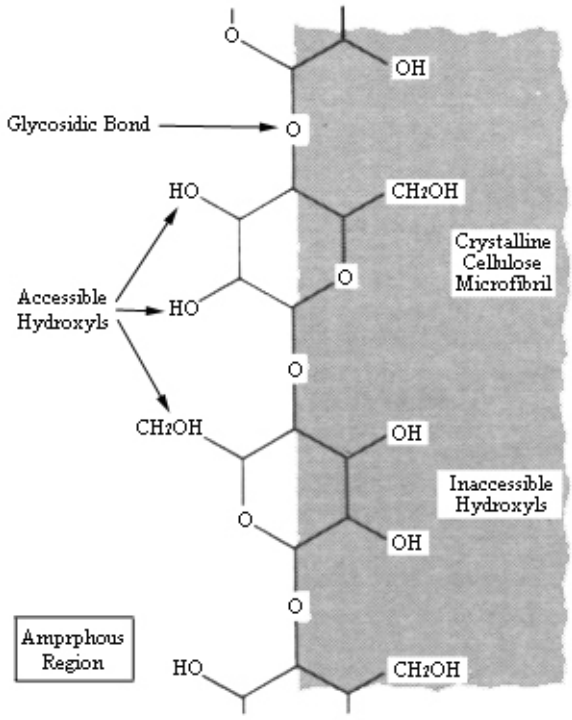

Figure 2.8 Microfibril surface [31].

2.4.2 Lignin

Lignin is a poorly understood hydrocarbon polymer with a highly complex structure consisting of aliphatic and aromatic constituents, which form a matrix sheath around the cellulose microfibrils and fibres [14]. Lignin provides compressive strength to the slender microfibrils, and prevents them from buckling under compressive loads. No regular structure for lignin has been demonstrated, and it is totally amorphous as opposed to the ordered structure of crystalline cellulose. Lignin is distributed throughout the primary and secondary cell walls, with the highest concentration being found in the middle lamella. The dissolution of lignin in the middle lamella using chemicals aids fibre separation, as is

commonly done in the pulp and paper industries. When exposed to ultraviolet light, lignin undergoes photochemical degradation [32].

2.4.3 Hemicelluloses

The hemicellulose fraction of the fibre contains a collection of polysaccharide polymers containing mainly the sugars D-xylopyranose, D-glocopyranose, D-galactopyranose, L-arabinofuranose, D-mannopyranose, and D-glucopyranosyluronic acid with small quantities of other sugars [16]. Hemicelluloses appear to form a link between cellulose and lignin, thus permitting the effective transfer of shear stresses between the cellulose microfibrils and the lignin [33]. Unlike cellulose, the hemicellulose polymer chains are rarely crystalline and are mainly responsible for the water absorption in the fibre wall. They are also heavily branched and have short side chains, whereas cellulose is a long unbranched polymer. It is suspected that no chemical bonding occurs between cellulose and hemicelluloses, but sufficient mutual adhesion is provided by hydrogen bonds and van der Waals forces [34]. Hemicelluloses have greater solubilities in solvents compared to cellulose, and can be broken down in high temperature environments.

2.4.4 Pectins

Pectins are a collective name for the heteropolysaccharides found in the primary cell walls of most non-wood plant fibres, and they consist of α-1, 4-linked galacturonic acid units, sugar units of various compositions, and their respective methyl esters [14]. Pectins, along with lignin and hemicelluloses, are used to connect the elementary fibres together and can easily be hydrolysed at elevated temperatures. Pectins are the most hydrophilic compounds in plant fibres due to the presence of carboxylic acid groups.

A summary of the cell wall polymers responsible for the properties of cellulose fibres can be seen in Figure 2.9:

Biological Degradation
Hemicelluloses
Accessible Cellulose
Non-Crystalline Cellulose

Moisture Sorption
Hemicelluloses
Accessible Cellulose
Non-Crystalline Cellulose
Lignin
Crystalline Cellulose

Ultraviolet Degradation
Lignin
Hemicelluloses
Accessible Cellulose
Non-Crystalline Cellulose
Crystalline Cellulose

Thermal Degradation
Hemicelluloses
Cellulose
Lignin

Strength
Crystalline Cellulose
Amorphous Constituents
Lignin

Figure 2.9 Cell wall polymers responsible for the properties of lignocellulosics in order of importance [35].

2.5 Thermoplastic Matrices

One of the main disadvantages of using lignocellulosic fibres as reinforcements in thermoplastic matrix composites is that they degrade at medium to high processing temperatures, which can result in reductions in composite mechanical

properties. The processing temperatures of natural fibre reinforced thermoplastic composites are limited to less than 200^{o}C, although it is possible to use higher temperatures for short periods of time [3]. Low temperature processes are desirable as the cause less fibre degradation, and are also cheaper and more environmentally friendly.

The first criterion for selecting a suitable composite matrix is the melting temperature (M.T) of the polymer, which needs to be below 200^{o}C. As seen in Table 2.6, some of the standard polymers that fit this requirement are polypropylene (PP), high-density polyethylene (HDPE) low-density polyethylene (LDPE) and polyvinylchloride (PVC). These plastics are all commonly used in the plastics industry, are not expensive and can be recycled.

Table 2.6 Physical properties of various polymers [36, 37].

Properties	**Limits**	**Type of Polymer**			
		PP	**LDPE**	**HDPE**	**PVC**
T.S (MPa)	Upper	38	17.3	37.3	62.1
	Lower	22	6.2	20	51.8
M.T (^{o}C)	Upper	177	120	130	204
	Lower	165	105	120	
ρ (g/cm^{3})	Upper	0.920	0.925	1.000	1.58
	Lower	0.899	0.910	0.941	1.49
W_{24h} (%)	Upper	0.02	<0.015	0.2	0.4
	Lower	<0.01		<0.01	0.04

A natural fibre reinforced composite needs to be lightweight in nature, and thus requires a thermoplastic matrix with a low density (ρ). PP and LDPE have the lowest densities of the thermoplastics summarised in Table 2.6, and are therefore the most suitable in this regard.

Water absorption in the matrix is a great drawback in composites, as water can migrate through the polymer to the fibre/matrix interface, resulting in a reduction in the strength of the composite. A matrix with a low level of moisture absorption

is thus desirable; hence PP and LDPE are the most suitable polymers as they absorb the least amount of water over a 24-hour period (W_{24h}).

The tensile strength (T.S) of the matrix material does not significantly affect the strength of composites containing 50% or more fibre volume fraction. Only a 5-10% difference in composite strength can be expected when using different thermoplastic matrices containing 50% volume fraction reinforcing fibres [36]. The strength of the matrix therefore only becomes important in composites with low fibre contents. PP is weaker than PVC, but generally has a greater tensile strength compared to LDPE and HDPE.

It is therefore thought that polypropylene is the most suitable thermoplastic for use in natural fibre composites as it has the lowest density, absorbs a low amount of water, and has a good tensile strength. PP is also the cheapest of the 4 polymers considered [38].

2.6 Issues Regarding the Use of Natural Cellulose Fibres in Composites

Natural fibres present many advantages compared to synthetic fibres, thus making them attractive reinforcements for composite materials. They are cheap, abundant and renewable, and have good specific properties such as tensile strength and stiffness. Unlike brittle synthetic fibres, natural fibres are flexible and are less likely to fracture during composite processing. This enables the fibres to maintain the appropriate aspect ratios to provide good composite reinforcement.

Despite these fibre advantages, untreated natural fibre composites have performed well below their potential capabilities, and have therefore not been used extensively in the thermoplastics industry.

The main reasons for this are as follows:

- Poor interfacial bonding between the cellulose fibres and the thermoplastic matrix
- Limited thermal stability of the composite
- High moisture absorption of the cellulose fibres
- Poor fibre separation and dispersion within the composite
- Biodegradability of the fibres

Other factors that govern the properties of short fibre reinforced composites are:

- Fibre aspect ratio
- Fibre orientation
- Fibre tensile strength, Young's modulus and volume fraction

2.6.1 Interfacial Bonding

All plant derived cellulose fibres are polar and hydrophilic in nature, mainly as a consequence of their chemical structure. Plant fibres contain non-cellulosic components such as hemicelluloses, lignin and pectins, of which the hemicelluloses and pectins are the most hydrophilic. These components contain many accessible hydroxyl (OH) and carboxylic acid groups, which are active sites for the sorption of water [29]. The cellulose component also contains many OH groups, but little water can be accommodated within the highly ordered and highly crystalline microfibrils. As a result of this, only un-bonded OH groups on the microfibril surfaces are available for sorption.

Polyolefins, such as polypropylene, are largely non-polar and hydrophobic in nature. The incompatibility of the polar cellulose fibres and non-polar thermoplastic matrix leads to poor adhesion, which then results in a composite material with poor mechanical properties [39]. To fully utilise the mechanical properties of the reinforcing fibres and thereby improve the composite properties, it is necessary to improve the adhesion between the fibres and matrix. This can be achieved by either modifying the surface of the fibres to make them more compatible with the matrix, or by modifying the matrix with the addition of a coupling agent that adheres well to both the fibres and matrix. When the fibres

and matrix have been brought into close proximity with one another, the following interfacial bonding mechanisms may occur:

- Mechanical interlocking
- Electrostatic bonding
- Chemical bonding
- Reaction or Interdiffusion bonding

It should be noted that it is possible for multiple bonding mechanisms to occur on the same interface at the same time.

Mechanical Interlocking

Mechanical interlocking on the fibre/matrix interface occurs when the fibre surface is rough and jagged (Figure 2.10). This mainly increases the interfacial shear strength, and makes the occurrence of fibre pullout less likely.

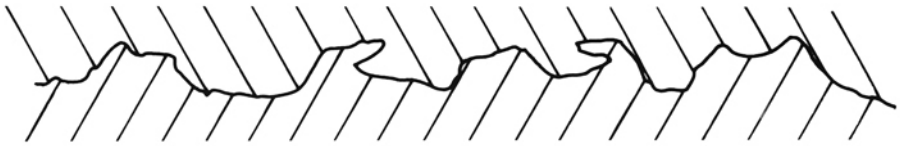

Figure 2.10 Schematic of mechanical interlocking [40].

Electrostatic Bonding

When the fibre or matrix is positively charged and the other is negatively charged, electrostatic bonding occurs (Figure 2.11). This electrostatic attraction only occurs when there is a difference in charge and intimate contact between the composite components.

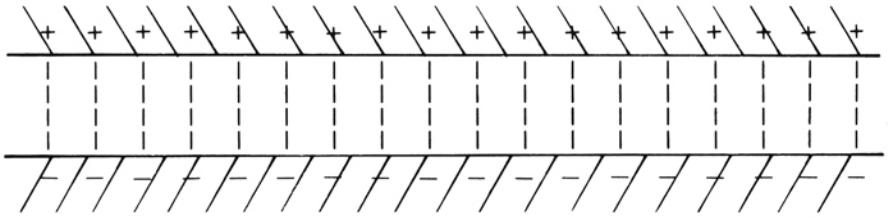

Figure 2.11 Schematic of electrostatic bonding [40].

Chemical Bonding

This type of bonding occurs when a reaction takes place between reactive chemical groups on the fibre surface and compatible groups in the matrix Figure 2.12). The strength of the bond depends on and the type of bond and the number of bonds per unit area. The most common chemical bonds and their relative bond strengths are as follows [31]:

Covalent Bond: 200 – 800 kJ mol^{-1}

Hydrogen Bond: 10 – 40 kJ mol^{-1}

Van der Waals: 1 – 10 kJ mol^{-1}

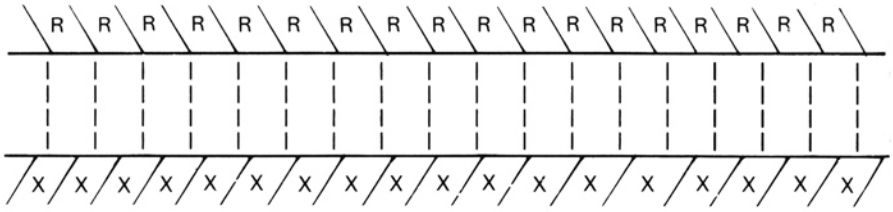

Figure 2.12 Schematic of chemical bonding, where R and X represent compatible chemical groups [40].

Reaction or Interdiffusion Bonding

Atoms or molecules of the fibre and matrix may interact or interdiffuse at the interface to give reaction or interdiffusion bonding. For interfaces involving polymers, reaction bonding may take place when polymer chains from each component entangle and intertwine together (Figure 2.13). The strength of this

bonding mechanism depends on the distance over which the chains are intertwined, the degree of entanglement and the number of chains per unit of area. For systems involving metals and ceramics, the interdiffusion of species from the two components can produce an interfacial layer of different composition and structure from either of the components (Figure 2.14). The interfacial layer will also have different mechanical properties from either the matrix or reinforcement and this consequently affects the characteristics of the interface [40].

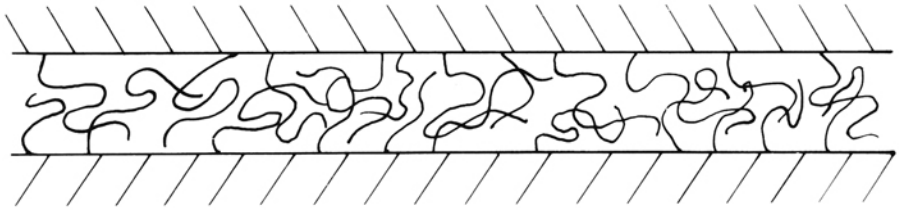

Figure 2.13 Schematic of reaction bonding involving polymers [40].

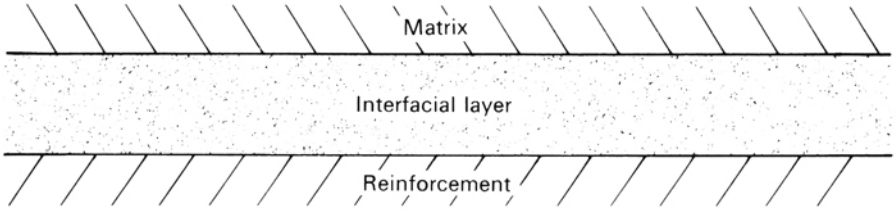

Figure 2.14 Schematic of interdiffusion bonding [40].

2.6.2 Thermal Stability

Unlike many synthetic fibres, lignocellulosic fibres are inherently thermally unstable, and thermal degradation starts to occur at temperatures of around 200^{o}C. This results in the exclusion of some manufacturing processes, and also limits the use of the composites to low temperature applications. It is suggested by Yildiz *et al.* [41] that temperatures above 150^{o}C can lead to permanent alterations of the physical and chemical properties of lignocellulosic fibres such as wood. It is also

stated that heat treatments at high temperatures can improve the biological durability of wood, but stiffness and strength are reduced.

It has, however, been shown by several authors [42-44] that the thermal stability of lignocellulosic fibres can be improved somewhat by means of alkali fibre treatment.

2.6.3 Moisture Absorption

A further problem associated with using lignocellulosic fibres in composite materials is high moisture absorption [3]. A moisture build up in the fibre cell wall can lead to fibre swelling and dimensional changes in the composite, particularly in the direction of the fibre thickness [35]. Another problem associated with fibre swelling is a reduction in the adhesion between the fibre and the matrix, leading to a reduction in the mechanical properties of the composite. The debonding between the fibre and matrix may be initiated by the development of osmotic pressure pockets at the surface of the fibre, which is a result of the leaching of water-soluble substances from the fibre surface [45].

Besides dimensional stability, the hydrophilic nature of lignocellulosic fibres also influences the process ability of the composite. The tendency of lignocellulosic fibres to absorb moisture results in the release of water vapour in the composite during high temperature compounding, leading to the formation of a highly porous material. These pores can act as stress concentration points, and can lead to premature failure of the composite during loading.

Joseph *et al*. [45] showed that the water uptake of natural fibre composites can be reduced considerably by using coupling agents to assist with fibre-matrix adhesion.

2.6.4 Fibre Separation and Dispersion

The incorporation of lignocellulosic fibres into a thermoplastic polymer is often associated with poor fibre dispersion due to the large differences in polarity

between the fibres and polymer, and the strong intermolecular hydrogen bonds between the fibres [3]. To obtain a satisfactory performance from the composite, it is necessary to have a good fibre distribution within the matrix. A good distribution implies that the fibres are fully separated from each other, and each fibre is fully surrounded by the matrix.

Insufficient fibre dispersion can lead to clumping and agglomeration of the fibres, resulting in an inhomogeneous mixture of resin-rich and fibre rich areas. This segregation is undesirable, as the resin rich areas are weak, while the fibre rich areas (clumps) are susceptible to micro cracking. Micro cracks contribute to inferior mechanical properties of the composite. It is therefore necessary to ensure a homogeneous fibre distribution in order to achieve maximum strength and performance of the composite material.

To ensure good distribution and dispersion of fibres within a composite matrix, it is necessary to separate the fibres from each other, modify the fibres and/or matrix to improve compatibility, and ensure that the fibre lengths are such that fibre entanglement does not occur.

To separate the fibres from their fibre bundles, it is necessary to dissolve the pectins and lignin that bind the individual fibres together. Fibre separation can easily be performed by treating the fibres with a strong alkali solution [46]. Fibre separation can also occur during composite compounding by means of high-energy processing techniques such as extrusion and injection moulding. Several factors contribute to this fibre attrition, such as the shearing forces generated in the compounding equipment, residence time, temperature and viscosity of the melt mixture [3].

Cellulose fibres and polypropylene generally do not mix well due to their polar and non-polar characteristics. It is therefore possible to improve compatibility by modifying the fibre surface using dispersing agents such as stearic acid, or by pre-treating the fibre with acetic anhydride [14, 47]. Fibre clumping is not as severe a problem with the treated fibre as it is with untreated fibre [48].

The length of fibres used in composites is a critical factor. They should not be too long, otherwise they may get entangled with each other resulting in clumping and reduced composite efficiency. If the fibres are too short, however, the stress transfer area will be too small for them to offer effective reinforcement. As fibre lengths are commonly reduced during compounding of the fibres and matrix, the ultimate fibre lengths present in a composite are dependent on the type and set-up of the composite processing equipment used.

2.6.5 Biodegradability

Natural lignocellulosic fibres degrade easily when exposed to nature. Some of these methods of degradation include biological, thermal, aqueous, photochemical, chemical and mechanical degradation processes [35]. In order to produce cellulose fibre-based composites with a long service life, it is necessary to retard this natural degradation. One way of preventing or slowing down the natural degradation process is by modifying the cell wall chemistry. Undesirable natural fibre characteristics such as dimensional instability, flammability, biodegradability, and chemical degradation can be eliminated or impeded in this manner [35]. Chemical treatments can reduce the water uptake in the fibres, and can therefore reduce the amount of fibre swelling and biological degradation by blocking the available OH groups on the fibre surface [45].

2.6.6 Fibre Aspect Ratio

The fibre aspect ratio (length/diameter) is a critical parameter in a composite material. For each short-fibre composite system, there is a critical fibre aspect ratio, which may be defined as the minimum fibre aspect ratio in which the maximum allowable fibre stress can be achieved for a given load [49]. The critical fibre aspect ratio of a composite can be calculated using the following equation [7]:

$$\frac{L_c}{D} = \frac{\sigma_f}{2_\tau} \qquad (2.1)$$

where L_c is the critical fibre length, D is the fibre diameter, σ_f is the tensile strength of the fibre and τ is the interfacial shear strength.

The critical fibre length is not only determined by fibre and matrix properties, but also by the quality of the fibre/matrix interface. Load is transferred from the fibre to the matrix by shear along the interface. A sub-critical length fibre will not make a significant contribution to composite strength, as it will be pulled out of the matrix before it can be fully stressed. A critical length fibre can be fully stressed, but only at a very small location in the middle of the fibre. A super-critical length fibre has a much greater proportion of the fibre that can be fully stressed, and can therefore contribute more to composite strength than a critical length fibre.

Longer reinforcing fibres are thus more desirable in a composite material, but if the fibre aspect ratio is too high, the fibres may get entangled during mixing resulting in poor fibre dispersion. An aspect ratio in the range of 100 – 200 after composite processing is recommended for high performance short-fibre reinforced composites [49].

2.6.7 Fibre Orientation

Fibre orientation is an important parameter that influences the mechanical behaviour of short-fibre reinforced composites. The maximum composite strength occurs when the reinforcing fibres are aligned and oriented parallel to the direction of the applied load. Short fibre composites, however, rarely consist of fibres oriented in a single direction. During extrusion, compounding and injection moulding processes, progressive and continuous changes in fibre orientation take place throughout the moulded components. These changes are complex, and are related to the size and concentration of the fibres, the viscoelastic properties of the melted polymer matrix, the mould cavity and processing conditions [50]. During extrusion, the polymer melt experiences both extensional and shear flow, which can result in the alignment of fibres in the flow direction (Figure 2.15).

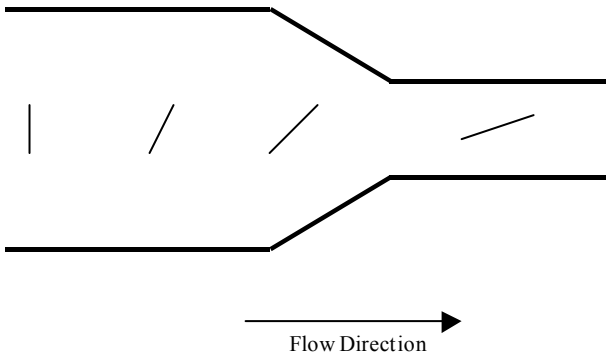

Figure 2.15 Fibre alignment as a result of extrusion.

During injection moulding, the fibre-polymer melt is subjected to complex and variable flow conditions that result in complex fibre orientation distributions within the composite. As the melt enters a mould, the sudden increase in channel dimensions causes deceleration along the flow front, resulting in a compressive force within the melt [12]. This compression aligns the fibres and polymer molecular chains transversely to the melt flow direction. The melt flowing along the mould walls moves at a lower velocity to the melt flowing through the channel due to the presence of frictional forces. The higher melt velocity at the centre of the channel, and the lower melt velocity near the walls causes the central material to splay outwards at the flow front, resulting in a phenomenon known as fountain flow (Figure 2.16) [51]. Fibres situated along the mould walls are aligned in the flow direction to form skin layers, whereas fibres in the centre of the channel are more transversely and randomly aligned and form a layer known as the core. The exact transition between the longitudinally aligned skin layers and the transversely aligned core is not always defined and can be difficult to identify.

A further technique for improving the fibre alignment in short fibre thermoplastic composites is compression moulding, whereby the polymer matrix is combined with a pre-fabricated aligned-fibre mat and consolidated at elevated temperatures and pressures in a hot-press.

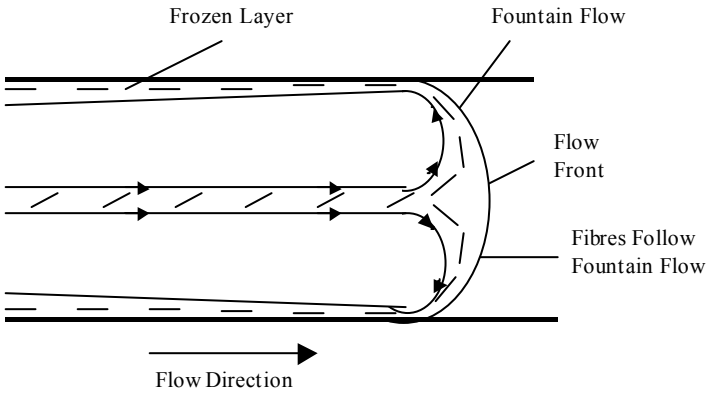

Figure 2.16 Fountain flow experienced during injection moulding [51].

Many composite strength prediction models require knowledge of the fibre orientation distribution within a composite [52-54]. However, while the fibre length distribution in composite samples can be easily determined by separating the fibres from the matrix and observing them under a microscope, measurements of fibre orientation are difficult because the fibres are concealed by the matrix material.

Both destructive and non-destructive techniques for measuring fibre orientation have been proposed in the literature. Destructive techniques generally consist of cutting a material sample and observing the elliptical shape of the fibres on the cutting plane [50, 52]. From the eccentricity of the ellipses, the angle between the fibre axis and the direction perpendicular to the cutting plane can be measured. However, these measurements can be inaccurate due to difficulties associated with distinguishing ellipses of low eccentricity. This technique can only be used for fibres with circular cross-sections and consistent fibre diameters.

Standard non-destructive techniques for evaluating fibre orientation involve the use of X-rays to obtain images of fibres situated on a plane perpendicular to the direction of irradiation [55]. This method allows for the determination of in-plane fibre orientation distributions only, and does not permit the measurement of fibre orientations along the thickness of the sample [56].

2.6.8 Fibre Tensile Strength, Young's Modulus and Volume Fraction

The properties of a composite are strongly influenced by the reinforcing fibre tensile strength, Young's modulus and volume fraction. Changes in composite properties with variations in fibre content, tensile strength and Young's modulus, can be predicted using failure prediction models such as the Modified Rule of Mixtures (as discussed further in this chapter) [7].

As reinforcing fibres are directly responsible for providing strength and stiffness to a composite, it is necessary to maximise the fibre tensile strength and Young's modulus to produce a composite material with enhanced properties.

Fibre volume fraction (V_f) also plays an important part in determining the composite mechanical properties. For composites consisting of brittle fibres in a ductile polymer matrix, two possible failure regimes exist depending on whether the fibre volume fraction is above or below a minimum value (V_{min}) (Figure 2.17). If a composite with $V_f < V_{min}$ is stressed, the polymer matrix is able to carry the applied load after fibre fracture. Failure of the fibres does not lead to composite failure but results in a stress increase in the matrix. The failed fibres, which now carry no load, can be regarded as holes in the polymer matrix. If a composite with $V_f > V_{min}$ is stressed, brittle failure of the fibres leads to failure of the whole composite, since the polymer matrix in unable to support the additional load which is transferred into the matrix from the fibres [57]. When $V_f > V_{min}$, a point exists where the strength of the composite reaches and then surpasses the strength of the matrix alone, and this is known as the critical fibre volume fraction (V_{crit}) [58].

At very high fibre volume fractions, the strength of a composite starts to decrease due to insufficient wetting of the fibres with the polymer matrix. Nishino *et al*. [59] produced a kenaf fibre reinforced poly-L-lactic acid composite, and found that the composite strength increase with an increase in fibre volume fraction was linear up until 70% fibre (by volume), after which a reduction in strength was observed.

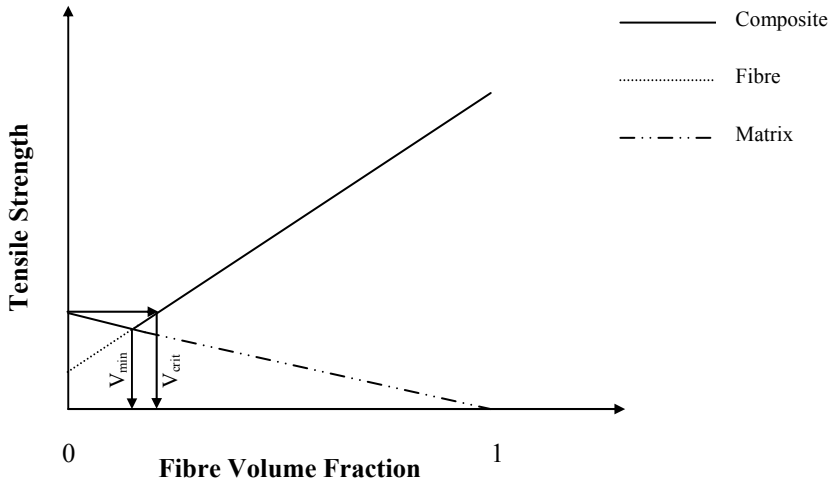

Figure 2.17 Theoretical relationship between tensile strength and fibre volume fraction for short-fibre reinforced composites.

Another explanation for the decrease in composite mechanical properties at high fibre volume fractions has been mentioned by Fu *et al.* [60]. During the injection moulding of short-fibre reinforced polymers, fibre breakages occur as a result of fibre-polymer interactions, fibre-fibre interactions, and fibre contact with the surfaces of the processing equipment. At high fibre volume fractions, there is an increase in fibre-fibre interaction and fibre-equipment contact, resulting in reductions in fibre length and fibre efficiency. A high fibre content therefore leads to a reduction in the mean fibre length, and if the mean fibre length is below the critical fibre length, the reinforcement efficiency is much reduced.

2.7 Fibre and Matrix Treatments

Natural fibre reinforced thermoplastic composites inherently have poor mechanical properties due to poor adhesion between the fibres and matrix. To improve interfacial bonding, modifications can be made to the fibres, the matrix or both the fibres and the matrix.

Matrix modifications generally involve the addition of chemical coupling agents and compatiblizers to the thermoplastic matrix, with the purpose of improving the polymer reactivity and wetting of the reinforcing fibres.

Fibre treatments may be biological, physical or chemical, and are performed to achieve one or more of the following objectives:

- Removal of undesirable fibre constituents
- Roughening of the fibre surface
- Separation of individual fibres from their fibre bundles
- Modification of the chemical nature of the fibre surface
- Reducing the hydrophilicity of the fibres

2.7.1 Biological Treatments

Biological treatments involve the use of naturally occurring microorganisms, namely bacteria and fungi. These treatments occur in aqueous environments and are relatively cheap to perform, but tend to be time consuming and water polluting. Two commonly used biological fibre treatments are retting and fungal treatment.

Retting

Retting is the controlled degradation of plant stems to free the bast fibres from their fibre bundles, as well as to separate them from the woody core and epidermis. During the retting process, bacteria (predominantly *Clostridia* species) and fungi, release enzymes to degrade pectic and hemicellulosic compounds in the middle lamella between the individual fibre cells [61]. This results in the separation of the bast fibres from the woody core, and leaves the fibres soft and clean (Figure 2.18). The retting duration is an important parameter, as under-retting can result in incomplete fibre separation, while over-retting can weaken the fibres and can lead to higher fibre mass losses during processing.

Retting may take the form of water retting where the plant stems are submerged in water, or dew retting, where plant stems are left in the field to partially degrade. Water retting requires abundant supplies of water and produces a more uniform and higher quality fibre [62], but is not generally practiced because of environmental pollution problems [22]. Dew retting, on the other hand, is a much

slower process [63] and can only be performed in regions where sufficient dew is released at night.

Generally, the retting process produces high quality fibre, but is very much dependent on weather conditions [64] and the skill and judgement of the farmer. If hemp is grown from seed, harvest does not occur until later on in the season when the weather is cool, and this can negatively affect the retting process and fibre quality.

Figure 2.18 Retted hemp stem.

Fungal Treatments

Natural cellulose fibres are prone to fungal attacks in damp and humid conditions. Fungal infestations of wood, especially by sapstain and white-rot fungi, have long caused serious wood quality problems such as decay and discolouration. These disadvantages, however, can be used in a positive manner in assisting the selective removal of plant fibre components (ie. cellulose, hemicelluloses, and lignin), and physically modifying the fibre wall for improved fibre/matrix interfacial bonding.

Sapstain fungi (*Ophiostoma*) grow in wood, and can cause severe wood discolouration due to the presence of pigmented hyphae (intertwined threads that bore into the wood). These fungi derive their nourishment from the plant cell contents, and can spread rapidly throughout a suitable growing medium. Sapstain fungi are significant because their hyphae can break into the plant fibres, and make fine holes as they pass through the cell wall. This leads to an increase in the permeability of the fibre, thus making it more susceptible to water absorption [65]. The sapstain activity has potential benefits for fibre treatment, as the holes in the cell wall created by the fungal hyphae increase the fibre surface area, and expose additional reactive hydroxyl (OH) groups for bonding with the matrix. These holes improve the surface roughness of the cell wall, which may lead to improvements in mechanical interlocking with the matrix.

White-rot fungi (*Basidiomycotina*) are responsible for some of the most destructive forms of wood degradation. They usually remove cell wall constituents (lignin, hemicelluloses and cellulose) simultaneously at approximately equal rates. However, a few varieties of white-rot fungi have the ability to degrade lignin and hemicelluloses at a faster rate than cellulose [66].

White-rot fungi form extensive hyphal networks that penetrate the wood tissues, forming large boreholes in the cell walls. As these fungi degrade the wood cell walls to derive nourishment, they quickly weaken the infected areas [65]. Wood under decay by white rot fungi maintains its fibrous nature and loses strength gradually until it is completely degraded. The wood appears stringy or lamellate in later stages of decay due to the degradation of lignin [67]. White-rot fungi may have the potential to assist with fibre treatment based on their ability to preferentially degrade lignin and hemicelluloses, they can assist with fibre separation and can also roughen the fibre surfaces to improve interfacial bonding.

2.7.2 Physical Treatments

Steam Explosion

Steam explosion is an effective and low energy method of fibre separation that could be used as an alternative to environmentally unsound fibre separation techniques such as water retting. Steam explosion requires less time and is better controlled than traditional retting procedures [19].

For the steam explosion method, semi-retted bast fibre is removed from the woody core and impregnated with a weak solution of sodium hydroxide under a vacuum. The fibres are drained prior to loading into a steam reactor, and steamed at 200^{o}C (1.5 MPa) for 90 seconds [19, 20]. The pressure is released suddenly from the steam reactor resulting in explosive decompression, and as the water in the fibres rapidly vaporises and increases in volume, the fibre bundles are blown apart and separated at the middle lamella. During the steam treatment, pectins, hemicelluloses and lignin are partially degraded and rendered soluble in the sodium hydroxide solution, which then ensures greater separation of the fibres.

Plasma Treatment

Several authors have used plasma treatment as a means of modifying the surface properties of reinforcing fibres [68-71]. A plasma is defined as a partially ionised gas composed of electrons, ions, atoms and molecules in excited and ground states. The formation of these states may be achieved by means of very high temperatures, strong electric fields, or magnetic fields. Two types of plasma can be produced by electrical discharge. The first type is known as hot or equilibrium plasma, and is characterized by high gas temperature and an approximately equal electron temperature. The second type is known as cold or non-equilibrium plasma, and is characterised by low gas temperature and high electron temperature. Cold plasma has proven to be the most suitable for organic material modification because the substrate remains at or near ambient temperature [70].

The main purpose of cold plasma treatment of composite reinforcing-fibres is to improve the fibre-matrix bond strength by modifying the chemical and physical

structure of the fibre surface layers, but without enhancing the bulk mechanical properties of the fibre. Physical modifications occur due to surface roughening of the fibre by means of the sputtering effect, which causes an enlargement of the fibre contact area and thus increases the friction between the fibre and the polymer matrix [69]. Chemical modifications depend on the type and nature of the plasma gases used, and a variety of fibre surface modifications can be achieved using this method. Cold plasma treatments of cellulose fibres commonly involve the implantation of active polar groups on the fibre surface, which reduces the fibre surface energy and promotes chemical bonding between the fibre and the polymer matrix. Additional fibre modifications that can be achieved by means of cold plasma treatment include increases in surface energies, surface cross linking and the formation of reactive free radicals [25].

2.7.3 Chemical Treatments

Fibre treatments involving the use of chemicals play an important role in improving the reinforcing capabilities of fibres. These treatments can either be classified as fibre pre-treatments, coupling agents, compatibilizers or dispersing agents. Pre-treatments involve the use of chemicals that remove undesirable and non-strength contributing fibre constituents such as lignin, pectins and hemicelluloses. Compatibilizers are chemicals that lower the surface energy of fibres to make them more non-polar and therefore more compatible with thermoplastic matrices. Dispersing agents are used to improve the dispersion of fibres in the matrix. Coupling agents are mainly responsible for improving the adhesion between reinforcing fibres and the matrix material, but can also reduce the water uptake of the fibres and assist with fibre dispersion as well. Due to this overlap in functions and to simplify matters, all bonding agents and surfactants have been grouped together as chemical treatments.

At present, over forty coupling agents have been used in the production and research of natural fibre composites [72]. The most popular treatments include the use of alkalis, anhydrides and anhydride-modified copolymers, silanes and isocyanates.

Alkali Treatments

Alkali fibre treatments using sodium hydroxide (NaOH), or combinations of sodium hydroxide and sodium sulphite (Na_2SO_3), have been used extensively in the pulping of wood fibre for paper use [31].

Some alkali treatments, especially those performed at elevated temperatures, can result in the selective degradation of lignin, pectins and hemicelluloses in the fibre wall, whilst having little effect on the cellulose components [31]. The removal of these cementing materials can result in stronger natural fibre reinforced thermoplastic composites. Miller *et al.* [48] produced wood fibre reinforced polypropylene and polyethylene composites, and found that composites containing fibres with the lowest surface lignin contents showed the largest increases in tensile properties, both on their own and with coupling agents added.

The removal of cementing materials facilitates the exposure of reactive OH groups on the fibre surface, thus enabling better bonding between the fibre and a matrix polymer or coupling agent [46]. The elementary fibres are also separated from their fibre bundles during alkali treatment, thus increasing the effective surface area for bonding with a matrix material [46, 73, 74]. Alkali treatments generally result in a rougher fibre topography, which can further improve fibre-matrix adhesion in a composite by providing additional sites for mechanical interlocking [75].

It has been reported that the removal of cementing materials from the fibre walls lead to better packing of the cellulose chains, thus increasing the crystallinity index of the fibre [76]. In addition, treatments with NaOH can lead to a decrease in the spiral angle and an increase in the molecular orientation of the cellulose chains [77]. These fibre changes may result in improvements in fibre strength, and hence stronger composite materials.

Rowell [32] has also reported that lignin is susceptible to photochemical degradation when exposed to ultraviolet light, further supporting the need for its

removal from fibres intended for use in composite materials that are to be exposed to sunlight.

Pectins, hemicelluloses and lignin are the main constituents in hemp fibre that are targeted for removal during alkali treatments. Pectins and hemicelluloses are easily removed by these methods, but lignin in hemp bast fibre can be difficult to remove [78]. It has been reported that lignin consists of strong carbon-carbon linkages and aromatic groups that are highly resistant to chemical attack, thus limiting the degradation and fragmentation of lignin [78].

The use of NaOH to treat natural fibres for use in composites is widely reported [46, 74, 77, 79-82]. NaOH plays the critical role of removing lignin by means of alkaline cleavage of ether linkages in the lignin, which may be accompanied by condensation reactions [78]. Pectins can be completely attacked and removed without any residue being left in the hemp fibre after NaOH treatment, but the rate of lignin removal is dependant on the NaOH concentration [78].

It has been reported by Wang *et al* [78] that a combination of NaOH and sodium sulphite (Na_2SO_3) can be used to remove lignin effectively from hemp fibre. The addition of a sufficient amount of Na_2SO_3 was shown to assist NaOH in the removal lignin, and was also shown to shorten the treatment time required to remove the lignin. These effects are facilitated by the presence of sulphite groups (SO_3^{2-}) in the Na_2SO_3 which are introduced into the lignin side chains by means of sulphonation, and enable the lignin to be quickly dissolved into the alkaline solution [78].

It is not always possible to remove all the lignin from the fibre by means of alkali treatment. The lignin in the middle lamella may be easily accessed and degraded, but access to lignin in the fibre secondary layers may be restricted due to coverage by the primary layer as well as the swelling of cellulose.

MAPP Treatments

Maleic anhydride (MA) grafted polypropylene (MAPP) is a coupling agent that also acts as a compatibilizer. It consists of long polymer chains with a MA functional group grafted onto one end. MAPP acts as a bridge between the non-polar polypropylene matrix and the polar fibres by chemically bonding with the cellulose fibres through the MA groups, and bonding to the matrix by means of polymer chain entanglement.

The MA functional group interacts strongly with the fibre surface through covalent and hydrogen bonding with the reactive OH groups on the surface of the cellulose and lignin (Figure 2.19). The polymer chains of MAPP then combine with the unreactive polypropylene matrix by means of chain entanglement. These entanglements function as physical cross-links that provide some mechanical integrity up to and above the glass transition temperature of the matrix [3]. The MAPP polymer chain length is an important factor regarding the level of chain entanglement that can be achieved by the coupling agent. When the MAPP polymer chains are very short, there is little chance of entanglement between coupling agent and matrix chains as they can easily slide past one another (Figure 2.20). When the MAPP polymer chains are longer, entanglement can then occur, but the viscosity of the coupling agent also becomes high resulting in poor fibre wetting. If the MAPP chains are extremely long, they may then entangle with the polypropylene molecules so that the MA groups on the MAPP have difficulty migrating to the OH groups on the fibre surface. An optimum chain length or a critical molecular weight is therefore necessary to develop sufficient entanglement with the matrix polymer.

Improvements in the mechanical properties of natural fibre reinforced thermoplastic composites as a result of the inclusion of MAPP have been shown by several researchers, including Sanadi *et al*. [83] and Pickering and Ji [84].

Sanadi *et al.* [83] used MAPP (Eastman Chemical Epolene G-3002) with kenaf fibre reinforced polypropylene composites. The resulting composites with 50wt% kenaf fibre and 3% MAPP displayed a tensile strength increase of 88% and a

Young's modulus increase of 350%. Pickering and Ji [84] used MAPP (Aldrich A-C 950P) to couple radiata pine fibres with polypropylene, and achieved increases in tensile strength and Young's modulus of 123% and 177% respectively with fibre weight fraction of 50% and a MAPP weight fraction of 2%.

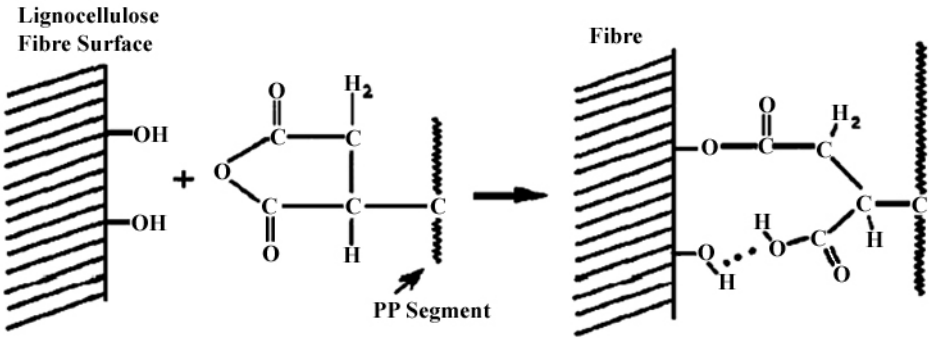

Figure 2.19 Reaction mechanisms of MAPP with the surface of a lignocellulosic fibre. Note the potential for both covalent and hydrogen bonding [3].

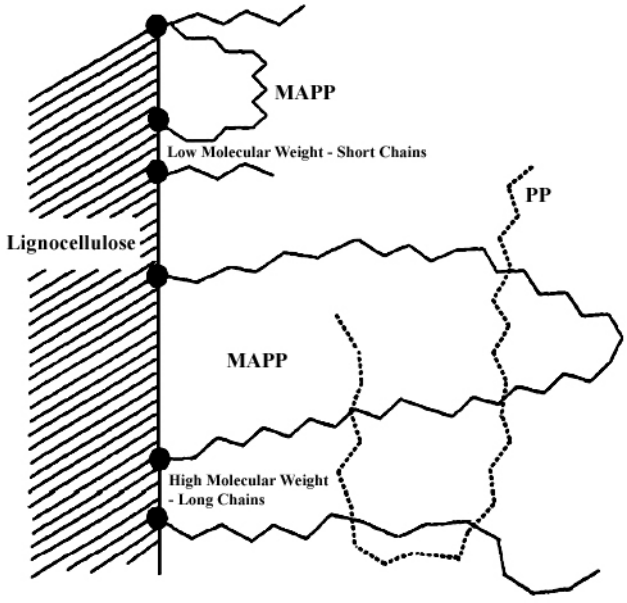

Figure 2.20 Schematic of possible PP molecular entanglements with the longer chains of MAPP. Shorter chains of MAPP have less opportunity to entangle with the PP molecules [3].

Acetic Anhydride Treatment

Fibre treatment with acetic anhydride (acetylation) is an effective method of reducing the hydrophilic characteristics of cellulose fibres [85], as well as improving fibre dispersion within a thermoplastic composite. Acetic anhydride is a compatibilizer that lowers the surface energy of the fibre to make it non-polar and more similar to the thermoplastic matrix [72]. This is achieved by the formation of stable acetate bonds with the reactive OH groups on the fibre surface. Once the acetic anhydride has bonded with the OH groups of the fibre, they are no longer reactive and are therefore no longer free to bond with other OH groups, water or other chemicals. Chemical modification of cellulose fibres with acetic anhydride is a good method of providing dimensional stability and decay resistance [86].

Baillie and Zafeiropoulos [14] treated dew-retted and green flax fibres with acetic anhydride. It was reported that acetylation slightly improved the interfacial bonding of dew retted flax fibre reinforced isostatic polypropylene composites, and caused a greater improvement for similar composites reinforced with green flax. An interfacial shear strength increase of 2.3% was observed for the acetylated dew-retted flax composites, and an interfacial shear strength increase of 83% was observed for the acetylated green flax composites.

Silane Treatments

Organic-inorganic silane coupling agents have been used for over 50 years to couple glass fibres with polymeric matrices. They have, however, been used recently to couple cellulose fibres to thermoplastic matrices such as polystyrene, polypropylene [87] and polyethylene [88]. Silane-based coupling agents are hydrophilic compounds based on a silicon molecule with different organic groups attached. One group interacts with the hydrophilic cellulose fibre, while another group reacts with the hydrophobic thermoplastic matrix material [89]. The reaction between cellulosic materials and silanes is highly complex. It is known that silane coupling agents react with cellulose water (or additional water) to form silanol (Si-OH) groups. After hydrolysis, the coupling agent can develop either

covalent or hydrogen bonds with the free OH groups on the fibre surface, but the degree of conversion of such OH groups is not well known [87].

Valadez-Gonzalez *et al*. [88] showed that the partial removal of lignin and other alkali soluble compounds from the fibre surface greatly increased the adsorption of the silane coupling agent onto the fibre wall.

Bataille *et al*. [90] produced a highly bleached hardwood pulp-fibre reinforced polypropylene composite using the silane coupling agent γ-metacryloxy-propyltrimethoxysilane (A-174). By including the silane coupling agent and processing the composite at 140^{o}C, they achieved a composite tensile strength increase of 50%.

Isocyanate Treatments

Polymeric isocyanates have been used as coupling agents to improve the interfacial bonding in natural fibre reinforced thermoplastic composites. Isocyanates contain a reactive isocyanate group (-N=C=O), which is able to react with the OH groups of cellulose. As a result, the hydrophilic nature of wood is reduced [45]. A number of isocyanates are available, but the most reactive isocyanate that can be used with cellulose fibres and a PVC (thermoplastic) matrix is Polymethylenepolyphenyl isocyanate (PMPPIC) [72]. Raj *et al*. [91] also showed that PMPPIC was the most reactive isocyanate when coupling chemi-thermomechanical pulp with polyethylene. The tensile strength and Young's modulus improvements of the chemi-thermomechanical pulp reinforced polyethylene composite containing a PMPPIC coupling agent were 60% and 90% respectively.

2.8 Processing of Fibre Reinforced Thermoplastic Composites

The processing methods used to fabricate natural fibre reinforced thermoplastic composites are generally the same as those used to produce similar composites containing synthetic fibres. The most commonly used techniques for mixing fibres with a thermoplastic polymer are melt mixing and extrusion. Injection moulding and compression moulding are the two most commonly used composite forming techniques, although extrusion is used in some instances. No serious attempts have yet been made to develop large-scale fabrication techniques for natural fibre reinforced thermoplastic composites with aligned fibre orientations.

2.8.1 Melt Mixing

Melt mixing using a radial flow (turbulent) mixer is a commonly used method in the scientific literature for compounding short reinforcing fibres with thermoplastic polymers. The thermoplastic polymer is initially heated to its melting temperature, and then reinforcing fibres are added to the mix [92]. After mixing has taken place, the composite mix can be rolled or formed into the desired shape. Various mixer settings, such as the mixing duration, rotor speed and melt-chamber temperature, can affect the composite properties. Joseph et al. [93] combined sisal fibres with polypropylene using a Haake Rheocord mixer. They showed that ineffective mixing and poor fibre dispersion occurred at short mixing times (<10 min) and low mixing speeds (<50 rpm), while low mixing temperatures (<170^{o}C) resulted in extensive fibre breakages. Composite strength losses due to fibre breakage also occurred at high mixing times (>10 min) and high mixing speeds (>50 rpm), with high mixing temperatures resulting in fibre degradation and poor fibre dispersion.

Melt mixing generally results in very good mixing of the fibres with the thermoplastic polymer, but is a non-continuous process that only allows the processing of a limited amount of material at any given time, and requires

stoppages to remove the material from the mixer. Melt mixing can only be used as a means of mixing the material, and further processing is required to fashion the material into its desired shape and form.

2.8.2 Extrusion Compounding

Extrusion is one of the most effective methods of compounding natural fibres and thermoplastic polymers. A thermoplastic polymer (which is usually obtained in pellet or powder form) and short reinforcing fibres are combined and drawn into a heated extrusion barrel by means of a single screw or two co-rotating screws, depending on the type of extruder (Figure 2.21). The polymer is melted and mixed with the fibres to form a composite melt, which is then drawn forward through the extruder barrel and further mixed and compressed to improve the melt homogeneity. The extruder melt then exits the barrel through a shaped die, which determines the shape of the extruded composite [92].

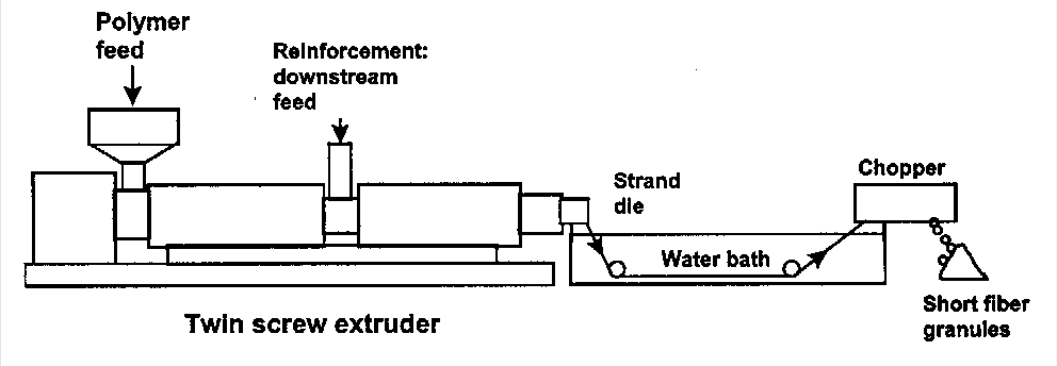

Figure 2.21 The extrusion compounding process for the manufacture of short fibre reinforced thermoplastic injection moulding granules [94].

Extrusion of short fibre reinforced thermoplastic composites using a twin-screw extruder is often carried out prior to injection moulding because of the excellent fibre distribution that can be achieved within the polymer matrix [95, 96]. The extruded composite can then be chopped into pellets that can easily be injection moulded into more complex shapes.

To produce composites with optimum mechanical properties and fibre distribution, it is necessary to optimise the extruder processing variables, such as

barrel length, temperature profile, screw configuration and screw speed. Incorrect extruder set-up can result in poor dispersion and wetting of the fibres with the polymer matrix, as well as severe fibre damage and length reductions.

Most fibre damage is caused by inter-fibre friction, friction between fibres and polymer, and friction between fibres and the extruder. One method of minimising fibre breakage is to feed the polymer into the main in-feed port and to feed the fibres into a second port further down the barrel, as can be seen in Figure 2.21 [97]. This enables the polymer to melt before coming into contact with the fibres, thus reducing the shear forces acting on the fibres. A second method of preserving the fibre integrity during compounding is to keep the compounding distance as short as possible, and also to minimise the number of kneading elements on the extruder screws [98].

Another variable that can affect the composite strength is processing temperature. If the temperature is too low, the polymer matrix will be too viscous to flow around the fibres, resulting in poor fibre wetting and hence a weaker composite. If the temperature is too high, degradation of the fibres and polymer will occur, also resulting in composite strength reductions.

Unlike melt mixing, extrusion is a continuous process that can accommodate high feed rates and allows the fast and efficient processing of materials. A shaped die can also be used to create a finished product with a desired profile.

2.8.3 Injection Moulding

Injection moulding is one of the most widely used processes for manufacturing moulded parts from thermoplastic and reinforced thermoplastic materials. It is one of the few manufacturing processes capable of producing net shape composite parts in high volumes and at high production rates [51].

Short fibre reinforced composites can be processed into complex shaped components using standard thermoplastic injection moulding equipment. Composite materials for use in injection moulding applications must be capable of

fluid-like flow during processing, and thus usually consist of short fibres with a relatively low fibre fraction (typically <50wt% or 30vol%). The composite fibre content needs to be carefully considered, as a low fibre content can result insufficient reinforcement, and a high fibre content can lead to poor moulding and reduced mechanical properties of the composite [51].

The injection moulder performs the function of melting the pre-formed (usually by extrusion) composite pellets in a heated barrel, delivering a homogeneous melt to the machine nozzle, and injecting the melt into a closed mould. The mould unit, which comprises of a fixed section and a movable section, encloses the shaped cavity into which the composite is injected and cooled, and is thus responsible for determining the final shape of the moulded part [99] (Figure 2.22).

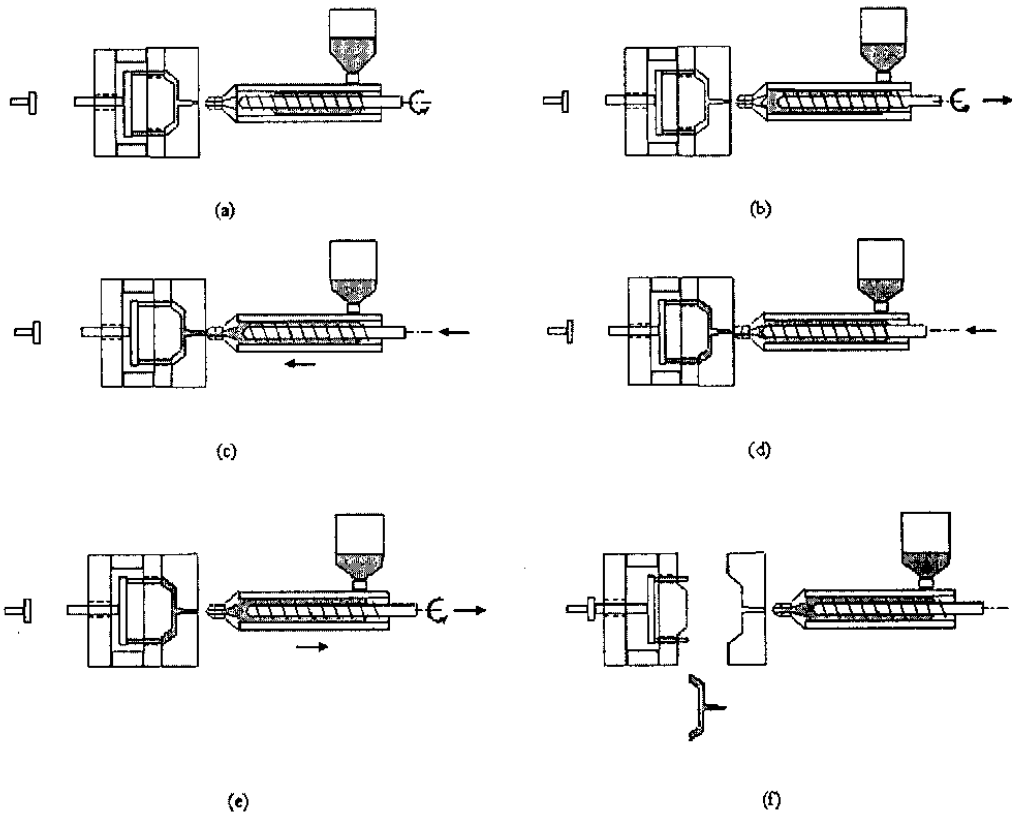

Figure 2.22 Basic operations of the injection moulding cycle: (a) start up; (b) screw back 1; (c) injection; (d) hold-on; (e) screw back 2; (f) cooling and ejection [51].

The injection moulding process does not induce the same level of mechanical friction on the composite melt as do other fabrication processes such as extrusion

and melt mixing, and it has been found that injection moulding does not lead to significant reinforcing fibre damage. Keller [98] compared the fibre length distribution of an extruded hemp fibre reinforced thermoplastic composite with the same composite that had been extruded and injection moulded. The results showed that average hemp fibre length after extrusion was 0.53mm (reduced from 8mm average length), and that there was no significant reduction in fibre length with the addition of the injection moulding process.

2.8.4 Compression Moulding

Compression moulding (hot pressing) is a commonly used processing technique for producing large, relatively simple composite parts with good mechanical properties. The compression moulding of glass mat reinforced thermoplastics is widely used in the production of complex semi-structural components, notably for the automotive industry [100]. Compression moulding basically involves the hot pressing of randomly orientated or aligned fibre mats, either chopped or in continuous form, with a thermoplastic material.

The compression moulding operation begins with the placement of a stack of alternating fibre-mat and thermoplastic sheets onto the bottom half of a preheated mould cavity [92]. The top half of the mould is lowered at a constant rate until the desired processing pressure is reached, thus causing melting of the polymeric matrix and consolidation of the composite. Once the composite has been pressed, it is cooled and removed from the mould.

2.8.5 Solution Mixing

Solution mixing is a suitable alternative to processing methods where the polymer is melted during compounding with the fibre, such as melt mixing, extrusion and injection moulding. This technique involves dissolving the polymer in a suitable solvent, adding the fibre to the polymer/solvent blend, precipitating the polymer from the solvent and then removing the solvent from the composite. The polymer precipitates are weakly bound to the fibres, and final consolidation of the fibre and polymer can be achieved by extrusion or compression moulding. Solution mixing

has an advantage over other fabrication methods in that it employs modest temperatures and shear stresses since the polymer and fibres are mixed in a low viscosity solution.

Solvents do not produce permanent chemical changes to thermoplastic polymer matrices, but instead produce physical changes that involve the separation of individual polymeric chains. Poulakis et al [101] showed that the mechanical properties of polypropylene were not affected by dissolution in xylene followed by precipitation. Solvents are also known to have little influence on the structure and integrity of cellulose fibres [99].

It is known that polymers have varying levels of solubility depending on which solvent is used. A solubility parameter δ can be defined for both the solvent and polymer (Table 2.7), and is a measure of the strength of the intermolecular cohesion in the pure solvent or in the pure polymer.

Table 2.7 Solubility parameters (δ) of polymers and solvents [99, 102].

Polymers	δ ($cal^{1/2}\ cm^{-3/2}$)	Solvents	δ ($cal^{1/2}\ cm^{-3/2}$)
PTFE	6.2	n-Pentane	6.3
Poly(dimethyl siloxane)	7.3	n-Hexane	7.3
PE	8.0	n-Octane	7.6
PP	7.9	Diisopropylketone	8.0
PIB	8	Cyclohexane	8.2
SBR	8.1-8.6	Carbon tetrachloride	8.6
Natural Rubber	8.1	Xylene	8.9
BR	8.5	Toluene	8.9
Polysulphide rubber	9.0-9.4	Ethyl acetate	9.1
PS	8.5-9.7	Dioxane	9.9
CR	9.2	Acetone	10.0
PVAC	9.4	Pyridine	10.9
PMMA	9.2	Ethanol	12.7
PVC	9.6	Methanol	14.5
PVDC	9.8	Glycerol	16.5
PETP	10.7	Water	23.4
Cellulose acetate	11.4		
EP	11.0		
POM	11.1		
Nylon 66	13.6		
PAN	15.4		

For a solvent, δ is calculated from the energy of vaporisation, and for a polymer, δ is estimated according to the primary structure of the polymer chain [99]. Polymers are able to dissolve in solvents with similar δ, as long as no strong polymer-solvent interactions occur. Thus, polypropylene (δ=7.9) can easily be dissolved in di*i*sopropylketone (δ=8.0), cyclohexane (δ=8.2), carbon tetrachloride (δ=8.6), xylene (δ=8.85) and toluene (δ=8.91).

2.8.6 Solution Mixing of Oriented Fibre Composites

The mechanical properties of composites depend on many factors such as fibre-matrix adhesion, volume fraction of the fibre, fibre aspect ratio (L/D) and fibre orientation. The fibre critical length/aspect ratio should be maintained above a critical value to ensure maximum stress transfer from the matrix to the fibre, and fibres should be oriented parallel to the direction of expected applied loading for optimum efficiency.

The fibre volume fraction obtainable for composites produced by melt mixing, injection moulding and extrusion is limited, as high fibre loadings can result in increases in composite viscosity to levels where processing becomes impossible. It is also known that these processing methods can influence the mechanical properties of a composite as a result of fibre breakage and polymer matrix degradation, due to the high frictional and shear forces involved [103]. The large forces experienced can therefore reduce fibre lengths to such an extent that their reinforcing capacities are diminished. Extrusion and injection moulding cannot be used to produce long fibre-reinforced composites due to fibre bending and curling during processing. Fibre bending causes a reduction in the effective length of a fibre below the critical fibre length in a particular direction, thus resulting in a decrease in the mechanical properties of the composite [73]. Fabrication techniques such as injection moulding also tend to produce composites with random or planar-random fibre alignments due to complex fluid dynamics and interactions between the molten material and the processing equipment.

The solution mixing method has the advantage of causing no significant fibre or polymer degradation, but is limited to producing randomly oriented fibre composites. Most researchers who have used solution mixing as a method of combining fibres and matrix have produced consolidated composites from the solution mixed material by means of extrusion [73, 93, 104], melt mixing [105] or grinding of the composite followed by compression moulding [106]. These additional processes result in significant fibre length reductions, and annul the benefits offered by the solution mixing method.

A new fabrication technique was therefore developed to produce composites with long axially oriented fibres and high fibre contents. The new technique is based on the solution mixing method, but instead of producing a slurry consisting of short, randomly oriented fibres, an aligned long-fibre composite is produced instead. The new method can also be used to graft a MAPP coupling agent onto the fibre surface to enhance the fibre-matrix adhesion.

2.9 Composite Interfacial Shear Strength

To better understand the mechanical performance of a fibre-reinforced composite, it is necessary to investigate the fibre and matrix properties, as well as the stress transfer that takes place at the interface between the fibre and matrix. Since the interface plays a major role in transferring the stress from the matrix to the fibre, it is important to be able to characterise the level of interfacial adhesion to properly understand the performance of the composite. Interfacial adhesion is usually characterised by the interfacial shear strength (IFSS), which can be determined by a number of micro mechanical tests such as the single fibre fragmentation test, the single fibre pull-out test, the micro-debond test and the single fibre compression test [107].

2.9.1 The Single Fibre Fragmentation Test

The single fibre fragmentation test (SFFT) is a widely used method for evaluating the *in situ* fibre-matrix adhesion and interfacial shear strength of fibres reinforcing a tough, transparent matrix with a high failure strain (greater than 3x the fibre failure strain). This test involves the application of increasing axial stress to a specimen containing a single fibre embedded in a polymer matrix. Load is transferred through the matrix into the fibre by means of shear stress at the interface, and stress transfer increases linearly from the tips of the fibre inwards to some maximum value. Fibre failure occurs when this transferred stress reached the tensile strength of the fibre. The fibre will continue to fracture into shorter lengths as the load increases, until the fibre fragments are so small that the tensile stresses induced in the fibre can no longer reach the fibre tensile strength. At this point a state of saturation is reached, and the final fragment length is referred to as the critical fibre length (L_c). Fibres exceeding L_c will break into two parts, yielding a random distribution of fragment lengths between $L_c/2$ and L_c, whereas fibres below L_c will be pulled out of the matrix before fibre failure [108]. The process of fibre fragmentation under increasing load is illustrated in Figure 2.23.

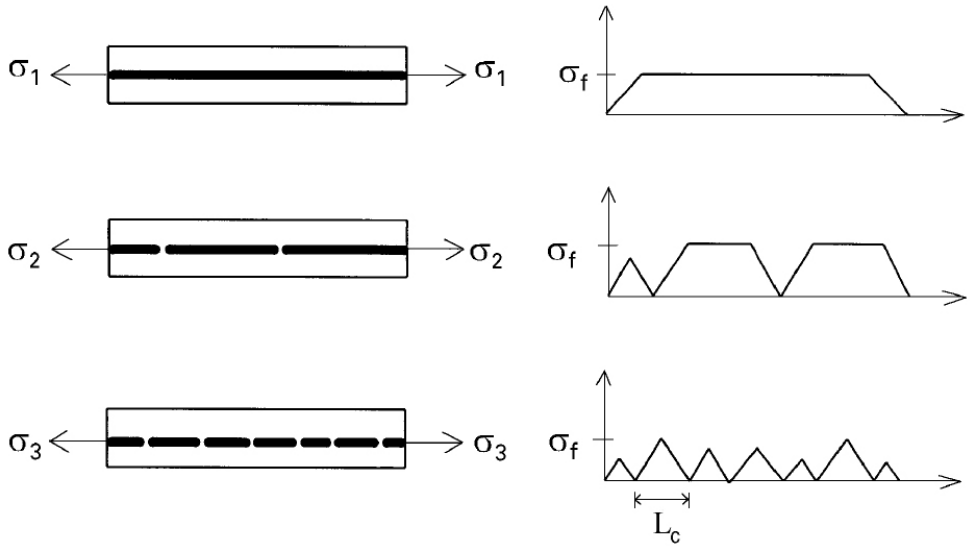

Figure 2.23 Schematic of the single fibre fragmentation test.

It is commonly accepted that L_c is a good indicator of the ability of the interface to transmit loads between the fibre and matrix, and a decrease in the interfacial adhesion leads to an increase in L_c [109]. The critical aspect ratio (L_c/D) can be calculated from SFFT results (assuming a random distribution of fragments between $L_c/2$ and L_c) using the following equation [108]:

$$\frac{L_c}{D} = \frac{4}{3}\left(\frac{L_{ave}}{D}\right) \qquad (2.2)$$

where D is the average fibre diameter and L_{ave} is the mean fragment length.

Once the critical aspect ratio has been determined, the interfacial shear strength (τ) can be calculated on the basis of the constant shear model proposed by Kelly and Tyson in 1965 [110]:

$$\tau = \frac{\sigma_{fc}}{2}\left(\frac{D}{L_c}\right) \qquad (2.3)$$

where σ_{fc} is the fibre tensile strength at L_c.

Drzal *et al.* [109] recognised that the distribution of fibre fragments fitted a two-parameter Weibull distribution, and rearranged the Kelly and Tyson equation in order to calculate the interfacial shear strength:

$$\tau = \frac{\sigma_{fc}}{2\beta}\Gamma\left(1 - \frac{1}{\alpha}\right) \qquad (2.4)$$

where α and β are the shape and scale parameters of the Weibull distribution, respectively, and Γ is the gamma function.

The shape and scale parameters of the Weibull distribution are commonly estimated by means of the linear regression method (graphical method), or the maximum likelihood method. It has been reported by Zafeiropoulos *et al.* [111] that both methods deliver similar estimations for these parameters.

It should be noted that the fragmentation test is used to estimate the cumulative effect of several different components which act together to form the interfacial

shear strength, i.e. the bond strength, the frictional contribution and the matrix yield strength [109].

2.9.2 The Single Fibre Pullout Test

The single fibre pullout test (SFPT) consists of a single fibre embedded in a matrix block (Figure 2.24). A steadily increasing axial force is applied to the free end of the fibre in order to pull it out of the matrix. As the fibre is pulled, the load and displacement are monitored until the fibre either pulls out of the matrix or is fractured.

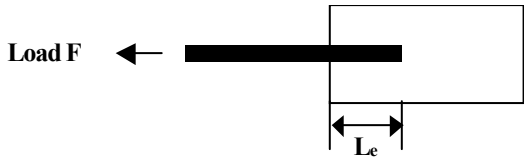

Figure 2.24 Schematic of the single fibre pullout test.

A typical force-displacement curve can be seen in Figure 2.25. The curve consists of three parts corresponding to the three stages of the pullout test [112]. At the first stage ($0<F<F_d$), where F is the applied force and F_d is the critical force at which debonding occurs, the fibre-matrix interface remains intact, and this part of the curve is considered to be mostly linear for a fibre-matrix system whose components are linearly elastic. When the external load reaches F_d, the fibre begins to debond from the matrix through interfacial crack propagation. During the second stage ($F_d<F<F_{max}$), where F_{max} is the peak force, debonding by means of crack propagation increases across the embedded fibre length. The applied force continues to increase due to the remaining adhesion of the intact part of the interface, and the presence of frictional forces between the fibre and matrix. After a peak load is reached, the crack propagation becomes unstable and the whole embedded fibre length becomes fully debonded. The third stage occurs after complete debonding has taken place, where the remaining force is due to frictional interactions between the fibre and the matrix (F_f).

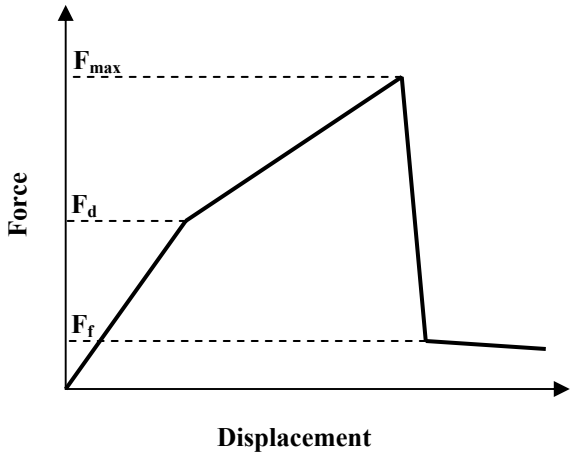

Figure 2.25 A typical force-displacement curve obtained from a single fibre pullout test.

The apparent interfacial shear strength (τ) can be calculated using the following equation [113]:

$$\tau = \frac{F_{max}}{\pi D L_e} \qquad (2.5)$$

where F_{max} is the peak force, D is the fibre diameter, and L_e is the embedded fibre length. It is assumed that the shear stress is uniformly distributed across the embedded length.

2.9.3 The Micro-Debond Test

The micro-debond test, also known as the microbond test, is a suitable test for determining the IFSS of composites with brittle matrices which fail due to the formation of multiple transverse cracks (with reinforcing fibres bridging the cracks) [114].

The micro-debond test is considered to be a modification of the SFPT as it consists of a single fibre embedded in the matrix [115], and only differs from the SFPT by having different boundary conditions (which can often be neglected) [114]. The experiment involves the deposition of a small amount of resin onto the fibre surface in the form of an ellipsoid-shaped droplet that forms concentrically around the fibre. The fibre is then pulled while the droplet is constrained by two blades or a micro-vice (Figure 2.26). In the case of the micro-debond test, it is

assumed that the interfacial shear strength is uniformly distributed along the embedded length of the fibre. When the shearing force reaches a critical value, pullout occurs and the droplet is displaced along the axis of the fibre. As with the SFPT, a force/displacement curve can be gained for each fibre tested, and the average shear stress can be calculated by dividing the maximum measured force of debonding by the embedded fibre length area.

The reliability of the test is very much dependant on the shape of the matrix droplet, and symmetric, round droplets are easier to test and analyse than droplets with flat surfaces. If the length of a droplet exceeds a critical value, the fibre will fracture prior to debonding and pullout.

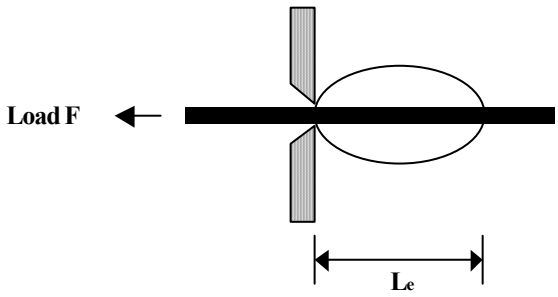

Figure 2.26 Schematic of the micro-debond test.

2.9.4 The Single Fibre Compression Test

The single fibre compression test, also known as the micro compression or micro indentation test, is a technique that enables the *in situ* interfacial bond testing of an actual unidirectional composite with a high volume fraction of fibres. The technique allows the evaluation of the processing or environmental exposure encountered by the composite either during manufacturing or in service. Moisture, solvent absorption, fatigue and thermal exposure can be properly evaluated for their effects on the fiber-matrix interface and composite properties [116].

The test requires a composite test coupon that has been cut perpendicular to the fibre axis to expose the two ends of the reinforcing fibres. The specimen is mounted in a device that allows a spherical or cylindrical indenter to be placed over a selected fibre end, and the fibre is compressively loaded to produce debonding and/or fibre slippage, as can be seen in Figure 2.27.

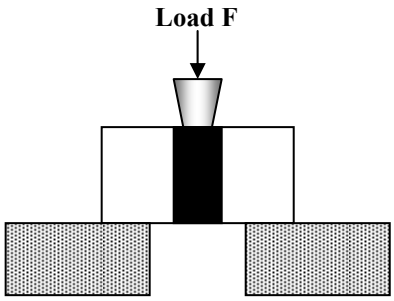

Figure 2.27 Schematic of single fibre compression test.

The load vs. displacement curve gained from the test is monitored until the fibre is completely debonded from the matrix. The interfacial shear strength (τ) can then be calculated using the following two equations which are based on the shear lag theory [117, 118]:

$$\tau = \left(\frac{n \mathrm{P_d}}{2\pi r} \right) \tag{2.6}$$

where:

$$n = \sqrt{\frac{2k}{r\mathrm{E}}} \tag{2.7}$$

P_d is the mean debonding load, k is a global stiffness constant including the elastic properties of the fibre and the matrix together with the local fibre environment, r is the fibre radius, and E is the fibre axial Young's modulus.

An alternative finite element method of determining the IFSS at debonding (τ) has been reported by Ho *et al.* [116]:

$$\tau = \sigma_{\mathrm{adj}} \left(\frac{\tau_{\max}}{\sigma_{\mathrm{app}}} \right)_{\mathrm{fem}} \tag{2.8}$$

where σ_{adj} is the adjusted compressive stress applied to the fiber end at debonding, and $(\tau_{max}/\sigma_{app})_{fem}$ is the ratio of the maximum interface shear stress to the applied stress resulting from a linear axis-symmetric finite element analysis.

2.9.5 Advantages and Limitations of IFSS Test Methods

The determination of IFSS is still a highly controversial topic that has been the subject of much debate over the past 30 years. It has been reported that measurements of interfacial properties by direct methods rely on risky assumptions which can lead to serious inaccuracies [119]. Problems may occur because the results are strongly influenced by unknown parameters such as pressure across the interface, variations in the coefficient of friction at the interface, and the possibility of mixed modes of failure during fibre fracture. Furthermore, the various test methods available can yield very different results [109]. However, IFSS testing still has an important part to play in composite evaluation, and since no exact method of IFSS determination exists, the most suitable test for a fibre matrix system needs to be determined and the advantages and limitations of the test method need to be carefully considered.

The most commonly used methods for determining IFSS are the single fibre fragmentation test (SFFT) and the single fibre pullout test (SFPT).

The SFFT is a convenient and reproducible test method where the fibre-matrix interface is subjected to pure shear [120]. The popularity of this test results from the fact that it yields much information for statistical sampling, data can be collected over a large area of interface, and the process itself somewhat replicates the *in situ* events that take place within an actual composite. The SFFT is very complex, and several micromechanical phenomena observed in real-life composites other than fibre fracture are observed during the test, namely shear yielding of the matrix, interfacial debonding and transverse matrix cracking [120].

In the SFFT, the load is applied directly to the matrix, and is then transferred to the fibre through the interface. During stressing of the composite, the tensile

forces result in cross sectional area reductions for both the fibre and matrix due to the Poisson's effect [109]. If the Poisson's ratio of the matrix is greater than that of the fibre, the matrix will induce radial compressive stresses on the fibre, and the frictional component of the interfacial adhesion will be increased depending on the net cross-sectional reduction between the fibre and matrix [121]. Furthermore, chemical and thermal shrinkage arising in specimens during cure and cool-down may also result in residual stresses that can greatly affect the fibre-matrix adhesion. Residual stresses may not always be evenly distributed in the composite, and it can be said that the IFSS obtained by means of SFFT is calculated by using an oversimplified representation of a uniform shear stress at the fibre-matrix interface.

To determine the IFSS from the SFFT, accurate fibre strength and fibre diameter measurements are required. Fibre strength is a function of the gauge length and is controlled by the flaw size distribution present within the fibre. Since it is not always possible to measure the fibre tensile strength at L_c by experimental methods, it is necessary to statistically extrapolate the fibre strength from fibres measured at larger gauge lengths. A review of the existing theories to calculate the Weibull statistics by which such scaling can be carried out from the experimental data is given by Asloun *et al* [122]. However, the extrapolation of fibre strength to the critical fibre length still remains highly controversial [120]. In addition, the fibre strength distribution may change upon processing, and so the Weibull parameters determined *ex situ* may be irrelevant for describing *in situ* fibre performance.

Since fibre fragmentation saturation is required for the SFFT, test specimens need to be strained to at least three times the fibre failure strain. This means that the SFFT cannot be used for composites consisting of matrices with low failure strains. The matrix should also have sufficient toughness to avoid fibre fracture-induced strain, and should be transparent to enable the fibre fragments to be observed.

There are concerns that the SFFT results may not correlate to the mechanical performances of high fibre-volume fraction composites [120]. Fibres within high

fibre content composites are subjected to stresses caused by adjacent fibres, which ultimately result in composite stress profiles that are different to composites containing less fibre. Due to the absence of a direct correlation between the interfacial properties measured by means of the SFFT and the macro-properties obtained from the testing of high fibre volume fraction composites, it is unlikely that the interface can be fully characterised by a single parameter such as IFSS [120]. It has, however, been reported by Valadez-Gonzalez *et al.* [121] that the results obtained from the SFFT show better agreement with composite mechanical properties than results obtained from the SFPT, especially for natural fibre reinforced polypropylene composites.

Single fibre pullout tests have the advantage that the debonding force can be plotted as a function of embedded length, and information can be gained about the failure process, e.g. a sudden drop in applied load indicates a brittle failure. As with the fragmentation test, the debonding is accompanied by an unknown coefficient of friction and pressure across the interface.

In the case of the SFPT and the micro-debond test, the fibre is subjected to an axial force resulting in a Poisson contraction in the radial direction, leading to a reduction in the fibre cross sectional area. This phenomenon may reduce the normal radial stresses induced on the fibre as a result of matrix shrinkage due the curing or cooling of the polymer. As a result, a decrease in the frictional component of the interfacial strength is observed, which may facilitate the initiation and propagation of interfacial failure.

Another problem associated with the SFPT is that a very large stress concentration is present at the fibre entry point, and another at the fibre end inside the polymer. For short embedded lengths, the IFSS at the entry point can be significantly lower than the IFSS at the end point [119]. The embedded length for small diameter fibres (ranging from 5 to 50μm) is also limited to a range of 0.05-1.0mm, as longer embedded fibre lengths result in fibre fracture.

The single fibre compression test has an advantage over other IFSS test methods in that real composites are tested, and the test is quick and easy to perform.

However, due to the compressive nature of the test, the interfacial pressure is increased due to Poisson expansions of the fibre resulting in an over estimation of the interfacial shear strength [119]. Many different types of damage other than interfacial debonding may also occur depending on the properties of the fibre and the matrix and the level of adhesion, such as cohesive failure of the matrix, matrix cracking and fibre breaking [123]. The single fibre compression test cannot be used with soft natural fibres and Kevlar™ due to the possibility of fibre crushing.

The single fibre fragmentation test (SFFT) was selected as the most suitable method for evaluating the interfacial shear strength (IFSS) of hemp fibre reinforced polypropylene composites. The SFFT provides a relatively accurate measurement of the IFSS as the fibre-matrix interface is subjected to pure shear, and the test provides a large amount of data for statistical sampling. The polypropylene/MAPP matrix has a failure strain greater than 3x the fibre failure strain thus ensuring full fibre fragmentation, and the matrix has a sufficient level of transparency to allow the fibre fragments to be observed and measured.

2.10 Composite Strength Predictions

Prediction of the load carrying capability of a structure is one of the most important tasks in structural design. In the last four decades, this need has prompted numerous researchers to develop a range of mathematical models to predict the strength of composites and their laminates. Despite the progress that has been made, it does not appear that there are any universally accepted models that account for the strength of composites, even under simple loading conditions. Although none of the strength prediction models have been rigorously verified experimentally, many have been formally introduced into textbooks on composite materials [124]. Despite the limitations associated with composite modelling, some models have been shown to predict composite strength with some degree of accuracy [73, 125, 126].

Fibre reinforced composites are classified into two groups from a viewpoint of fibre length, that is, continuous fibre composites and discontinuous fibre composites. Most of the early strength prediction models are based on the assumption that reinforcing fibres are continuous and are aligned axially to the applied load. However, aligned continuous fibre composites are difficult to produce, and existing fabrication methods for such composites are time consuming and labour intensive. Discontinuous fibres are commonly used in many composites as a result of the increasing use of fast and efficient moulding techniques adopted from the plastics manufacturing industry. The strength prediction of discontinuous fibre composites is far more complex than that of composites reinforced with continuous fibres, and further difficulties are experienced in modelling composites with off-axis fibre alignments.

Most strength prediction models are based on the assumption of a two-dimensional plane-stress field in the composite, and some of the most commonly used models are summarised below.

2.10.1 Rule of Mixtures Model (Parallel Model)

Kelly and Tyson [110] first proposed the rule of mixtures model to predict the strength (σ_c) of unidirectional, continuous fibre composites:

$$\sigma_c = V_f\sigma_f + V_m\sigma_m \qquad (2.9)$$

where:

$$V_m = 1 - V_f \qquad (2.10)$$

such that V_f and V_m are the volume fractions of the fibre and matrix, respectively; σ_f is the mean fibre tensile strength of the fibre and σ_m is the matrix stress when the fibres reach their ultimate tensile stress in the composite. In the case of the Parallel model, it is assumed that iso-strain conditions exist for both matrix and

fibre. A schematic representation of the parallel model can be seen in Figure 2.28.

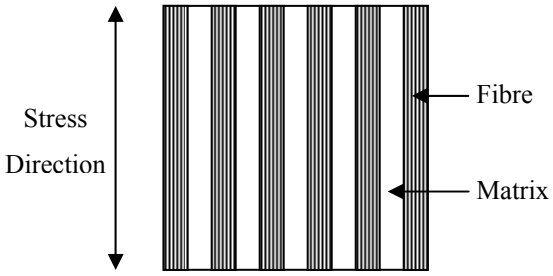

Figure 2.28 Schematic representation of the Parallel Model.

2.10.2 Inverse Rule of Mixtures Model (Series Model)

An inverse variation of the Kelly-Tyson model can be used to predict the strength (σ_c) of unidirectional, continuous fibre composites that are loaded in a perpendicular direction to the fibre alignment [125, 126]:

$$\sigma_c = \frac{\sigma_f \sigma_m}{\sigma_m V_f + \sigma_f V_m} \qquad (2.11)$$

In the case of the Series model, stress is assumed to be uniform in both the matrix and the fibre. A schematic representation of the series model can be seen in Figure 2.29.

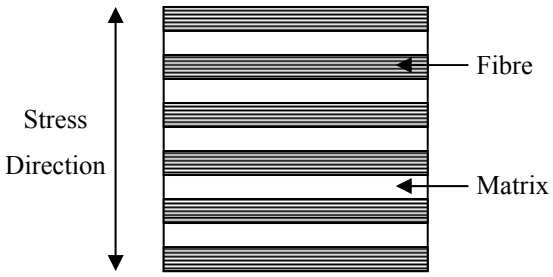

Figure 2.29 Schematic representation of the Series Model.

2.10.3 Hirsch Model

Hirsch [73, 126, 127], proposed a model based on a weighted average of the Series and Parallel models, and introduced a parameter related to efficiency of the fibre-matrix interface:

$$\sigma_c = x\left(\sigma_m V_m + \sigma_f V_f\right) + \left(1 - x\right)\frac{\sigma_f \sigma_m}{\sigma_m V_f + \sigma_f V_m} \qquad (2.12)$$

where x is an efficiency factor that accounts for the fibre orientation, fibre length, stress transfer between the fibre and matrix, and stress amplification at the fibre ends [125]. The efficiency factor, x, cannot be derived by mathematical means, and is instead empirically fitted to the model.

For the Hirsch model, good agreement between the theoretical and experimental values have been observed for axially aligned fibre composites when x = 0.4, and for randomly oriented fibre composites when x = 0.1 [125]. A schematic representation of the Hirsch model can be seen in Figure 2.30.

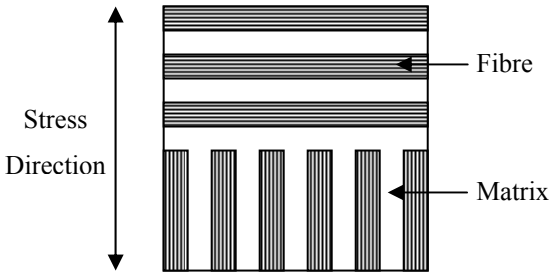

Figure 2.30 Schematic representation of the Hirsch Model.

2.10.4 Halpin-Tsai Model

The Halpin-Tsai model [73, 125, 128, 129] has been used by several researchers to determine the strength of polymeric blends consisting of continuous and discontinuous phases. It has also been reported that this model is useful for determining the properties of composites that contain discontinuous fibres

oriented in the loading direction [125]. According to Halpin and Tsai, tensile strength can be given by:

$$\sigma_c = \sigma_m\left(\frac{1+\zeta\eta V_f}{1-\eta V_f}\right) \tag{2.13}$$

where:

$$\eta = \frac{\frac{\sigma_f}{\sigma_m}-1}{\frac{\sigma_f}{\sigma_m}+\zeta} \tag{2.14}$$

such that η is the relative strength of the fibre and matrix, and ζ is an empirically fitted measurement of reinforcement geometry which depends on loading conditions.

2.10.5 Modified Halpin-Tsai Equation

The Halpin-Tsai model was modified to account for the packing fraction of the reinforcing fibres, as can be seen in Equations 2.15 and 2.16 [73, 125, 130]:

$$\sigma_c = \sigma_m\left(\frac{1+\zeta\eta V_f}{1-\eta\psi V_f}\right) \tag{2.15}$$

where:

$$\psi = 1+\left(\frac{1-\varphi_{max}}{\varphi_{max}^2}\right)V_f \tag{2.16}$$

φ_{max} is the maximum fibre packing fraction. φ_{max} equals 0.785 for a square arrangement of fibres, 0.907 for a hexagonal array of fibres and 0.82 for random packing of fibres. η is determined by Equation 2.14, and ζ is determined empirically.

2.10.6 Modified Rule of Mixtures (Kelly-Tyson Model)

The Rule of Mixtures model was further developed by Kelly and Tyson [110] to predict the strength of axially aligned discontinuous fibre composites, taking into account the strength contribution of fibres and also whether the average fibre length (L) is greater than the critical fibre length ($L>L_c$) or less than the critical fibre length ($L<L_c$).

The critical fibre length (L_c) can be determined by experimental methods such as the single fibre fragmentation test, or can be calculated using the mean fibre strength (σ_f), the mean fibre diameter (D) and the interfacial shear strength (τ) as determined by means of micro-mechanical tests:

$$L_c = \sigma_f \left(\frac{D}{2\tau} \right) \qquad (2.17)$$

For composites containing discontinuous fibres, the applied load is transferred to the fibres by means of shear forces at the fibre-matrix interface, and high shear stresses are experienced at the fibre ends [110]. Composite failure mechanisms are governed by fibre length, and sub-critical length fibres ($L<L_c$) cannot be fully stressed and will eventually debond and be pulled out of the matrix. Critical length fibres ($L=L_c$) can only be fully stressed at a very small location in the middle of the fibre, whereas supercritical length fibres ($L>L_c$) can be stressed over a much greater proportion of the fibre. Once the stress in the fibre reaches the fibre tensile strength, fibre fracture occurs.

Kelly and Tyson modified the rule of mixtures model (Equation 2.9) by replacing the mean fibre strength (σ_f) with the average stress along the fibre. The average stress of a sub-critical length fibre is given by the area under the curve in Figure 2.31(a) divided by the fibre length, and the average stress of a critical length fibre or super-critical length fibre is given by the area under the curve in Figure 2.31(b) divided by the fibre length.

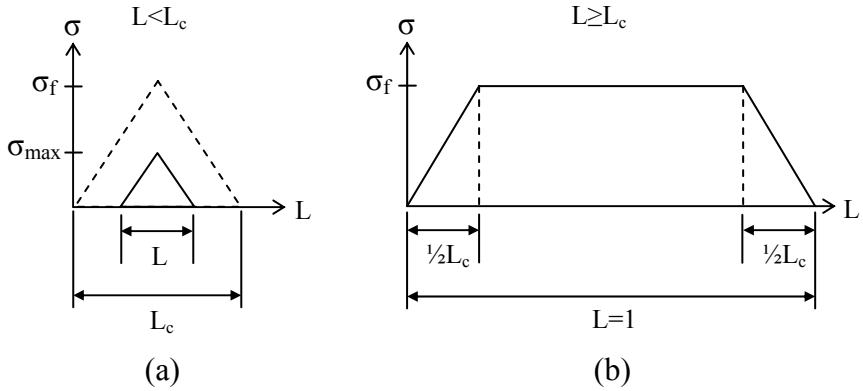

Figure 2.31 Linear build-up of stress inside a fibre: (a) $L<L_c$; (b) $L \geq L_c$.

Thus, the tensile strength (σ_c) of composites containing fibres shorter than L_c is given by:

$$\sigma_c = V_f \sigma_f \left(\frac{L}{2L_c} \right) + V_m \sigma_m \qquad \text{for } L<L_c \qquad (2.18)$$

and the tensile strength of composites containing fibres longer than L_c is given by:

$$\sigma_c = V_f \sigma_f \left(1 - \frac{L_c}{2L} \right) + V_m \sigma_m \qquad \text{for } L \geq L_c \qquad (2.19)$$

Equations 2.18 and 2.19 can be combined into the following equation to determine the composite tensile strength:

$$\sigma_c = K_2 V_f \sigma_f + V_m \sigma_m \qquad (2.20)$$

where K_2 is a fibre length factor, which can be determined by:

$$K_2 = \frac{L}{2L_c} \qquad \text{for } L<L_c \qquad (2.21)$$

or

$$K_2 = 1 - \left(\frac{L_c}{2L}\right) \qquad \text{for } L \geq L_c \qquad (2.22)$$

2.10.7 Bowyer-Bader Model

Bowyer and Bader proposed a model based on the Kelly-Tyson Modified Rule of Mixtures where the tensile strength of a discontinuous fibre composite could be determined from the sum of the sub-critical and super-critical fibre contributions, as well as that of the matrix [54].

The Kelly-Tyson model only accounts for composites with all the fibres aligned in the loading direction, and the equation cannot be integrated to give a factor which accounts for the complex fibre orientations in many moulded thermoplastic composites [131].

To enable the strength determination of composites containing off-axis fibres, it was necessary to consider the fibre orientation distribution in the composite. A simple numerical fibre orientation factor (K_1), was thus empirically fitted to the Rule of Mixtures equation [132]:

$$\sigma_c = K_1 K_2 V_f \sigma_f + V_m \sigma_m \qquad (2.23)$$

In the case of the Bowyer-Bader model, good agreement between the theoretical and experimental values are observed for axially aligned fibre composites when K_1=1, and for randomly oriented fibre composites when K_1=0.2 [125, 133].

Instead of using an average fibre length, as done in the Kelly-Tyson model, the effect of fibre length distribution on the composite properties was taken into account in the Bowyer-Bader model:

$$\sigma_c = K_1 \left\{ \sum_i \left[\frac{V_i \sigma_f L_i}{2L_c} \right] + \sum_j \left[V_j \sigma_f \left(1 - \frac{L_c}{2L_j} \right) \right] \right\} + V_m \sigma_m \qquad (2.24)$$

where V_i and V_j are the volume fractions of the sub-critical and super-critical fibre lengths, respectively; and L_i and L_j are the sub-critical and super-critical fibre lengths, respectively. Subscripts *i* and *j* refer to the sub-critical and super-critical lengths, respectively.

2.10.8 Problems and Limitations Associated with Strength Prediction Models

Each of the composite strength prediction models that have been reviewed in this section are based on various assumptions that need to be identified and considered.

All the summarised models assume that the reinforcing fibres are isotropic in nature, and this is unlikely for natural fibres as they are expected to be weaker in the transverse direction than the axial direction. The strength prediction models only consider the in-plane failure of composites, and do not consider the large fibre strength distributions that are associated with natural fibres. It is also likely that *in situ* fibre strengths are lower than *ex situ* fibre strengths as a result of fibre damage induced during composite processing.

The models all assume that the reinforcing fibres are cylindrically shaped. However, the actual shape of the hemp fibre is not perfectly cylindrical due to surface irregularities and fibre damage caused by composite processing. The non-uniform shape of hemp fibres can also account for deviations in composite experimental properties from the theoretical predictions.

Each model is based on the assumption that the composite is void-free, and do not incorporate a factor that accounts for the presence of voids. This may lead to strength prediction inaccuracies, as micro-voids formed between the fibres and matrix during composite preparation can influence the composite tensile properties.

Usually, the Parallel and Series models are used to predict the strength of continuous fibre reinforced polymeric composites. These models assume either uniform stress or uniform strain, which is clearly an over-simplification considering the inherent variations in fibre and fibre-interface properties.

The stress transfer mechanisms of continuous fibre reinforced composites are different from those of short fibre reinforced composites. In the case of short fibre composites, the stress transfer depends largely on the fibre orientation, stress concentration at the fibre ends, fibre length, fibre dispersion and fibre-matrix interfacial bond strength [125]. The strength theory for short fibre composites is still under development [134], and most proposed models are based on the Kelly-Tyson Modified Rule of Mixtures model [50, 73, 110, 126, 133-135].

The Bowyer-Bader and Hirsch models are the most reliable of the strength prediction models, especially for composites with low fibre contents where the applied load is uniformly distributed in the composite [126]. At higher fibre contents, these two models become less accurate due to fibre agglomeration, which leads to an uneven distribution of the applied load in the composite. Since fibre agglomeration is not accounted for in any of the models, the theoretical strength values deviate somewhat from the experimental values at high fibre contents.

Many composite fabrication processes result in test samples with complex, unknown fibre orientation functions, which can complicate data analysis and comparisons with model predictions [133]. Fibre orientations are difficult to measure because the fibres are concealed by the matrix and cannot be viewed easily in three dimensions. Some models, such as those proposed by Fu and Lauke [50], and Van Hattum and Bernardo [52], provide means for determining the fibre efficiency factor, but at the cost of introducing other intrinsic material parameters such as bridging stress and strengths of oblique fibres. Consequently, simplifying assumptions on the modelling of fibre orientation are usually made in order to define strength prediction models. Thus, fibre orientation factors are given as fitting factors and are derived implicitly from tests, rather than being evaluated on the basis of fibre angle measurements [56]. Of all the models

reviewed, only the Boyer-Bader and Hirsch models were found to account for off-axis fibre orientation.

2.11 X-Ray Diffraction Analysis

X-ray diffraction (XRD) is a versatile and non-destructive technique that reveals detailed information about the chemical composition and crystallographic structure of solid materials.

Many solid materials are crystalline in nature, and consist of a regular three-dimensional distribution of atoms in space (eg body-centred cubic, hexagonal close-packed). These atoms are arranged such that they form a series of parallel planes separated from one another by a distance *d* (or *d*-spacing) which varies according to the nature of the material.

Each plane of atoms in a crystalline material can act as a reflecting surface. When X-rays are directed at such a material, they hit each plane of atoms in turn, diffracting first off the surface layer, and then the layers below it (Figure 2.32). Since the wavelengths of some X-rays are about equal to the distance between the planes of atoms in crystalline solids (*d*), reinforced diffraction peaks of radiation of varying intensities can be produced when a beam of X-rays strikes a crystalline solid.

If the crystalline planes are parallel and are at an angle with the incoming X-ray beam such that the diffracted X-rays are in-phase, the diffracted X-rays will reinforce one another resulting in a strong diffracted signal (i.e. for constructive interference to occur, crystals must have the correct orientation with respect to the incoming beam). At some arbitrary angles of incidence between the X-ray beam and the crystalline planes of the material, the diffracted X-rays are not in phase, resulting in destructive interference of the diffracted X-ray beams, and hence no refracted signal. It is therefore necessary to orient the X-ray beam at many angles with respect to the crystalline planes of a material to ensure that a strong refracted signal can be achieved. The angular positions and intensities of the resultant

diffraction signals are detected and recorded, and provide a characteristic diffraction "fingerprint" of the sample examined.

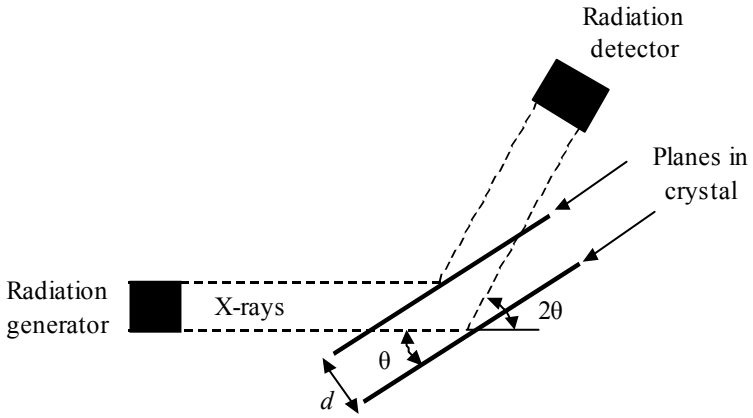

Figure 2.32 Schematic of the X-ray diffraction method.

Modern powder X-ray diffractometers consist of an X-ray source, a movable sample platform, an X-ray detector, and associated computer-controlled electronics. A powdered sample is utilised to provide a random distribution of crystal orientations, so that some of the particles will be correctly oriented in the X-ray beam to allow diffraction to occur [37]. The sample is either packed into a shallow cup-shaped holder, and the sample holder spins slowly during the experiment to reduce sample heating. The X-ray source is usually Mo or Cu. The X-ray beam is fixed and the sample platform rotates with respect to the beam by an angle theta (θ). The detector rotates at twice the rate of the sample and is at an angle of 2-theta (2θ) with respect to the incoming X-ray beam.

2.12 Thermal Analysis

Organic materials, including natural fibres and synthetic polymers, experience degradation of their physical and mechanical properties at elevated temperatures in the presence of oxygen. Since composite forming methods such as extrusion and injection moulding occur at elevated temperatures, it is important to evaluate the thermal oxidative reactions that occur within the composite at those temperatures. The thermal stability of hemp fibre, polypropylene and hemp fibre

reinforced polypropylene composites can be evaluated by means of thermogravimetric analysis (TGA) and differential thermal analysis (DTA).

TGA is an analytical technique used for determining the thermal stability and fraction of volatile components in a material by monitoring the weight change as the material is heated. The measurements are usually carried out in air or an inert atmosphere, and the weight change is recorded as a function of increasing temperature.

DTA is a technique used for providing information on the chemical reactions, phase transformations, and structural changes that occur in a material during heating. DTA measures the temperature difference between a reference (e.g. an empty alumina crucible) and the sample (placed within a crucible identical to the reference) during heating. The differences in released and absorbed energies of the sample material can therefore be determined, as well as changes in the heat capacity of the material as a function of temperature. Endothermic and exothermic processes that occur in the sample are reflected by changes in the temperature difference between the sample and the reference.

2.12.1 Thermal Oxidative Degradation of Polypropylene

Thermoplastic polymers inherently experience degradation of their physical and mechanical properties at elevated temperatures. When the polymer is heated, the molecular chain length is reduced as a function of time by the thermal cleavage of intra-chain covalent bonds. This chain scission at elevated temperatures results in a reduction in the polymer molecular weight and mechanical properties over time. In addition to thermal degradation, the chains can be broken mechanically by shear stresses induced during processing, and also by exposure to ultraviolet radiation.

Thermoplastic polymers are also somewhat susceptible to degradation in the presence of an oxidative atmosphere such as air, and polymer oxidation reactions occur more rapidly at high temperatures [99]. The auto-oxidation degradation of

PP at elevated temperature follows a process involving several steps, including initiation, propagation, chain branching, and termination [136]. Degradation is initiated when a hydrogen atom is removed from the polymer chain (RH) as a result of the thermal energy input. This hydrogen atom removal results in the formation of a highly reactive and unstable free radical (R·) (Equation 2.25). This free radical reacts with an oxygen molecule to form a peroxide radical (ROO·) (Equation 2.26), which can then react with a hydrogen atom from another polymer chain to form a hydroperoxide group (ROOH) and another free radical (R·) (Equation 2.27). This free radical again reacts with oxygen to form another peroxide radical, thus ensuring the propagation of the oxidation reaction to other polymer molecules (Equation 2.26). In the case of PP, a polymer chain containing a free radical is likely to split into two smaller chains, and the process can therefore accelerate depending on how easy it is to remove the hydrogen from the polymer chain. Chain branching occurs when the hydroperoxide (ROOH) decomposes by unimolecular mechanisms (Equation 2.28a), bimolecular mechanisms (Equation 2.28b), or other proposed methods (Equation 2.28c) [137]. Chain branching ultimately causes cross-linking of the polymer chains, which then results in embrittlement of the polymer.

The termination of degradation is achieved by the 'mopping up' of free radicals to create inert products (Equations 2.29a – 2.29c). This can occur naturally by combining free radicals or can be assisted by using stabilizers in the polymer.

The thermal oxidative degradation of polypropylene can be summarised as follows [136-138]:

Polymer Thermolysis:

$$RH \longrightarrow R\cdot \qquad (2.25)$$

Propagation:

$$R\cdot + O_2 \longrightarrow ROO\cdot \qquad (2.26)$$

$ROO\cdot + RH \longrightarrow R\cdot + ROOH$ (2.27)

Chain Branching (including chain scission):

$ROOH \longrightarrow RO\cdot + OH$ (2.28a)

$ROOH + ROOH \longrightarrow RO\cdot + ROO\cdot + H_2O$ (2.28b)

$ROOH + RH \longrightarrow RO\cdot + R\cdot + H_2O$ (2.28c)

Termination:

$2ROO\cdot \longrightarrow$ Non-radical products (2.29a)

$ROO\cdot + R\cdot \longrightarrow ROOR$ (2.29b)

$R\cdot + R\cdot \longrightarrow RH$ (2.29c)

Polypropylene can be protected from thermal oxidative degradation by incorporating a stabilizer into the polymer. Stabilizers are used to keep the polymer chains and the original molecular structure intact, thus enabling properties such as strength, stiffness and toughness to be retained over a longer period of time. Most stabilizers (AH) slow down polymer degradation by reacting rapidly with available peroxide radicals (ROO·) to produce another less active radical (A·), as can be seen in Equation 2.30.

$ROO\cdot + AH \longrightarrow ROOH + A\cdot$ (2.30)

Other stabilizers interrupt the thermal oxidative degradation cycle at the hydroperoxide propagation step to slow down or prevent the cycle from completing.

The polypropylene used in this research incorporates a mixture of stabilizers that are designed to work as a system to reduce the thermal oxidative degradation during processing.

2.12.2 Thermal Oxidative Degradation of Hemp

The decomposition process of hemp is very complicated and involves the combined degradation of several fibre constituents, each of which have varying levels of thermal stability. Hemp bast fibres have been found to contain 55% cellulose, 16% hemicellulose, 18% pectin and 4% lignin as well as small amounts of wax, ash and protein [20]. It has been widely reported that hemicellulose is the least thermally stable fibre component, followed by cellulose and then lignin [44, 139-141].

Very little research has been done to investigate the thermal decomposition of the hemicelluloses found specifically in hemp fibre. It has therefore been assumed that hemicelluloses in hemp react in similar ways to hemicelluloses found in wood. Hemicelluloses present in deciduous and coniferous woods are present almost entirely as hexosanes, and undergo thermal decomposition very readily [140]. Hemicelluloses are less thermally stable than crystalline cellulose as a result of their amorphous nature, and evolve more non-combustible gases and tar when compared to cellulose. During the thermal oxidative degradation of hemicellulose, water vapour and non-combustible gases are released, and acetic acid is liberated in a process of deacetylation [44].

The pectins found in hemp have similar thermal stabilities to hemicelluloses, and decompose when the heteropolysaccharides structures are hydrolysed at elevated temperatures. The thermal degradation residue of pectin is a black char powder [142].

The thermal degradation of cellulose is thought to occur through dehydration, hydrolysis, oxidation, decarboxylation and transglycosylation (the transfer of a glycosidically bound sugar to another hydroxyl group) [44]. Degradation at low

temperature starts with gradual degradation, decomposition and charring, followed by a rapid volatilization accompanied by the formation of levoglucosan on pyrolysis at higher temperatures [140]. The non-combustible volatiles produced are mostly H_2O, with the emission of some CO_2 and CO [141].

Thermal degradation of lignin occurs by the extensive cleavage of α- and β-aryl-ether linkages, the splitting off of aliphatic side chains from the aromatic ring, and the cleavage of the carbon-carbon linkage between lignin structural units [44]. Char is formed from lignin at higher temperatures as a result of cleavage of the alkyl-aryl-ether bonds, with the consequent formation of a more resistant and condensed structure.

Chapter 3: Materials and Methods

3.1 Experimental Overview

The purpose of this research was to improve the tensile strength and Young's Modulus of hemp-fibre reinforced polypropylene composite materials over what has already been presented in the literature. Improvements to these properties were endeavoured by optimising various composite parameters, such as the fibre strength, fibre processing methods, composite processing methods and fibre-matrix interfacial adhesion.

In order to achieve this objective, hemp fibres were chemically treated to improve the fibre strength, improve fibre separation and to modify the fibre surface. Composites were produced by compounding chopped fibres and polypropylene powder in a twin-screw extruder, and the extruded composites were then granulated and injection moulding into tensile test specimens. A maleated polypropylene (MAPP) coupling agent was added to some composites to improve the fibre-matrix adhesion, and the fibre and MAPP contents were varied to produce a series of composites with differing mechanical properties.

A second composite fabrication technique was investigated whereby an oriented fibre mat was impregnated with a polymer-solvent mixture. The solvent was then evaporated, leaving a mass of fine polypropylene precipitates distributed throughout the mat. The impregnated mat was finally consolidated by means of hot pressing.

Fibres and composites were analysed to evaluate various physical and chemical attributes, such as strength, Young's modulus, lignin content, crystallinity, interfacial adhesion and thermal stability.

3.2 Fibre Modification and Evaluation

3.2.1 Alkali Solution Preparation

Chemical fibre treatments using NaOH are commonly used in the pulp and paper industries to delignify wood fibres and to separate the fibre bundles into elementary fibres. This method can also be used for separating and delignifying hemp bast fibre [143]. The following two alkali solutions were prepared and used in this investigation, each with the purpose of achieving good fibre separation, maximising lignin removal and minimising fibre degradation.

NaOH Treatment

Retted industrial hemp fibre (*Cannabis Sativa L.)* supplied by Hemcore (UK), was treated with a 10wt% solution of NaOH, such that the fibre:liquor ratio was 1:6 (by weight). In order to treat a 70g sample of hemp fibre with the required alkali solution concentration and fibre:liquor ratio, 42g analytical grade NaOH (98% purity) was dissolved in 378ml water and added to the pre-weighed quantity of fibre.

This particular treatment was found in a previous study [144, 145] to be the optimum for improving the tensile strength and fibre separation of semi-retted hemp fibre grown in New Zealand, where a tensile strength increase of 12% was observed for the treated fibres over the untreated control.

NaOH/Na_2SO_3 Treatment

Retted industrial hemp fibre (*Cannabis Sativa L.)* supplied by Hemcore (UK), was treated with a 5wt% NaOH / 2wt% Na_2SO_3 solution, such that the fibre:liquor ratio was 1:7 (by weight). In order to treat a 70g sample of hemp fibre with the required alkali solution concentration and fibre:liquor ratio, 17.5g analytical grade NaOH (98% purity) and 2.8g Na_2SO_3 powder (98% purity) were dissolved in 469.7ml water and added to the pre-weighed quantity of fibre.

This treatment is a modification of the hemp fibre treatment used by Islam *et al* [43].

3.2.2 Fibre Processing

Hemp fibres were combined with the appropriate alkali solutions and processed at elevated temperatures and pressures inside a lab-scale pulp digester (Figure 3.1 and Figure 3.2). The processing temperature was regulated by PID-controlled heating elements situated throughout the shell, while the pressures inside the digester and digester canisters were dependant on the temperature of the digester water and thus corresponded with the saturation pressure for saturated water at that temperature. During operation, the entire vessel was rotated cyclically through 110^{o} (from an upright position) to ensure good mixing and an even distribution of heat throughout the contents.

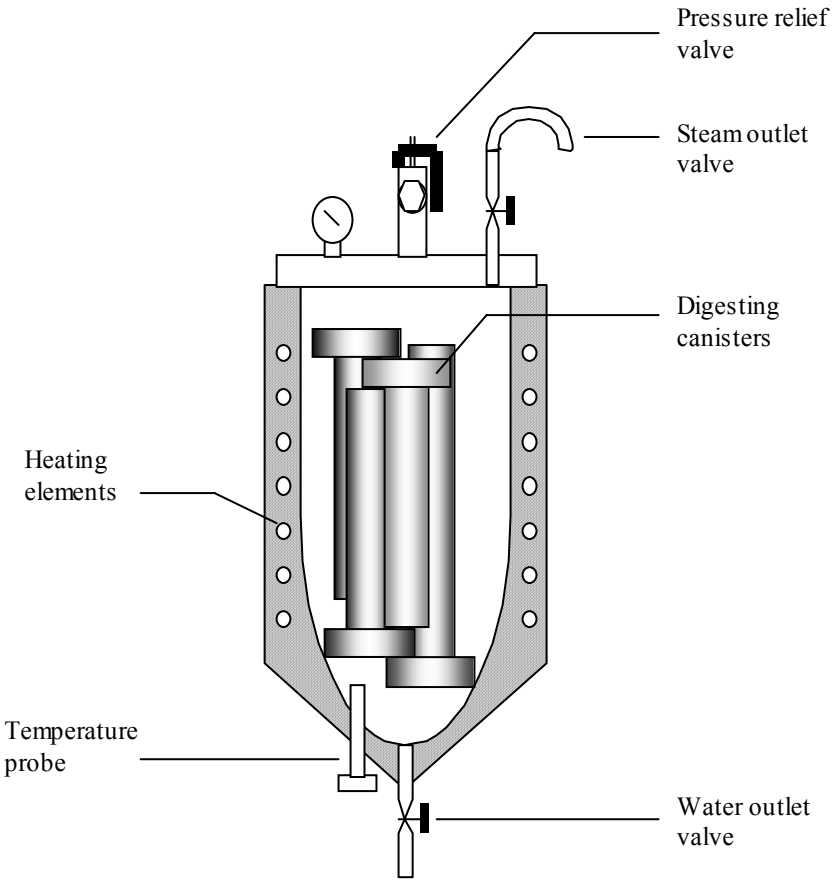

Figure 3.1 Schematic of a pulp digester.

Figure 3.2 Lab-scale pulp digester.

The internal volume of the digester was 15L, thus requiring large amounts of alkali liquor and fibre to fill the digester to capacity. Smaller batches of hemp (70g) were therefore digested in 1L capacity stainless steel canisters, which were placed inside the digester cavity. Four canisters could be fitted inside the digester in an arrangement shown in Figure 3.1.

Once the fibre and liquor containing canisters were placed inside the digester, the remaining space in the digester cavity was filled with water so that heat could be transferred from the heating elements to the canisters. A cook schedule was programmed into the temperature controller to control the digestion process. Figure 3.3 and Figure 3.4 show the response of the system to the programmed cook schedule.

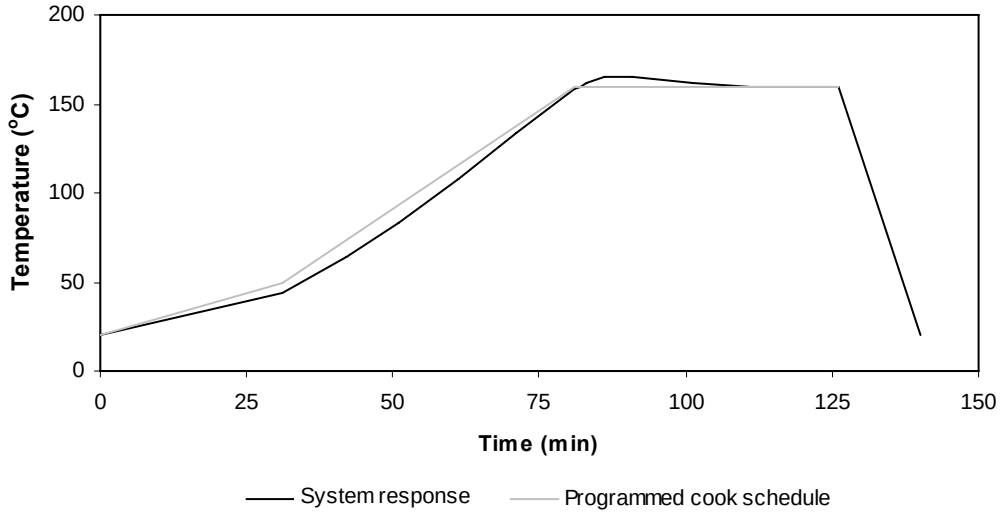

Figure 3.3 Digester cook schedule for NaOH treatment.

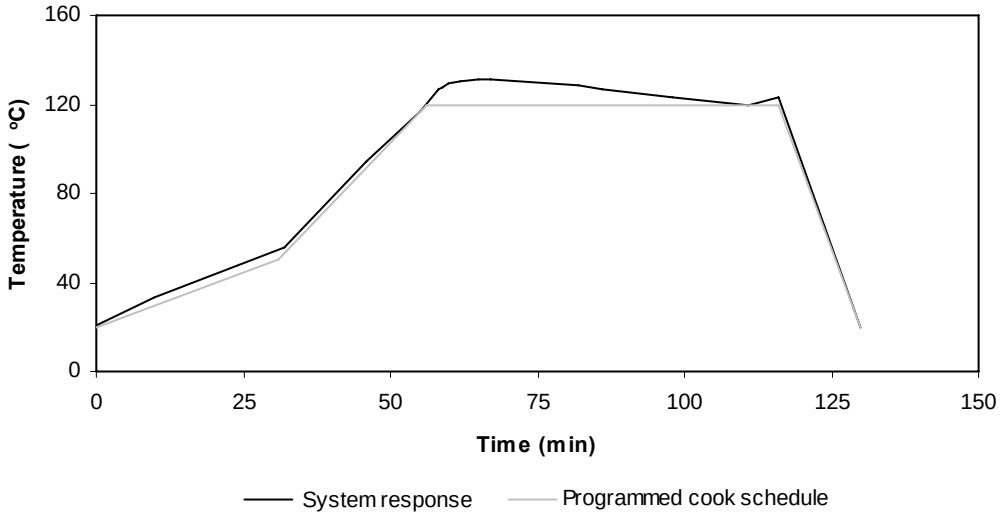

Figure 3.4 Digester cook schedule for NaOH/Na_2SO_3 treatment.

Once the digestion process was completed, the digester and its contents were crash cooled (rapidly cooled from the maximum process temperature to 30°C) to reduce the hemp fibre exposure with the alkali solution. This crash cooling process involved the rapid release of pressure within the digester by means of opening the steam outlet valve. Once the pressure had been released and the internal temperature had dropped to below 100°C, the water outlet valve was opened to drain the hot water from inside the digester. A cold-water hose was then attached to the steam outlet pipe, so that cold water could be circulated in

through the steam outlet valve and then out through the water outlet valve. The crash cool process took about 14-15 minutes to perform.

Once the crash cooling process was completed and the digesting canisters had reached a manageable temperature of between 30°C and 40°C, the digested fibre was removed from each of the canisters and placed in a pulp and paper fibre-washer (Figure 3.5). Fibres were washed for 10 minutes in clean water, before being dried in a drying oven at 80°C for 48 hours.

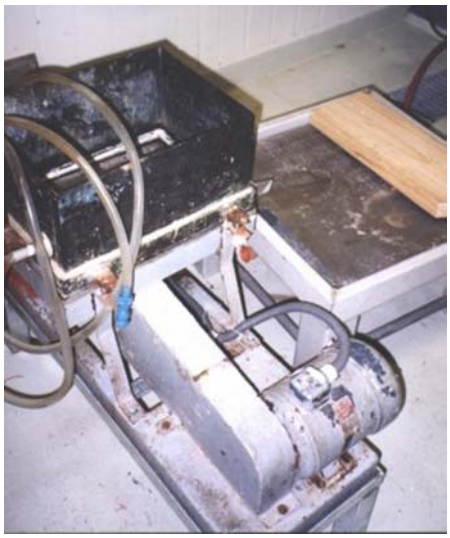

Figure 3.5 Pulp and paper fibre washer.

It was found after digestion that the NaOH treatment resulted in fibre dry mass losses of 41.3%, while the NaOH/Na_2SO_3 treatment resulted in fibre dry mass losses of 32.1%.

3.2.3 Lignin Measurement

Lignin measurements for untreated, NaOH treated and NaOH/Na_2SO_3 treated hemp fibre were performed by Veritec Laboratories, Rotorua, New Zealand.

The TAPPI Standard Method T 222 om-88 was used to determine acid-insoluble lignin content, and the TAPPI Useful Method UM 250 was used to determine acid-soluble lignin content.

Samples of approximately 0.25g were ground into a fine powder, and the cell wall material was isolated (including starch removal) by extraction with a series of solutions and solvents before being analysed for lignin content.

A filtrate dilution of 1:5 was used in these experiments, and an extinction coefficient (absorptivity) of 110 L/g.cm was used in the calculations for acid soluble lignin (as per TAPPI UM 250 NOTE 2).

3.2.4 Single Fibre Tensile Testing

The tensile strength and Young's modulus of NaOH treated, NaOH/Na_2SO_3 treated and untreated hemp fibres were determined according to the ASTM D3379-75 Standard Test Method for Tensile Strength and Young's Modulus for High-Modulus Single Filament Materials.

Elementary hemp fibres were separated from their fibre bundles by hand, and then mounted on 2mm thick cardboard mounting-cards with either 5mm, 8mm, 10mm and 12.5mm holes punched into them, such that the hole diameter determined the fibre gauge length (Figure 3.6). Mounting cards with 1.5mm and 3mm windows for use with short gauge length fibres were made by hand. A small amount of PVA glue was applied to the two edges on either side of the hole/window along the length of the card, and the fibres were carefully put into place.

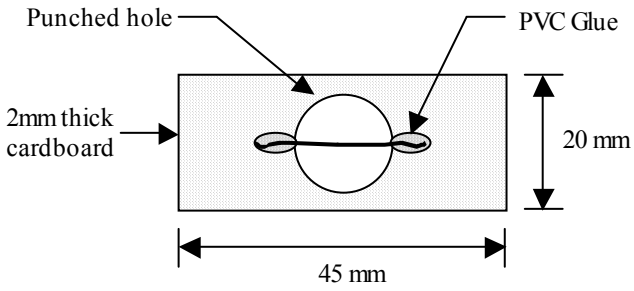

Figure 3.6 Single fibre mounting.

Mounted fibres were inspected under an Olympus BX60F5 metallurgical microscope to ensure that only a single fibre was present on each card.

Diameters of selected fibres were then measured under the same microscope by means of a calibrated eyepiece. For fibres with a gauge length of 5mm, 8mm, 10mm and 12.5mm, the average fibre diameter was determined by measuring the diameter at 5 locations along the fibre length, and then taking the average. The diameters of 1.5mm and 3mm fibres were determined by averaging 3 measurements along the fibre length.

The mounted fibres were then placed in the grips of an Instron-4204 tensile testing machine (Figure 3.7), and the supporting sides of the mounting cards were carefully cut using a hot-wire cutter. The fibres were then tensile tested to failure at a rate of 0.5mm/min using a 10N-load cell. Average fibre tensile strengths were obtained using the results from thirty specimens.

Figure 3.7 Instron-4204 tensile testing machine.

3.2.5 Compliance and Young's Modulus Determination

To calculate the Young's modulus of a single fibre using tensile test data, it is necessary to obtain accurate values for tensile load and displacement (elongation). The load cell of the Instron tensile tester measures the load exerted on a fibre specimen, and an extensometer or strain gauge attached to the specimen is required to accurately measure the displacement. Unfortunately, the use of a standard extensometer or strain gauge on single hemp fibres is not possible due to the small diameters of the fibres. The fibre displacement experienced during tensile testing can therefore only be measured from the displacement of the testing machine crosshead. The crosshead displacement, however, is actually a combination of the fibre elongation as well as the crosshead deformation, specimen grips, and the cardboard mounting card. It is therefore necessary to utilise a correction factor to determine the true displacement of the fibre, which involves the calculation of the testing system compliance.

System compliance (C_s), as defined by the ASTM Standard Test Method D 3379-75, is the portion of the indicated elongation contributed by the load train system and the specimen gripping system. The system compliance must be determined experimentally for a given combination of test machine conditions, grip system and mounted specimen. System compliance must therefore be subtracted from the apparent fibre elongation to yield the true fibre elongation for the given fibre length.

The procedure for determining system compliance is described in the ASTM D 3379-75 Standard Test method for Tensile Strength and Young's Modulus for High Modulus Single-Filament Materials, and was also used by Kromm *et al*. [146]. The procedure involves the tensile testing of filaments of a material with a known Young's modulus over a range of gauge lengths. For this experiment, E-glass was chosen as it has a known Young's modulus of 69 GPa, which is in the same range as that of hemp fibre. From the corresponding load-displacement curves obtained for each E-glass fibre length, the apparent compliance (C_a) for each length could be determined by inverting the gradient obtained from the

straight-line section of each curve. The apparent compliance is a linear function of gauge length, which can then be extrapolated to zero gauge length to give the system compliance (C_s) (testing system compliance), as can be seen in Figure 3.8.

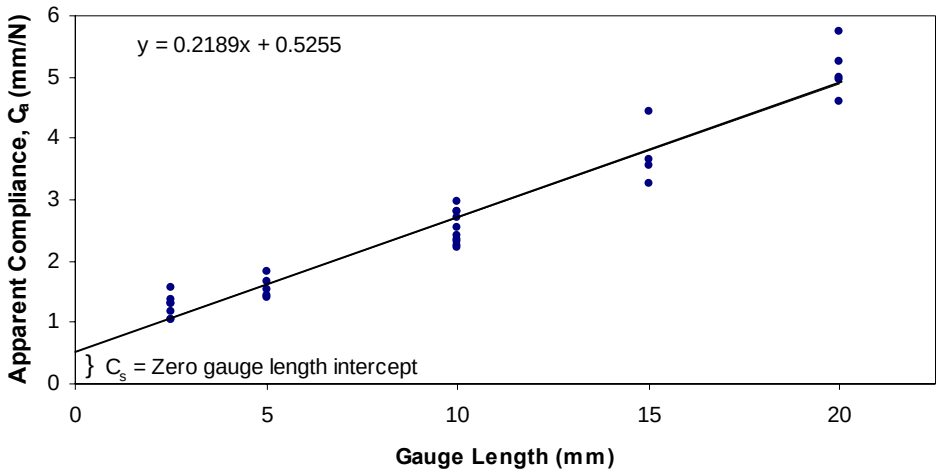

Figure 3.8 System compliance of the tensile testing system based on data obtained from E-glass fibres.

The true compliance (C) for any test specimen is thus the difference between the apparent compliance (C_a) and the system compliance (C_s):

$$C = C_a - C_s \qquad (3.1)$$

C_a and C_s can be determined from the system compliance trend-line equation as seen in Figure 3.8:

$$y = 0.2189x + 0.5255 \qquad (3.2)$$

where y is the apparent compliance (C_a) of the fibre, x is the gauge length of the fibre and the intercept (0.5255) is the system compliance (C_s).

To calculate the Young's modulus of a fibre (E_f), the following equation can then be used:

$$E_f = \frac{L}{CA} \qquad (3.3)$$

where L is the specimen gauge length, C is the true compliance and A is the average fibre cross sectional area.

The Young's modulus of a 10mm gauge length E-glass fibre, with a cross sectional area of 7.178 $x10^{-11}$ m^2 (an average CSA for all E-glass fibres tested) was calculated as 64 GPa using Equations 3.1, 3.2 and 3.3. This Young's modulus is comparable to the manufacturer specified value of 69 GPa, thus verifying that the above method has a sufficient level of accuracy to be used to calculate the Young's modulus of single hemp fibres using the same tensile testing system.

3.2.6 X-Ray Diffraction Analysis of Fibres

Untreated hemp fibre, NaOH treated hemp fibre and $NaOH/Na_2SO_3$ treated hemp fibre was chopped into fine particles and compressed into disks using a cylindrical steel mould (Ø = 15mm) with an applied pressure of 32 MPa. A Philips X'Pert diffractometer fitted with a ceramic X-ray diffraction tube was used to assess the influence of the alkali treatments on fibre crystallinity. The diffracted intensity of CuKα radiation (wavelength of 0.1542 nm) was recorded between 5^o and 40^o (2θ angle range) at 40 kV and 40 mA.

3.3 Fabrication and Evaluation of Composites

3.3.1 Composite Extrusion and Injection Moulding

All extruded and Injection moulded composites were reinforced with retted industrial hemp fibre (*Cannabis Sativa L.)* supplied by Hemcore (UK), except for the composites produced to show the effects of fibre content on composite mechanical properties, where retted New Zealand grown hemp fibre was used instead. Fibres were either used in their untreated state, or were treated with

NaOH or NaOH/Na_2SO_3. A polypropylene copolymer (Icorene™ PP CO14RM) with a density of 0.9 gm/cc, a melting temperature of 165^{o}C and a melt flow index of 13 g/10min was used as the composite matrix. The coupling agent used was A-C 950P high molecular weight maleic anhydride modified polypropylene (MAPP), with a saponification value of 35–40mg KOH/gm, a density of 0.93 gm/cc and free maleic anhydride content of less than 0.5%, and was supplied by Honeywell International Inc, USA. The MAPP contents referred to for extruded and injection moulded composites are given as a percentage of the total composite weight.

Treated fibres were chopped into lengths of 1-3mm using an industrial granulator, and dried at 80^{o}C for 48 hours (referred to as 'normal' fibre length distribution). The chopped hemp fibre, polypropylene and MAPP were compounded in a ThermoPrism TSE-16-TC twin-screw extruder (Figure 3.9), such that composites with varying MAPP and polypropylene contents were produced. The extruder barrel consisted of 5 heating zones, which were set at 80^{o}C (barrel entrance), 110^{o}C, 155^{o}C, 180^{o}C, and 175^{o}C (barrel exit). The twin co-rotating screws were operated at 160 revolutions per minute (rpm).

Figure 3.9 ThermoPrism TSE-16-TC twin-screw extruder.

After air-cooling, the extruded composite material was granulated in an industrial granulator to produce composite pellets suitable for injection moulding, with dimensions ranging from 3 to 6mm. The composite pellets were then dried at 80^{o}C for 24 hours before being injection moulded into Type 1 tensile test specimens (as specified by the ASTM D638-91 standard) using a BOY15-S injection-moulding machine (Figure 3.10). Composites were injection moulded at the lowest temperatures that enabled adequate filling of the mould, which was found to be equal to a barrel temperature of 180^{o}C for composites containing alkali treated fibres, and a barrel temperature of 145^{o}C for composites containing untreated treated fibres. Other barrel temperatures were also used in order to determine the effects of injection moulding temperature on composite tensile strength, and this data was used to assist with composite thermal analysis. It should be noted that these temperatures represent the temperatures of the injection moulder barrel, and not necessarily those of the composite melt.

Figure 3.10 BOY15-S injection-moulding machine.

The injection moulder processing variables that were used for the majority of the composites are as follows: 83% injection pressure, 40% back pressure, and 250 rpm screw rotation speed (referred to as 1st I.M Setup). A second set of

variables was used to investigate the effects of injection moulding variables on composite mechanical properties, and these are as follows: 55% injection pressure, 30% back pressure, and 100 rpm screw rotation speed (referred to as 2nd I.M Setup).

Injection moulded test specimens were tensile tested to determine composite tensile strength and Young's modulus.

An additional investigation was performed to determine the effects of fibre length on the mechanical properties of injection-moulded composites. The same batch of Hemcore hemp fibre used in previous experiments was used in this investigation, but it was observed that some fibre degradation had occurred due to the presence of moisture in the fibre storage area. It was therefore suspected that the mechanical properties of the fibres used in this particular investigation were somewhat lower than those used in the fabrication of the other extruded and injection moulded composites.

Hemp fibres were treated with $NaOH/Na_2SO_3$, and were granulated and separated according to length by means of a sieve with aperture dimensions of 710μm x 710μm. Fibres that passed through the sieve are referred to as 'short', and fibres that were retained by the sieve are referred to as 'long'. A 'normal' fibre length distribution was made up of un-sieved long and short fibres. Composites containing 40wt% fibre, 4wt% MAPP and 56wt% polypropylene were fabricated from the three fibre length separations by means of extrusion and injection moulding. Type 1 tensile test specimens were produced and tensile tested.

A summary of all the injection moulded composite parameters and results can be seen in the appendix.

3.3.2 Solution Mixing of Composites

The solution mixing method involves dissolving the polymer in a solvent, adding the solvent/polymer mixture to a pre-prepared stacked fibre mat consisting of layers of oriented fibres, precipitation of the polymer within the fibre mat and the

removal and recovery of the solvent. Solution mixed composites were made from retted industrial hemp bast fibre, supplied by Hemcore (UK). The fibre used in the solution mixing experiments was taken from the same batch that was used for the injection moulding experiments and fragmentation tests. It was observed that some fibre degradation had occurred due to the presence of moisture in the fibre storage area, so fibre mechanical properties were expected to be significantly lower than fibres used in previous experiments.

Hemp fibre was treated with a 5wt% NaOH / 2wt% Na_2SO_3 solution. Fibres were dried at 80^{o}C for 48 hours, and formed into aligned fibre mats using a hand-operated carding machine. A thicker fibre mat with axially oriented fibres was then produced by stacking up several thinner carded fibre mats, as can be seen in Figure 3.11.

Figure 3.11 Stack of carded hemp fibre mats.

A polypropylene copolymer (Icorene™ PP CO14RM) with a density of 0.9 gm/cc, a melting temperature of 165^{o}C and a melt flow index of 13 g/10min was used as the composite matrix. The coupling agent used was A-C 950P high molecular weight maleic anhydride modified polypropylene (MAPP), with a

saponification value of 35–40mg KOH/gm, a density of 0.93 gm/cc and free maleic anhydride content of less than 0.5%, was supplied by Honeywell International Inc, USA. Analytical grade xylene was used as the polymer solvent.

For each composite, 765ml of xylene was heated to 130^{o}C in a round-bottomed flask, and a pre-determined amount of MAPP was then dissolved in the heated xylene. A MAPP/PP ratio of 7.14g MAPP/100g PP was used for all composites, which is equivalent to 4wt% MAPP in a composite containing 40wt% hemp and 56wt% PP (i.e. the optimum MAPP content found in previous experiments).

The xylene/MAPP mixture was then poured into a pre-heated aluminium evaporating-tray lined with a wire basket. A pre-determined mass of polypropylene powder, depending on the intended fibre/PP content of the composite, was then dissolved in the xylene/MAPP mixture. Once the polypropylene had dissolved, the aligned fibre mat was added to the evaporating tray, and wetted with the xylene/polymer mixture. The contents of the evaporating tray were then covered to prevent solvent evaporation, and cooled to 70^{o}C to enable the polypropylene to become a viscous gel within the fibre mat. The evaporating tray was then inserted into a specially designed solvent evaporator fitted with a Liebig condenser (Figure 3.12), and heated at 95^{o}C for between 23 to 28 hours to evaporate and condense the solvent. Approximately 75% of the xylene could be recovered and reused from each evaporation procedure. The fibre mat containing polypropylene precipitates (Figure 3.13) was then heated in a drying oven at 104^{o}C for 24 hours to remove xylene residues.

The polypropylene impregnated mat was then hot pressed in a heated hydraulic press by means of one of the following procedures:

1. The composite was pressed at 180^{o}C for 5 minutes at a pressure of 115 KPa, followed by cooling under pressure.
2. The composite was pressed at 180^{o}C for 5 minutes at a pressure of 115 KPa, and then cooled under pressure. The composite was then pressed a second time at 180^{o}C for 5 minutes at a pressure of 121 KPa, and again cooled under pressure.

Figure 3.12 Solution mixing apparatus including evaporating tray, solvent evaporator and Liebig condenser.

Figure 3.13 Solution mixed hemp fibre mat containing loosely bound polypropylene precipitates.

A relatively high temperature was used during hot pressing to ensure that the polymer viscosity was low enough for the polypropylene to flow freely around the fibres and into voids, thus producing a consolidated composite (Figure 3.14). A low consolidation pressure was used during pressing to prevent the molten polymer from being squeezed out of the composite. Composites were then weighed, and the composite fibre contents were determined by dividing the mass of the fibre mat prior to processing by the mass of the composite after hot pressing. Composites were then cut into Type 1 tensile test specimens (as specified by the ASTM D638-91 standard) by means of a CNC mill.

A summary of all the solution mixed and hot pressed composite parameters and results can be seen in the appendix.

Figure 3.14 Solution mixed and hot pressed hemp fibre composite.

3.3.3 Composite Tensile Testing

Tensile test specimens were placed in a conditioning chamber at 23^{o}C ± 3^{o}C and 50% ± 5% relative humidity for 40 hours. The specimens were then tested according to the ASTM D638-91 standard using an Instron-4204 tensile testing

machine fitted with either a 5kN or 10kN load cell, and operated at a rate of 5mm/min. An Instron 2630-112 extensometer was used to measure the composite strain. Composite specimens were tested to failure, whereas non-fibre containing specimens were only tested to the point of maximum stress due to excessive necking. Ten specimens were evaluated for each extruded and injection moulded composite, whereas four specimens were tested for each solution mixed and hot pressed composite.

3.3.4 Fibre Extraction and Length Analysis

Injection moulded composites containing 4wt% MAPP, 56wt% polypropylene and fibres that had been separated according to length, were boiled in xylene to dissolve the polypropylene matrix and to enable the extraction of the fibres from the composite.

Approximately 5g of each composite was dissolved in 150ml of boiling xylene (135^{o}C) for 20 minutes, and then filtered through a mesh with aperture dimensions of 600µm x 600µm to remove the majority of the fibres from the xylene filtrate. The filtrate was then filtered through a mesh with aperture dimensions of 150µm x 150µm to remove the fines. This process was repeated twice more using 100ml of clean xylene. The fibres were then dried, and the longer fibres and fines were combined and mixed with water in a low speed Waring blender. A small amount of dishwashing detergent was added to the fibre-water suspension to assist with fibre dispersal. A sample of the fibres extracted from the 'short', 'normal' and 'long' fibre composites were analysed by means of a Kajaani Fibrelab electronic sequential fibre length analyser. Approximately 4000 fibres were analysed, and a mean fibre length and normal fibre distribution were determined for each composite.

Injection moulded composites containing 40wt% $NaOH/Na_2SO_3$ treated hemp fibre, polypropylene and either 0wt% MAPP or 4wt% MAPP were similarly dissolved in boiling xylene, and the fibres were extracted and washed in additional solvent. The extracted fibres were viewed microscopically to ascertain

whether or not the MAPP coupling agent had successfully bonded to the fibre surfaces.

3.3.5 Single Fibre Fragmentation Testing

The single fibre fragmentation test (SFFT) was selected as the most suitable method for evaluating the interfacial shear strength (IFSS) of hemp fibre reinforced polypropylene composites. The SFFT provides a relatively accurate measurement of the IFSS as the fibre-matrix interface is subjected to pure shear, and the test provides a large amount of data for statistical sampling. The polypropylene/MAPP matrix has a failure strain greater than 3x the fibre failure strain thus ensuring full fibre fragmentation, and the matrix has a sufficient level of transparency to allow the fibre fragments to be observed and measured.

It was found experimentally that the extruded and injection moulded composite with the greatest tensile strength and Young's modulus consisted of $NaOH/Na_2SO_3$ treated hemp fibre, polypropylene and 4wt% MAPP. It was therefore decided to further evaluate the interfacial adhesion of composites containing the same constituents. It should be noted that SFFT's were only performed on fibres that had not suffered moisture-induced degradation, hence the data gathered from these tests is only applicable to the extruded and injection moulded composites containing non-degraded fibres. The SFFT is not strictly standardised for natural fibre composites, and the following test procedure was derived from techniques that have been widely used on synthetic fibres:

$NaOH/Na_2SO_3$ treated hemp fibres were separated from their fibre bundles by hand (taking care to handle the fibre ends so not to contaminate the fibre) and viewed under an optical microscope to ensure the presence of only a single fibre. Fibres were then mounted on paper frames with PVA glue, such that fibre gauge lengths were maintained at 20mm. The sides of each window were cut away, so that a small paper tab was left attached to each end of the fibre.

Polypropylene with 4wt% MAPP was compounded in a ThermoPrism TSE-16-TC twin-screw extruder, and then hot pressed at 180°C to form a 0.5mm thick polymer sheet. Pure polypropylene without a coupling agent was pressed into sheet form in a similar manner. The polymer sheets were cut into small pieces (approximately 10mm x 10mm), and each fibre was carefully aligned between two polymer pieces and hot pressed between two Teflon™-coated steel plates at 180°C for 4 minutes, whilst the pressure was gradually increased to 5 MPa to attain a specimen thickness of 0.15mm.

After hot pressing, the SFFT specimens were cooled under pressure and cut so that the fibres were positioned axially along the length of the specimens. Masking tape was attached to the ends of each specimen to limit the fibre gauge length to 18mm, and also to provide a larger area on which to grip the specimen in the tensile tester. A schematic of the procedure undertaken to produce fragmentation test specimens can be seen in Figure 3.15.

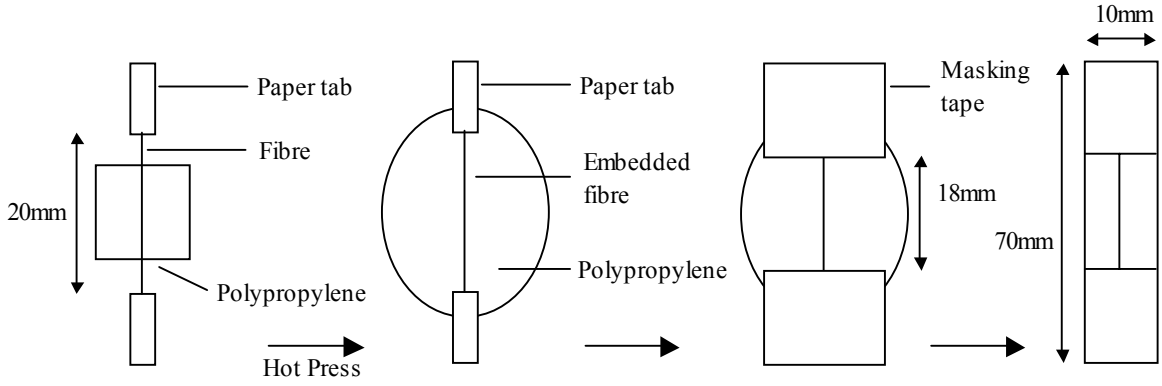

Figure 3.15 Fabrication of single fibre fragmentation test specimens.

An Instron-4204 universal testing machine operated at a crosshead speed of 2mm/min was used to subject SFFT specimens to an increasing tensile load. The load was released after full fibre fragmentation had occurred, and just before the polypropylene matrix started to yield (at around 50% strain). Twenty-five tests were performed for specimens containing a polypropylene matrix, as well as for specimens containing polypropylene and 4wt% MAPP.

After testing, the individual fibre fragment lengths and fibre diameters were measured at a magnification of 50x using an optical microscope with a calibrated eyepiece. An average fibre diameter was determined by taking the average of five diameter measurements across the length of each fibre. For the purpose of this study, it was assumed that fibres were circular in cross-section. Only fibre fragments present within the 18mm gauge length of each SFFT specimen were considered for analysis.

3.3.6 Microscopic Analysis of Fibres and Composites

Optical Microscope Imaging

Composites containing 40wt% $NaOH/Na_2SO_3$ treated hemp fibre, 57wt% polypropylene and 3wt% MAPP were injection moulded using the following injection moulder settings: 40% back pressure, 83% injection pressure, 250 rpm screw speed. Composite test specimens were then cut, ground and polished with a Struers Rotopol-21 grinding and polishing machine to reveal the fibre orientations in different planes.

Macroscopic images were taken of polished composite surfaces by means of a Wild M3B stereo-microscope fitted with a Nikon Digital Sight DS-SMc digital camera at a 6.4x magnification. Microscopic images of the polished composite surfaces were obtained by stitching together 8 different micrographs taken with an Olympus BX60F5 metallurgical microscope, fitted with a Nikon Digital Sight DS-SMc digital camera at a 50x magnification.

Scanning Electron Microscope Imaging

Fracture surfaces of composite tensile test specimens and the surfaces of chemically treated and untreated fibres were examined my means of a Hitachi S-4100 field emission scanning electron microscope (SEM), operated at 5 kV. Samples were mounted onto aluminium stubs with carbon tape and then sputter coated with platinum and palladium to make them conductive prior to SEM observation.

3.3.7 Thermal Analysis

Thermal analysis results, especially those for DTA analysis, can vary substantially by altering the experimental variables such as sample size and form, heating rate, purge gas and pressure. Usually, low heating rates, low sample weights, and samples in the form of fine powders have negligible effects on the overall decomposition curves [44].

The following materials were evaluated by means of TGA and DTA thermal analysis methods: Extruded polypropylene (containing 4wt% MAPP), untreated hemp fibre, $NaOH/Na_2SO_3$ treated hemp fibre, as well as extruded composites containing 56wt% polypropylene, 4%wt MAPP and either 40wt% untreated hemp fibre or 40wt% $NaOH/Na_2SO_3$ treated hemp fibre.

Thermal analysis was carried out using a TA Instruments SDT 2960 Simultaneous DTA-TGA analyser, as can be seen in Figure 3.16. Measurements were taken whilst maintaining a static airflow of 150 ml/min with a constant heating rate of 2^oC/min in an open alumina crucible. Each specimen weighed 10mg (± 1mg), with a scanning temperature range of 25^oC – 500^oC.

Figure 3.16 SDT 2960 Simultaneous DTA-TGA analyser.

Chapter 4: Results and Discussion

4.1 Fibre Evaluation

4.1.1 The Effects of Alkali Treatment on Diameter, Tensile Strength and Young's Modulus of Fibres

Adhesives in the fibre cell wall, such as lignin, pectins and hemicelluloses are responsible for binding cellulose microfibrils together as fibre units, as well as joining adjacent fibres together to form fibre bundles. These compounds must be removed to initiate fibre separation, and hence enable better fibre distribution within fabricated composites. In Table 4.1, it can be seen that the two alkali treatments resulted in decreases in fibre diameter, which can be attributed to the removal of alkali-soluble cementing materials from the fibre cell walls.

Table 4.1 Mechanical properties of untreated and alkali treated fibres. Standard deviations are included in parenthesis.

Fibre Treatment	Fibre Diameter (µm)	Tensile Load (N)	Tensile Strength (MPa)	Young's Modulus (GPa)
Untreated	26.5 (6.7)	0.276 (0.187)	514 (274)	24.8 (16.3)
NaOH	21.7 (5.7)	0.121 (0.095)	347 (106)	20.3 (8.4)
$NaOH/Na_2SO_3$	23.6 (5.2)	0.264 (0.119)	616 (260)	30.2 (11.8)

The NaOH treatment resulted in greater fibre diameter reductions than the $NaOH/Na_2SO_3$ treatment, as more cementing materials could be removed from the fibre due to the use of a higher alkali concentration. This data was statistically

analysed using a one-tailed Student's t-test at a confidence level of 95% (P<0.05). According to the Student's t-test results, the diameters between the two types of alkali treated fibre and the untreated control are significantly different.

It can also be seen in Table 4.1 that each of the alkali treatments had a different effect on the fibre tensile strength and Young's modulus. When looking at the average values, the $NaOH/Na_2SO_3$ treatment appeared to increase the fibre tensile strength and Young's modulus in relation to those of the control (untreated fibres), whereas the NaOH treatment appeared to reduce the fibre tensile strength and Young's modulus. The data was statistically analysed using a one-tailed Student's t-test at a confidence level of 95% (P<0.05) to determine the significance of the difference in the fibre tensile strength and Young's modulus of each of the fibre treatments in relation to that of the control. According to the Student's t-test results, there are no significant increases in fibre tensile strength and Young's modulus of the $NaOH/Na_2SO_3$ treated fibres when compared to the control, although the averaged test results would suggest that the tensile strength and Young's modulus of the $NaOH/Na_2SO_3$ treated fibres are slightly superior. The Student's t-test results also indicate that there is a significant decrease in tensile strength of NaOH treated fibres when compared to the control, but there is no significant decrease in fibre Young's modulus for this treatment.

It can thus be seen that the $NaOH/Na_2SO_3$ fibre treatment did not dramatically affect the tensile strength and Young's modulus of hemp fibres, suggesting that no degradation occurred to the cellulose microfibrils during the alkali treatment. The NaOH treatment, however, resulted in a significant reduction in fibre strength as a result of cellulose degradation, which is often associated with treatments involving the use of high NaOH concentrations [75].

It therefore appears that the treatment using $NaOH/Na_2SO_3$ is the most suitable alkali fibre treatment for producing strong and stiff fibres for use in composite materials.

4.1.2 Lignin Content of Fibres

The lignin contents of untreated and alkali treated hemp fibres are listed in Table 4.2. It can be seen that the NaOH treatment, which had the higher alkali concentration, was more effective than the NaOH/Na_2SO_3 treatment in the removal of lignin from hemp fibre. It can also be seen in Figure 4.1 that the NaOH treated fibre is much lighter in colour than the untreated and NaOH/Na_2SO_3 treated fibre due to the lower lignin content.

Table 4.2 Lignin content of untreated and alkali treated fibres.

Fibre Treatment	Acid Insoluble Lignin (wt%)	Acid Soluble Lignin (wt%)	Total Lignin (wt%)
Untreated	3.8	1.2	5.0
NaOH	1.7	0.4	2.1
NaOH/Na_2SO_3	2.8	0.7	3.5

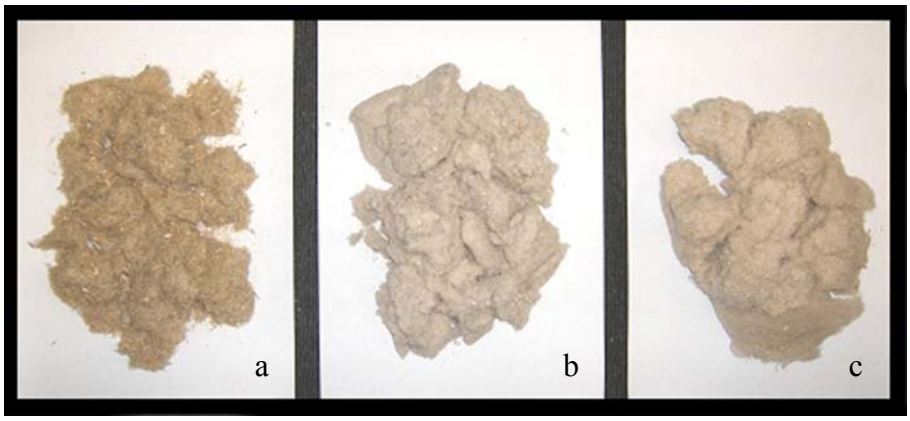

Figure 4.1 Granulated hemp fibre showing colour differences: a) Untreated hemp fibre, b) NaOH treated hemp fibre and c) NaOH/Na_2SO_3 treated hemp fibre.

As mentioned previously, reductions in the average alkali treated fibre diameters were thought to be due to the removal of alkali-soluble compounds from the fibre wall. The relationship between fibre diameter and fibre lignin content can be seen in Figure 4.2. This figure provides further evidence that the average fibre

diameter does in fact decrease with the removal of lignin from the fibre. As the lignin content of untreated hemp bast fibre is relatively low in comparison to the hemicellulose and pectin contents (Table 2.5 in Chapter 2), it is unlikely that the diameter reductions observed for alkali treated fibres are only due to the removal of lignin. It is known that lignin is less soluble in solvents and less prone to thermal degradation than hemicelluloses and pectins [14, 16, 32, 35], so it can be assumed that these two constituents are removed to a greater extent than lignin during the alkali fibre treatment processes.

The fibre mass losses of 41.3% experienced during the NaOH fibre treatment and 32.1% experienced during the NaOH/Na_2SO_3 fibre treatment further verify that other cementing materials are removed along with lignin during fibre treatment.

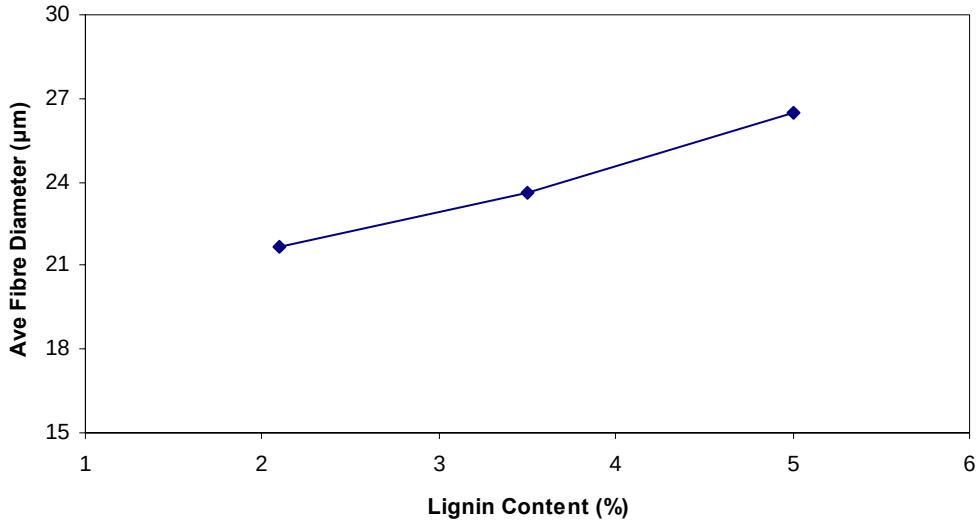

Figure 4.2 Relationship between lignin content and fibre diameter of untreated and alkali treated hemp fibres.

4.1.3 Fibre Separation

Scanning electron micrographs of untreated and alkali treated fibres (Figure 4.3, Figure 4.4 and Figure 4.5) were examined to evaluate the degree of fibre separation. Both alkali treatments resulted in greater levels of fibre separation when compared to the untreated fibre, but it was observed that the NaOH

treatment resulted in fewer numbers of unseparated fibre bundles compared to the $NaOH/Na_2SO_3$ treatment. This was expected, as the NaOH treatment is more effective than the $NaOH/Na_2SO_3$ treatment in removing the lignin and pectins that bind the individual fibres together.

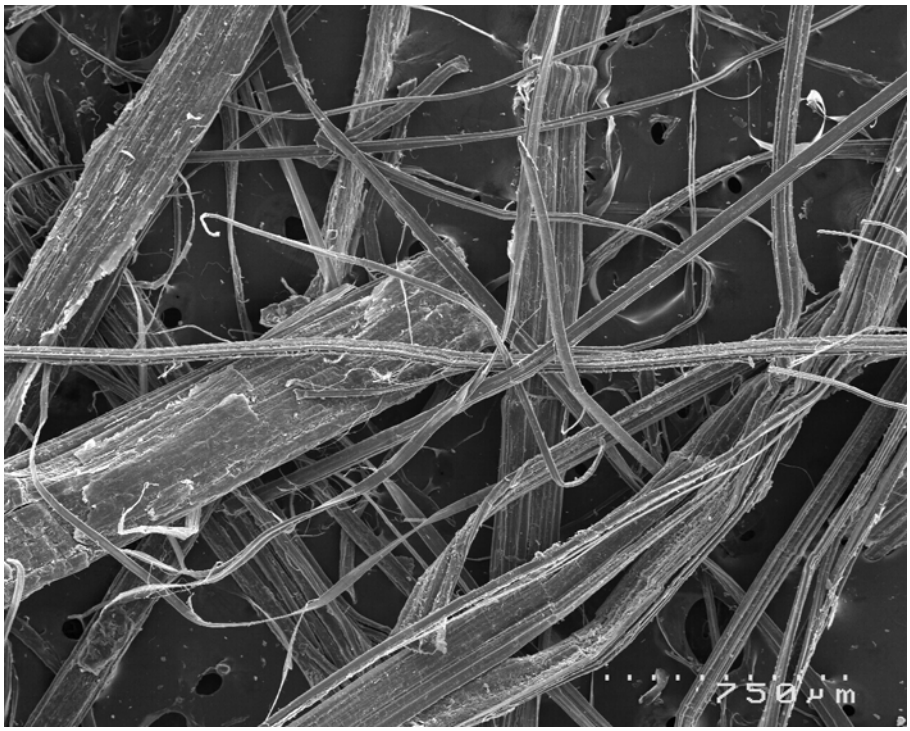

Figure 4.3 Scanning Electron Micrograph (SEM) of untreated hemp fibres showing poor fibre separation.

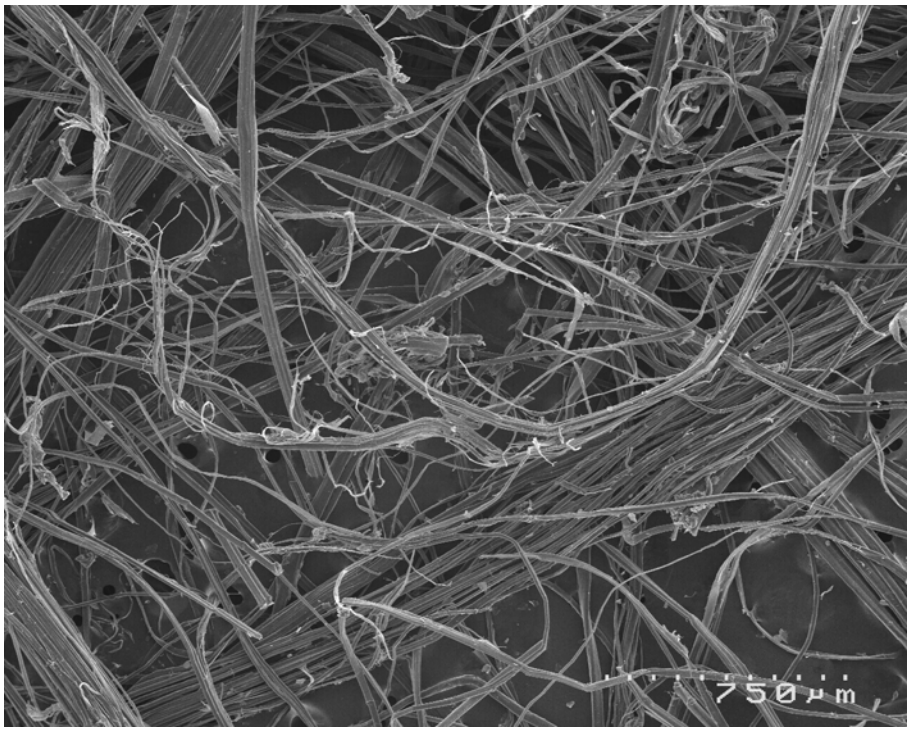

Figure 4.4 Scanning Electron Micrograph (SEM) of NaOH treated hemp fibres showing good fibre separation.

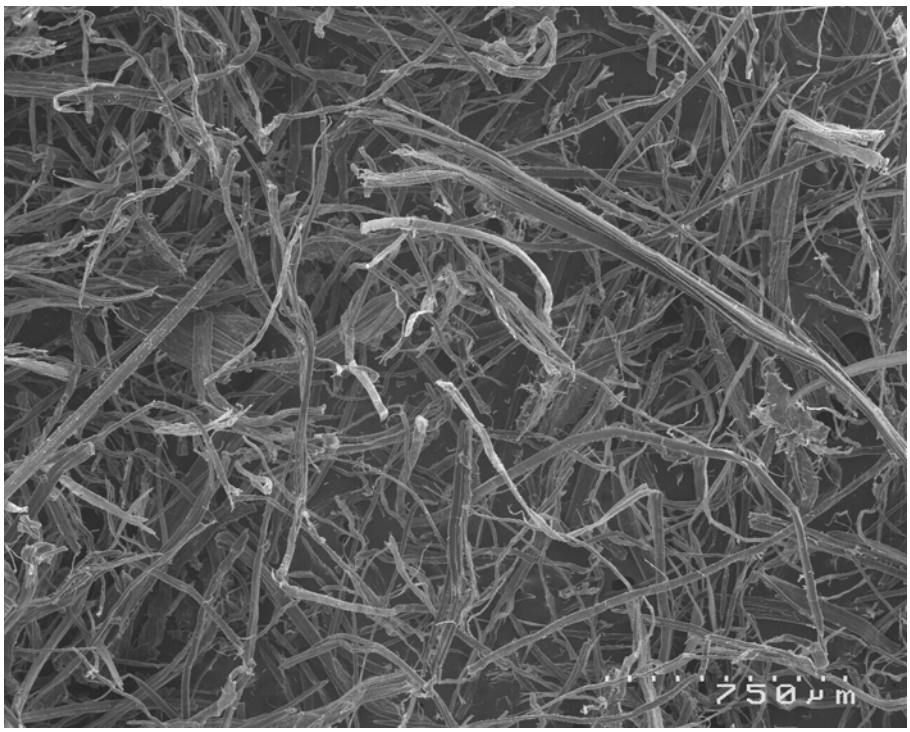

Figure 4.5 Scanning Electron Micrograph (SEM) of NaOH/Na_2SO_3 treated hemp fibres showing good fibre separation.

4.1.4 Microscopic Evaluation of Untreated and Alkali Treated Fibres

The surfaces of untreated and alkali treated fibres were observed by means of a scanning electron microscope (SEM). Untreated fibres can be seen in Figures 4.6(a) and 4.6(b), NaOH treated fibres can be seen in Figures 4.7(a) and 4.7(b), and NaOH/Na_2SO_3 treated fibres can be seen in Figures 4.8(a) and 4.8(b). From the SEM micrographs, it can be observed that the gummy polysaccharides of lignin, pectin and hemicellulose are localized on the surfaces of the untreated fibres. In contrast, the NaOH and NaOH/Na_2SO_3 treated fibres appear to have clean but rough surfaces containing large numbers of etched striations. The rough surface morphologies of these alkali treated fibres are expected to assist with mechanical interlocking bonding mechanisms when used in composites, and the clean surfaces are expected to provide direct bonding between the MAPP coupling agent and the microfibril cellulose OH groups.

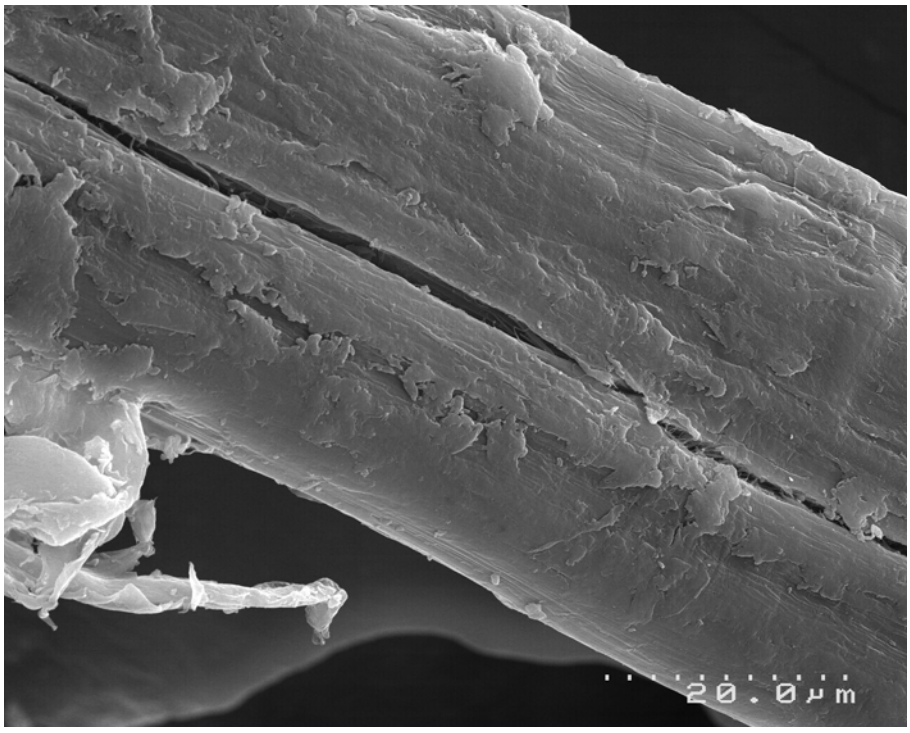

Figure 4.6(a) Scanning Electron Micrograph (SEM) of untreated hemp fibre surface.

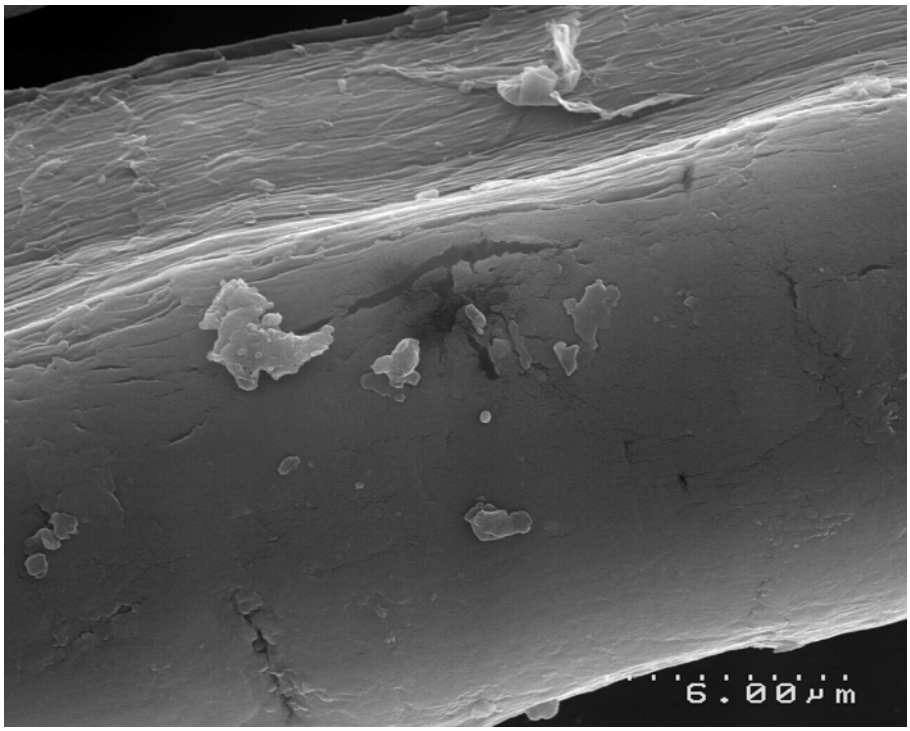

Figure 4.6(b) Scanning Electron Micrograph (SEM) of untreated hemp fibre surface.

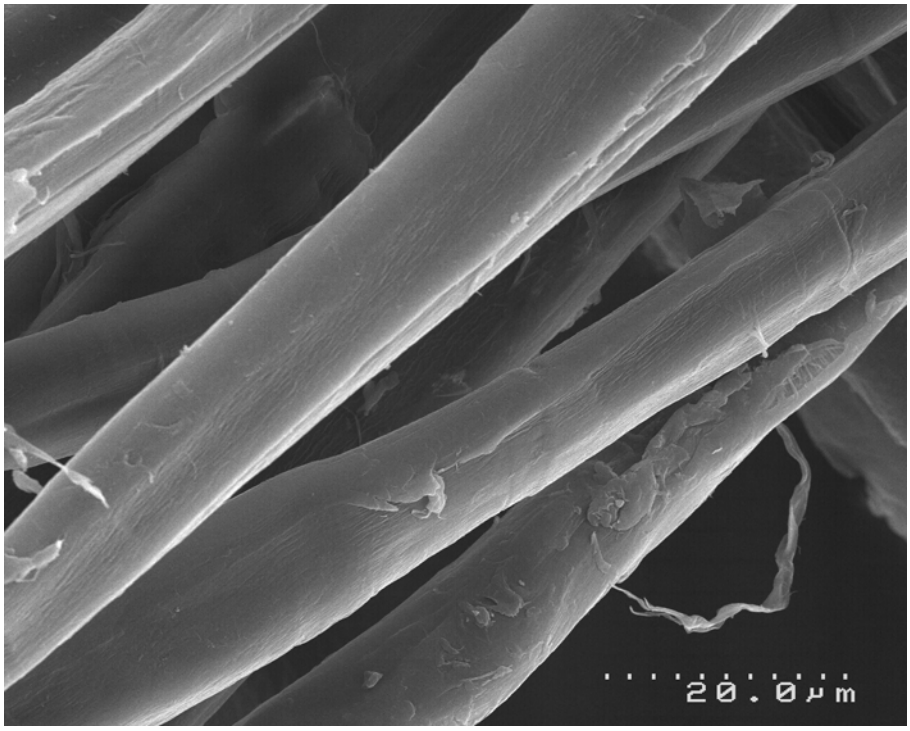

Figure 4.7(a) Scanning Electron Micrograph (SEM) of NaOH treated hemp fibre surface.

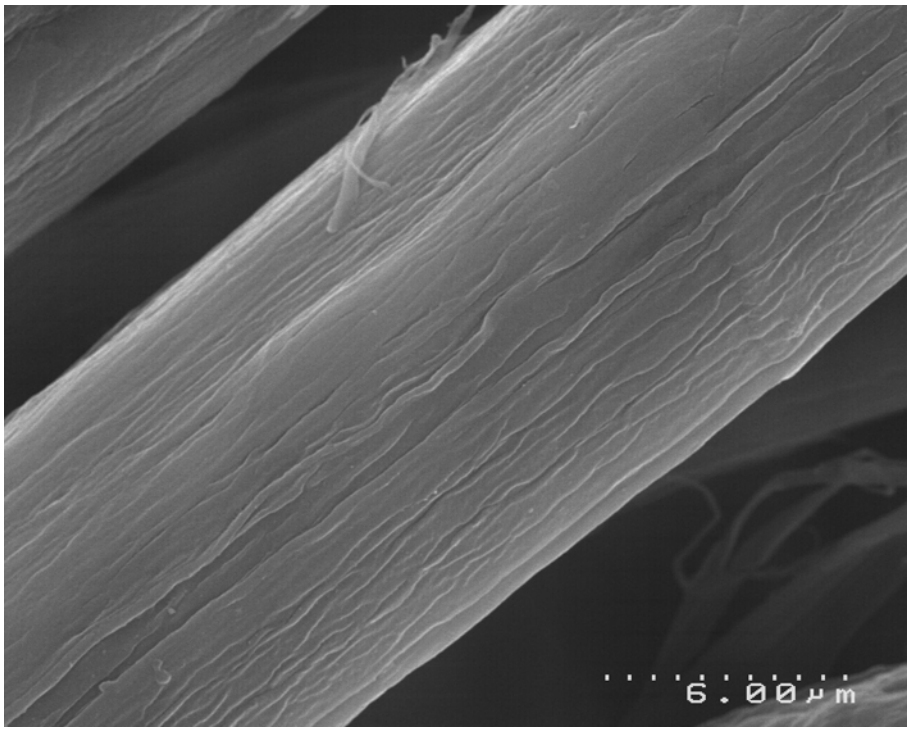

Figure 4.7(b) Scanning Electron Micrograph (SEM) of NaOH treated hemp fibre surface.

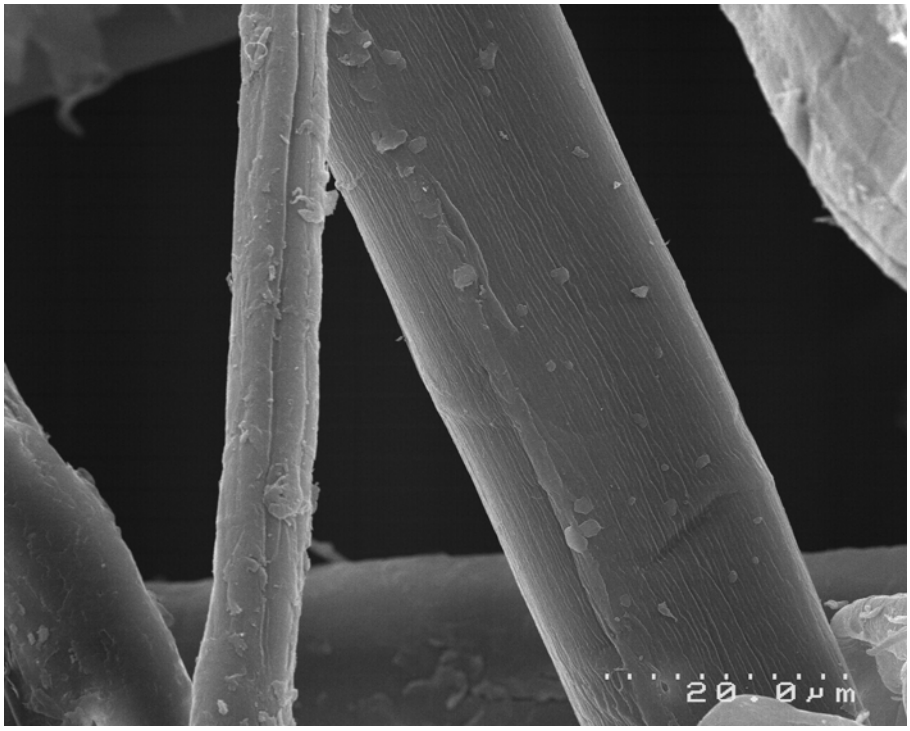

Figure 4.8(a) Scanning Electron Micrograph (SEM) of NaOH/Na_2SO_3 treated hemp fibre surface.

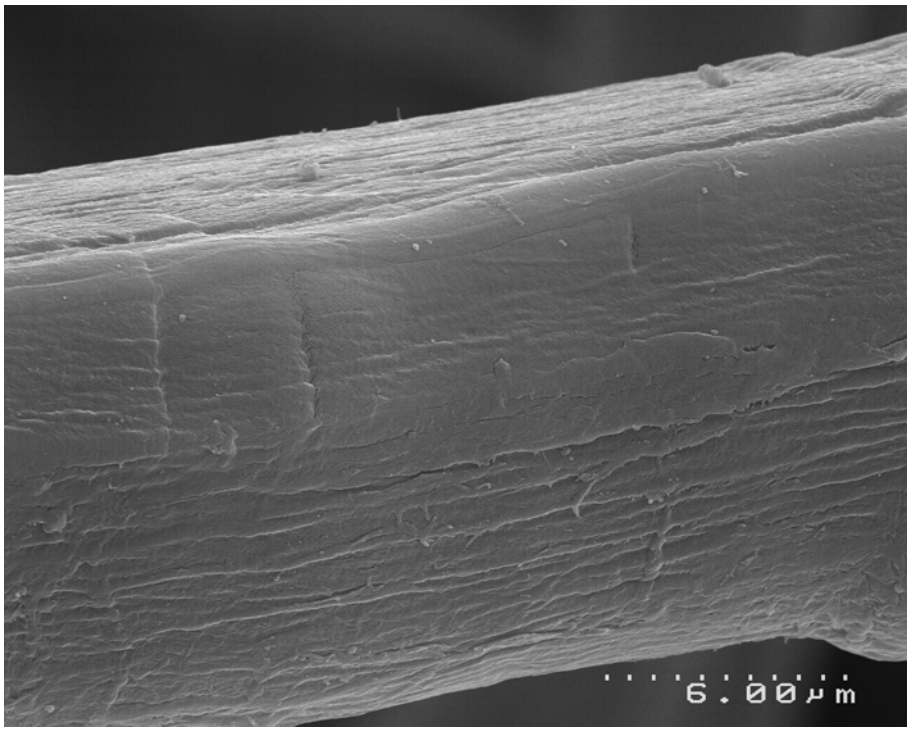

Figure 4.8(b) Scanning Electron Micrograph (SEM) of NaOH/Na_2SO_3 treated hemp fibre surface.

4.1.5 Determination of Fibre Crystallinity Index by Means of X-Ray Diffraction

X-ray diffraction is a useful method for evaluating the crystallographic structure of semi-crystalline materials such as hemp fibre. It can be used to evaluate the crystallinity of crystallographic planes present within the sample material, from which it is possible to determine the crystallinity index of the sample.

The X-ray diffractograms of untreated, NaOH treated and NaOH/Na_2SO_3 treated hemp fibre can be seen in Figure 4.9. It can be observed that the major crystalline peak of each profile occurred at around $2\theta = 22.7^{o}$, which represents the cellulose crystallographic plane (002). The X-ray diffractograms show that the intensity of the (002) crystallographic plane was increased significantly as a result of the alkali fibre treatments.

The fibre crystallinity index (I_c) of the treated and untreated hemp samples was calculated using Equation 4.1 [147], and the results are summarised in Table 4.3.

$$I_c = \left(\frac{I_{002} - I_{am}}{I_{002}} \right) x100 \qquad (4.1)$$

where I_{002} is the maximum intensity of diffraction of the (002) lattice peak at a 2θ angle of between 22° and 23°; and I_{am} is the intensity of diffraction of the amorphous material, which is taken at a 2θ angle between 18° and 19° where the intensity is at a minimum [148]. It should be noted that the crystallinity index is useful only on a comparison basis as it is used to indicate the order of crystallinity rather than the crystallinity of crystalline regions [76].

Table 4.3 Crystallinity index of untreated and alkali treated hemp fibre.

	I_{am} (2θ = 18.3°)	I_{002} (2θ = 22.7°)	Crystallinity Index (%)
Untreated Hemp	828	5409	84.7
NaOH treated hemp	791	7622	89.6
NaOH/Na_2SO_3 treated hemp	885	8087	89.1

It can be seen in Table 4.3 that the crystallinity index of hemp fibre was increased by alkali treatment. As previously mentioned, this is thought to be due to better packing and stress relaxation of cellulose chains as a result of the removal of pectins and other amorphous constituents from the fibre. It can also be seen that fibre treated with NaOH has a slightly higher crystallinity index compared to fibre treated with NaOH/Na_2SO_3.

Other well-defined peaks present on the X-ray diffractograms are at 2θ = 15.2° and 2θ = 16.6°, and these reflections correspond with the (110) and ($1\bar{1}0$) crystallographic planes, respectively [76]. When the crystalline cellulose content is high, these two peaks are more pronounced, and when the fibre contains large amounts of amorphous material (such as lignin, hemicelluloses, pectins and

amorphous-cellulose), these two peaks are smeared and appear as one broad peak [147]. It can be seen in Figure 4.9 that the peaks at 15.2° and 16.6° are well defined for both the NaOH and the NaOH/Na_2SO_3 treated hemp fibres. The peaks for NaOH treated fibre, however, are better defined than those for NaOH/Na_2SO_3 treated fibre, suggesting that the NaOH treatment was responsible for the removal of a greater amount of amorphous material from the fibre than the NaOH/Na_2SO_3 treatment. This is also supported by the fact that the crystallinity index of the NaOH fibre is higher than that of the NaOH/Na_2SO_3 treated fibre.

The increase in fibre crystallinity is thought to be the main factor contributing to the increase in tensile strength of NaOH/Na_2SO_3 treated fibres, as seen in Table 4.1. The decrease in tensile strength of NaOH treated fibres may be due to the removal of excessive amounts of amorphous material, including pectins and lignin, which are responsible for binding the cellulose microfibrils together in the fibre.

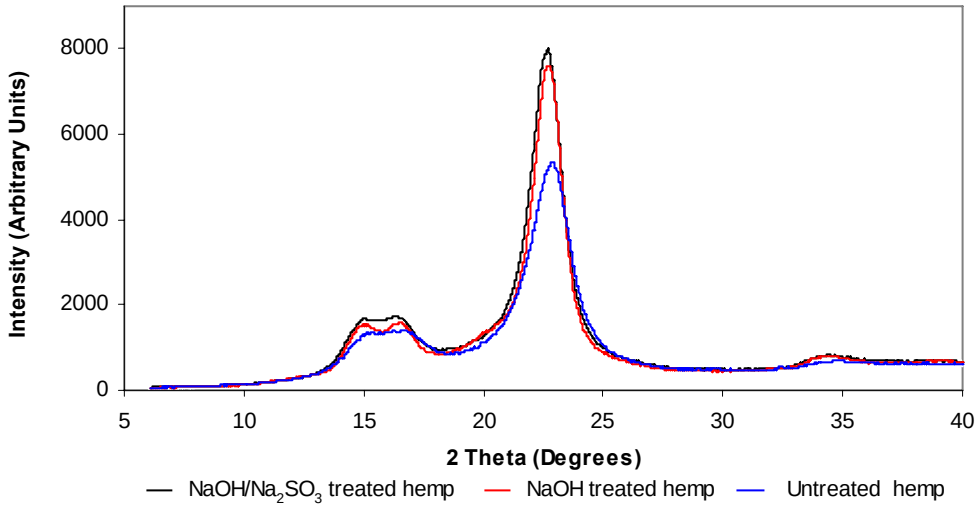

Figure 4.9 X-ray diffraction profiles of untreated and alkali treated hemp fibre.

4.2 Evaluation of Extruded and Injection Moulded Composites

4.2.1 The Effects of Injection Moulder Processing Conditions on Composite Mechanical Properties

It is known that the mixing of a polymer melt can be enhanced during the injection moulding process by optimising processing conditions such as screw rotation speed, back pressure and injection pressure [149].

Screw rotation speed is a measure of the number of revolutions per minute (rpm) of the injection screw, and faster screw speeds can lead to better mixing of polymeric melts [149]. This improvement in mixing is due to the generation of higher shear forces at higher screw speeds, which can cause large agglomerates to break down into small particles and distribute uniformly throughout the melt [149].

Back pressure is the counter pressure or force applied to the back of the injection screw during screw recovery (when the screw returns to it's injection position), to provide a constant pressure on the polymer melt as additional polymer is drawn into the injection barrel. An increase in back pressure results in improvements in dispersion and distribution of the melt due to increased levels of shear stress. An increase in back pressure also induces more frictional heat inside the barrel, which reduces the melt viscosity and increases the pressure flow and circulation of the melt inside the barrel [149].

Injection pressure is the pressure on the face of the injection screw when injecting material into the mould. Higher injection pressures can result in higher shear and frictional forces within the melt material.

It can thus be said that improved mixing of a polymeric melt or a particle-filled polymeric melt can be achieved by increasing the screw rotation speed, back pressure and injection pressure. However, increases in these variables can lead to fibre damage in short fibre reinforced composites, and hence reductions in mechanical properties in the final part [51]. Screw rotation speed, back pressure and injection pressure should therefore be kept low to minimize fibre damage.

In this investigation, it was attempted to ascertain the effects of two different injection moulder set-ups on the mechanical properties of composites containing 40wt% NaOH treated hemp fibre, polypropylene, and either 4wt% or 5wt% maleic anhydride modified polypropylene (MAPP).

The first set-up consisted of relatively high injection moulder settings, which are as follows: 83% injection pressure, 40% back pressure, and 250 rpm screw rotation speed. The second set-up consisted of relatively low injection moulder settings, which are as follows: 55% injection pressure, 30% back pressure, and 100 rpm screw rotation speed.

It can be seen in Figure 4.10 and Figure 4.11 that variations in the injection moulder settings made virtually no difference to the tensile strength and Young's modulus of injection moulded composites. It is known that extensive fibre and polymer mixing occurs during composite extrusion; and it is thought that no further improvements in mixing were achieved by means of injection moulding, even though relatively high injection pressures, back pressures and screw speeds were used. It is also suspected that the two injection moulder set-ups resulted in the same amount of fibre damage during injection moulding, which may explain why no differences were observed in the composite mechanical properties associated with each set-up.

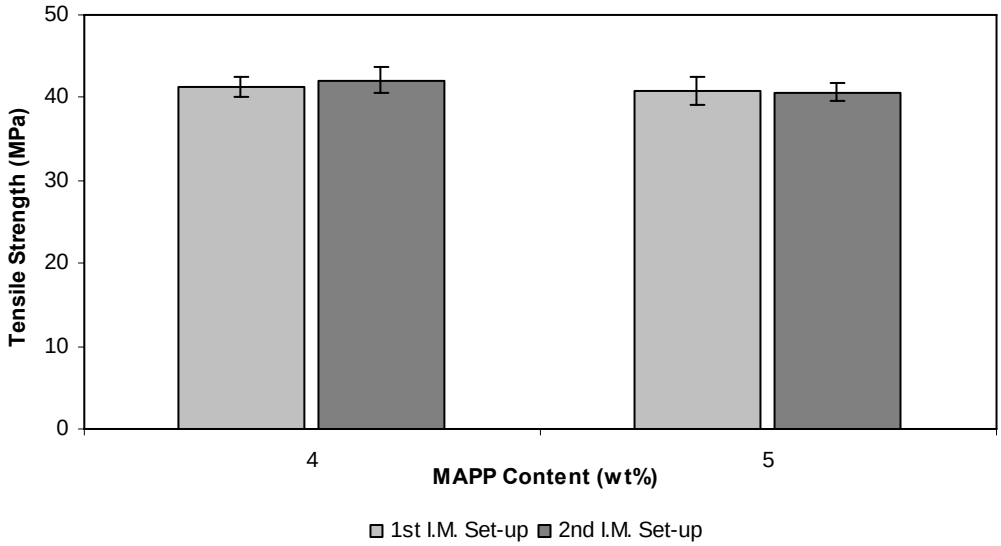

Figure 4.10 Effects of injection moulder processing conditions on the tensile strength of composites containing 40wt% NaOH treated hemp fibre. The error-bars each represent ± 1 standard deviation.

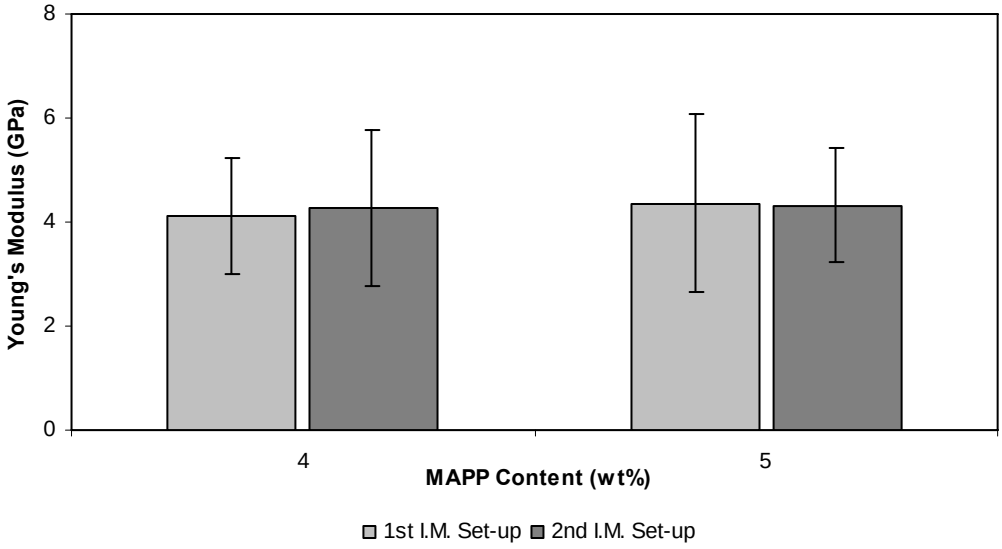

Figure 4.11 Effects of injection moulder processing conditions on the Young's modulus of composites containing 40wt% NaOH treated hemp fibre. The error-bars each represent ± 1 standard deviation.

4.2.2 The Effects of Fibre Content on Composite Mechanical Properties

In this investigation, a range of composites was produced using different quantities of NaOH treated NZ hemp fibre, polypropylene and 2wt% MAPP. From the results in Figure 4.12, it can be seen that composite tensile strength increased with increasing hemp fibre content up to a maximum of 37.6 MPa at a fibre content of 40wt%, after which a decrease was observed. This decrease in composite strength was shown to be statistically significant by means of a one-tailed Student's t-test at a confidence level of 95% (P<0.05). As the fibres are much stronger than the matrix material, and because there is sufficient fibre-matrix interfacial adhesion due the presence of MAPP, it is understandable that an increase in fibre content resulted in increases in composite strength. However, this trend is only true up to a certain fibre content, after which there is insufficient polymer in the composite to provide adequate wetting of the fibres. It was observed that composites containing 50wt% hemp were extremely difficult to extrude and injection mould, as the high fibre and low polymer contents resulted in highly viscous melts with poor fibre wetting with the polymer matrix. The increase in fibre content beyond 40wt% also resulted in reductions in fibre dispersion in the composites, which may have further contributed to the observed decreases in composite strength.

The results in Figure 4.13 show that an increase in fibre content greatly improved the Young's modulus of the composites, and the relationship between fibre content and Young's modulus appears almost linear. It can be seen that the stiffest composite contained 50wt% fibre, and had a Young's modulus of 5.93 GPa. The increase in Young's modulus with increasing fibre content is well documented [91, 150, 151], and is due to the fact that the fibres possess much higher Young's moduli than the matrix material.

From this investigation, it was concluded that a composite containing 40wt% fibre provided the best combination of tensile strength, Young's modulus and process ability.

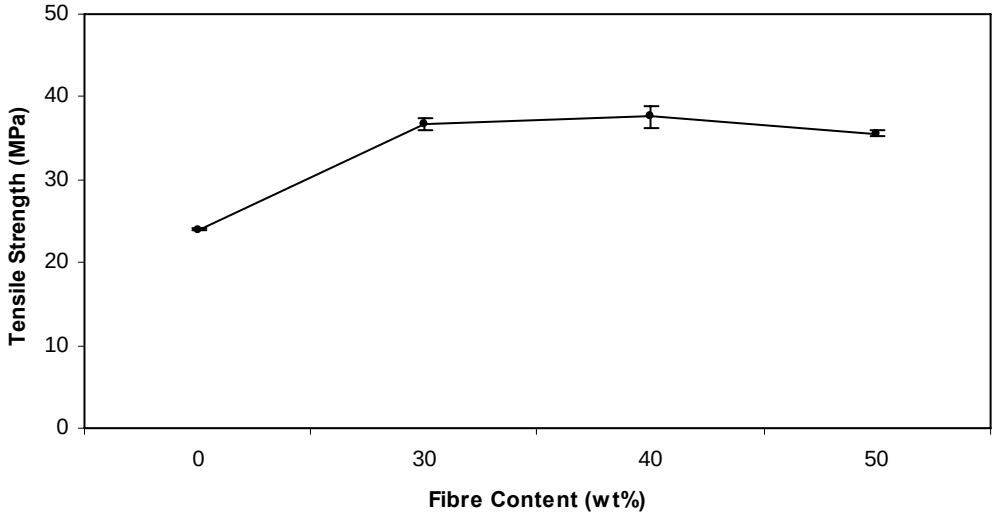

Figure 4.12 Effects of fibre content on the tensile strength of composites containing NaOH treated NZ hemp fibre. The error-bars each represent ± 1 standard deviation.

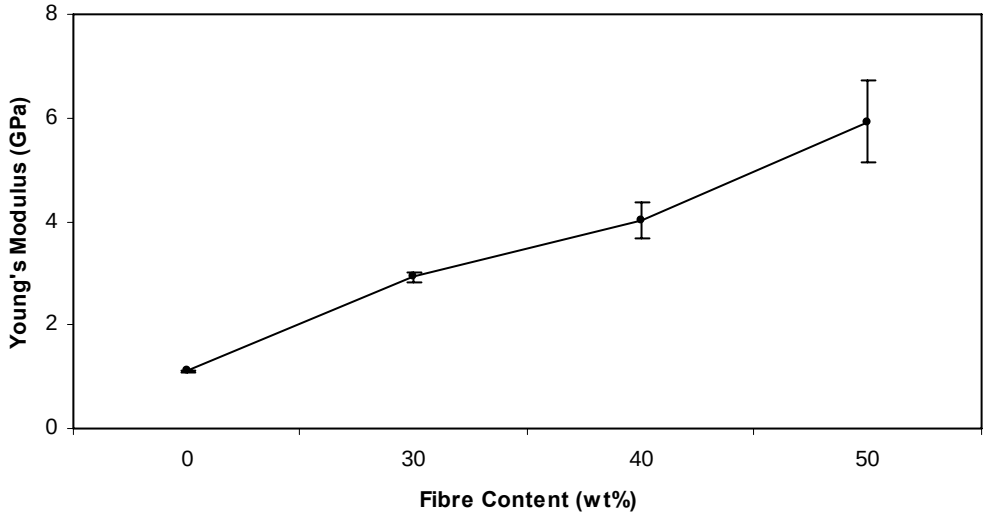

Figure 4.13 Effects of fibre content on the Young's modulus of composites containing NaOH treated NZ hemp fibre. The error-bars each represent ± 1 standard deviation.

4.2.3 The Effects of Fibre Treatment and MAPP Content on Composite Mechanical Properties

A range of composites was produced from 40wt% untreated, NaOH and $NaOH/Na_2SO_3$ treated hemp fibre, polypropylene and varying MAPP contents. From the results in Figure 4.14, it can be seen that all composites showed an increase in tensile strength with the addition of MAPP. MAPP improves the adhesion between fibre and matrix by chemically bonding to available OH groups on the fibre surface, and then adhering to the matrix through molecular chain entanglement. Not all OH groups on the fibre surface are available for bonding with MAPP, as many are bonded to cementing materials (i.e. lignin, hemicelluloses and pectins) and water.

For composites containing untreated fibre, there was no significant increase in strength when the MAPP content was increased from 2wt% to 5wt%. This was thought to be due to the fact that 2wt% MAPP was sufficient to saturate most of the available OH groups present on the surfaces of the untreated fibres.

Composites containing NaOH treated fibres showed a progressive strength increase when the MAPP content was increased from 0wt% to 4wt%, and a slight strength decrease at 5wt% MAPP. Alkali treatments separate the fibre bundles into elementary fibres by degrading the cementing materials that bind the fibres together. This separation results in an increase in the effective surface area of the fibre which is available for bonding with the MAPP coupling agent [74]. As alkali treated fibres collectively have larger surface areas, it is assumed that there are more OH groups available on the fibre surfaces for chemical bonding, and thus more MAPP is required to saturate these OH groups. A MAPP content of 4wt% was thought to be sufficient to saturate most of the available OH groups present on the NaOH treated fibres.

The results in Figure 4.14 also show that composites containing 4wt% MAPP and reinforced with NaOH and NaOH/Na_2SO_3 treated fibres appeared stronger than composites containing the same MAPP content and untreated fibre. It is assumed that alkali treated fibres have greater numbers of OH groups available for bonding with MAPP, resulting in improved fibre-matrix adhesion and stronger composites when sufficient MAPP is provided [75].

Composites containing NaOH/Na_2SO_3 treated fibre and 4wt% MAPP appeared significantly stronger than composites containing NaOH treated fibre and 4wt% MAPP. As both fibre treatments resulted in adequate levels of fibre separation and subsequent increases in fibre surface area, the difference in composite strength was attributed to the higher tensile strength of the NaOH/Na_2SO_3 treated fibres.

From the results in Figure 4.15, it can be seen that there is no particular trend linking MAPP content or fibre treatment to composite Young's modulus. The results of Maldas and Kokta [39] and Mutjé *et al.* [152] also showed no distinct connection between MAPP concentration and composite Young's modulus for wood flour filled polypropylene composites and hemp fibre reinforced polypropylene composites, respectively. It can also be seen in Figure 4.15 that there are large data standard deviations, indicating that there were significant variations in Young's modulus between composite specimens during testing.
It can thus be seen in Figure 4.14 and Figure 4.15 that the strongest and stiffest composite produced by means of extrusion and injection moulding consisted of 40wt% NaOH/Na_2SO_3 treated fibre, polypropylene and 4wt% MAPP. The tensile strength and Young's modulus of this composite are 50.5 MPa and 5.3 GPa, respectively.

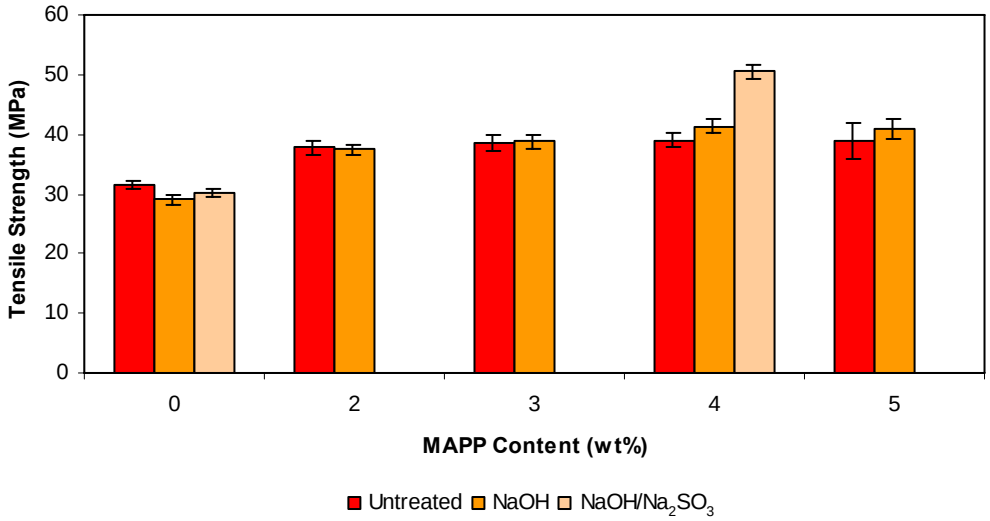

Figure 4.14 Effects of fibre treatment and MAPP content on the tensile strength of composites containing 40wt% hemp fibre. The error-bars each represent ± 1 standard deviation.

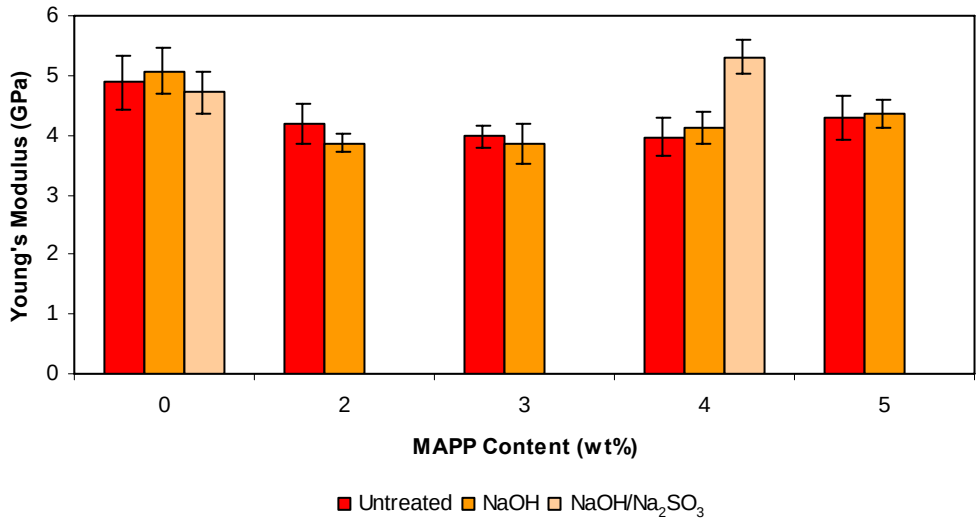

Figure 4.15 Effects of fibre treatment and MAPP content on the Young's modulus of composites containing 40wt% hemp fibre. The error-bars each represent ± 1 standard deviation.

The fracture surfaces of composites containing untreated, NaOH and $NaOH/Na_2SO_3$ treated hemp fibre, polypropylene and either 0wt% or 4wt% MAPP were viewed by means of a scanning electron microscope, and the associated micrographs can be seen in Figures 4.16a to 4.21b.

It can be seen in Figure 4.16(a, b), Figure 4.18(a, b) and Figure 4.20(a, b) that the composites without the MAPP coupling agent showed very poor fibre-matrix interfacial adhesion. There is much fibre-pullout, as is evident by the large number of unbroken fibres sticking out of the fracture surfaces, as well as the large number of holes present in the matrix from which the fibres were pulled out. The protruding fibres that are visible in these micrographs appear smooth and clean, and there is no evidence of polypropylene adhering to the fibre surfaces. It is apparent that composites without MAPP fail by means of fibre de-bonding and tensile failure of the matrix.

It can be seen in Figure 4.17(a, b), Figure 4.19(a, b) and Figure 4.21(a, b) that the addition of 4wt% MAPP greatly improved the fibre-matrix adhesion. There is less evidence of fibre pullout, and the polypropylene matrix appears to have adhered strongly to the fibre surfaces. Very few fibres can be observed on the fracture surfaces due to fibre concealment by the matrix material, although a few severely damaged fibres can be seen protruding out of the matrix. These fibres appear to have split longitudinally down the fibre length, and this is thought to be the result of microfibril shearing within fibres that were not positioned axially to the direction of induced stress. These micrographs provide strong evidence that the MAPP containing composites fail mostly by local shear yielding of the matrix around the fibre, rather than tensile failure of the fibres or fibre de-bonding.

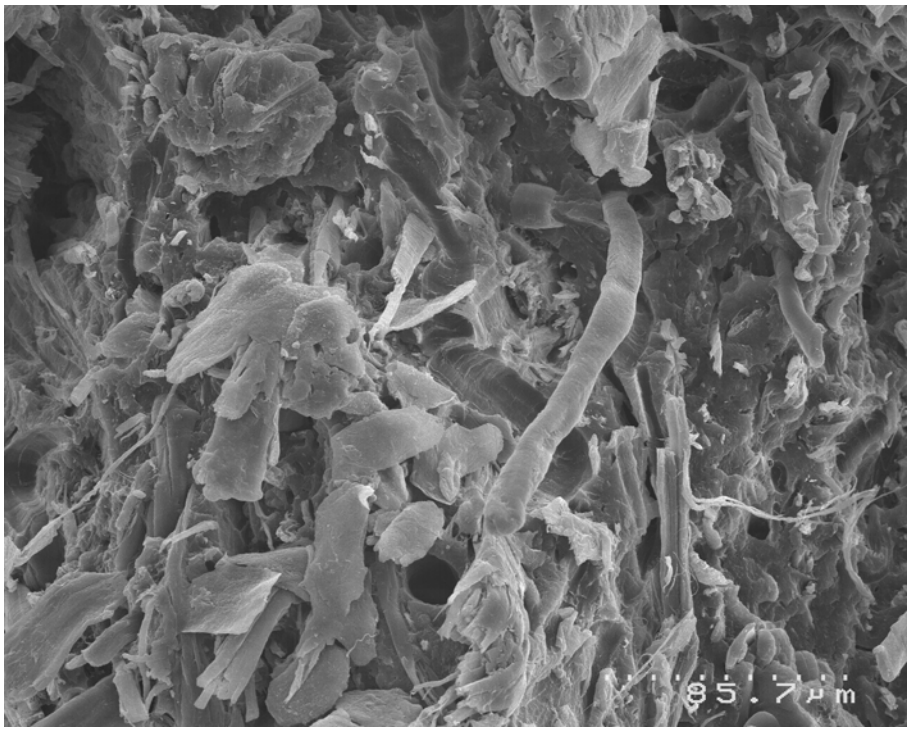

Figure 4.16(a) Scanning Electron Micrograph (SEM) of the fracture surface of an extruded and injection moulded composite [40wt% untreated hemp fibre, PP and 0wt% MAPP].

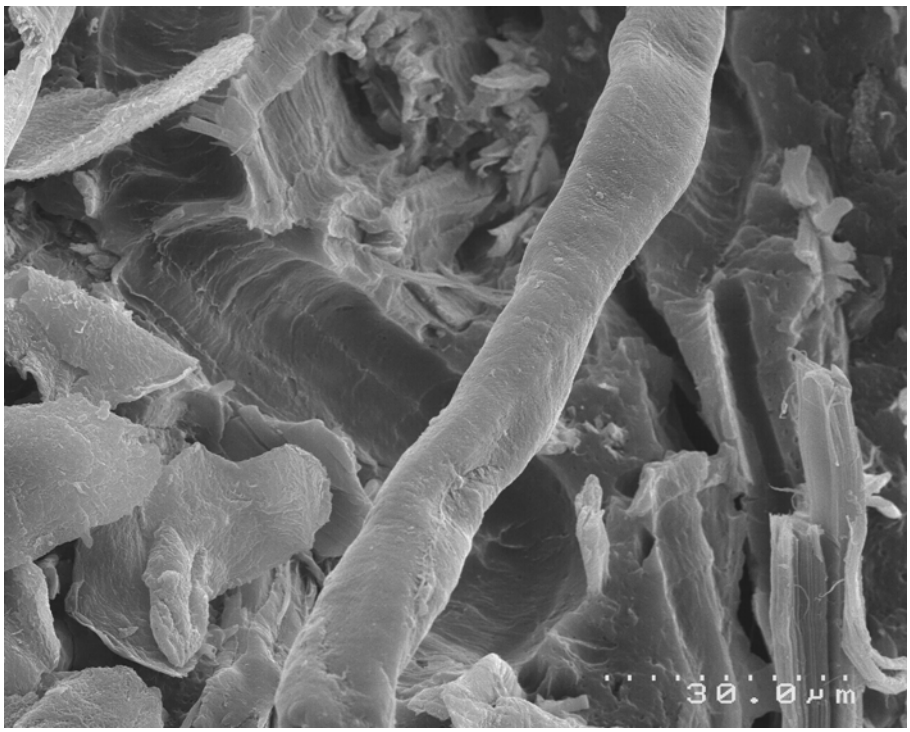

Figure 4.16(b) Scanning Electron Micrograph (SEM) of the fracture surface of an extruded and injection moulded composite [40wt% untreated hemp fibre, PP and 0wt% MAPP].

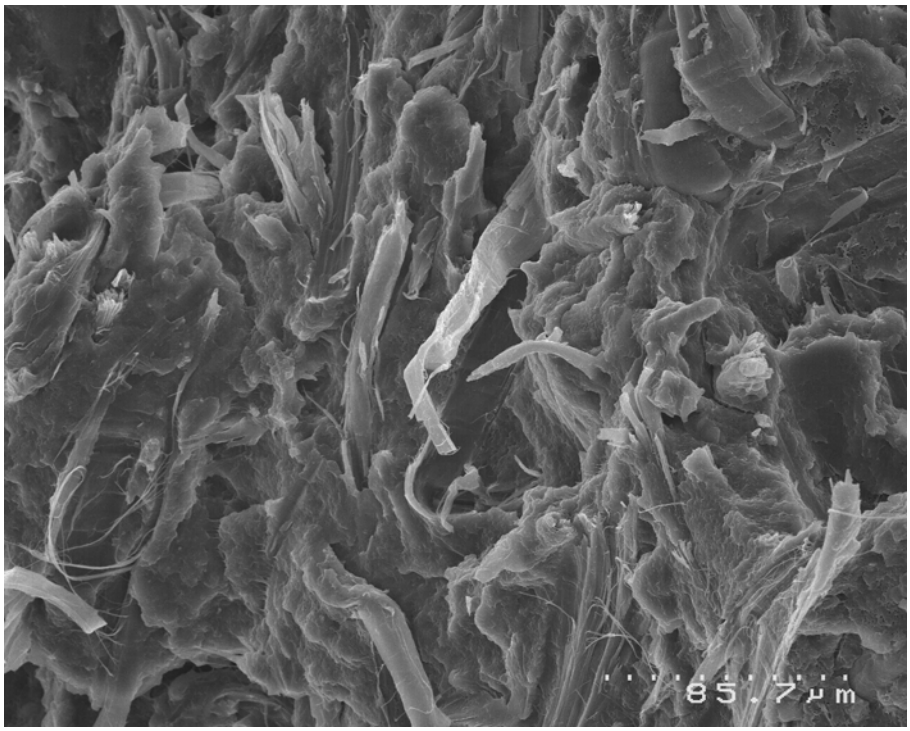

Figure 4.17(a) Scanning Electron Micrograph (SEM) of the fracture surface of an extruded and injection moulded composite [40wt% untreated hemp fibre, PP and 4wt% MAPP].

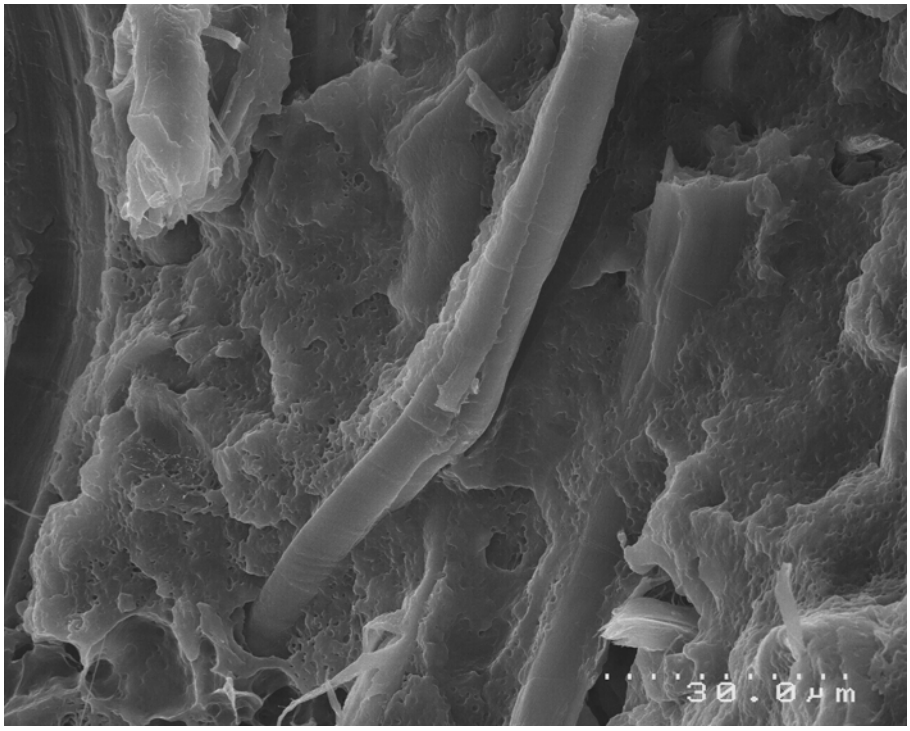

Figure 4.17(b) Scanning Electron Micrograph (SEM) of the fracture surface of an extruded and injection moulded composite [40wt% untreated hemp fibre, PP and 4wt% MAPP].

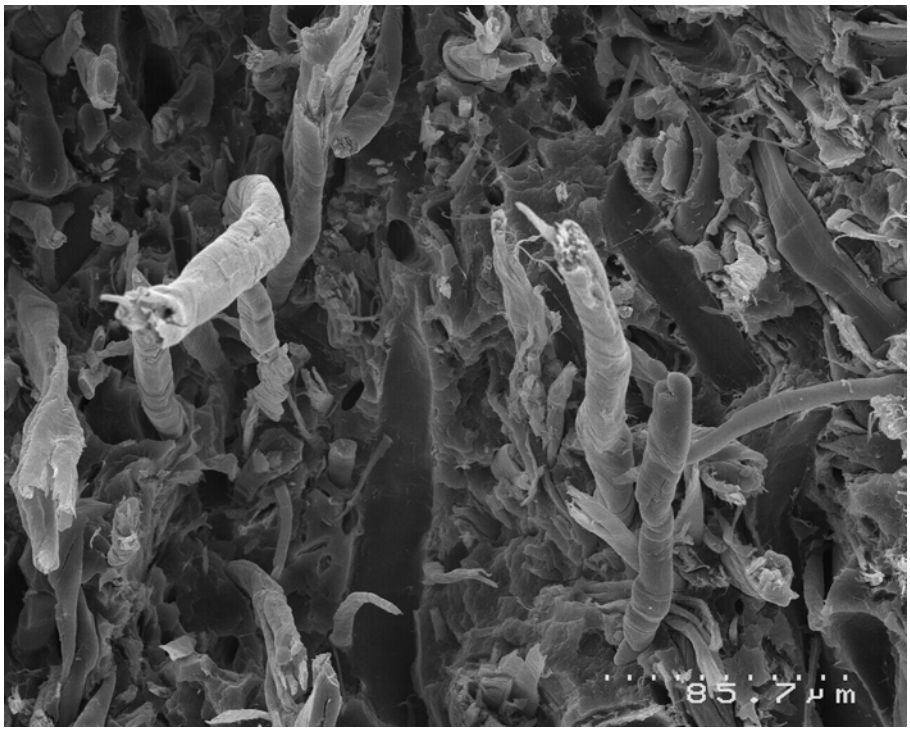

Figure 4.18(a) Scanning Electron Micrograph (SEM) of the fracture surface of an extruded and injection moulded composite [40wt% NaOH treated hemp fibre, PP and 0wt% MAPP].

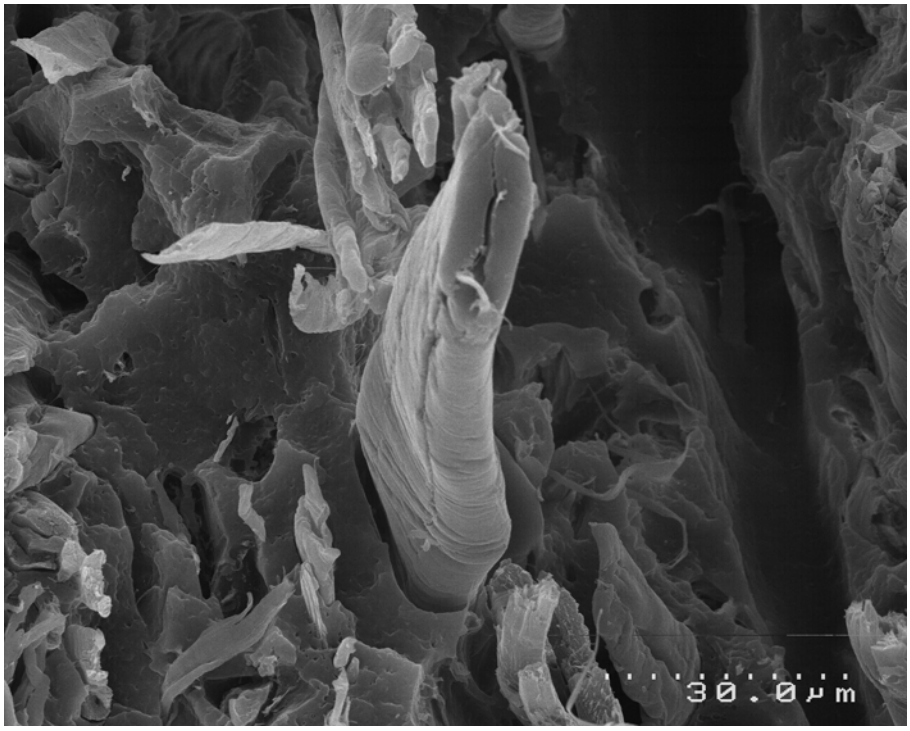

Figure 4.18(b) Scanning Electron Micrograph (SEM) of the fracture surface of an extruded and injection moulded composite [40wt% NaOH treated hemp fibre, PP and 0wt% MAPP].

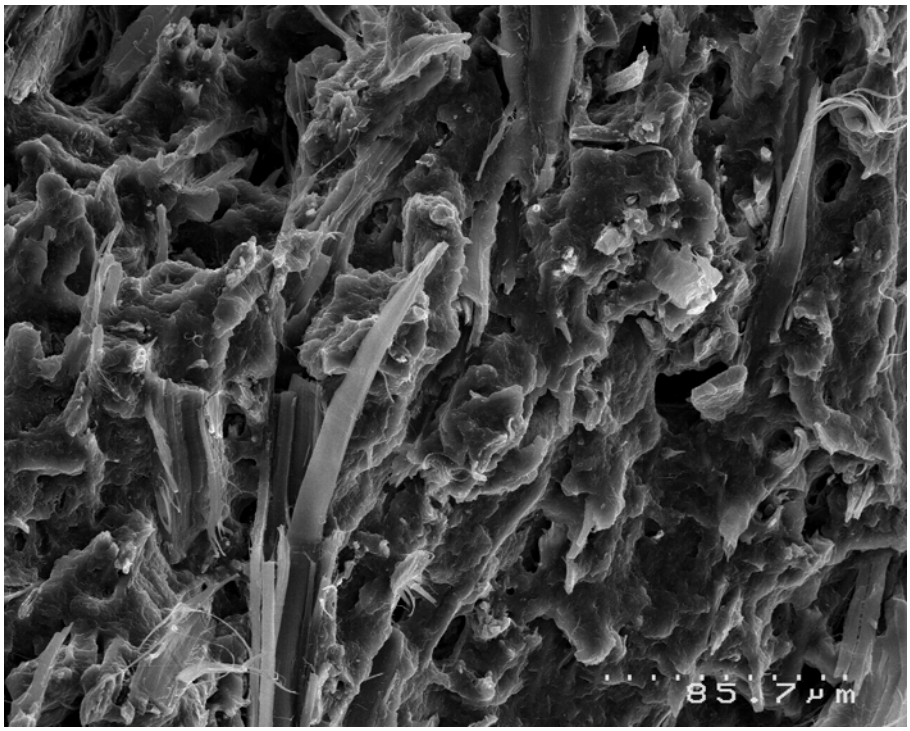

Figure 4.19(a) Scanning Electron Micrograph (SEM) of the fracture surface of an extruded and injection moulded composite [40wt% NaOH treated hemp fibre, PP and 4wt% MAPP].

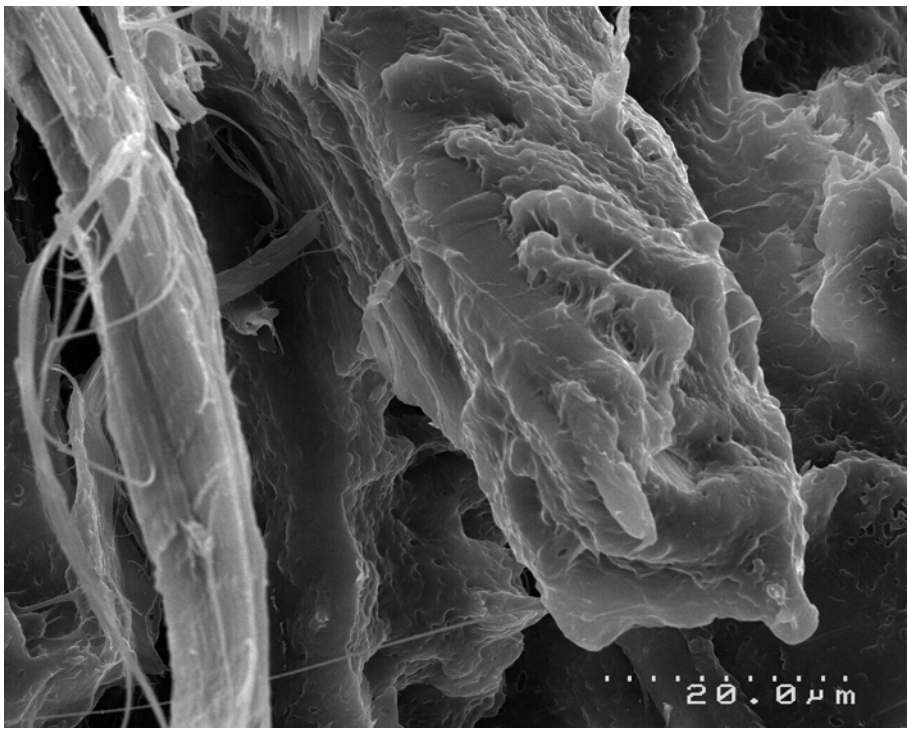

Figure 4.19(b) Scanning Electron Micrograph (SEM) of the fracture surface of an extruded and injection moulded composite [40wt% NaOH treated hemp fibre, PP and 4wt% MAPP].

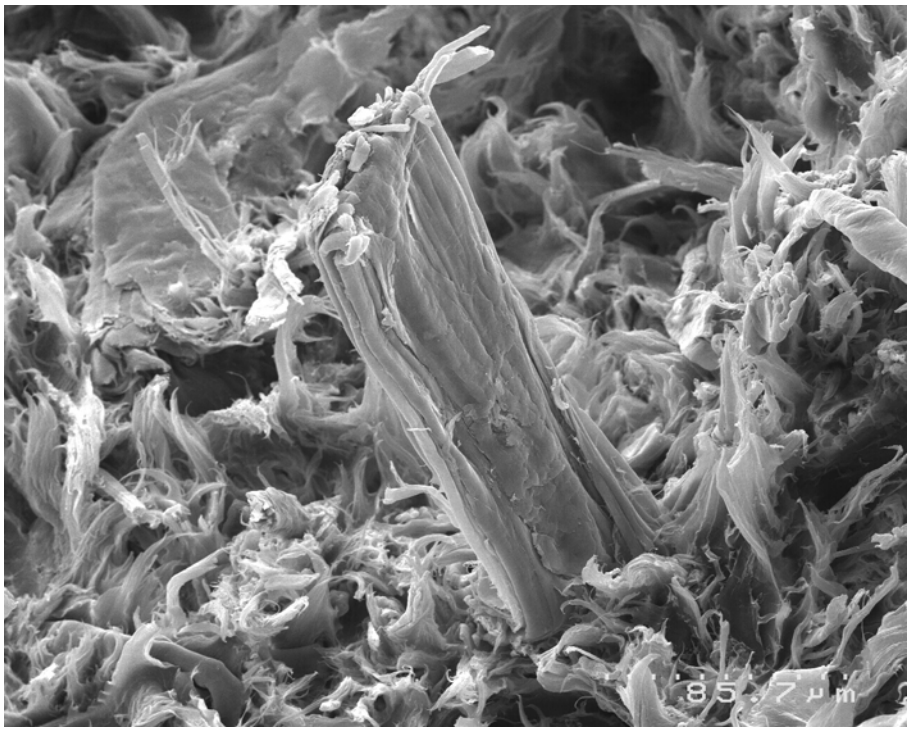

Figure 4.20(a) Scanning Electron Micrograph (SEM) of the fracture surface of an extruded and injection moulded composite [40wt% NaOH/Na_2SO_3 treated hemp fibre, PP and 0wt% MAPP].

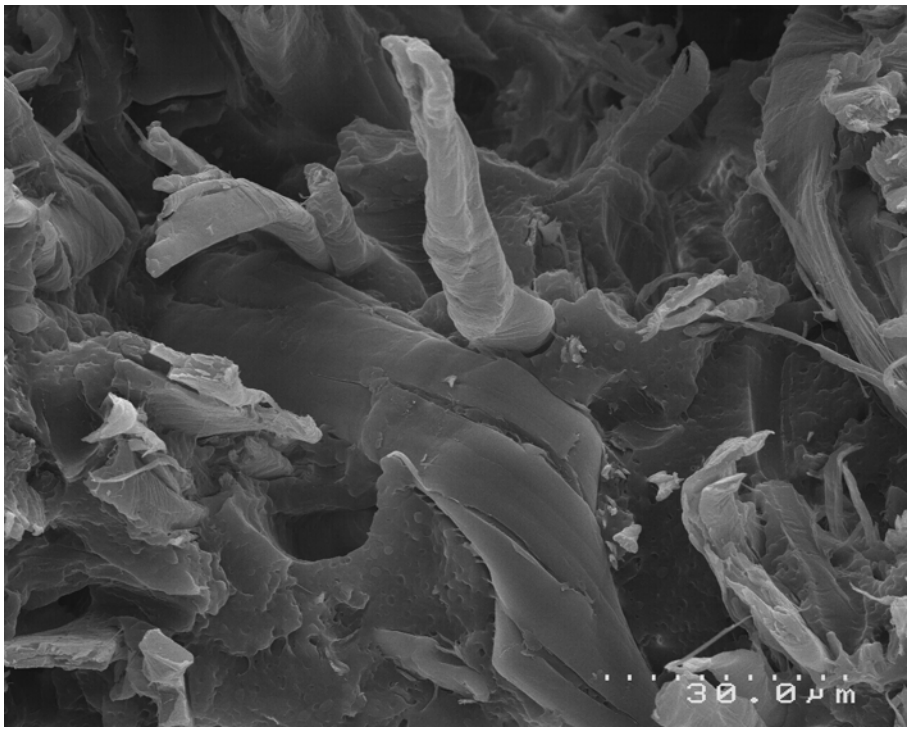

Figure 4.20(b) Scanning Electron Micrograph (SEM) of the fracture surface of an extruded and injection moulded composite [40wt% NaOH/Na_2SO_3 treated hemp fibre, PP and 0wt% MAPP].

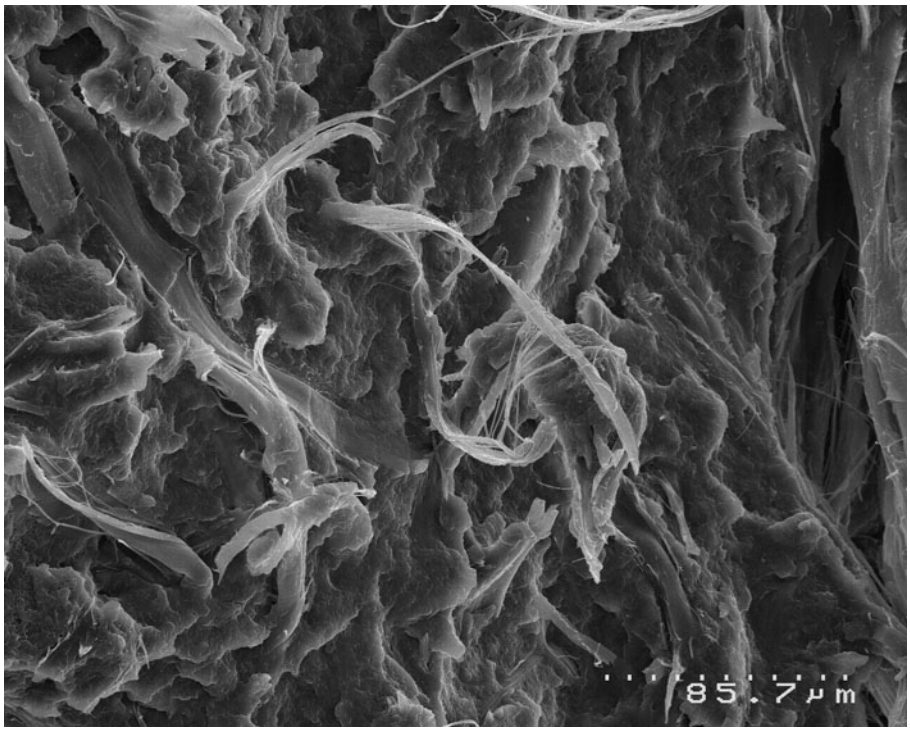

Figure 4.21(a) Scanning Electron Micrograph (SEM) of the fracture surface of an extruded and injection moulded composite [40wt% NaOH/Na_2SO_3 treated hemp fibre, PP and 4wt% MAPP].

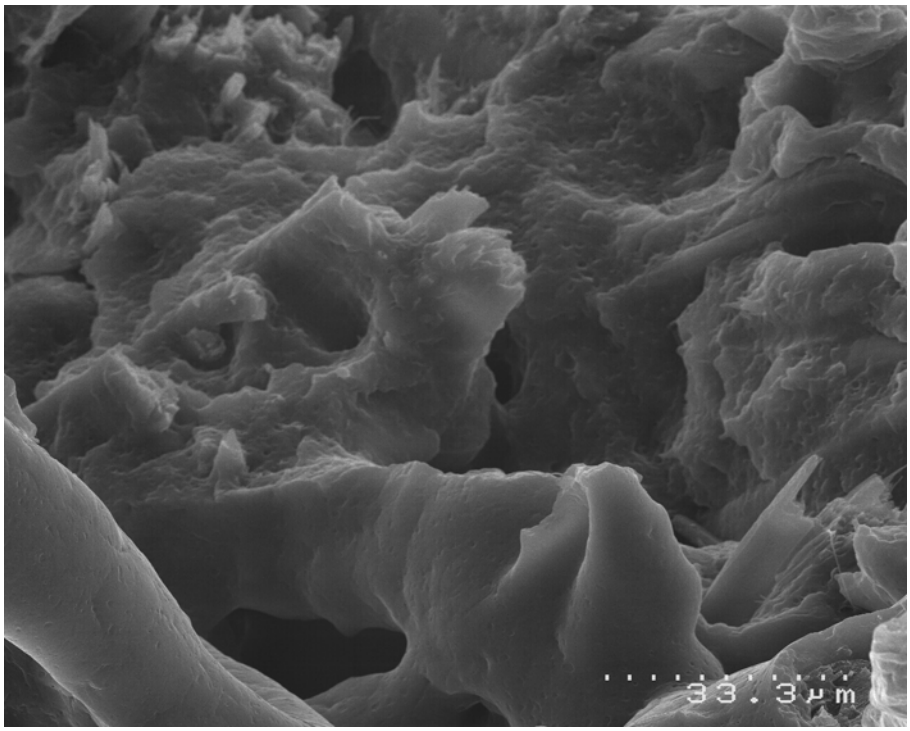

Figure 4.21(b) Scanning Electron Micrograph (SEM) of the fracture surface of an extruded and injection moulded composite [40wt% NaOH/Na_2SO_3 treated hemp fibre, PP and 4wt% MAPP].

To further investigate the bonding of MAPP to the surface of hemp fibres, the polypropylene matrices of composites containing 40wt% $NaOH/Na_2SO_3$ treated hemp fibre, polypropylene and either 0wt% MAPP or 4wt% MAPP were dissolved in hot xylene, and the fibres were extracted and washed in additional xylene. Scanning electron micrographs of hemp fibres extracted from these composites can be seen in Figure 4.22(a, b) and Figure 4.23(a, b).

As can be seen in Figure 4.22(a, b), several polymer particles are present and appear to be loosely bound to fibres extracted from composites produced without MAPP. These particles are not chemically bonded to the fibre surface, and are thought to be matrix residues that were not removed when the fibres were rinsed with the hot solvent.

The micrographs of fibres extracted from composites produced with 4wt% MAPP (Figure 4.23(a, b)) show many polymer particles that appear to be chemically bonded to the fibre surfaces. Since strong covalent bonds are formed between the maleic anhydride functional group of MAPP and the OH groups present on the fibre surface, the MAPP component of the composite matrix cannot be removed from the fibre by means of solvent dissolution. It can be observed that the MAPP particles are not evenly distributed on the fibre surfaces, but rather form particle clusters that are bonded at random intervals along the length of the fibres.

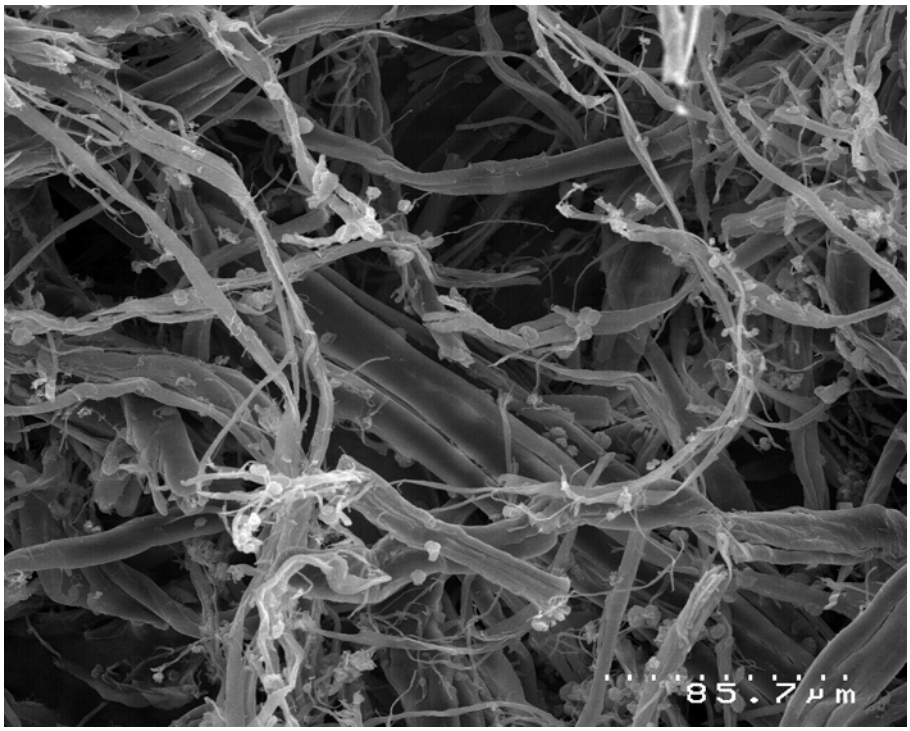

Figure 4.22(a) Scanning Electron Micrograph (SEM) of a NaOH/Na_2SO_3 treated hemp fibre extracted from a composite containing PP and 0wt% MAPP.

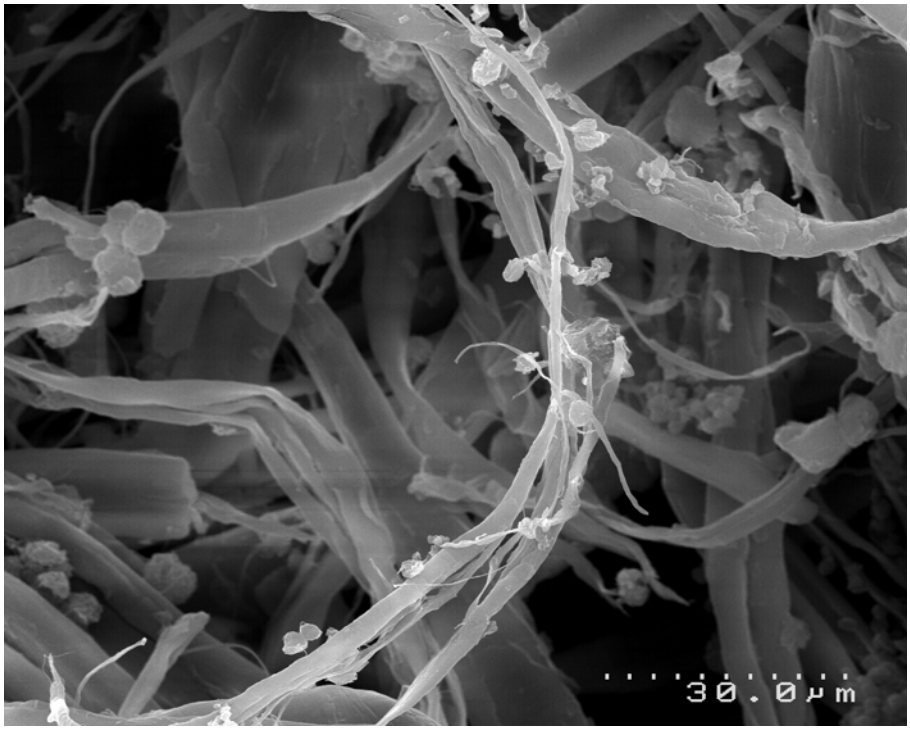

Figure 4.22(b) Scanning Electron Micrograph (SEM) of a NaOH/Na_2SO_3 treated hemp fibre extracted from a composite containing PP and 0wt% MAPP.

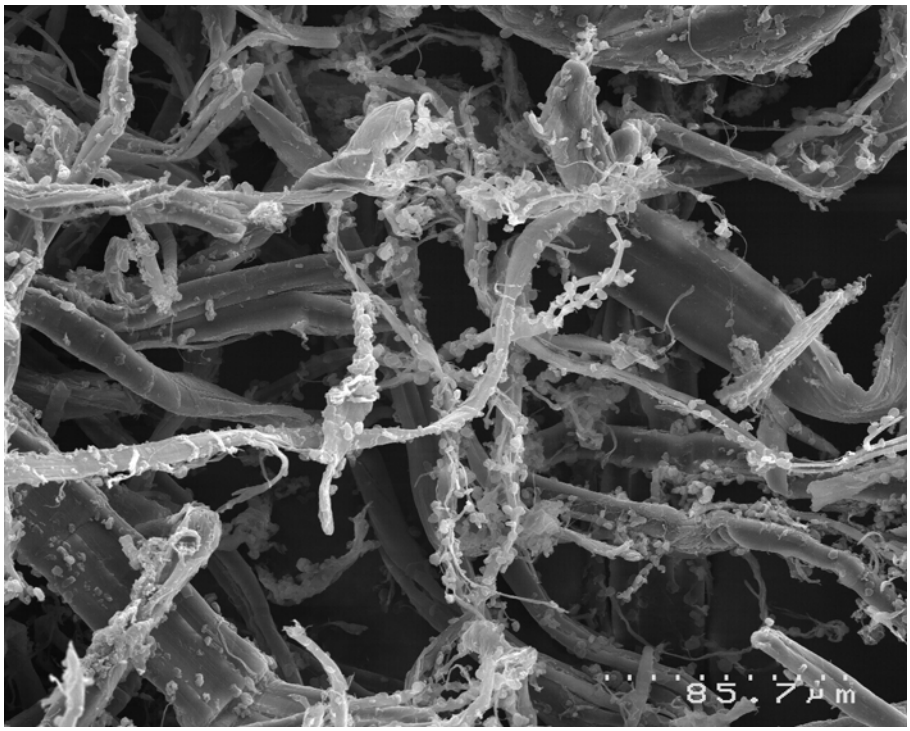

Figure 4.23(a) Scanning Electron Micrograph (SEM) of a NaOH/Na_2SO_3 treated hemp fibre extracted from a composite containing PP and 4wt% MAPP.

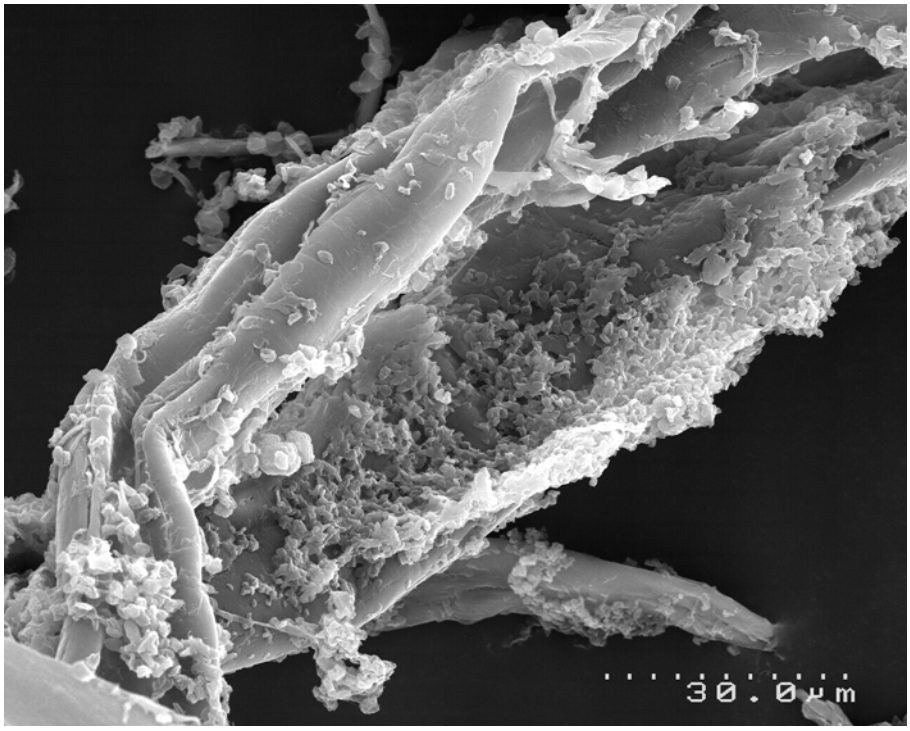

Figure 4.23(b) Scanning Electron Micrograph (SEM) of a NaOH/Na_2SO_3 treated hemp fibre extracted from a composite containing PP and 4wt% MAPP.

4.2.4 Fibre Length Analysis and the Effects of Fibre Length on Composite Properties

Fibre length is one of the major factors affecting the ultimate mechanical properties of a composite. Long fibres provide reinforcement for the composite, whereas very small fibres, or fines, do not contribute to composite strength and act more as fillers. It is generally regarded that a fibre aspect ratio of above 10 is required to ensure adequate load transmission from a composite matrix to a reinforcing fibre [152], but the effective fibre length is ultimately determined by the strength of the fibre-matrix interfacial bond.

The purpose of this investigation was therefore to evaluate the mechanical properties of extruded and injection moulded composites made from different fibre length separations. The composite mechanical properties for composites made from fibres separated into 'short', 'normal' and 'long' fibre lengths can be seen in Table 4.4.

It can be seen from these results that the use of different fibre lengths did not result in significant differences in composite tensile strength and Young's modulus.

Table 4.4 Mechanical properties of injection moulded composites reinforced with fibres separated by length. Standard deviations are included in parenthesis.

Composite Fibre Length Distribution	Composite Tensile Strength (MPa)	Composite Young's Modulus (GPa)
Short	42.0 (1.2)	4.82 (0.82)
Normal	42.2 (1.2)	4.60 (0.35)
Long	41.0 (1.8)	4.99 (0.67)

It is widely known that significant fibre length reductions are made during the compounding and moulding of composites [153], with most fibre breakages

occurring during extrusion [98]. In order to further evaluate the composites, it was necessary to determine the actual fibre length distribution inside each composite after processing. Fibres were therefore extracted from injection-moulded composites by dissolving the polymer matrix in a solvent, and the length distributions of the extracted fibres were analysed.

The fibre length distributions for composites made from short, normal and long fibres can be seen in Figure 4.24, Figure 4.25 and Figure 4.26, respectively. It can be seen that the short fibre composites contained the highest proportion of short fibres and fines, and had a mean fibre length of 400μm. The composites containing normal length fibres had a mean fibre length of 520μm and the composites containing long fibres had a mean fibre length of 530μm. Both the normal and long fibre composites appeared to have very similar fibre length distributions, which is contrary to what was anticipated.

These similarities in fibre length distribution are thought to be due to fibre breakages induced by the extrusion, granulating and injection moulding processes. Since composites were granulated into pellets that ranged from 1mm to 5mm in dimensions, it is suspected that fibres classified as "long" were shortened significantly as a result of composite granulating. Fibre damage leading to fibre breakage is also likely to have occurred during extrusion and injection moulding as a result of fibre-polymer interactions, fibre-fibre interactions and fibre contact with surfaces of processing equipment [154]. Due to the relatively high fibre content of the composites (40wt% hemp fibre), the fibre damage caused by friction between fibres was expected to be more pronounced [155].

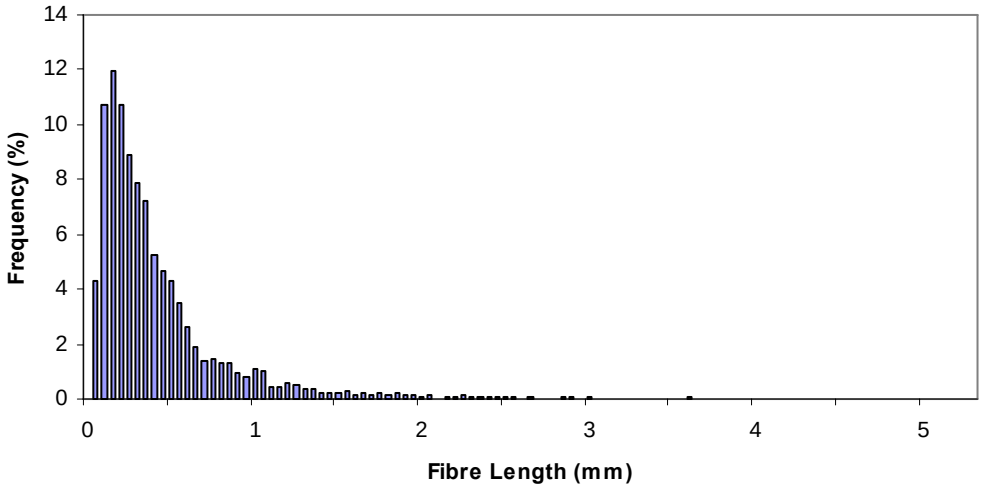

Figure 4.24 Fibre distribution for short fibre length composites.

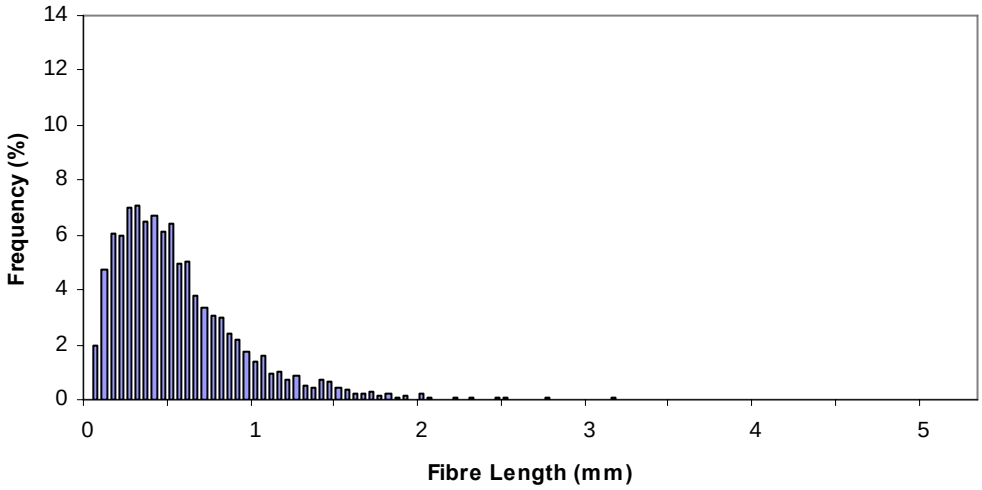

Figure 4.25 Fibre distribution for normal fibre length composites.

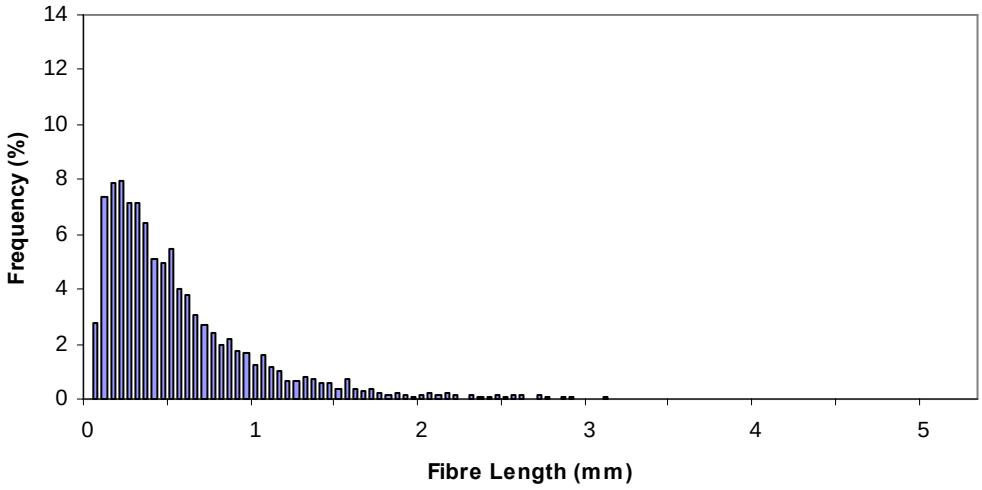

Figure 4.26 Fibre distribution for long fibre length composites.

A micrograph of a few extracted fibres can be seen in Figure 4.27. The fibres show signs of de-fibrillation and structural damage in some regions along the fibre length. It is known that de-fibrillation increases the fibre surface area and hence area available for bonding with the matrix, and may lead to increases in tensile strength for some composites [156]. Despite possible improvements in fibre-matrix bonding, significant damage appears to have been induced in the fibres, resulting in likely fibre strength reductions that would ultimately limit the strength of composites produced using these processing methods.

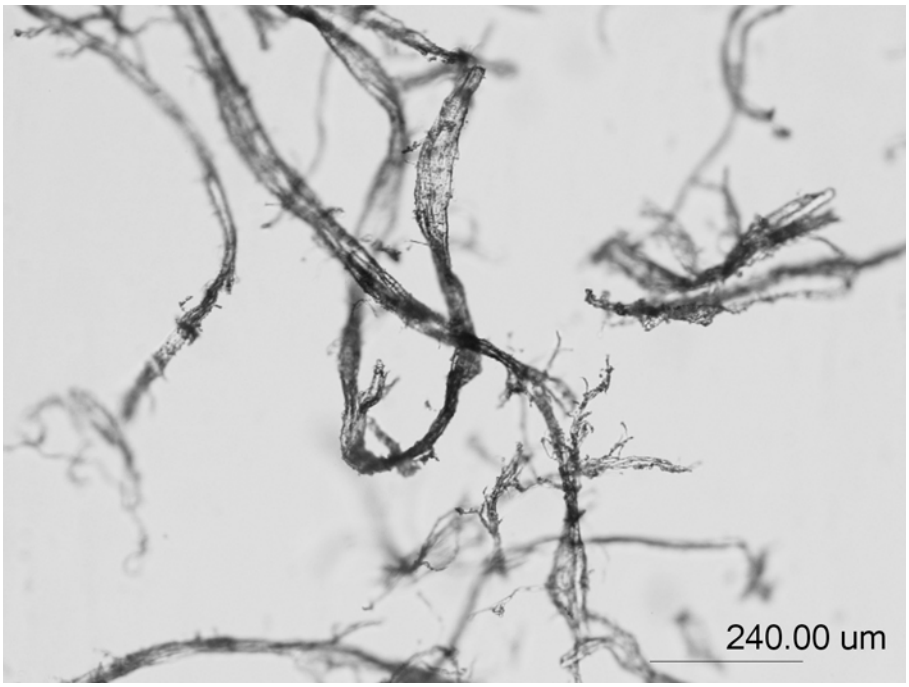

Figure 4.27 Optical micrograph of extracted hemp fibres showing composite processing induced damage.

4.2.5 Fibre Orientations of Injection Moulded Composites

During injection moulding, the fibre-polymer melt is subjected to complex and variable flow conditions that result in complex fibre orientation distributions within the composite. Differences in the melt velocities along the walls of the mould and the mould channel can often result in the formation of surface and core layers in the composite, and a 'fountain flow' fibre orientation.

Several composite samples, cut from injection moulded composite test specimens containing 40wt% NaOH/Na_2SO_3 treated hemp fibre, 57wt% polypropylene and 3wt% MAPP, were viewed macroscopically and microscopically. The sample viewing orientations and internal fibre orientations can be seen in Figures 4.28, 4.29, 4.30 and 4.31. In reference to these samples, the *X*-direction corresponds to the mould-filling direction, the *Y*-direction corresponds to the sample width and the *Z*-direction corresponds to the sample thickness.

It can be seen in Figure 4.29 and Figure 4.31 that fibres are oriented in a three-layer structure that is commonly found in injection-moulded composites [51, 53, 157, 158]. There are two skin layers (*S*), and a core region of fibres (*C*) showing the unique structure caused by fountain flow. The sample shown in Figure 4.31 was ground and polished such that half the composite was removed (in the *Z*-direction) to reveal the fountain flow structure of the core region. The core layer appears to have a lower polymer content compared to the skin layers, and large lightly-coloured regions can be seen which are thought to be collections of large un-separated fibre bundles and pieces of hurd material.

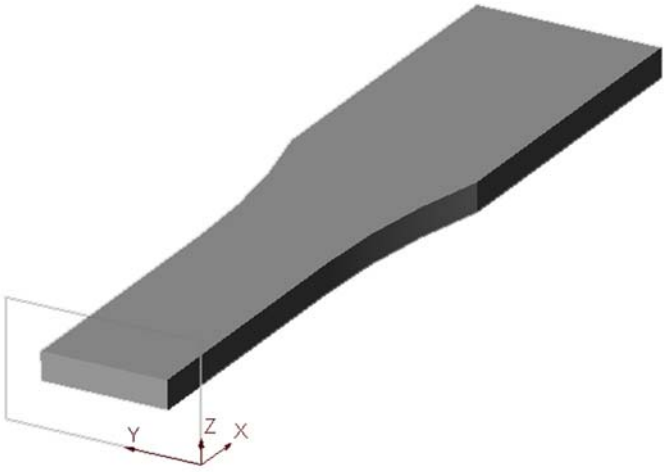

Figure 4.28 Schematic of a composite test specimen showing the cross-sectional view.

Figure 4.29 Macroscopic view of a test specimen cross-section showing a distinct core layer (*C*), and two skin layers (*S*).

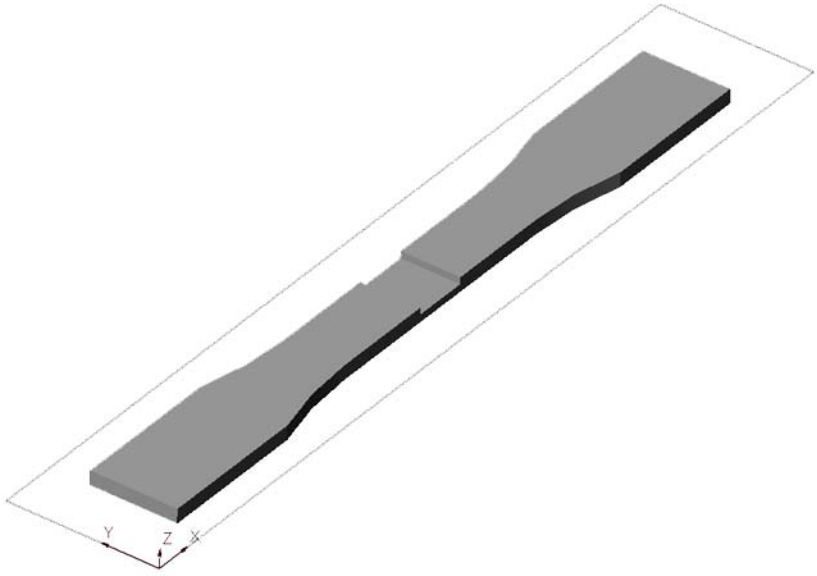

Figure 4.30 Schematic of a composite test specimen showing a cut-away plan view.

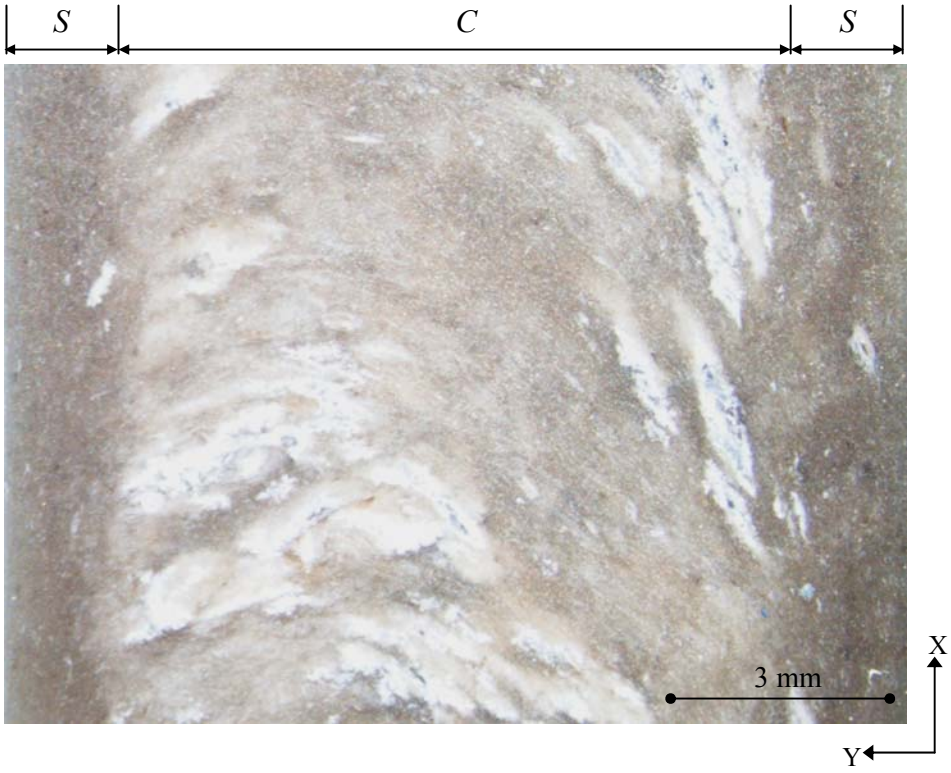

Figure 4.31 Macroscopic plan view of a test specimen with half the thickness removed, showing a distinct core layer (*C*), and two skin layers (*S*).

The polished cross-section of an injection-moulded specimen viewed microscopically can be seen in Figure 4.32. The large number of fibre cross-sections that can be viewed along the edges of the composite suggests that the majority of the fibres in the skin layers have been oriented in the flow direction along the sides of the mould (the *X*-direction). It can also be seen that the fibres are more transversely oriented in the composite core.

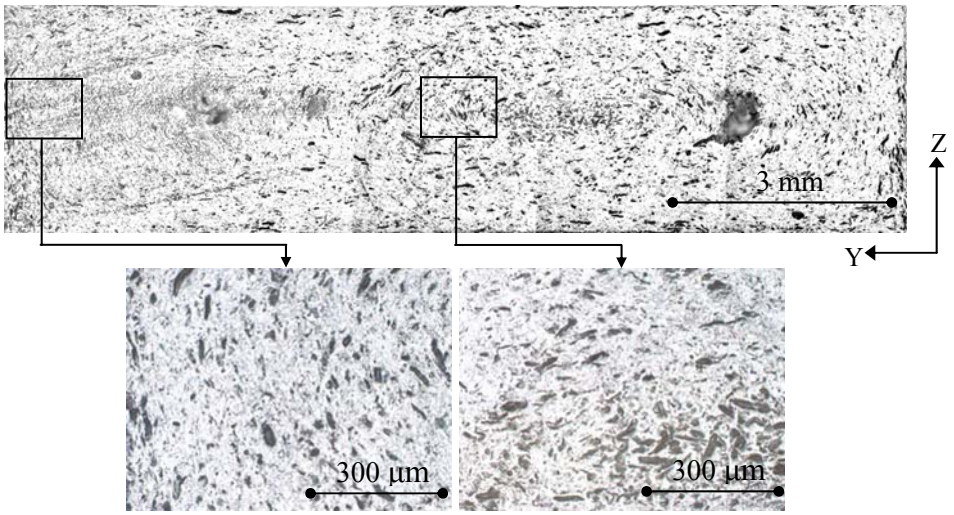

Figure 4.32 Optical micrograph showing the cross-sectional view of a composite specimen.

The fibre orientations in the core layer can be seen in Figure 4.33. The sample was ground and polished such that half the composite was removed (in the *Z*-direction) to reveal the core layer. It can be seen that there is good fibre alignment along the edges of the composite in the skin layers, and that the fibres in the core are aligned in an arc formation in the *X*-*Y* plane by the fountain flow.

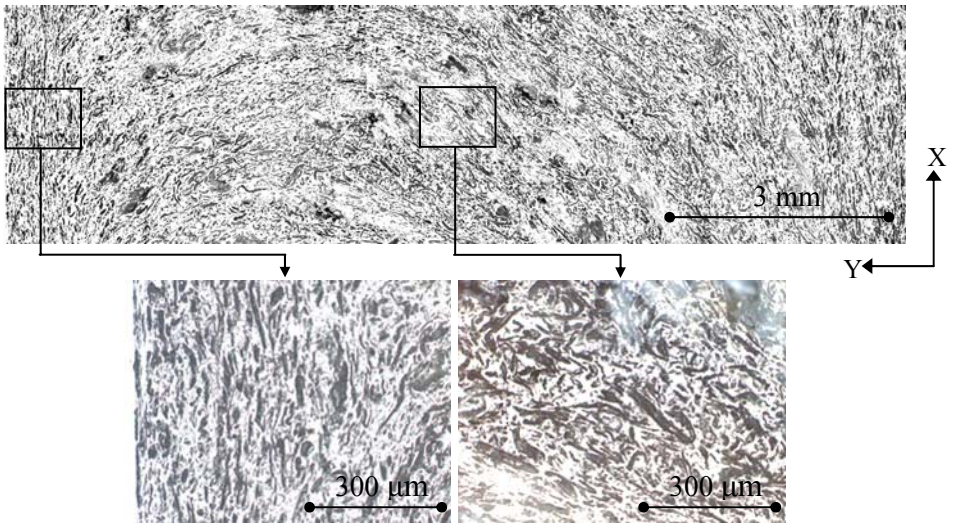

Figure 4.33 Optical micrograph showing a plan view of a specimen with the top half removed (core layer).

The fibre orientations in the transitional area between the core and skin can be seen in Figure 4.34. The sample was ground and polished such that the top quarter of the composite was removed (in the *Z*-direction). It can be seen that there is good fibre alignment along the edges of the composite in the skin layers, but no distinct fountain flow pattern can be seen in the core. Instead, the core shows a random fibre orientation.

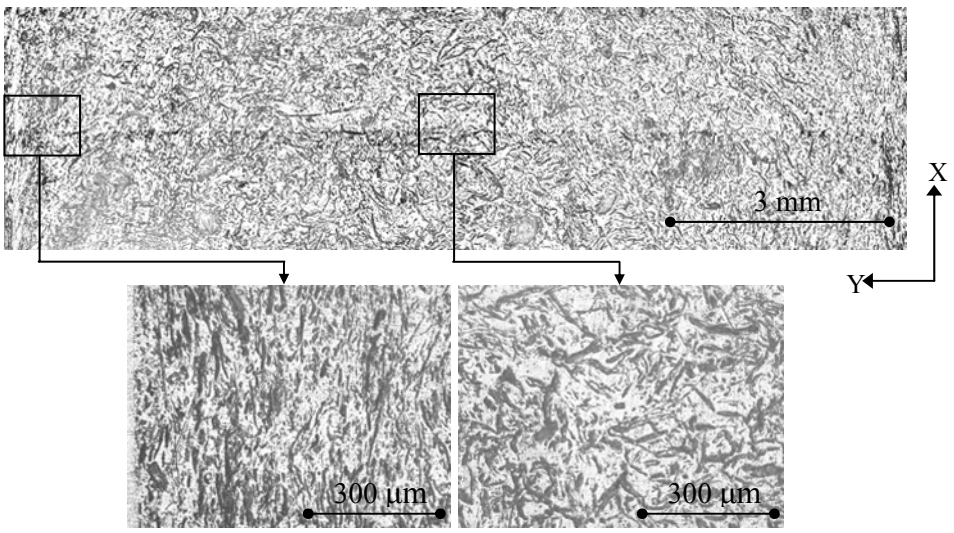

Figure 4.34 Optical micrograph showing a plan view of a specimen with the top quarter removed (transition between core and skin layer).

The fibre orientations in the composite surface layers can be seen in Figure 4.35. It can be seen that the fibres are somewhat aligned in the flow direction, but not to the same extent as seen in the skin layers further inside the composite. The fibres at the surface also appear to be longer than those in the skin and core layers.

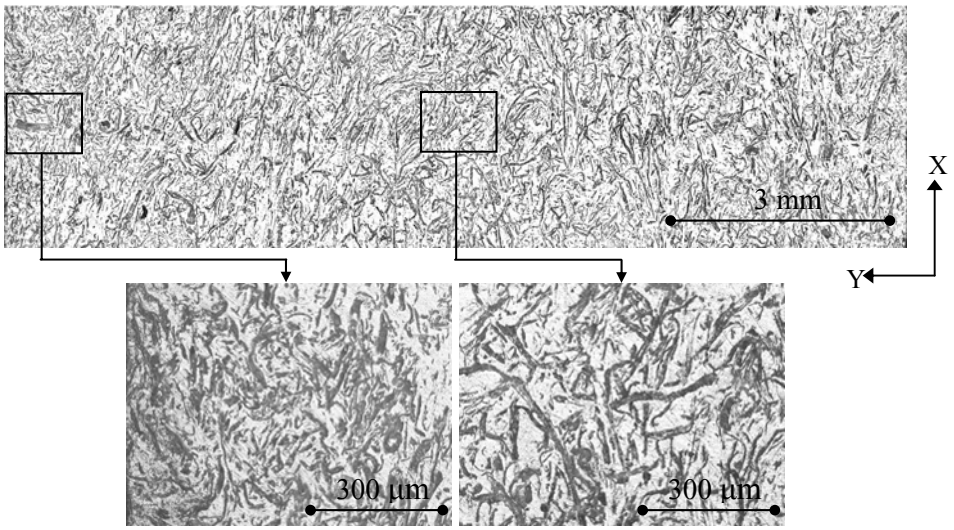

Figure 4.35 Optical micrograph showing a specimen surface plan view (skin layer).

From the observations made based on these micrographs, it can be seen that there are very few fibres oriented through the mould thickness (*Z*-direction) for injection moulded composites containing 40wt% fibre with average fibre length of between 1-3mm. The fibres also appear to be somewhat oriented in the test direction (*X*-direction). It can therefore be concluded that the fibre orientation within these composites is planar-random.

It has been reported that increased injection speeds result in thicker core layers, but this effect is more pronounced in thin composites (2mm thickness) than in thicker composites (4mm thickness) [51]. Increases in the fibre content and the inclusion of longer fibres have been found to increase the core thickness of injection-moulded composites [51, 158]. Gate location, mould geometry, melt rheology and temperature distributions in the mould have also been shown to affect fibre orientation [159]. Fibre orientation and the observed fountain flow structure are not affected by the presence of MAPP in the composite [53]

Some authors [50, 52] have been able to determine the fibre orientations of synthetic fibre composites by means of observing the elliptical shape of fibre cross-sections on a polished cutting plane. This method was not considered in this investigation due to the large size and cross-sectional shape variations associated with hemp fibres, which would result in significant inaccuracies in fibre orientation determination.

4.3 Evaluation of Solution Mixed Composites

4.3.1 Comparisons Between Short Randomly Oriented Fibre Composites Produced by Extrusion/Injection Moulding and Solution Mixing Methods

Solution mixing is a convenient alternative to composite fabrication techniques that involve the melt mixing of a polymer with reinforcing fibres. It is known that solvents such as xylene do not cause permanent chemical changes to polypropylene, but it is unknown how the dissolution of MAPP in xylene would affect the coupling agent's ability to enhance the fibre-matrix adhesion of a composite.

A composite containing 40wt% $NaOH/Na_2SO_3$ treated hemp fibre, 56wt% polypropylene and 4wt% MAPP was prepared by solution mixing, and instead of hot pressing, the composite was dried, granulated and injection moulded to produce tensile test specimens. The solution mixed and injection moulded composite was then compared to an extruded and injection moulded composite containing the same weight content of constituents.

It can be seen in Table 4.5 that there are no significant differences in tensile strength and Young's modulus between composites produced by the two different processing methods. It can therefore be assumed that the levels of interfacial

adhesion are equivalent for composites produced by each method, and that the efficiency of the MAPP coupling agent was not affected by the solvent.

Table 4.5 Tensile strength and Young's modulus of randomly oriented fibre reinforced composites prepared by solution mixing/injection moulding and extrusion/injection moulding. Standard deviations are included in parenthesis.

Composite Fabrication Method	Tensile Strength (MPa)	Young's Modulus (GPa)
Extrusion and Injection Moulding	42.2 (1.2)	4.60 (0.35)
Solution Mixing and Injection Moulding	43.1 (2.5)	4.99 (0.72)

The fracture surfaces of extruded and injection moulded composites (Figures 4.36(a) and 4.36(b)) and solution mixed composites (Figures 4.37(a) and 4.37(b)) provide further evidence of good fibre-matrix interfacial adhesion. The micrographs all show very little fibre pullout and many fractured fibres can be seen. It can also be seen that the polypropylene has adhered to most fibre surfaces as a result of the presence of MAPP. Composite fracture is thus thought to have occurred by means of fibre fracture and shear failure of the polypropylene matrix. It can also be observed that the reinforcing fibres in both composites are well dispersed throughout the matrix and are separated from their fibre bundles. Since the solution mixing method does not provide much mechanical energy for fibre separation, it can be concluded that the high shear forces experienced by the composite melt during injection moulding are responsible for the improvements in fibre separation and dispersion.

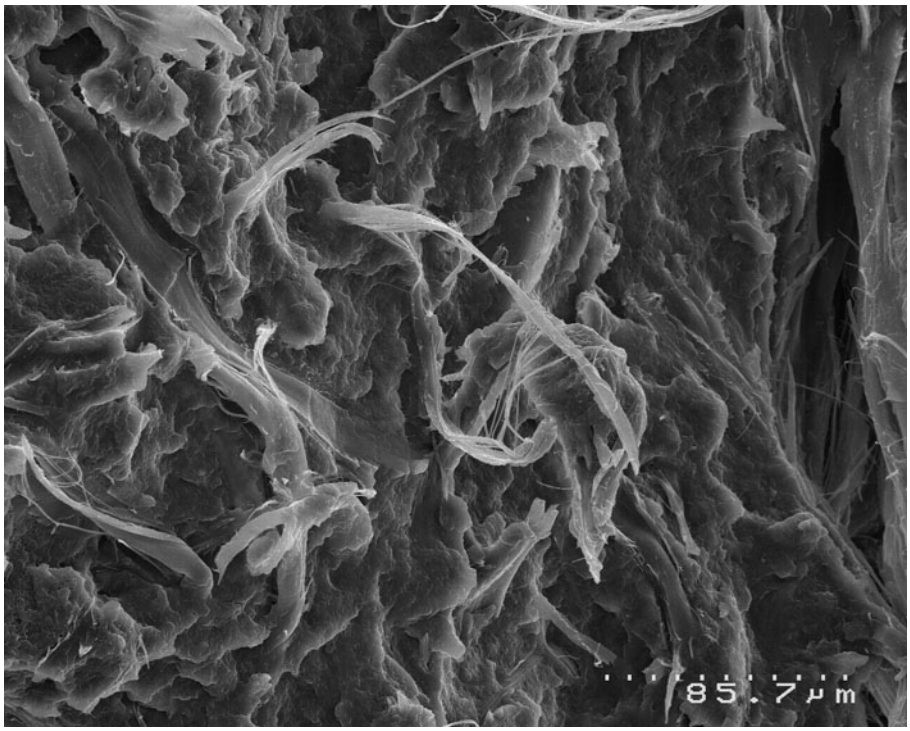

Figure 4.36(a) Scanning Electron Micrograph (SEM) of the fracture surface of an extruded and injection moulded composite [40wt% NaOH/Na_2SO_3 treated hemp fibre, PP and 4wt% MAPP].

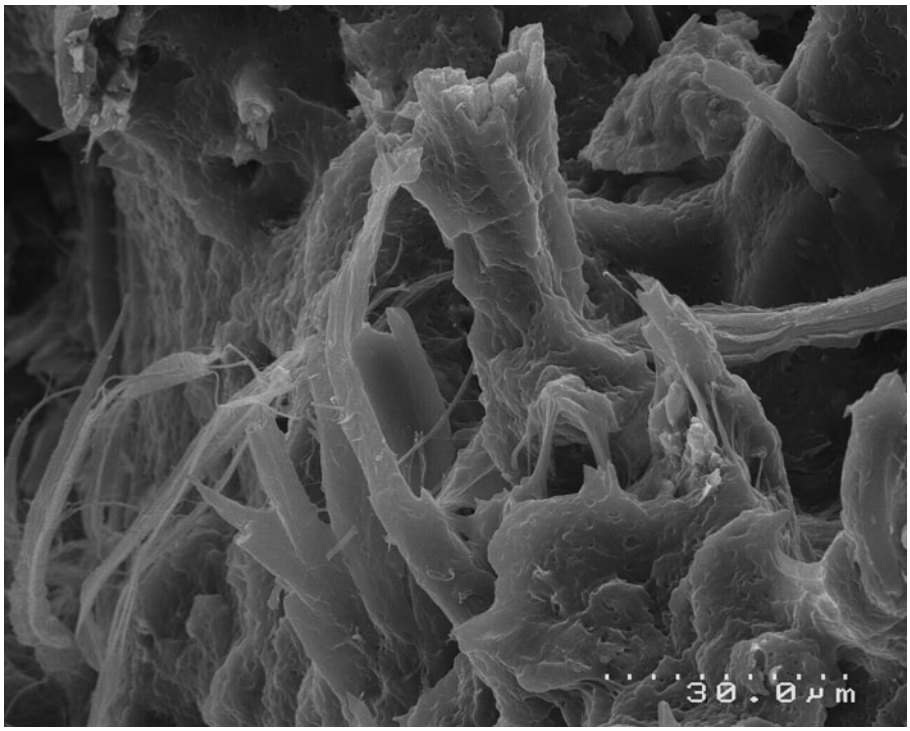

Figure 4.36(b) Scanning Electron Micrograph (SEM) of the fracture surface of an extruded and injection moulded composite [40wt% NaOH/Na_2SO_3 treated hemp fibre, PP and 4wt% MAPP].

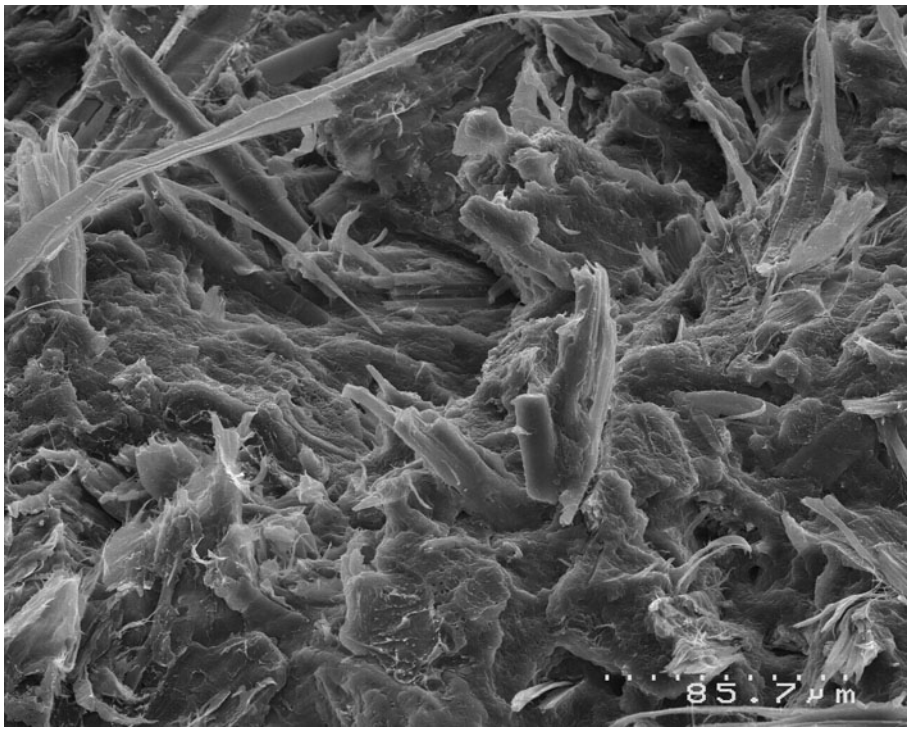

Figure 4.37(a) Scanning Electron Micrograph (SEM) of the fracture surface of a solution mixed and injection moulded composite [40wt% NaOH/Na_2SO_3 treated hemp fibre, PP and 4wt% MAPP].

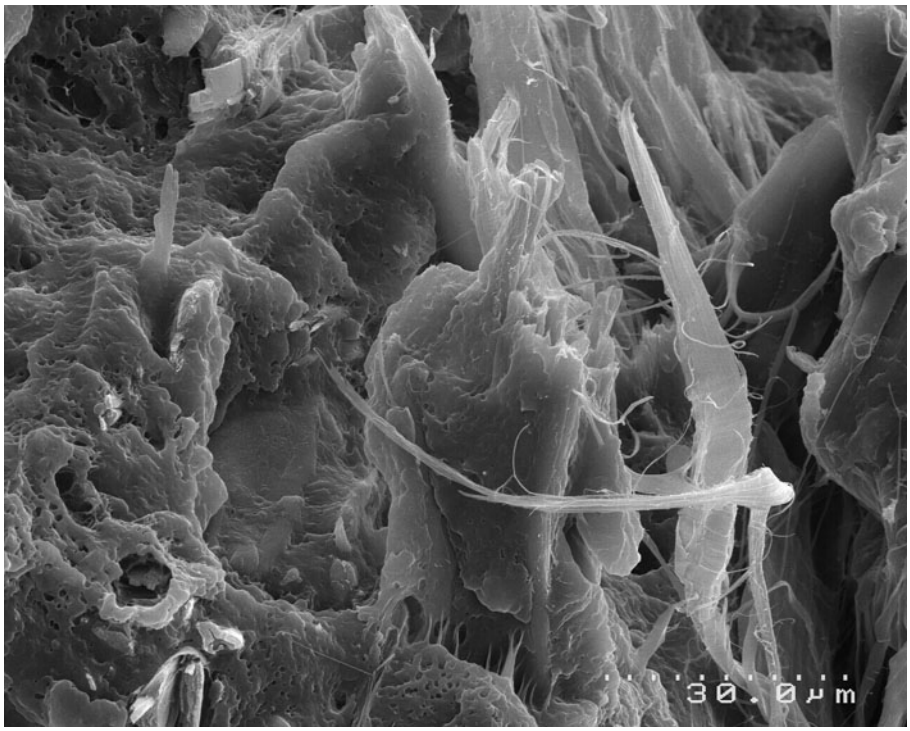

Figure 4.37(b) Scanning Electron Micrograph (SEM) of the fracture surface of a solution mixed and injection moulded composite [40wt% NaOH/Na_2SO_3 treated hemp fibre, PP and 4wt% MAPP].

4.3.2 Long Oriented Fibre Composites Produced by Solution Mixing

The tensile strength and Young's modulus of composites containing long, axially oriented fibres as produced by solution mixing and hot pressing can be seen in Figure 4.38 and Figure 4.39. Composites were either hot-pressed once or twice in the heated hydraulic press. A MAPP/PP ratio of 7.14g MAPP/100g PP was used for all solution mixed and hot pressed composites.

It can be seen in Figure 4.38 that the composite tensile strength increased steadily as the fibre content was increased to 56wt%, and a strength decrease was seen thereafter. The data was statistically analysed using a one-tailed Student's t-test at a confidence level of 95% (P<0.05), and it was found that statistically significant increases in tensile strength occurred for both the 1x and 2x hot-pressed composites as the fibre contents were increased to 56wt%. According to the Student's t-test results, there were no significant decreases in tensile strength for 1x and 2x hot-pressed composites as the fibre contents were increased beyond 56wt%. It was observed during tensile testing that composites with fibre contents above 56wt% appeared to have reduced levels of fibre wetting on their fracture surfaces due to insufficient amounts of polymer being available to cover the fibres. No significant differences in tensile strength were observed for 1x and 2x hot-pressed composites.

In Figure 4.39, it can be seen that the composite Young's modulus increased almost linearly with an increase in fibre content. It can also be seen that by pressing the composite twice, significant improvements in Young's Modulus could be made. This is thought to be due to the reduction of fibre spring-back in the composite. Spring-back is a condition that often occurs in compression-moulded components when the compaction pressure is released suddenly and the material partially returns to its original shape due to elastic recovery.

The strongest composite produced by means of solution mixing and hot pressing contained 56wt% hemp fibre, was hot pressed twice and had an average tensile

strength of 84.7 MPa. The stiffest composite contained 63wt% hemp fibre, was also hot pressed twice, and had an average Young's modulus of 16.0 GPa.

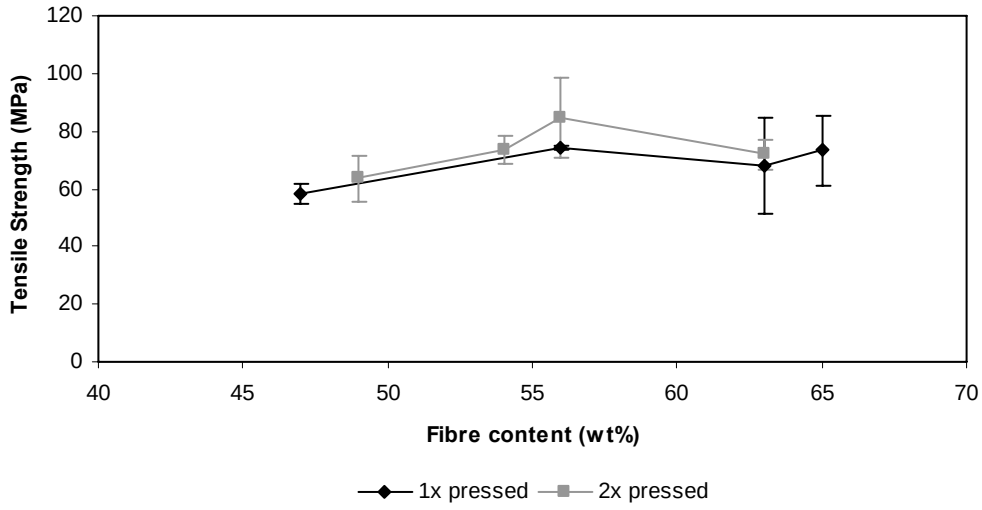

Figure 4.38 Tensile strength of solution mixed and hot pressed composites containing $NaOH/Na_2SO_3$ treated hemp fibre. The error-bars each represent ± 1 standard deviation.

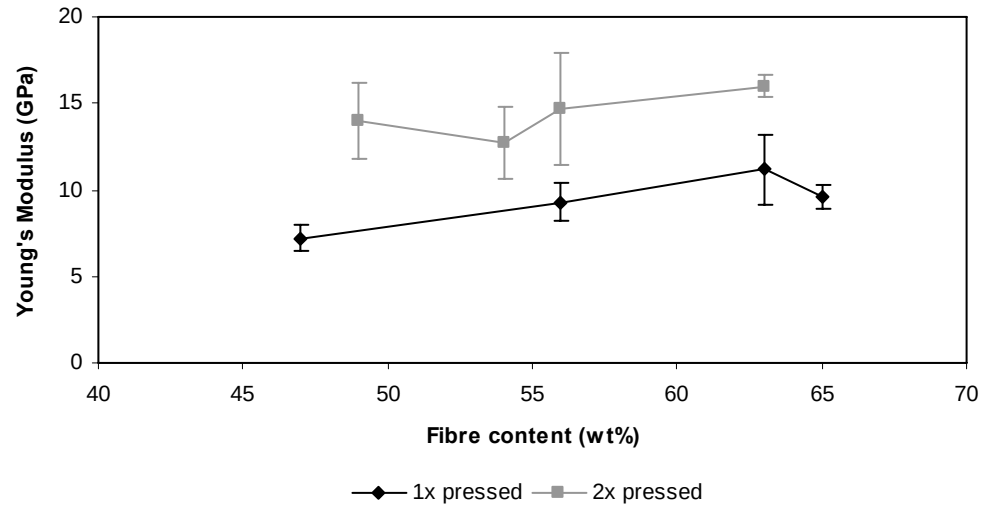

Figure 4.39 Young's modulus of solution mixed and hot pressed composites containing $NaOH/Na_2SO_3$ treated hemp fibre. The error-bars each represent ± 1 standard deviation.

The fracture surfaces of composites produced by means of solution mixing and hot pressing can be seen in Figure 4.40(a) and Figure 4.40(b). The composite fracture surface in Figure 4.40(a) shows many fractured fibres with no obvious signs of fibre pullout. The fibres all appear to be axially oriented, and are mostly

bound together in the form of fibre bundles. A single fractured fibre is shown in Figure 4.40(b), and it can be seen that the fibre is well covered with the polypropylene matrix, and the adhesion between the fibre and matrix is excellent. It appears that the composite failed by means of fibre fracture, although shear failure of the matrix is evident on the sides of most fibre bundles. From these micrographs, it can be seen that solution mixing in conjunction with hot-pressing is a suitable method for producing long, axially aligned fibre composites with good wetting of the fibres with the matrix, and excellent fibre-matrix interfacial adhesion.

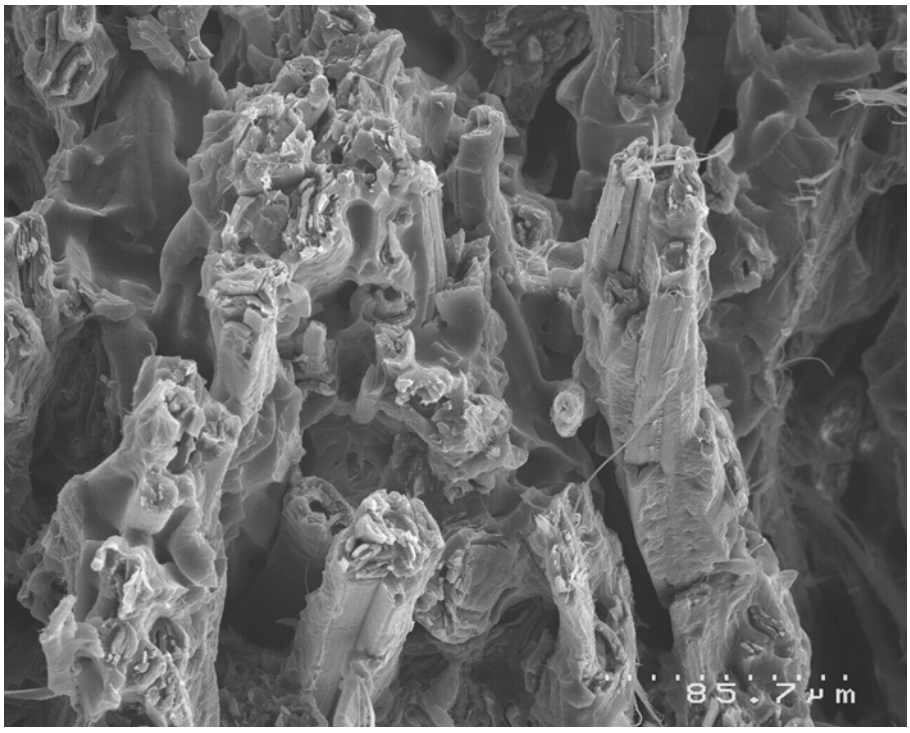

Figure 4.40(a) Scanning Electron Micrograph (SEM) of the fracture surface of a solution mixed and hot pressed composite [56wt% NaOH/Na_2SO_3 treated hemp fibre, PP and 4wt% MAPP].

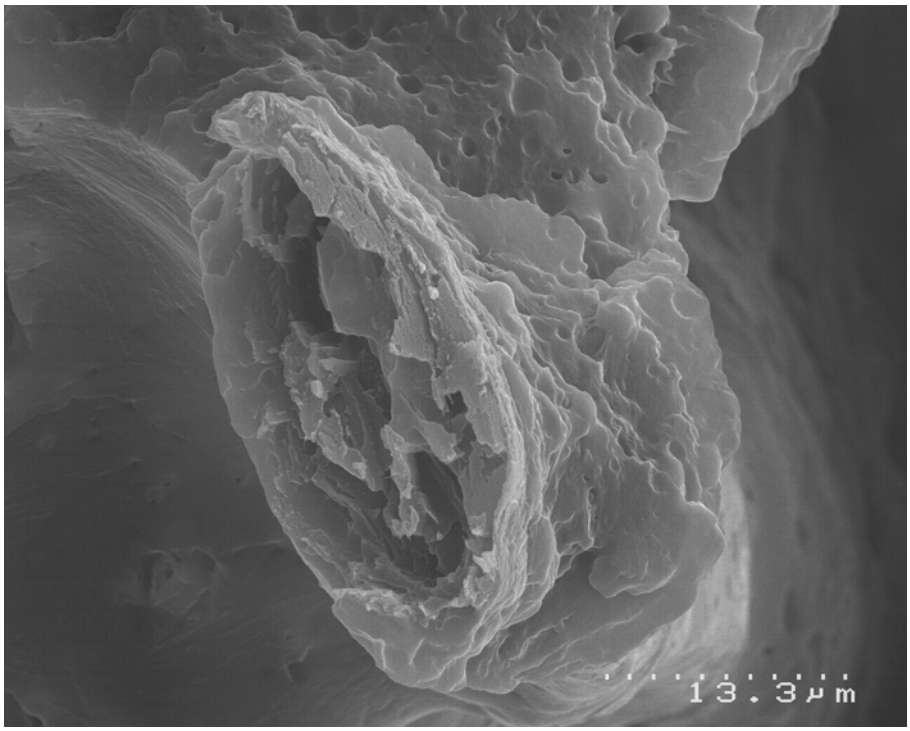

Figure 4.40(b) Scanning Electron Micrograph (SEM) of the fracture surface of a solution mixed and hot pressed composite [56wt% NaOH/Na_2SO_3 treated hemp fibre, PP and 4wt%MAPP].

It should be noted, however, that the tensile strength and Young's modulus of solution mixed and hot pressed composites were thought to be below their potential values for the following reasons:

- Despite the fact that the fibres were carded, they appeared to be somewhat crimped and were not held under tension during composite hot pressing to ensure a near perfect fibre alignment.
- Most fibres were bound together in the form of fibre bundles, resulting in a lower fibre surface area available for bonding with the matrix when compared to well-separated fibres.
- Some voids were present in the composites.
- The fibres used to reinforce these composites were found to have experienced moisture induced degradation, and were thought be weaker and less stiff than those used to reinforce the extruded and injection moulded composites discussed in Section 4.2. It can be seen in Table 4.6. that an injection moulded and extruded composite containing degraded

fibres showed a decrease in tensile strength of 16% and decrease in Young's modulus of 13% compared to a similar composite containing non-degraded fibres. If the strength and stiffness of the solution mixed and hot pressed composite were reduced by the same margins as a result of the inclusion of degraded fibres, it may have been possible to achieve a composite tensile strength of 98 MPa and a Young's modulus of 18 GPa if non-degraded fibres had been used instead.

Table 4.6 Tensile strength and Young's modulus of extruded/injection moulded composites containing non-degraded fibres and degraded hemp fibres. Composites contain 40wt% $NaOH/Na_2SO_3$ treated fibre and 4wt% MAPP, and standard deviations are included in parenthesis.

Fibre Used	Tensile Strength (MPa)	Young's Modulus (GPa)
Non-degraded	50.5 (1.1)	5.31 (0.29)
Degraded	42.2 (2.1)	4.60 (0.35)

4.4 Composite Modelling

In this section, single fibre fragmentation tests and single fibre tensile tests were performed on $NaOH/Na_2SO_3$ treated fibres that had not experienced degradation due to the presence of moisture in the fibre storage area. Since it is expected that the tensile strength and the interfacial shear strength of moisture-degraded fibres would be different to those of fibres that had not experienced moisture-induced degradation, the results obtained in this section can only be attributed to composites containing fibres that were not degraded (i.e. the results are applicable to extruded and injection moulded composites and not to solution mixed composites).

4.4.1 Determination of Critical Fibre Length

Single fibre fragmentation test (SFFT) specimens were stressed, and final fibre fragment lengths were measured and evaluated. A typical micrograph of a

fragmented $NaOH/Na_2SO_3$ treated fibre in a matrix of PP containing 4% MAPP can be seen in Figure 4.41. The failure at the interface is typical of a strong interfacial bond, as the breaks appear to have extended transversely into the matrix [120].

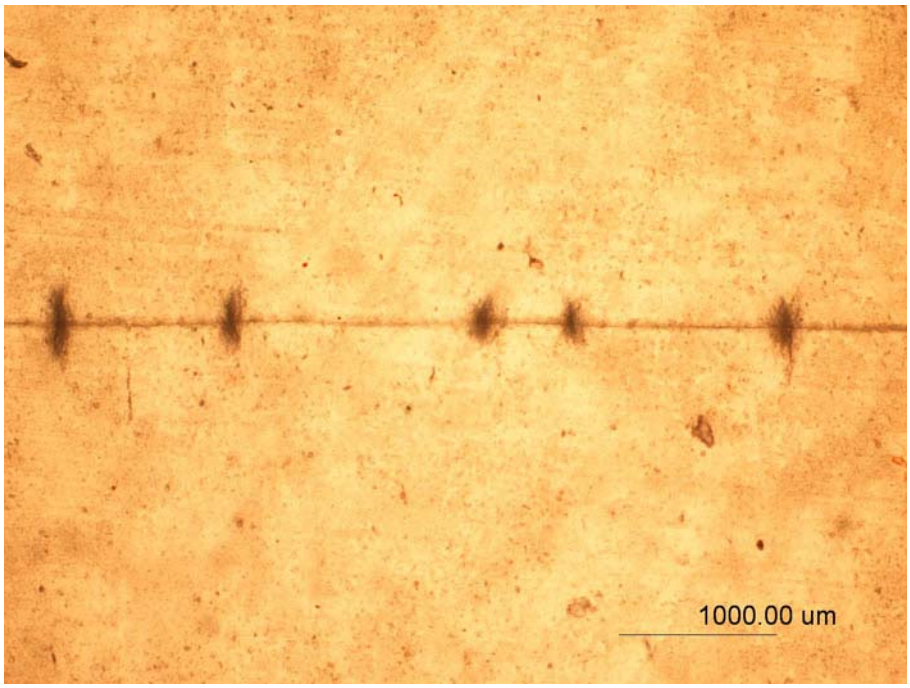

Figure 4.41 Micrograph showing fibre breaks after the fragmentation test.

Fragmentation tests involving $NaOH/Na_2SO_3$ treated fibres mounted in pure polypropylene without MAPP proved to be unsuccessful due to a lack of adhesion between the fibres and matrix, resulting in fibre pullout rather than fibre fragmentation. The treated fibres appeared to have a smooth surface, thus reducing the likelihood of stress transfer between the matrix and fibre by frictional and/or mechanical interlocking mechanisms. Due to elementary fibre length limitations, it was not practical to extend the fibre length used in the SFFT to above the 18mm used in this investigation.

Due to the absence of fibre fragmentation experienced by specimens without MAPP, it was not possible to obtain any meaningful fragmentation test data for further evaluation. The determination of fibre-matrix interfacial strength was

therefore limited to the evaluation of fragmentation test specimens containing 4% MAPP.

Once fibre fragment lengths had been measured, they were divided by the average fibre diameter (23.6μm) to give the distribution of fibre fragment aspect ratios (L/D). The cumulative distribution of fibre fragments was then plotted against L/D, as can be seen in Figure 4.42.

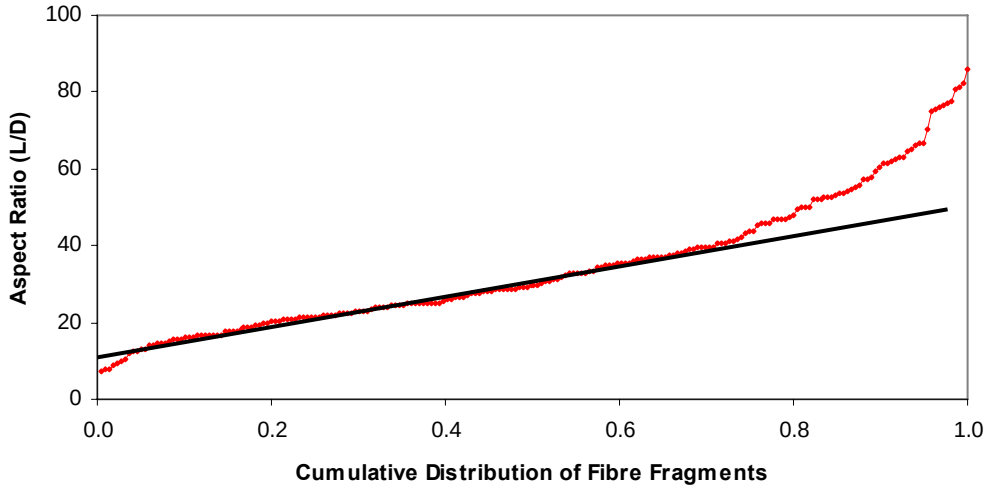

Figure 4.42 Fragment L/D values for treated hemp fibre with a polypropylene/4% MAPP matrix.

The cumulative distribution of fibre fragment aspect ratios was determined by ranking all fibre fragments in an ascending order, and then dividing the rank number of each fragment by the total number of fragments. This resulted in a value between 0 and 1 for each fragment [108].

Theoretically, when a fragmentation test specimen is strained, any fibre fragment longer than the critical fibre length (L_c) will be broken in two, and any fibre fragment shorter than L_c will not be broken. Consequently, the longest fibre existing after fragmentation saturation will be equal to L_c while the shortest will be equal to $\frac{1}{2}L_c$. Thus, the fibre fragment aspect ratios should vary uniformly between L_c/D and $\frac{1}{2}(L_c/D)$, as can be seen in Figure 4.43.

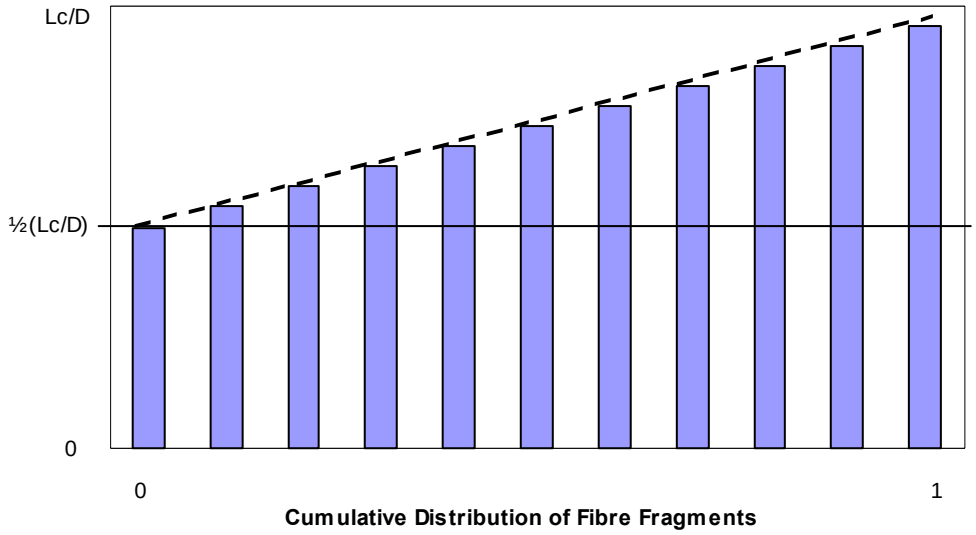

Figure 4.43 Theoretical fibre fragment aspect ratio distribution [108].

In reality, fragments below ½(L_c/D) can occur due to incidental defects in the fibres leading to premature failure. Fragments longer than L_c/D can be found in the case of local imperfect wetting, imperfect alignment and imperfect fragmentation saturation [108]. It is therefore possible to identify and remove these anomalies from the data by adding a trend line to the curve (Figure 4.42), and eliminating the data above and below the line (Figure 4.44). The result is a set of data that more closely resembles a uniform fragment distribution between L_c/D and ½(L_c/D).

An arithmetic mean aspect ratio (L_{ave}/D) of 26.4 was derived from the data in Figure 4.44 by adding up all the fragment aspect ratios and dividing the total by the number of fragments analysed.

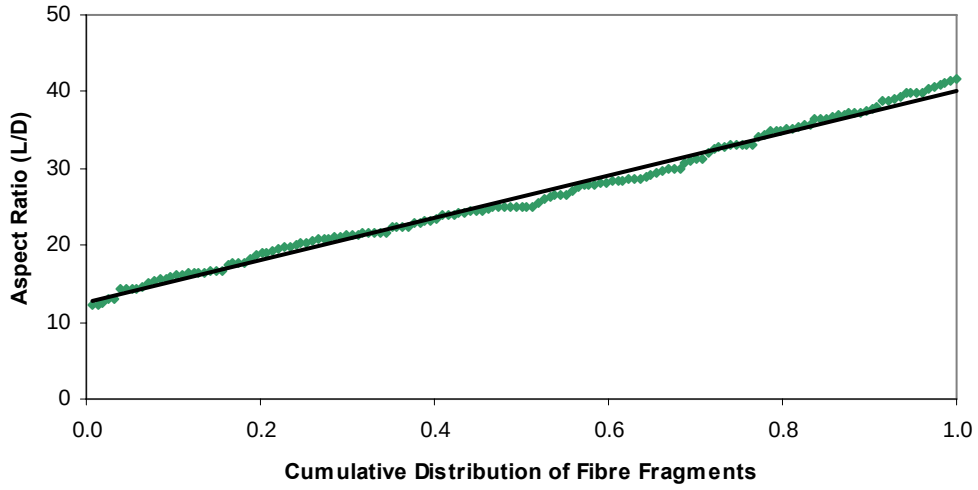

Figure 4.44 Fragment L/D values for treated hemp fibres with a polypropylene/4% MAPP matrix (anomalies removed).

The L_c/D for NaOH/Na_2SO_3 treated hemp fibre composites (no moisture-induced fibre degradation) with a matrix of polypropylene and 4% MAPP was then calculated by substituting the value obtained for L_{ave}/D into Equation 4.2:

$$\frac{L_c}{D} = \frac{4}{3}\left(\frac{L_{ave}}{D}\right) \qquad (4.2)$$

where D is the average fibre diameter and L_{ave} is the mean fragment length.

The mean fibre diameter as measured before fragmentation was 23.6μm, resulting in an L_c of 0.83mm. This compares well with the L_c value of 0.82mm for flax fibre reinforced polypropylene/MAPP as reported by Andersons *et al.* [134].

4.4.2 Fibre Strength Prediction at the Critical Fibre Length

The use of Equation 4.3 to calculate the value of the interfacial shear strength (τ) from the SFFT requires the input of fibre strength at the critical fibre length (σ_{fc}):

$$\tau = \frac{\sigma_{fc}}{2\beta}\Gamma\left(1-\frac{1}{\alpha}\right) \qquad (4.3)$$

where α and β are the shape and scale parameters of the Weibull distribution, respectively, and Γ is the gamma function.

It is widely known that fibre strength is dependant on gauge length, thus it is necessary to test the strength of fibres at a gauge length equal to L_c. As L_c is very small in most situations, direct fibre strength measurement by means of single fibre tensile testing is not possible and alternative methods need to be used. Asloun *et al*. [122] studied the dependence of high strength carbon fibres on gauge length by means of weak-link scaling using Weibull statistics. They showed that two and three-parameter Weibull distributions are not appropriate for describing fibre strength dependence on gauge length. Instead, a logarithmic dependence of strength on gauge length was identified as a simple yet accurate method of extrapolating the fibre tensile strength to shorter lengths, i.e. a plot of logarithmic fibre strength versus fibre gauge length revealed an approximately linear relationship.

Several fibre gauge lengths were tensile tested, and the relationship between gauge length and fibre strength can be seen in Figure 4.45. A graph showing fibre strength vs. gauge length was used in this investigation rather than a ln fibre strength vs. ln gauge length graph (as used by Asloun *et al*.), as it produced a trend line that more closely fitted the data. The R^2 value of 0.86 for the trend line is reasonably close to 1, thus indicating a good degree of linearity. The error bars in Figure 4.45 each represent ± 1 standard deviation. It should be noted that this method cannot be used to determine the strength of a fibre at a gauge length of 0, and cannot be used to accurately predict the strength of fibres longer than 12.5mm.

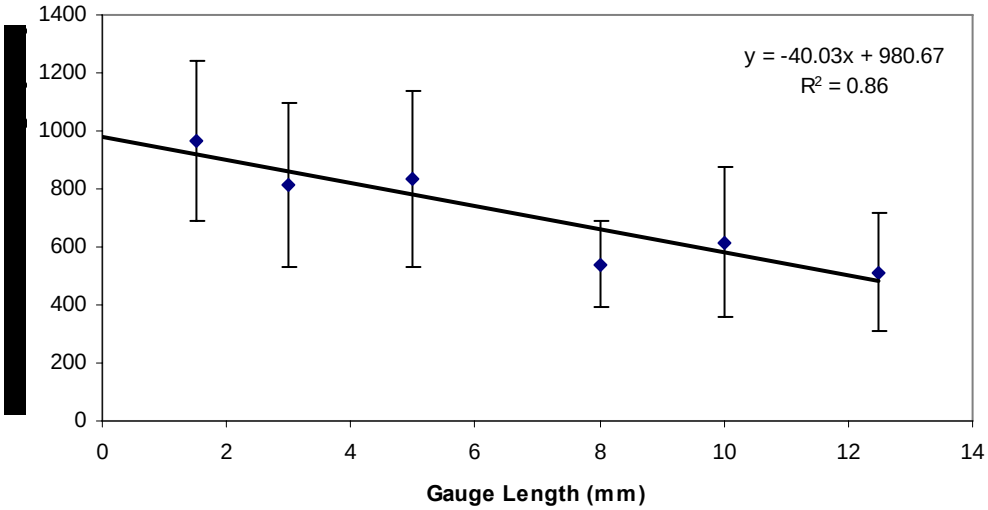

Figure 4.45 Mean fibre tensile strength plotted against gauge length for NaOH/Na_2SO_3 treated hemp fibres.

By using the trend line equation in Figure 4.45, it was possible to calculate the fibre tensile strength at L_c = 0.83mm. The fibre tensile strength at the critical fibre length (σ_{fc}) was thus found to be σ_{fc} = 947.4 MPa. It should be noted that natural fibres exhibit large variations in tensile strength as can be seen by the error bars in Figure 4.45. An average standard deviation in tensile strength for all fibre gauge lengths was found to be 245.4 MPa, thus the fibre tensile strength at the critical fibre length (σ_{fc}) is 947.4 MPa ± 245.4 MPa.

4.4.3 Interfacial Shear Strength Determination

Equation 4.3 was used to calculate the interfacial shear strength (IFSS) using the fibre tensile strength at the critical fibre length (σ_{fc}) that was previously calculated, and the Weibull shape (α) and scale (β) parameters were estimated using the linear regression method (graphical method) [111].

The aspect ratio for each fibre fragment length (using data from Figure 4.44) was ranked in an ascending order, and the failure probability was calculated using the following probability estimator [111, 122, 160]:

$$P_f = \frac{(j - 0.5)}{n} \qquad (4.4)$$

where P_f is the probability of failure, *j* is the rank number and *n* is the number of data points. This estimator was used as it is suitable for sample sizes larger than 20.

A Weibull plot (Figure 4.46) was produced by plotting ln(aspect ratio) against lnln(1/1- P_f), from which the shape parameter (α) could be obtained by assuming the gradient of the trend line, and the scale parameter (β) could be obtained from the trend line intercept with the *x*-axis. The R^2 coefficient of the Weibull plot is very close to 1, indicating a good degree of linearity and thus verifying the validity of the linear regression method.

The IFSS of NaOH/Na_2SO_3 treated hemp fibre composites with a matrix of polypropylene and 4% MAPP was thereby found to be equal to 15.4 MPa, which indicates a relatively high level of interfacial bonding when compared to other natural fibre reinforced thermoplastic composites presented in the literature [105, 121, 161]. Due to the large standard deviations in fibre tensile strength at the critical fibre length (σ_{fc}), the IFSS exhibits a large variation of 4.0 MPa. Thus the IFSS is 15.4 MPa ± 4.0 MPa.

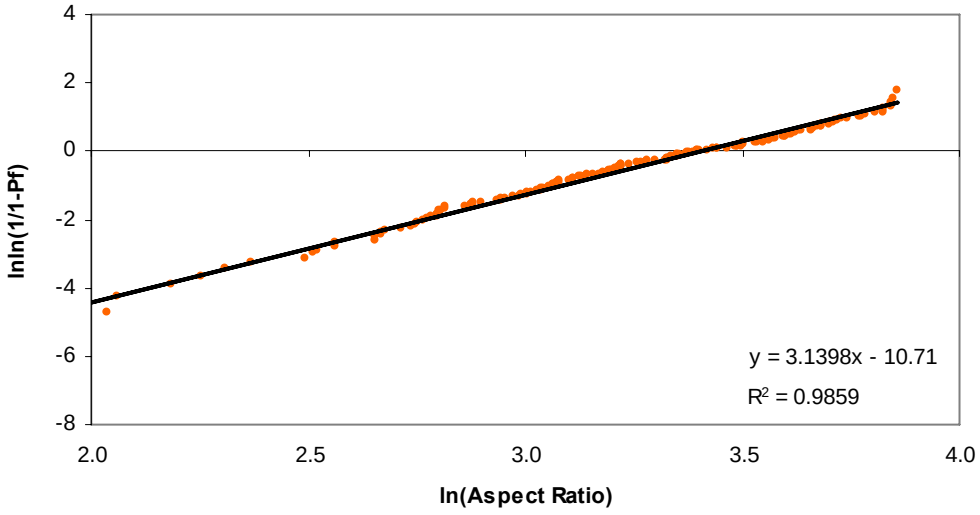

Figure 4.46 Fragment lengths of treated hemp fibres with a polypropylene/4% MAPP matrix presented as a Weibull distribution.

Interfacial failure can result from of one the following two failure mechanisms: failure of the interfacial bond between the matrix and the fibre, and matrix shear

yield failure. It is therefore necessary to determine the shear yield strength of the matrix to determine which of these failure mechanisms are most likely to occur in the composite.

The shear strength of the matrix (τ_m) was estimated using the Von Mises yield criterion, as can be seen in Equation 4.5 [52, 135, 162]:

$$\tau_m = \frac{\sigma_m}{\sqrt{3}} \qquad (4.5)$$

where σ_m is the matrix tensile strength.

It has been assumed in this investigation that the polypropylene/4% MAPP matrix is elastic-perfectly plastic in nature. The tensile strength of polypropylene containing 4% MAPP is 24.4 MPa, which results in a matrix shear strength estimation of 14.1 MPa. It can be seen that the IFSS is slightly higher than the estimated shear strength of the matrix. This indicates that the composite is most likely to fail by local shear yielding of the matrix around the fibre, assuming that all the fibres in the composite are longer than L_c. It can be seen, however, that the IFSS has a relatively large standard deviation. This would suggest that a significant proportion of fibres have IFSS values below the matrix shear strength, and that some fibre de-bonding is likely to occur as well.

4.4.4 Composite Tensile Strength Predictions

In order to evaluate the performance of a composite, it is important to be able to compare the experimental results with results predicted by alternative means, such as mathematical modelling. Composite strength prediction models generally require the mechanical properties and volume fractions of the individual composite components, as well as factors related to stress transfer in the composite.

The following strength prediction models have been used to predict the theoretical strength as well as to evaluate the performance of composites fabricated and tested in this investigation.

The Modified Rule of Mixtures Model

The Kelly-Tyson Modified Rule of Mixtures can be used to determine the tensile strength (σ_c) of axially aligned discontinuous fibre composites:

$$\sigma_c = K_2 V_f \sigma_f + V_m \sigma_m \qquad (4.6)$$

where V_f and V_m are the volume fractions of the fibre and matrix, respectively; σ_f is the mean fibre tensile strength of the fibre and σ_m is the matrix stress at the fibre failure strain. Alternatively, σ_m can be taken as the matrix stress at the failure strain of the composite [50].

K_2 is a fibre length factor, which can be determined by:

$$K_2 = \frac{L}{2L_c} \qquad \text{for } L<L_c \qquad (4.7)$$

or

$$K_2 = 1 - \left(\frac{L_c}{2L}\right) \qquad \text{for } L \geq L_c \qquad (4.8)$$

where L is the fibre length, and L_c is the critical fibre length. $L<L_c$ refers to sub-critical fibre lengths, and $L \geq L_c$ refers to super-critical fibre lengths.

The Kelly-Tyson Modified Rule of Mixtures was used to predict the theoretical tensile strength of composites containing 40wt% hemp fibre, 4wt% MAPP and 56wt% polypropylene, with the assumption that all the reinforcing fibres in the composite are the same length and all fibres are perfectly aligned in the axial direction. It has also been assumed that no fibre-matrix debonding occurs, there

are no voids present in the composite and the composite matrix properties are the same as those of the un-reinforced polypropylene.

Another assumption made by the Kelly-Tyson model is that the stresses experienced by fibres in an axially loaded composite are negligible at the fibre ends, and increase rapidly towards the middle of the fibre, reaching a plateau when the distance from the ends is larger than $½L_c$. As can be seen in Figure 4.47, a fibre below L_c cannot be fully loaded, unlike a fibre equal to or longer than L_c. A sub-critical length fibre will not make a significant contribution to composite strength, as it will be pulled out of the matrix before it can be fully stressed. A critical length fibre can be fully stressed, but only at a very small location in the middle of the fibre. A super-critical length fibre has a much greater proportion of the fibre that can be fully stressed, and can therefore contribute more to composite strength than a critical length fibre.

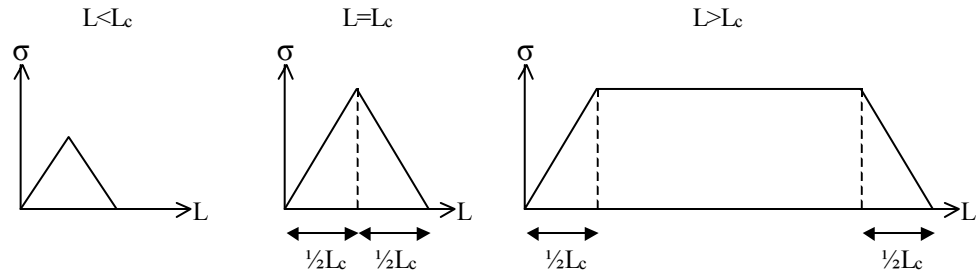

Figure 4.47 Linear build-up of stress inside a fibre.

The critical fibre length used in this model was determined by means of the single fibre fragmentation test (as described in Section 4.3.1), and was found to be L_c = 0.83mm for a composite containing NaOH/Na2SO3 treated hemp fibre with a matrix of polypropylene and 4wt% MAPP.

Since fibre tensile strength varies according to fibre length, the value for σ_f will vary according to L. The fibre strength at each fibre length was thus determined using the linear relationship found between fibre strength and fibre gauge length in Figure 4.45.

The fibre volume fraction (V_f) is calculated from the fibre weight fraction (W_f) using the following equation:

$$V_f = \left(1 + \frac{\rho_f}{\rho_m}\frac{1 - W_f}{W_f}\right)^{-1} \qquad (4.9)$$

where the hemp fibre density ρ_f = 1.48g/cm^3 [1], and is the matrix density ρ_m = 0.9g/cm^3 (as specified by the manufacturer). For a composite containing 40wt% hemp fibre and polypropylene, V_f = 0.288.

The failure strain (ε_c) of an injection moulded composite containing 40wt% hemp fibre, 4wt% MAPP and 56wt% polypropylene was found to be ε_c = 3.3% by means of tensile testing. The matrix stress at the failure strain of the composite was then determined from a stress-strain curve for polypropylene. The matrix stress was thus found to be σ_m = 20 MPa at a strain of ε_m = 3.3%, as can be seen in Figure 4.48.

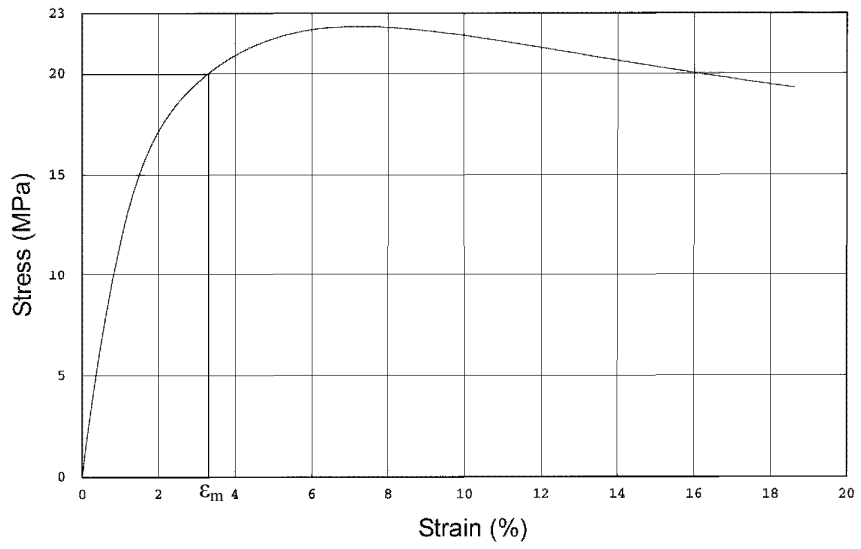

Figure 4.48 Stress-Strain curve for polypropylene, showing the stress of the matrix at the failure strain of the composite.

The composite tensile strength predictions for axially aligned discontinuous fibre composites were determined using Equation 4.6, and are shown in Figure 4.49. Tensile strengths were predicted for composites with differing fibre lengths,

ranging from an average fibre length of 0.1mm to an average fibre length of 12.5mm. The strengths of fibres at these lengths were determined using the trend line equation in Figure 4.45.

Since the contribution of sub-critical length fibres are relatively small to begin with and rapidly increase as the fibres approach L_c, the composite strength increases rapidly as the fibres approach L_c. Once the fibre length exceeds L_c, the fibres can be fully stressed over a greater area than fibres at L_c, thus resulting in further increases in composite strength. However, at fibre lengths above L_c, the model predicts that composite strength starts to level off due to the reduction of fibre tensile strength associated with the increases in fibre length (as can be seen in Figure 4.45). A maximum theoretical composite strength is obtained at a fibre length of $4L_c$ (3.3mm), after which the benefits offered by the longer fibres become offset by reductions in fibre strength, giving an overall reduction in predicted composite strength.

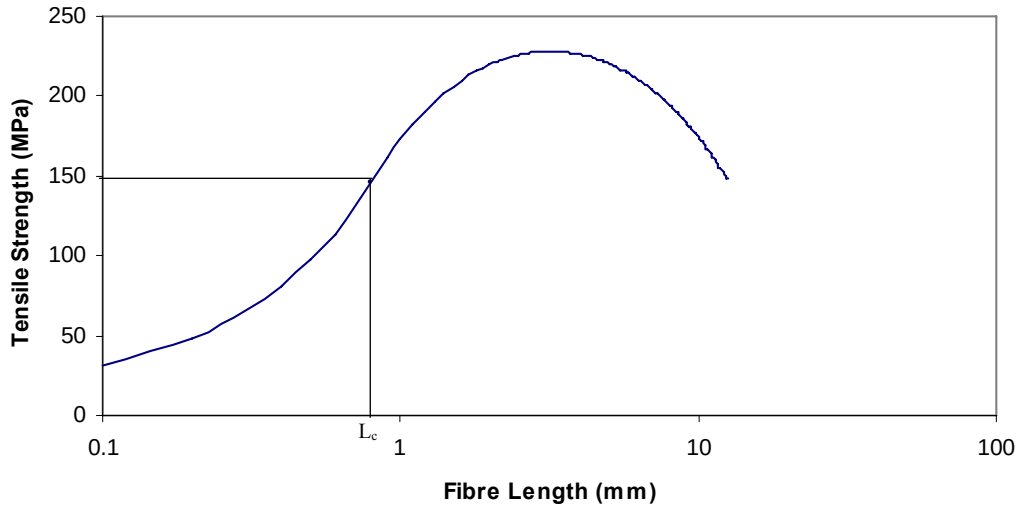

Figure 4.49 Kelly-Tyson prediction of composite tensile strength vs. fibre length for composites with fibre contents of 40wt% and perfect fibre alignment. The strength of a composite with fibre length equal to L_c is indicated.

It can thus be seen in Figure 4.49 that the maximum theoretical tensile strength of an axially aligned composite containing 40wt% $NaOH/Na_2SO_3$ treated hemp fibre, 4wt% MAPP and 56wt% polypropylene is 228 MPa, which could theoretically be achieved if all the fibres were 3.3mm in length.

The theoretical strength of a composite in which all the fibres lengths are equal to L_c (i.e. 0.83mm) is 150.6 MPa, which is only 66% of the maximum theoretical strength of a composite containing 3.3mm fibres, as proposed by the Kelly-Tyson model. It can thus be seen that fibre length plays an important part in determining the composite strength, and fibre lengths need to be equivalent to $4L_c$ in order to achieve the maximum theoretical composite strength.

In reality, however, a composite with fibres longer than $4L_c$ would not be expected to be weaker than a composite containing fibre lengths equal to $4L_c$. The Kelly-Tyson model effectively assumes that fibres can only be broken once prior to composite failure. In reality, however, long fibres can break into shorter fibre lengths without causing composite failure, and these shorter fibres can be reloaded to continue providing composite reinforcement.

Since this model assumes that fibres can only break once when stressed, it's accuracy is limited to fibre lengths in the range of L_c where the fibres can only be broken once. The accuracy of the model is thus reduced at fibre lengths where multiple fibre fractures are likely to occur, and the composite strength predictions become increasingly underestimated as the fibre length is increased. Thus, the maximum theoretical composite strength at $L = 4L_c$ is likely to be undervalued, and the reductions in composite strength at lengths above $4L_c$ (as seen in Figure 4.49) would not necessarily occur.

It can therefore be concluded that fibres need to be equal to or longer than $4L_c$ in order to achieve the maximum theoretical composite strength.

The Bowyer-Bader Model

The Hirsch and Bowyer-Bader models have both been shown to provide results that most closely match the experimentally obtained tensile strengths of short natural fibre reinforced thermoplastic composites [73, 125, 126]. The Bowyer-Bader model was selected for this study as it takes into consideration the super-critical and sub-critical length distributions of fibres extracted from an actual composite:

$$\sigma_c = K_1 \left\{ \sum_i \left[\frac{V_i \sigma_f L_i}{2L_c} \right] + \sum_j \left[V_j \sigma_f \left(1 - \frac{L_c}{2L_j} \right) \right] \right\} + V_m \sigma_m \quad (4.10)$$

where K_1 is a fibre orientation factor, V_i and V_j are the volume fractions of the sub-critical and super-critical fibre lengths, respectively; and L_i and L_j are the sub-critical and super-critical fibre lengths, respectively. Subscripts *i* and *j* refer to the sub-critical and super-critical lengths, respectively.

As with any model, a number of assumptions need to be identified and considered [131]. The assumptions for the Bowyer-Bader model are as follows:

- Stress transfer across the interface increases linearly from the tips of the fibre inwards to some maximum value
- No fibre-matrix debonding occurs
- An orientation correction factor (K_1) may be applied to account for fibres not oriented in the loading direction
- K_1 is independent of strain and is the same for all fibre lengths
- The composite matrix properties are the same as for the un-reinforced polypropylene
- The interfacial shear stress is independent of loading angle
- Porosity in the composite is negligible

The fibre length and diameter distributions used in this model were obtained by analysing the fibres extracted from injection moulded composites consisting of 40wt% NaOH/Na_2SO_3 treated normal-length hemp fibre, 56wt% polypropylene and 4wt% MAPP (as seen in Figure 4.25).

As can be seen in Equation 4.10, the Bowyer-Bader model accounts for the sum of all the sub-critical and super-critical fibre strength contributions, as well as the matrix contribution and a fibre orientation factor. It is therefore possible to divide the fibres that make up the fibre length distribution into sub-critical and super-critical fibre lengths, and then to determine the contribution of each of those fibres to the overall strength of the composite. The individual fibre contributions can

then be added together with the matrix contribution, and then multiplied by a fibre orientation factor to determine the composite strength.

In order to calculate the fibre contributions to composite strength, it was first necessary to determine the volume fraction (V_i or V_j) of each fibre in the fibre distribution. The volume of each individual fibre was calculated by multiplying the fibre cross-sectional area (obtained from diameters measured by the fibre length analyser) by the fibre length. It was then necessary to determine the volume fraction of each fibre in the fibre sample, which was done by dividing the volume of each fibre by the sum of all the fibre volumes.

Once the volume fraction of each fibre in the fibre sample was known, it was then necessary to determine the volume fraction of each fibre in the composite. It is known that the total volume fraction of fibres in an injection-moulded composite containing 40wt% hemp is $V_f = 0.288$ (i.e. the sum of all individual fibre volume fractions in the composite is equal to 0.288). The volume fraction of each fibre in the composite could thus be determined by multiplying the fibre volume fractions in the sample by 0.288.

The strength contribution of each individual sub-critical and super-critical length fibre was determined using Equation 4.10, where V_f for each fibre was determined by the method described above, L_i and L_j are the sub-critical and super-critical fibre lengths measured by means of a Kajaani fibre length analyser, and $L_c = 0.83$mm as determined in Section 4.3.1. Since the fibre length distribution in the composite is small, and all the fibres are short and in the range of L_c, the fibre tensile strength at the critical fibre length (σ_{fc}) was used in this model. The fibre tensile strength at the critical fibre length (σ_{fc}) was thus found to be 947.4 MPa (as described in Section 4.3.2). The strength contribution of the matrix was also determined, where $V_m = 0.712$ and $\sigma_m = 20$ MPa.

Assuming all the fibres are perfectly aligned in the axial direction (i.e. $K_1 = 1$), a composite containing 40wt% $NaOH/Na_2SO_3$ treated normal-length hemp fibre, 4wt% MAPP and 56wt% polypropylene would have a theoretical tensile strength of 149 MPa, based on the Bowyer-Bader model. Fibres shorter than L_c make up

49.6% of the total fibre volume, and yet account for only 31.9% of the fibre contribution to composite strength. Fibres longer than L_c make up 50.4% of the total fibre volume and account for 68.1% of the fibre contribution to composite strength.

It can be seen that the collective grouping of super-critical length fibres are more effective in contributing to the overall composite strength compared to sub-critical length fibres. As suggested by the strength predictions in Figure 4.49, fibre length is an important variable in determining composite strength, along with fibre orientation and fibre-matrix adhesion. It is therefore necessary to maximise the reinforcing fibre lengths to achieve improvements in composite strength.

The experimentally obtained tensile strength of an injection-moulded composite containing 40wt% $NaOH/Na_2SO_3$ treated normal-length hemp fibre, 4wt% MAPP and 56wt% polypropylene is 50.5 MPa (as described in Section 4.2.3), which is only one-third of the theoretical composite strength determined by means of the Bowyer-Bader model. Using Equation 4.10 and the experimentally obtained composite strength, the fibre orientation factor for the injection moulded composite was found to be $K_1 = 0.34$.

It is reported that a three-dimensional random fibre alignment yields a value of $K_1 = 0.2$, and an axially aligned fibre arrangement yields a value of $K_1 = 1$ [125, 133]. A value of $K_1 = 0.34$ therefore suggests that the fibre orientation in this particular composite is slightly better than a typical random fibre orientation. This is verified by the micrographs in Section 4.2.5, where it can be seen that the fibres are oriented in a planar-random manner.

The value of $K_1 = 0.34$ also indicates that only a small fraction of the fibres effectively contribute to the strength of the composite. It is well known from the analysis of the off-axis properties of unidirectional composites that the reinforcing effect of a fibre drops off rapidly as the angle between the loading direction and the fibre is increased [133]. It therefore seems likely that the tensile strengths of planar-randomly oriented injection moulded composites are governed by the

fibres that have an orientation close to parallel with the loading direction. As those fibres fail, the composite as a whole fails.

K_1 accounts mostly for fibre orientation, but as it is essentially a fitting factor, it also represents a combination of other factors including fibre strength distribution, imperfect interfacial bonding and fibre end effects that are commonly found in short discontinuous fibre composites [163].

The fibre strength at L_c has been used for the purpose of simplifying the calculations. It is widely known that fibre strength is dependent on fibre length. Since the composite consists of a range of fibre lengths, it is expected that there would be variations in fibre strength as well. These variations in fibre strength with fibre length are insignificant for this composite, as they are much smaller than the large strength variations that are usually associated with natural fibres. Also, the fibre strength used in these calculations was determined by *ex situ* test methods, as it is not possible to determine the fibre strength *in situ*. This may result in an over-estimation of fibre strength, as it is thought that fibres *in situ* are weaker due to fibre damage inflicted during composite processing.

In this investigation, an average interfacial shear strength has been used. The interfacial shear strength, however, may not be uniform in the composite due to imperfect mixing of the coupling agent with the matrix, and differences in fibre surface chemistry due to the variable removal of non-cellulosic fibre compounds during alkali treatment.

It is also known that interfacial shear stresses reach a maximum value at the fibre ends and then decrease towards the middle of the fibre, reaching zero when the distance exceeds $L_c/2$ [110, 119, 163]. The high interfacial shear stresses experienced at the fibre ends may initiate interfacial failure, which may then propagate along the fibre length, further reducing the ability of the fibre to transfer stresses [163]. The high interfacial shear stresses experienced at the fibre ends may also result in yielding of the matrix. Once interfacial failure is initiated and propagated along the fibre length, the load carrying abilities of short

discontinuous fibres may quickly be made ineffectual, as opposed to those of long, continuous fibres.

In this investigation, it is also assumed that small fibres and fibre fragments contribute to composite strength. These small fibres may actually act as fillers rather than reinforcements, and may not actually contribute to the strength of the composite. However, small fibres and fibre fragments may fit in-between the larger fibres in the composite, resulting in improvements in fibre packing, which may then lead to improvements in composite Young's modulus.

It can thus be concluded that in order to produce a strong composite material, the following are required:

- Strong reinforcing fibres and a matrix with a shear strength above the composite interfacial shear strength to prevent shear yielding
- Good fibre-matrix interfacial adhesion (i.e. a low L_c)
- Fibres need to be longer than L_c in order for them to be fully loaded at the fibre centre, but need to be longer than $4L_c$ to make a greater contribution to the composite strength
- Fibres need to be oriented in the loading direction
- Fibres need to be evenly distributed throughout the matrix.

4.5 Thermal Analysis of Fibres and Composites

The TGA and DTA plots of untreated and alkali treated hemp can be seen in Figure 4.50. The onset of thermal degradation can be identified by a dramatic decrease in sample weight and increase in the temperature difference due to the exothermic combustion reactions taking place. The thermal degradation of untreated hemp fibre begins at around 205^{o}C, and the thermal degradation of alkali treated hemp fibre starts at around 240^{o}C. Untreated fibre degrades at lower temperatures due to the presence of thermally unstable fibre constituents such as hemicelluloses and pectins, whereas the alkali treated fibre is more stable due to the removal of these constituents.

The two main DTA peaks of untreated hemp fibre appear to be made up of several smaller peaks, indicating the multiple exothermic degradation reactions of cellulose, lignin, hemicelluloses and pectins. The much narrower DTA peaks of treated hemp indicate a more homogeneous composition containing mostly cellulose, with fewer other decomposition reactions taking place. The first exotherm has a peak temperature of 276^{o}C for untreated fibre and 316^{o}C for alkali treated fibre, and is most likely caused by the decomposition of cellulose, leading to the formation and volatilisation of levoglucosan and other volatile products as reported by Dahiya and Rana [164]. The exothermic peaks at 384^{o}C for untreated fibre and 425^{o}C for alkali treated fibre may be attributed to the oxidation of volatile and charred products. Since the two exothermic peaks of the alkali treated hemp fibre have shifted to higher temperatures when compared to the untreated fibre, it can be concluded that alkali treatment increases the thermal stability of hemp.

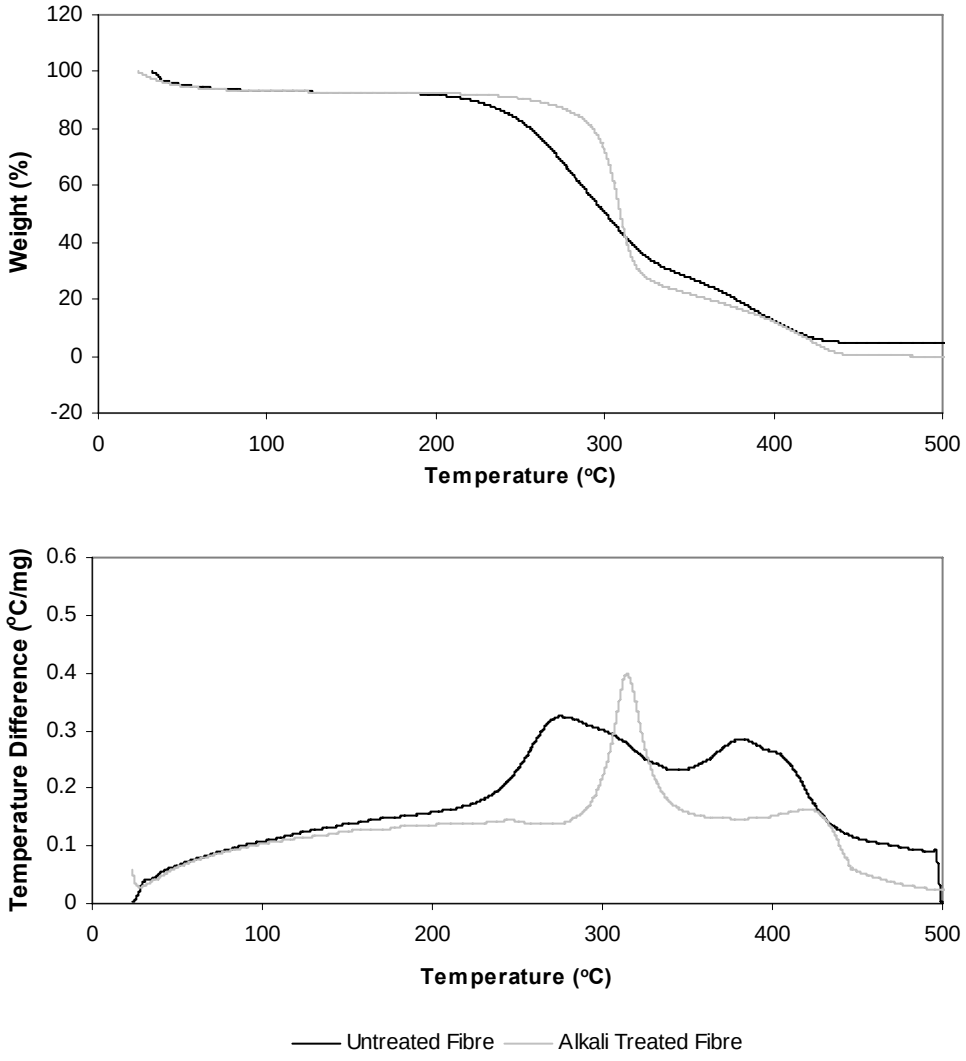

Figure 4.50 TGA and DTA curves for alkali treated and untreated hemp fibre.

The TGA and DTA plots of polypropylene, composites containing untreated hemp fibre, and composites containing alkali treated hemp fibre can be seen in Figure 4.51. It can be seen that both composites start to lose weight at lower temperatures when compared to polypropylene, thus indicating that polypropylene has a higher thermal stability. High shear and frictional forces are experienced by polypropylene and the two composites during extrusion, and it was observed that the composites were more viscous than polypropylene due to their high fibre contents. The high shear and frictional forces that occur between the fibres and polypropylene matrix during extrusion are thought to have caused breakage of the polypropylene polymeric chains, resulting in a decrease in thermal stability of the composite.

It can be seen from the TGA plot in Figure 4.51 that composite weight loss began at 214^{o}C for both composites. This is in contrast to what was expected, as it was thought that the composite containing untreated hemp fibre would be less thermally stable than the treated fibre composite due to the higher hemicellulose and pectin contents of the untreated fibre. This apparent improvement in thermal stability of the untreated fibre composite could be attributed to the presence of the MAPP coupling agent. MAPP is able to bond with the hemicellulose in the untreated fibre, thus stabilizing its structure and improving the thermal stability of the composite [165]. Several other authors have also reported the thermal stabilization of non-cellulosic fibre constituents by means of a coupling agent [166-168]. The poor thermal stability of hemicelluloses and pectins in a composite can thus be negated by the inclusion of a coupling agent.

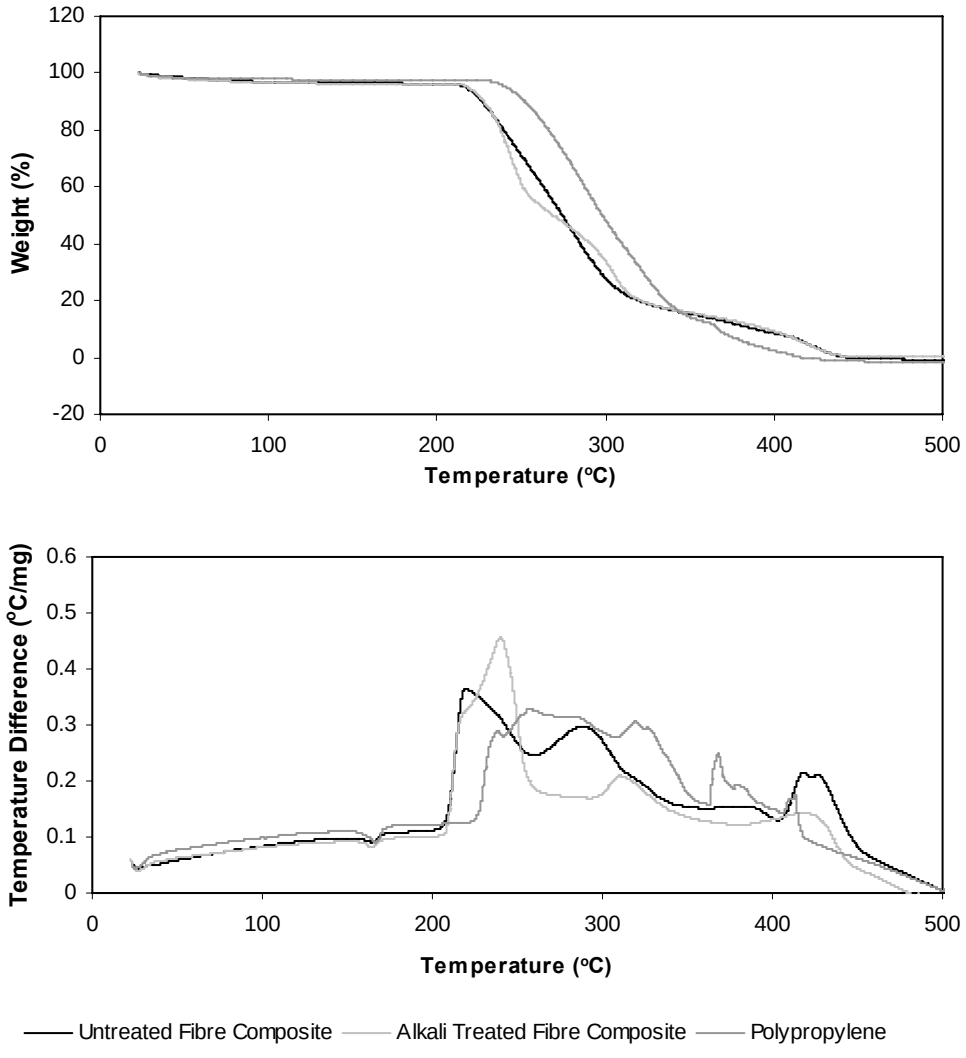

Figure 4.51 TGA and DTA curves for polypropylene, the composite containing untreated hemp and the composite containing alkali treated hemp.

From the TGA and DTA plots in Figure 4.52 and Figure 4.53, it can be seen that both composites are less thermally stable than their constituents. The DTA plots of each composite are also not exact summations of the plots obtained for hemp fibre and polypropylene. This indicates that unknown complex interactions/reactions are likely to have taken place between the fibre constituents, the MAPP coupling agent and the polypropylene matrix of each composite.

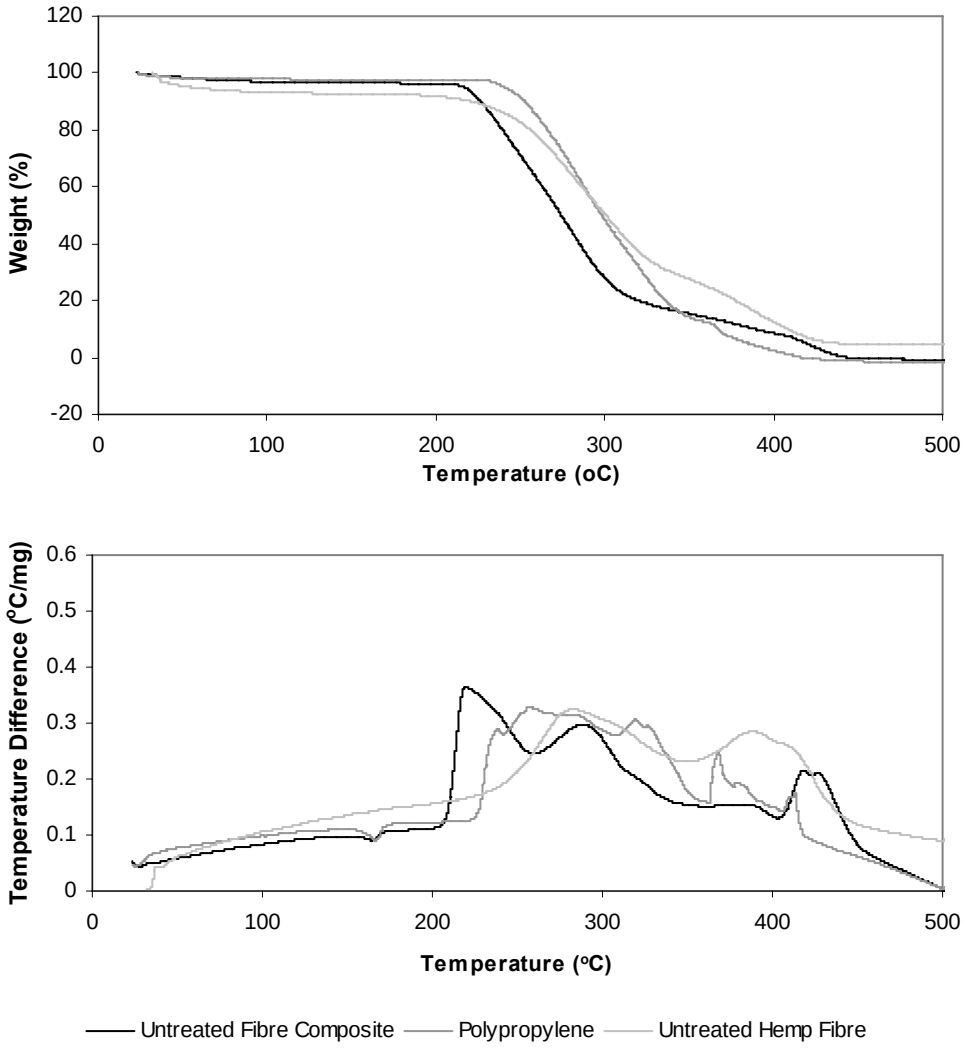

Figure 4.52 TGA and DTA curves for polypropylene, untreated hemp fibre and the composite containing untreated hemp.

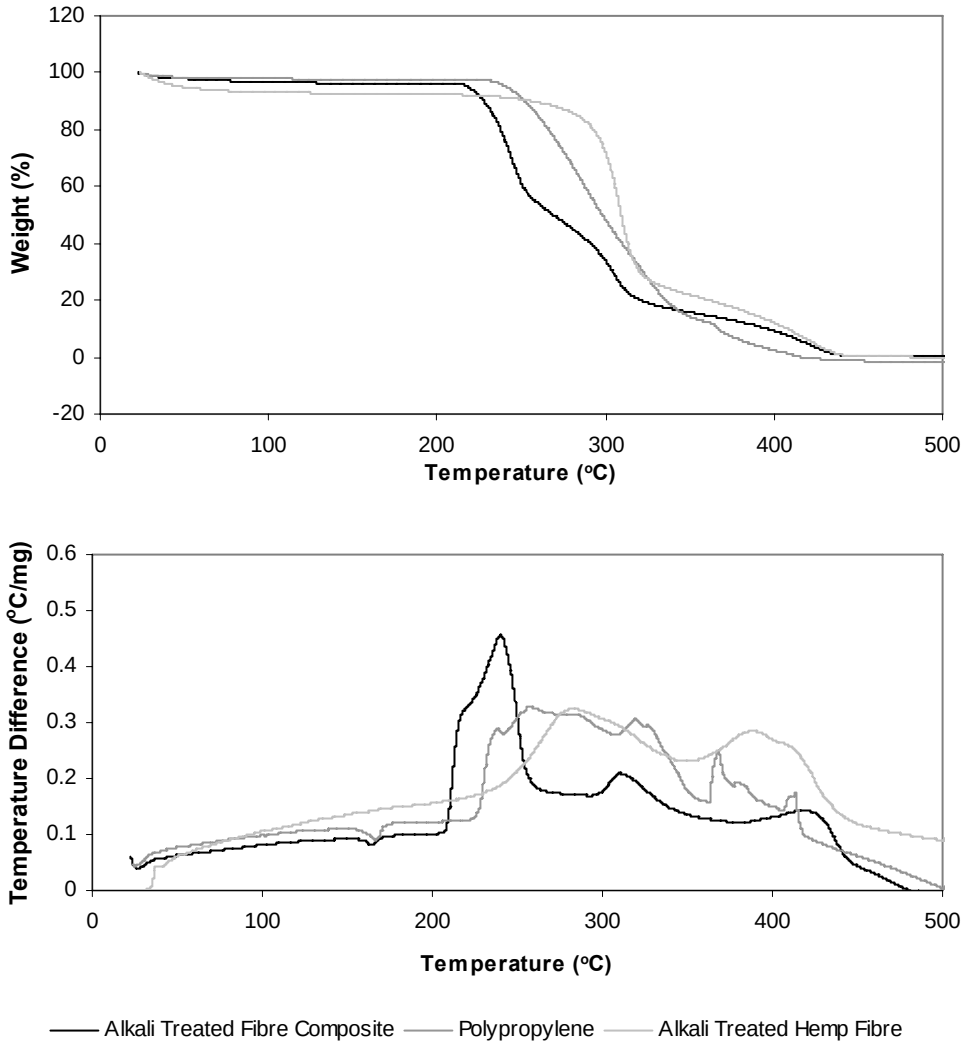

Figure 4.53 TGA and DTA curves for polypropylene, alkali treated hemp fibre and the composite containing alkali treated hemp.

The thermal analysis of extruded polypropylene and extruded composites does not necessarily give a true representation of the thermal reactions that may take place during the injection moulding process. It is difficult to determine the exact conditions experienced by the composite material during injection moulding, and the conditions in an open system as such as a TGA and DTA analyser are expected to vary considerably to a closed system such as an injection moulder.

During injection moulding, it was observed that alkali treated fibre composites could be processed at a set temperature of 180°C without evidence of burning, whereas untreated fibre composites had to be processed at 145°C, and showed evidence of burning when processed at 155°C. Despite the fact that the melting

temperature of the polypropylene copolymer is 165^{o}C, it was possible to melt the polymer at lower temperatures due to the high-pressure and high friction conditions experienced in the injection moulder. It is interesting to see from Figure 4.51 that the onset of thermal oxidative degradation in the DTA-TGA analyser occurs at 214^{o}C for both the untreated and alkali treated composites, whereas degradation occurred at a much lower temperature for the untreated fibre composite during the injection moulding process. It is known that much higher pressures are experienced during injection moulding compared to extrusion, and it is thought that high pressures have an important part to play in accelerating the degradation of hemicelluloses and pectins in the fibre.

When the untreated fibre composite was injection moulded at a set temperature of 155^{o}C, a colour change and burning smell were observed. At 160^{o}C the composite appeared to be a darker shade of brown with a more intense smell, and at 170^{o}C the composite appeared burned and contained voids caused by the release of combustion gases. The alkali treated fibre composites appeared unchanged at all processing temperatures up to 190^{o}C.

The colour change of the untreated fibre composite was most likely due to the formation of tar from the degradation of hemicelluloses, and the formation of black char powder as a result of pectin degradation. The distinct burning smell was thought to be a product of hemicellulose degradation. Even though degradation of the untreated fibre composite appeared to have begun at 155^{o}C, a small reduction in fibre strength was only observed at 170^{o}C, as can be seen in Figure 4.54. This suggests that the cellulose component of the fibre, which is responsible for fibre strength, had not been affected by the conditions in the injection moulder. According to some researchers, the crystalline structure of cellulose can be improved up to a certain temperature, which may be as high as 200^{o}C [41]. It is therefore likely that the combination of heat and pressure in the injection moulder resulted in the degradation of hemicelluloses and pectins, without affecting the integrity of the cellulose.

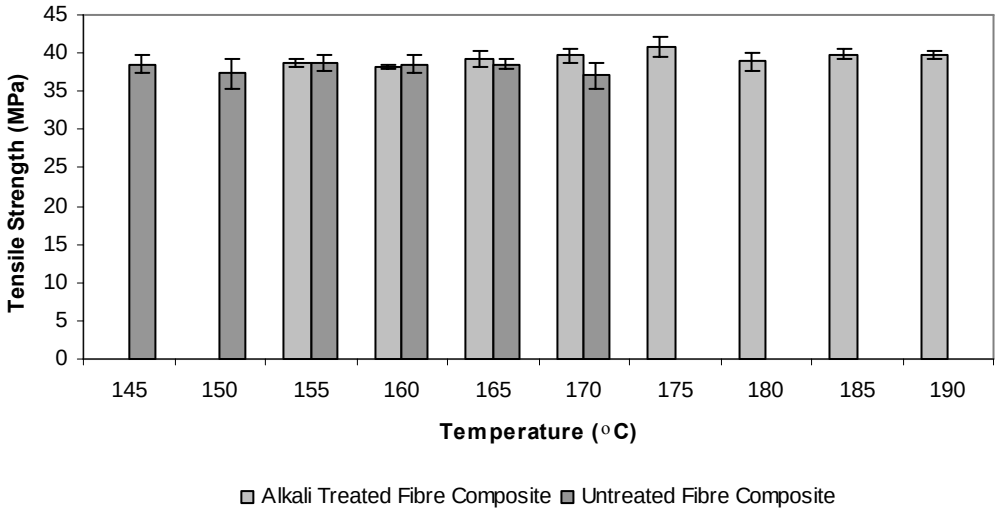

Figure 4.54 Effect of injection moulder temperature settings on the tensile strength of composites containing 40wt% NaOH treated hemp fibre and 3wt% MAPP. The error-bars each represent ± 1 standard deviation.

Chapter 5: Conclusions

5.1 Alkali Fibre Treatments

In this investigation it was shown that a 5wt% NaOH / 2wt% Na_2SO_3 fibre treatment could be used to delignify and separate hemp fibres from their fibre bundles without reducing the fibre tensile strength and Young's modulus. A second treatment involving the use of a 10wt% NaOH solution was found to reduce the fibre tensile strength considerably as well as to negatively affect the fibre Young's modulus.

The crystallinity index of untreated hemp fibre was shown to be 84.7%, and this was increased to 89.6% for fibre treated with NaOH and 89.1% for fibre treated with NaOH/Na_2SO_3. The increase in fibre crystallinity as a result of alkali treatment was thought to be due to better packing and stress relaxation of the cellulose chains as a result of the removal of amorphous fibre constituents.

Untreated fibres were found to contain 5wt% lignin, and were un-separated and bound together in the form of fibre bundles. Considerable fibre separation was achieved by means of alkali treatment, and the NaOH/Na_2SO_3 and NaOH treatments were found to have reduced the fibre lignin contents to 3.5wt% and 2.1wt%, respectively.

Observations of fibre surfaces by means of SEM imaging showed that the untreated fibres were covered in the gummy polysaccharides of lignin, pectin and hemicellulose, whereas the alkali treated fibres appeared to have clean but rough surfaces containing large numbers of etched striations. It is thought that these striations would provide enhanced mechanical interlocking with the polymer matrix, and the removal of cementing materials would allow direct bonding between the fibre microfibril cellulose and the MAPP coupling agent.

The thermal stability of hemp fibre was analysed by means of TGA and DTA, and it was found that untreated fibre was less thermally stable than $NaOH/Na_2SO_3$ treated fibre, with degradation starting at 205^oC and 240^oC for each, respectively.

5.2 Extruded and Injection Moulded Composites

In this investigation, it was found that an injection moulded hemp fibre reinforced polypropylene composite containing 40wt% fibre provided the best combination of tensile strength, Young's modulus and ease of processing.

It was also found that the addition of a MAPP coupling agent resulted in increases in composite tensile strength due to improvements in the fibre-matrix interfacial adhesion. The optimum MAPP content observed in this investigation was 4wt%.

A composite consisting of 40wt% $NaOH/Na_2SO_3$ treated fibre, 4% MAPP and polypropylene was thus found to have the highest tensile strength (50.5 MPa) and Young's modulus (5.31 GPa) of all the composites tested, due to the inclusion of the strongest, well separated fibres and an optimum fibre and MAPP content. This composite appears to have the highest tensile strength for any injection moulded hemp fibre reinforced polypropylene composite reported in the literature.

Single fibre fragmentation tests of $NaOH/Na_2SO_3$ treated fibres in a matrix of 4wt% MAPP and polypropylene revealed a critical fibre length (L_c) of 0.83mm. A two-parameter Weibull distribution of fibre fragments was used to determine the interfacial shear strength of this composite, which was found to be 16.1 MPa. The magnitude of this interfacial shear strength indicated a relatively high level of fibre/matrix adhesion for composites consisting of 40wt% $NaOH/Na_2SO_3$ treated fibre, 4% MAPP and polypropylene.

SEM analysis of composite fracture surfaces showed that composites without MAPP failed by means of fibre de-bonding and tensile failure of the matrix. Composites containing 4wt% MAPP failed mostly by local shear yielding of the

matrix around the fibre, rather than tensile failure of the fibres or fibre de-bonding.

Composite extrusion, granulating and injection moulding were found to cause significant fibre damage and reductions in fibre length, which limited the tensile strength of composites fabricated in this manner. It was also found that injection moulded composites displayed a planar-random fibre orientation as a result of the fountain flow effect.

TGA and DTA analysis showed that untreated hemp fibre composites and $NaOH/Na_2SO_3$ treated hemp fibre composites, each with a matrix of 4% MAPP and polypropylene, were less thermally stable than the polypropylene matrix alone; this was thought to be due to polymer chain breakages that occur in the composite matrix as a result of extrusion and injection moulding. The thermal stabilities of composites containing untreated fibre and $NaOH/Na_2SO_3$ treated fibre were found to be similar to each other.

5.3 Solution Mixed Composites

Composites with long, axially aligned fibres were successfully produced using a novel solution mixing technique and hot pressing. Significant improvements in tensile strength and Young's modulus were achieved for solution mixed composites compared to composites produced by means of extrusion and injection moulding. The strongest solution mixed composite had a tensile strength of 84.7 MPa, and consisted of 56wt% $NaOH/Na_2SO_3$ treated fibre, 4% MAPP and polypropylene; and the stiffest injection moulded composite had a Young's modulus of 16.0 GPa, and consisted of 63wt% $NaOH/Na_2SO_3$ treated fibre, 4% MAPP and polypropylene. Improvements in tensile strength of 68% were gained over the strongest injection moulded composite, and improvements in Young's modulus of 201% were gained over the stiffest injection moulded composite.

Despite these improvements, it was thought that the tensile strength and Young's modulus of solution mixed and hot pressed composites were below their potential

values because of fibre degradation, crimping of the fibres, poor fibre separation and the presence of voids within the composites.

5.4 Composite Modelling

Based on the results obtained from the Modified Rule of Mixtures Model, it was found that the reinforcing fibres in a composite need to be axially aligned in the loading direction and need to be equal to or longer than $4L_c$ in order to achieve the maximum theoretical composite strength.

The Bowyer-Bader model was used to predict the strength of an injection moulded composite with a normal fibre length distribution, consisting of 40wt% $NaOH/Na_2SO_3$ treated fibre, 4% MAPP and 56wt% polypropylene. A theoretical composite tensile strength of 149 MPa was obtained from the model, based on the assumption that all the fibres were axially aligned in the composite. The experimentally obtained tensile strength for the composite was 50.5 MPa, which is only one-third of the theoretical composite strength determined by means of the Bowyer-Bader model. The difference between the experimentally obtained composite strength and theoretical composite strength was thought to be mainly due to the planar-random orientation of the reinforcing fibres in the composite.

It is believed that all of the research objectives stated in the introduction have been met with the completion of this thesis. A greater understanding of the parameters that influence the strength and stiffness of natural fibre reinforced thermoplastic composites has been achieved, and it is believed that advances in the mechanical properties of such composites have been attained. Several original contributions have also been made, the most important being the fabrication of oriented fibre composites by means of solution mixing, and the use of synthetic fibre modelling techniques to predict the strength of natural fibre reinforced thermoplastic composite materials.

Chapter 6: Recommendations for Future Work

The results obtained during the course of this research have laid an important platform from which to further improve the properties of hemp fibre reinforced thermoplastic composites. Some recommendations for future work have been proposed:

- The true benefits offered by using natural fibres such as hemp lie in the fact that they are sustainable, bio-derived and biodegradable. It is therefore suggested that bio-derived and/or biodegradable polymer matrices be used instead of petroleum-derived polymers. Natural fibre reinforced composites containing bio-derived matrices could potentially be incinerated after use for energy recovery, and natural fibre reinforced composites containing biodegradable matrices could potentially be composted after use to provide soil nutrients.

- It was found that composites with good fibre-matrix adhesion failed mostly by local shear yielding of the matrix around the fibre, rather than tensile failure of the fibres or fibre de-bonding. A polymer with a shear strength greater than that of polypropylene should therefore be used as the composite matrix to avoid such failure.

- The use of coupling agents other than MAPP, or combinations of coupling agents, could be investigated to improve the fibre-matrix interfacial adhesion of composites with matrices other than polypropylene.

- To produce a genuine environmentally friendly composite material, it is necessary that the fibre and composite processing methods are

environmentally sound. It may therefore be necessary to investigate environmentally friendly alternatives to alkali fibre treatment, which may involve the use of lignin-degrading fungi and enzymes.

- To improve the strength of fibre reinforced composites, it is necessary to achieve good fibre alignment in the direction of the applied load. This may involve the use of continuous hemp yarns to produce uniaxially aligned thermoplastic matrix pre-preg composites for the compression moulding of composite components.

- Hemp fibre is often obtained commercially in bales of tangled and twisted strips of retted bast fibre, which can be difficult to straighten for use in axially aligned composites. Since the fibres are originally straight and aligned in the outer bark of the hemp plant, it may be possible to alkali treat strips of hemp bark without bending the fibres and causing permanent fibre disfigurement.

- An alternative fabrication method to produce axially aligned fibre composites could involve the fabrication of fibres made from a thermoplastic polymer and coupling agent, and then commingling these polymer fibres with hemp fibres by means of carding. The resulting oriented fibre mats could then be stacked and consolidated by means of compression moulding.

- To reduce the hydrophilicity of natural fibres and to improve the water resistance of natural fibre reinforced composites, the fibres could be pressure-treated with a low viscosity chemical solution that could penetrate the amorphous regions of the fibre and bond with available OH groups.

- Many composite strength prediction models require inputs of single fibre tensile strength and Young's modulus in the longitudinal fibre direction (i.e. along the fibre length). Since many composites consist of fibres

oriented transversely to the direction of applied load, it is necessary to determine the tensile strength and Young's modulus of single fibres in the transverse direction (i.e. across the fibre thickness).

- Since the average fibre lengths in extruded and injection moulded composites were found to be below the critical fibre length, it is suggested that an investigation be performed to determine the effects of each composite processing step on the composite fibre length distribution (i.e. extrusion, granulating and injection moulding). Once it has been established which step/steps are responsible for reducing fibre length, changes could then be made to the processing equipment to reduce fibre breakages and to ensure that the fibre lengths are maintained above the critical fibre length. It is also suggested that a study be performed to determine the optimum fibre length for injection moulded composites, as sub critical length fibres provide poor composite reinforcement, and long fibres tend to become entangled.

References

1. Wambua, P., Ivens, J., and Verpoest, I., *Natural fibres: can they replace glass in fibre reinforced plastics?* Composites Science and Technology, 2003. **63**(9): p. 1259-1264.
2. Bos, H.L., Van Den Oever, M.J.A., and Peters, O.C.J.J., *Tensile and compressive properties of flax fibres for natural fibre reinforced composites.* Journal of Materials Science, 2002. **37**: p. 1683-1692.
3. Sanadi, A.R., Caulfield, D.F., and Jacobson, R.E., *Agro-fiber / thermoplastic composites*, in *Paper and composites from agro-based resources*. 1997, CRC Lewis Publishers. p. 377-401.
4. Pervaiz, M. and Sain, M.M., *Carbon storage potential in natural fiber composites.* Resources, Conservation and Recycling, 2003. **39**(4): p. 325-340
5. Mohanty, A.K., Misra, M., and Drzal, L.T., *Sustainable bio-composites from renewable resources: Opportunities and challenges in the green materials world.* Journal of Polymers and the Environment, 2002. **10**: p. 19-26.
6. Plackett, D. *The natural fiber-polymer composite industry in Europe - technology and markets*. in *7th Toronto Conference on "Progress in Woodfibre-plastic Composites"*. 2002. Toronto, Canada.
7. Sanadi, A.R., Young, R.A., Clemons, C.M., and Rowell, R.M., *Recycled newspaper fibers as reinforcing fillers in thermoplastics: Part 1 - Analysis of tensile and impact properties in polypropylene.* Journal of Reinforced Plastics and Composites, 1994. **13**: p. 54-67.
8. Marsh, G., *Composites on the road to the big time?* Reinforced Plastics, 2003. **47**(2): p. 33-36.
9. Lee, S.M., *International Encyclopedia of Composites - Vol. 2*. 1990: New York. p. 35.
10. Karus, M. and Kaup, M., *Natural fibres in the European automotive industry.* Journal of Industrial Hemp, 2002. **7**(1): p. 119-131.
11. Marsh, G., *Next step for automotive materials.* Materials Today, 2003. **6**(4): p. 36-43.
12. Clemons, C.M., *Wood plastic composites in the United States.* Forest Products Journal, 2002. **52**(6): p. 10-18.
13. Nickel, J. and Riedel, U., *Acticities in Biocomposites.* Materials Today, 2003: p. 44-48.
14. Eichhorn, S.J., Baillie, C.A., Zafeiropoulos, N., Mwaikambo, L.Y., Ansell, M.P., Dufresne, A., Entwistle, K.M., Herrera-Franco, P.J., Escamilla, G.C., Groom, L., Highes, M., Hill, C., Rials, T.G., and Wild, P.M., *Current international research into cellulosic fibres and composites.* Journal of Materials Science, 2001. **36**(9): p. 2107-2131.
15. Robson, D. and Hague, J. *A comparison of wood and plant fiber properties*. in *3rd International Conference on Woodfiber-Plastic Composites*. 1995. Madison, Wisconsin, USA: Forest Products Society.

16. Rowell, R.M., Han, J.S., and Rowell, J.S., *Characterization and factors effecting fiber properties*, in *Natural Polymers and Agrofibres Composites*, E.L.A.L.a.M. Frolline, L.H.C., Editor. 2000, Embrapa Instrumentacao Agropecuaria: Sao Carlos, Brazil. p. 115-134.
17. Mohanty, A.K., Misra, M., and Hinrichsen, G., *Biofibres, biodegradable polymers and biocomposites: An overview.* Macromolecular Materials and Engineering, 2000. **276**(1): p. 1-24.
18. Pickering, K.L., Priest, M., Watts, T., Beckermann, G.W., and Alam, S.N., *Feasibility study for NZ hemp fibre composites.* SAMPE Journal of Advanced Materials, 2005. **37**(3).
19. Vignon, M.R., Dupeyre, D., and Garcia-Jaldon, C., *Morphological characterization of steam-exploded hemp fibers and their utilization in polypropylene-based composites.* Bioresource Technology, 1996. **58**(2): p. 203-215.
20. Garcia-Jaldon, C., Dupeyre, D., and Vignon, M.R., *Fibres from semi-retted hemp bundles by steam explosion treatment.* Biomass and Bioenergy, 1998. **14**(3): p. 251-260.
21. Mediavilla, V., Leupin, M., and Keller, A., *Influence of the growth stage of industrial hemp on the yield formation in relation to certain fibre quality traits.* Industrial Crops and Products, 2001. **13**: p. 49-56.
22. Keller, A., Leupin, M., Mediavilla, V., and Wintermantel, E., *Influence of the growth stage of industrial hemp on chemical and physical properties of the fibres.* Industrial Crops and Products, 2001. **13**(1): p. 35-48.
23. Correia, F., Roy, D.N., and Goel, K., *Pulping of Canadian industrial hemp.* Pulp and Paper Canada, 1998. **99**(9): p. 39-41.
24. Dickison, W.C., *Plant growth, development, and cellular organization*, in *Integrative Plant Anatomy*. 2000, Academic Press: Burlington. p. 3-49.
25. Bledzki, A.K. and Gassan, J., *Composites reinforced with cellulose based fibres.* Progress in Polymer Science, 1999. **24**(2): p. 221-274.
26. Bennett, S.J., Snell, R., and Wright, D., *Effect of variety, seed rate and time of cutting on fibre yield of dew-retted hemp.* Industrial Crops and Products, 2006. **24**(1): p. 79-86.
27. *TPP Industrial Hemp Guide*. 1998, Health Canada. p. 4.
28. Milner, K.C., Anacker, R.L., Fukushi, K., Haskins, W.T., Landy, M., Malmgren, B., and Ribi, E., *Structure and biological properties of surface antigens from gram-negative bacteria*, in *Symposium on Relationship of Structure of Microorginasms to their Immunological Properties*. 1963: American Society for Microbiology, Cleveland, Ohio.
29. Lilholt, H. and Lawther, J.M., *Natural Organic Fibers*, in *Comprehensive composite materials*, T.-W. Chou, Editor. 2000, Elsevier Science: Oxford. p. 303-325.
30. Wallenberger, F.T., Weston, N.E., Ford, R., Wool, R.P., and Chawla, K. *Advanced fibers, plastics, laminates and composites*. in *Materials Research Society Symposium*. 2001. Boston, Massachusetts, U.S.S.: Materials Research Society.
31. Walker, J.C.F., *Wood chemistry and cell wall ultrastructure*, in *Primary Wood Processing*. 1993, Chapman and Hall: London. p. 44-51.
32. Rowell, R.M. *A new generation of composite materials from agro-based fiber*. in *The 3rd International Conference on Frontiers of Polymers and Advanced Materials*. 1995. Kuata Lumpur, Malaysia: Plenum Press.

33. Walker, J.C.F., *Basic wood chemistry and cell wall ultrastructure*, in *Primary Wood Processing*. 1993, Chapman and Hall: London. p. 23-67.
34. Sjöström, E., *Wood Chemistry: Fundamentals and Applications*. 1981: Academic Press.
35. Rowell, R.M., *Chemical modification of agro-resources for property enhancement*, in *Paper and Composites from Agro-based Resources*. 1997, CRC Press. p. 351-375.
36. Van de Velde, K. and Kiekens, P., *Thermoplastic polymers: overview of several properties and their consequences in flax fibre reinforced composites.* Polymer Testing, 2001. **20**(8): p. 885-893.
37. Smith, W.F., *Foundations of Materials Science and Engineering*. 2nd ed. 1993: McGraw-Hill.
38. Van de Velde, K. and Kiekens, P., *Thermoplastic pultrusion of natural fibre reinforced composites.* Composite Structures, 2001. **54**(2-3): p. 355-360.
39. Maldas, D. and Kokta, B.V., *Role of coupling agents on the performance of woodflour-filled polypropylene composites.* International Journal of Polymeric Materials, 1994. **27**: p. 77-88.
40. Matthews, F.L. and Rawlings, R.D., *Composite Materials: Engineering and Science*. 1 ed. 1994: Chapman and Hall.
41. Yildiz, S., Gezer, E.D., and Yildiz, U.C., *Mechanical and chemical behavior of spruce wood modified by heat.* Building and Environment, 2006. **41**(12): p. 1762-1766.
42. Ray, D., Sarkar, B.K., Basak, R.K., and Rana, A.K., *Study of the thermal behavior of alkali treated jute fibers.* Journal of Applied Polymer Science, 2001. **85**: p. 2594-2599.
43. Islam, M.S., Pickering, K.L., and Beckermann, G.W. *The effect of fibre treatment using alkali on industrial hemp fibre/epoxy resin composites*. in *ICME*. 2005. Dhaka, Bangladesh.
44. Vichnevsky, S., Fuhr, B., and Melnichuk, J., *Characterization of wood and non-wood mechanical pulps by differential thermal analysis.* Journal of Pulp and Paper Science, 2003. **29**(1): p. 17-20.
45. Joseph, P.V., Rabello, M.S., Mattoso, L.H.C., Joseph, K., and Thomas, S., *Environmental effects on the degradation behaviour of sisal fibre reinforced polypropylene composites.* Composites Science and Technology, 2002. **62**(10-11): p. 1357-1372.
46. de Albuquerque, A.C., Joseph, K., Hecker de Carvalho, L., and d'Almeida, J.R.M., *Effect of wettability and ageing conditions on the physical and mechanical properties of uniaxially oriented jute-roving-reinforced polyester composites.* Composites Science and Technology, 2000. **60**(6): p. 833-844.
47. Zafeiropoulos, N.E., Baillie, C.A., and Matthews, F.L., *A study of transcrystallinity and its effect on the interface in flax fibre reinforced composite materials.* Composites Part A: Applied Science and Manufacturing, 2001. **32**(3-4): p. 525-543.
48. Miller, N.A., Stirling, C.D., and Van Tilburg, V.S.M., *Effects of fibre treatment on fibre/matrix interfacial bonding in Pinus Radiata fibre/thermoplastic composites.* Polymers and Polymer Composites, 1995. **3**(2): p. 117-126.

49. Nando, G.B. and Gupta, B.R., *Short fiber-thermoplastic elastomer composites*, in *Short Fibre-Polymer Composites*, J.R. White, Editor. 1996, Woodhead Publishing: Cambridge.
50. Fu, S.Y. and Lauke, B., *Effects of fiber length and fiber orientation distributions on the tensile strength of short-fiber reinforced polymers.* Composites Science and Technology, 1996. **56**: p. 1179-1190.
51. Brooks, R., *Injection molding based techniques*, in *Comprehensive Composite Materials*, A. Kelly and C. Zweben, Editors. 2000, Elsavier Science Ltd: Oxford.
52. Van Hattum, F.W.J. and Bernardo, C.A., *A model to predict the strength of short fiber composites.* Polymer Composites, 1999. **20**(4): p. 524-533.
53. Thomason, J.L., *Micromechanical parameters from macromechanical measurements on glass reinforced polypropylene.* Composites Science and Technology, 2002. **62**(10-11): p. 1455-1468.
54. Bowyer, W.H. and Bader, M.G., *On the re-inforcement of thermoplastics by imperfectly aligned discontinuous fibres.* Journal of Materials Science, 1972. **7**(11): p. 1315-1321.
55. Kim, E.G., Park, J.K., and Jo, S.H., *A study on fiber orientation during the injection molding of fiber-reinforced polymeric composites: (Comparison between image processing results and numerical simulation).* Journal of Materials Processing Technology, 2001. **111**(1-3): p. 225-232.
56. Bernasconi, A., Rossin, D., and Armanni, C., *Analysis of the effect of mechanical recycling upon tensile strength of a short glass fibre reinforced polyamide 6,6.* Engineering Fracture Mechanics, 2007. **74**(4): p. 627-641.
57. Bowen, C.R., Dent, A.C., Stevens, R., Cain, M., and Stewart, M., *Determination of critical and minimum volume fraction for composite sensors and actuators*, in *4M2005 Conference on Multi-Material Micro Manufacture* 2005, Elsevier: Karslruhe, Germany.
58. Alger, M.S.M., *Polymer Science Dictionary*. 2nd ed. 1996: Chapman and Hall.
59. Nishino, T., Hirao, K., Kotera, M., Nakamae, K., and Inagaki, H., *Kenaf reinforced biodegradable composite.* Composites Science and Technology, 2003. **63**: p. 1281-1286.
60. Fu, S.Y., Lauke, B., Mader, E., Yue, C.Y., and Hu, X., *Tensile properties of short-glass-fiber- and short-carbon-fiber-reinforced polypropylene composites.* Composites: Part A, 2000. **31**: p. 1117-1125.
61. Di Candilo, M., Ranalli, P., Bozzi, C., Focher, B., and Mastromei, G., *Preliminary results of tests facing with the controlled retting of hemp.* Industrial Crops and Products, 2000. **11**(2-3): p. 197-203.
62. Morrison, W.H., Archibald, D.D., Sharma, H.S.S., and Akin, D.E., *Chemical and physical characterization of water- and dew-retted flax fibres.* Industrial crops and products, 2000. **12**: p. 39-46.
63. Sharma, H.S.S., Faughey, G., and Lyons, G., *Comparison of physical, chemical and thermal characteristics of water-, dew-, and enzyme-retted fibers.* Journal of Applied Polymer Science, 1999. **74**: p. 139-143.
64. Hepworth, D.G., Hobson, R.N., Bruce, D.M., and Farrent, J.W., *The use of unretted hemp fibre in composite manufacture.* Composites Part A: Applied Science and Manufacturing, 2000. **31**(11): p. 1279-1283.

65. Walker, J.C.F., *Timber preservation*, in *Primary Wood Processing*. 1993, Chapman and Hall: London. p. 285-289.
66. Dorado, J., Almendros, G., Field, J.A., and Sierra-Alvarez, R., *Infrared spectroscopy analysis of hemp (Cannabis sativa) after selective delignification by Bjerkandera sp. at different nitrogen levels.* Enzyme and Microbial Technology, 2001. **28**(6): p. 550-559.
67. Alexopoulos, C.J., Mims, C.W., and Blackwell, M., *Phylum Basidiomycota: Order Aphyllophorales*, in *Introductory Mycology*. 1996, John Wiley and Sons.
68. Yuan, X., Jayaraman, K., and Bhattacharyya, D., *Effects of plasma treatment in enhancing the performance of woodfibre-polypropylene composites.* Composites Part A: Applied Science and Manufacturing, 2004. **35**(12): p. 1363-1374.
69. Li, R., Ye, L., and Mai, Y.-W., *Application of plasma technologies in fibre-reinforced polymer composites: a review of recent developments.* Composites Part A: Applied Science and Manufacturing, 1997. **28**(1): p. 73-86.
70. Sabharwal, H.S., Denes, F., Nielsen, L., and Young, R.A., *Free-radical formation in jute from argon plasma treatment.* Journal of Agriculture and Food Chemistry, 1993. **40**: p. 2202-2207.
71. Chen, J.-R., *Study on free radicals of cotton and wool fibers treated with low-temperature plasma.* Journal of Applied Polymer Science, 1996. **62**(9): p. 1325-1329.
72. Lu, J.Z., Wu, Q., and McNabb, H.S., *Chemical coupling in wood fiber and polymer composites: A review of coupling agents and treatments.* Wood and Fiber Science, 2000. **32**(1): p. 88-104.
73. Li, Y., Mai, Y.-W., and Ye, L., *Sisal fibre and its composites: a review of recent developments.* Composites Science and Technology, 2000. **60**(11): p. 2037-2055.
74. Ray, D., Sarkar, B.K., Rana, A.K., and Bose, N.R., *The mechanical properties of vinylester resin matrix composites reinforced with alkali-treated jute fibers.* Composites Part A: Applied Science and Manufacturing, 2001. **32**(1): p. 119-127.
75. Mwaikambo, L.Y. and Ansell, M.P., *Hemp fibre reinforced cashew nut shell liquid composites.* Composites Science and Technology, 2003. **63**: p. 1297-1305.
76. Ouajai, S. and Shanks, R.A., *Composition, structure and thermal degradation of hemp cellulose after chemical treatments.* Polymer Degradation and Stability, 2005. **89**(2): p. 327-335.
77. Gassan, J. and Bledzki, A.K., *Possibilities for improving the mechanical properties of jute/epoxy composites by alkali treatment of fibres.* Composites Science and Technology, 1999. **59**(9): p. 1303-1309.
78. Wang, H.M., Postle, R., Kessler, R.W., and Kessler, W., *Removing pectin and lignin during chemical processing of hemp for textile applications.* Textile Research Journal, 2003. **73**(8): p. 664-669.
79. Gumuskaya, E. and Usta, M., *Dependence of chemical and crystalline structure of alkali sulfite pulp on cooking temperature and time.* Carbohydrate Polymers, 2006. **65**(4): p. 461-468.

80. Mwaikambo, L.Y. and Ansell, M.P., *The effect of chemical treatment on the properties of hemp, sisal, jute and kapok for composite reinforcement.* Die Angewandte Makromolekulare Chemie, 1999. **272**(1): p. 108-116.
81. Bismarck, A., Aranberri-Askargorta, I., Springer, J., Lampke, T., Wielage, B., Stamboulis, A., I, S., and Limbach, H.-H., *Surface characterization of flax, hemp and cellulose fibers; Surface properties and the water uptake behavior.* Polymer Composites, 2002. **23**(5): p. 872-894.
82. Correia, F., Roy, D.N., and Goel, K., *Chemistry and delignification kinetics of Canadian industrial hemp.* Journal of Wood Chemistry and Technology, 2001. **21**(2): p. 97-111.
83. Sanadi, A.R., Caulfield, D.F., Jacobson, R.E., and Rowell, R.M., *Renewable agricultural fibers as reinforcing fillers in plastics: Mechanical properties of kenaf fiber-polypropylene composites.* American Chemical Society, 1995. **34**: p. 1889-1896.
84. Pickering, K.L. and Ji, C., *The effect of poly[methylene(polyphenyl isocyanate)] and maleated polypropylene coupling agents on New Zealand Radiata pine-polypropylene composites.* Journal of Reinforced Plastics and Composites, 2003.
85. Zafeiropoulos, N.E., Williams, D.R., Baillie, C.A., and Matthews, F.L., *Engineering and characterisation of the interface in flax fibre/polypropylene composite materials. Part I. Development and investigation of surface treatments.* Composites Part A: Applied Science and Manufacturing, 2002. **33**(8): p. 1083-1093.
86. Rowell, R.M., *Distribution of acetyl groups in Southern Pine reacted with acetic anhydride.* Wood Science, 1982. **15**(2): p. 172-182.
87. Matias, M.C., De La Orden, M.U., Gonzalez Sanchez, C., and Martinez Urreaga, J., *Comparative spectroscopic study of the modification of cellulosic materials with different coupling agents.* Journal of Applied Polymer Science, 1999. **75**: p. 256-266.
88. Valadez-Gonzalez, A., Cervantes-Uc, J.M., Olayo, R., and Herrera-Franco, P.J., *Chemical modification of henequen fibers with an organosilane coupling agent.* Composites Part B: Engineering, 1999. **30**(3): p. 321-331.
89. Pickering, K.L., Abdalla, A., Ji, C., McDonald, A.G., and Franich, R.A., *The effect of silane coupling agents on radiata pine fibre for use in thermoplastic matrix composites.* Composites Part A: Applied Science and Manufacturing, 2003. **34**(10): p. 915-926.
90. Bataille, P., Ricard, L., and Sapieha, S., *Effects of cellulose fibers in polypropylene composites.* Polymer Composites, 1989. **10**(2): p. 103-107.
91. Raj, R.G., Kokta, B.V., Grouleau, G., and Daneault, C., *The influence of coupling agents on mechanical properties of composites containing cellulosic fillers.* Polymer.-Plast.Technol.Eng, 1990. **29**(4): p. 339-353.
92. Michaeli, W., Kaufmann, H., Greif, H., and Vosseburger, F.-J., *Training In Plastics Technology*. 1995: Hanser Publishers.
93. Joseph, P.V., Joseph, K., and Thomas, S., *Effect of processing variables on the mechanical properties of sisal-fiber-reinforced polypropylene composites.* Composites Science and Technology, 1999. **59**(11): p. 1625-1640.

94. Gibson, A.G., *Continuous molding of thermoplastic composites*, in *Comprehensive Composite Materials*, A. Kelly and C. Zweben, Editors. 2000, Elsevier Science Ltd: Oxford.
95. Wielage, B., Lampke, T., Utschick, H., and Soergel, F., *Processing of natural-fibre reinforced polymers and the resulting dynamic-mechanical properties.* Journal of Materials Processing Technology, 2003. **139**(1-3): p. 140-146.
96. Krzysik, A.M., Youngquist, J.A., Myers, G.E., Chahyadi, I.S., and Kolosick, P.C. *Wood-polymer bonding in extruded and nonwoven web composite panels*. in *Wood adhesives 1990*. 1991. Madison, WI: Forest Products Research Society.
97. Yam, K.L., Gogoi, B.K., Lai, C.C., and Selke, S.E., *Composites from compounding wood fibres with recycled high density polyethylene.* Polymer Engineering and Science, 1990. **30**(11): p. 693-699.
98. Keller, A., *Compounding and mechanical properties of biodegradable hemp fibre composites.* Composites Science and Technology, 2003. **63**(9): p. 1307-1316.
99. Hall, C., *Polymer Materials: An introduction for technologists and scientists*. 1981: Macmillan.
100. Wakeman, M.D. and Rudd, C.D., *Compression moulding of thermoplastic composites*, in *Comprehensive Composite Materials*, A. Kelly and C. Zweben, Editors. 2000, Elsevier Science Ltd: Oxford.
101. Poulakis, J.G. and Papaspyrides, C.D., *Recycling of polypropylene by the dissolution/reprecipitation technique: I. A model study.* Resources, Conservation and Recycling, 1997. **20**(1): p. 31-41.
102. Perisanu, S.T., *Estimation of solubility of carbon dioxide in polar solvents.* Journal of Solution Chemistry, 2001. **30**(2): p. 183-192.
103. Baroulaki, I., Karakasi, O., Pappa, G., Tarantili, P.A., Economides, D., and Magoulas, K., *Preparation and study of plastic compounds containing polyolefins and post used newspaper fibers.* Composites Part A: Applied Science and Manufacturing, 2006. **37**(10): p. 1613-1625.
104. Joseph, K., Thomas, S., Pavithran, C., and Brahmakumar, M., *Tensile properties of short sisal fiber-reinforced polyethylene composites.* Journal of Applied Polymer Science, 1993. **47**: p. 1731-1739.
105. Herrera-Franco, P.J. and Valadez-Gonzalez, A., *A study of the mechanical properties of short natural-fiber reinforced composites.* Composites Part B: Engineering, 2005. **36**(8): p. 597-608
106. Coutinho, F.M.B. and Costa, T.H.S., *Performance of polypropylene-wood fiber composites.* Polymer Testing, 1999. **18**(8): p. 581-587.
107. Joffe, R., Andersons, J., and Wallstrom, L., *Strength and adhesion characteristics of elementary flax fibres with different surface treatments.* Composites Part A: Applied Science and Manufacturing, 2003. **34**(7): p. 603-612.
108. Vlasveld, D.P.N., Parlevliet, P.P., Bersee, H.E.N., and Picken, S.J., *Fibre-matrix adhesion in glass-fibre reinforced polyamide-6 silicate nanocomposites.* Composites Part A: Applied Science and Manufacturing, 2005. **36**(1): p. 1-11.
109. Drzal, L.T., Herrera-Franco, P.J., Ho, H., Kelly, A., and Zweben, C., *Fiber-Matrix Interface Tests*, in *Comprehensive Composite Materials*. 2000, Pergamon: Oxford. p. 71-111.

110. Kelly, A. and Tyson, W.R., *Tensile properties of fibre-reinforced metals: Copper/Tungsten and Copper/Molybdenum.* Journal of the Mechanics and Physics of Solids, 1965. **13**: p. 329-350.
111. Zafeiropoulos, N.E. and Baillie, C.A., *A study of the effect of surface treatments on the tensile strength of flax fibres: Part II Application of Weibull statistics.* Composites Part A: Applied Science and Manufacturing, 2006. **38**(2): p. 629-638.
112. Gao, S.-L., Mader, E., and Zhandarov, S.F., *Carbon fibers and composites with epoxy resins: Topography, fractography and interphases.* Carbon, 2004. **42**(3): p. 515-529.
113. Mader, E., Jacobasch, H.J., Grundke, K., and Gietzelt, T., *Influence of an optimized interphase on the properties of polypropylene/glass fibre composites.* Composites Part A: Applied Science and Manufacturing, 1996. **27**(9): p. 907-912
114. Zhandarov, S. and Mader, E., *Characterization of fiber/matrix interface strength: applicability of different tests, approaches and parameters.* Composites Science and Technology, 2005. **65**(1): p. 149-160.
115. George, J., Sreekala, M.S., and Thomas, S., *A review on interface modification and characterization of natural fiber reinforced plastic composites.* Polymer Engineering & Science, 2001. **41**(9): p. 1471-1485.
116. Ho, H. and Drzal, L.T., *Evaluation of interfacial mechanical properties of fiber reinforced composites using the microindentation method.* Composites Part A: Applied Science and Manufacturing, 1996. **27**(10): p. 961-971.
117. Zidi, M., Carpentier, L., Chateauminois, A., Kapsa, P., and Sidoroff, F., *Development of a micro-indentation model simulating different mechanical responses of the fibre/matrix interface.* Composites Science and Technology, 2001. **61**(3): p. 369-375.
118. Kharrat, M., Chateauminois, A., Carpentier, L., and Kapsa, P., *On the interfacial behaviour of a glass/epoxy composite during a micro-indentation test: assessment of interfacial shear strength using reduced indentation curves.* Composites Part A: Applied Science and Manufacturing, 1997. **28**(1): p. 39-46.
119. Piggott, M.R., *Why interface testing by single-fibre methods can be misleading.* Composites Science and Technology, 1997. **57**(8): p. 965-974
120. Tripathi, D. and Jones, F.R., *Single fibre fragmentation test for assessing adhesion in fibre reinforced composites.* Journal of Materials Science, 1998. **33**(1): p. 1-16.
121. Valadez-Gonzalez, A., Cervantes-Uc, J.M., Olayo, R., and Herrera-Franco, P.J., *Effect of fiber surface treatment on the fiber-matrix bond strength of natural fiber reinforced composites.* Composites Part B: Engineering, 1999. **30**(3): p. 309-320.
122. Asloun, E.M., Donnet, J.B., Guilpain, G., Nardin, M., and Schultz, J., *On the estimation of the tensile strength of carbon fibres at short lengths.* Journal of Materials Science, 1989. **24**(10): p. 3504-3510.
123. Pochiraju, K.V., Tandon, G.P., and Pagano, N.J., *Analyses of single fiber pushout considering interfacial friction and adhesion.* Journal of the Mechanics and Physics of Solids, 2001. **49**(10): p. 2307-2338.

124. Sun, C.T., Kelly, A., and Zweben, C., *Strength Analysis of Unidirectional Composites and Laminates*, in *Comprehensive Composite Materials*. 2000, Pergamon: Oxford. p. 641-666.
125. Kalaprasad, G., Joseph, K., Thomas, S., and Pavithran, C., *Theoretical modelling of tensile properties of short sisal fibre-reinforced low-density polyethylene composites* Journal of Materials Science, 1997. **32**(16): p. 4261-4267.
126. Joseph, P.V., Mathew, G., Joseph, K., Thomas, S., and Pradeep, P., *Mechanical properties of short sisal fiber-reinforced polypropylene composites: Comparison of experimental data with theoretical predictions.* Journal of Applied Polymer Science, 2002. **88**(1): p. 602-611.
127. Hirsch, T.J., *Modulus of elasticity of concrete affected by elastic moduli of cement paste matrix and aggregate.* Journal of the American Concrete Institute, 1962. **59**: p. 427-447.
128. Halpin, J.C. and Tsai, S.W., *Effects of environmental factors on composite materials*. 1969, Air Force Materials Laboratory AFML-TR-67-423.
129. Halpin, J.C. and Kardos, J.L., *The Halpin-Tsai equations: A review.* Polymer Engineering & Science, 1976. **16**(5): p. 344-352.
130. Yeh, M.-K., Tai, N.-H., and Liu, J.-H., *Mechanical behavior of phenolic-based composites reinforced with multi-walled carbon nanotubes.* Carbon, 2006. **44**(1): p. 1-9.
131. Thomason, J.L., *Micromechanical parameters from macromechanical measurements on glass reinforced polyamide 6,6.* Composites Science and Technology, 2001. **61**(14): p. 2007-2016.
132. Vu-Khanh, T., Denault, J., Habib, P., and Low, A., *The effects of injection moulding on the mechanical behaviour of long-fibre reinforced PBT/PET blends.* Composites Science and Technology, 1991. **40**(4): p. 423-435.
133. Thomason, J.L., Vlug, M.A., Schipper, G., and Krikor, H.G.L.T., *Influence of fibre length and concentration on the properties of glass fibre-reinforced polypropylene: Part 3. Strength and strain at failure.* Composites Part A: Applied Science and Manufacturing, 1996. **27**(11): p. 1075-1084.
134. Andersons, J., Sparnins, E., and Joffe, R., *Stiffness and strength of flax fiber/polymer matrix composites.* Polymer Composites, 2006. **27**(2): p. 221-229.
135. Garkhail, S.K., Heijenrath, R.W.H., and Peijs, T., *Mechanical properties of natural fibre mat reinforced thermoplastics based on flax fibres and polypropylene.* Applied Composite Materials, 2000. **7**: p. 351-372.
136. Nakatani, H., Suzuki, S., Tanaka, T., and Terano, M., *New kinetic aspects on the mechanism of thermal oxidative degradation of polypropylenes with various tacticities.* Polymer, 2005. **46**(26): p. 12366-12371.
137. Achimsky, L., Audouin, L., and Verdu, J., *Kinetic study of the thermal oxidation of polypropylene.* Polymer Degradation and Stability, 1997. **57**(3): p. 231-240.
138. Brydson, J.A., *Plasic Materials*. 6th ed. 1995: Butterworth Heinemann.
139. Wielage, B., Lampke, T., Marx, G., Nestler, K., and Starke, D., *Thermogravimetric and differential scanning calorimetric analysis of natural fibres and polypropylene.* Thermochimica Acta, 1999. **337**(1-2): p. 169-177.

140. Demirbas, A., *Mechanisms of liquefaction and pyrolysis reactions of biomass.* Energy Conversion and Management, 2000. **41**(6): p. 633-646.
141. Beall, F.C. and Eickner, H.W., *Thermal degradation of wood components: A review of the literature*. 1970, U.S.D.A Forest Service. p. 1-27.
142. Einhorn-Stoll, U., Kunzek, H., and Dongowski, G., *Thermal analysis of chemically and mechanically modified pectins.* Food Hydrocolloids, 2007. **21**(7): p. 1101-1112
143. Biermann, C.J., *Handbook of Pulping and Papermaking*. 2nd Edition ed. 1996: Academic Press.
144. Beckermann, G.W., Pickering, K.L., and Foreman, N.J. *The processing, production and improvement of hemp-fibre reinforced polypropylene composite materials*. in *2nd International Conference on Structure, Processing and Properties of Materials*. 2004. Dhaka, Bangladesh: Department of Materials and Metallurgical Engineering, BUET.
145. Pickering, K.L., Beckermann, G.W., Alam, S.N., and Foreman, N.J., *Optimising industrial hemp fibre for composites.* Composites Part A: Applied Science and Manufacturing, 2007. **38**(2): p. 461-468
146. Kromm, F.X., Lorriot, T., Coutand, B., Harry, R., and Quenisset, J.M., *Tensile and creep properties of ultra high molecular weight PE fibres.* Polymer Testing, 2003. **22**(4): p. 463-470.
147. Tserki, V., Zafeiropoulos, N.E., Simon, F., and Panayiotou, C., *A study of the effect of acetylation and propionylation surface treatments on natural fibres.* Composites Part A: Applied Science and Manufacturing, 2005. **36**(8): p. 1110-1118.
148. Roncero, M.B., Torres, A.L., Colom, J.F., and Vidal, T., *The effect of xylanase on lignocellulosic components during the bleaching of wood pulps.* Bioresource Technology, 2005. **96**(1): p. 21-30.
149. Latif, L. and Saidpour, H., *Assessment of plastic mixture quality in injection moulding process.* Polymer Testing, 1997. **16**(3): p. 241-258.
150. Newson, W.R. and Maine, F.W. *Second generation woodfibre-polymer composites*. in *Progress in Woodfibre-Plastic Composites*. 2002. Toronto, Canada.
151. Abdul Khalil, H.P.S., Chow, W.C., Rozman, H.D., Ismail, H., Ahmad, M.N., and Kumar, R.N., *The effect of anhydride modification of sago starch on the tensile and water absorption properties of sago-filled linear low-density polyethylene (LLDPE).* Polym.-Plast.Technol.Eng, 2001. **40**(3): p. 249-263.
152. Mutje, P., Lopez, A., Vallejos, M.E., Lopez, J.P., and Vilaseca, F., *Full exploitation of Cannabis sativa as reinforcement/filler of thermoplastic composite materials.* Composites Part A: Applied Science and Manufacturing, 2007. **38**(2): p. 369-377.
153. Dalvag, H., Klason, C., and Stromvall, H.-E., *The efficiency of cellulosic fillers in common thermoplastics. Part ii. Filling with processing aids and coupling agents.* International Journal of Polymeric Materials, 1985. **11**: p. 9-38.
154. Fu, S.Y., Lauke, B., Mader, E., Yue, C.Y., and Hu, X., *Tensile properties of short-glass-fiber and short-carbon-fiber-reinforced polypropylene composites.* Composites Part A: Applied Science and Manufacturing, 2000. **31**(10): p. 1117-1125.

155. Doan, T.-T.-L., Gao, S.-L., and Mader, E., *Jute/polypropylene composites I. Effect of matrix modification.* Composites Science and Technology, 2006. **66**(7-8): p. 952-963.
156. Mohr, B.J., Nanko, H., and Kurtis, K.E., *Durability of kraft pulp fiber-cement composites to wet/dry cycling.* Cement and Concrete Composites, 2005. **27**(4): p. 435-448.
157. Clemons, C.M., Caulfield, D.F., and Giacomin, A.J., *Dynamic fracture toughness of cellulose-fiber-reinforced polypropylene: Preliminary investigation of microstructural effects.* Journal of Elastomers and Plastics, 1999. **31**(4): p. 367-378.
158. Spahr, D.E., Friedrich, K., Schultz, J.M., and Bailey, R.S., *Microstructure and fracture behaviour of short and long fibre-reinforced polypropylene composites.* Journal of Materials Science, 1990. **25**(10): p. 4427-4439.
159. Skourlis, T.P., Pochiraju, K., Chassapis, C., and Manoochehri, S., *Structure-modulus relationships for injection-molded long fiber-reinforced polyphthalamides.* Composites Part B: Engineering, 1998. **29**(3): p. 309-319.
160. Kompella, M.K. and Lambros, J., *Micromechanical characterization of cellulose fibers.* Polymer Testing, 2002. **21**(5): p. 523-530.
161. Torres, F.G. and Cubillas, M.L., *Study of the interfacial properties of natural fibre reinforced polyethylene.* Polymer Testing, 2005. **24**(6): p. 694-698
162. Pegoretti, A., Fambri, L., and Migliaresi, C., *Interfacial stress transfer in nylon-6/E-Glass microcomposites: Effect of temperature and strain rate.* Polymer Composites, 2000. **21**(3): p. 466-475.
163. Fan, C.F. and Hsu, S.L., *A spectroscopic analysis of the stress distribution along the reinforcement fibers in model composites: End effects.* Macromolecules, 1988. **22**: p. 1474-1479.
164. Dahiya, J.B. and Rana, S., *Thermal degradation and morphological studies on cotton cellulose modified with various arylphosphorodichloridites.* Polymer International, 2004. **53**(7): p. 995-1002.
165. Kim, H.-S., Kim, S., Kim, H.-J., and Yang, H.-S., *Thermal properties of bio-flour-filled polyolefin composites with different compatibilizing agent type and content.* Thermochimica Acta, 2006. **451**(1-2): p. 181-188.
166. Mohanty, S., Verma, S.K., and Nayak, S.K., *Dynamic mechanical and thermal properties of MAPE treated jute/HDPE composites.* Composites Science and Technology, 2006. **66**(3-4): p. 538-547.
167. Gañán, P. and Mondragon, I., *Thermal and degradation behavior of fique fiber reinforced thermoplastic matrix composites.* Journal of Thermal Analysis and Calorimetry, 2003. **73**(3): p. 783-795.
168. Ray, D., Sarkar, B.K., Basak, R.K., and Rana, A.K., *Thermal behavior of vinyl ester resin matrix composites reinforced with alkali treated jute fibres.* Journal of Applied Polymer Science, 2004. **94**: p. 123-129.

Appendix

Summary of Results for Solution Mixed and Hot Pressed Composites

Fibre Origin	No. Times Pressed	Fibre Treatment	Fibre Length	Fibre Content (wt%)	MAPP/PP Ratio (g MAPP/100g PP)	Tensile Strength (MPa)	T.S. Std Dev (MPa)	Young's Modulus (GPa)	Y.M. Std Dev (GPa)
UK[a]	1	$NaOH/Na_2SO_3$	Continuous	47	7.14	58.4	3.4	7.20	0.78
UK[a]	1	$NaOH/Na_2SO_3$	Continuous	56	7.14	74.2	0.8	9.29	1.12
UK[a]	1	$NaOH/Na_2SO_3$	Continuous	63	7.14	68.1	16.8	11.18	2.03
UK[a]	1	$NaOH/Na_2SO_3$	Continuous	65	7.14	73.2	12.2	9.65	0.69
UK[a]	2	$NaOH/Na_2SO_3$	Continuous	49	7.14	63.6	8.0	14.00	2.17
UK[a]	2	$NaOH/Na_2SO_3$	Continuous	54	7.14	73.6	4.9	12.74	2.05
UK[a]	2	$NaOH/Na_2SO_3$	Continuous	56	7.14	84.7	14.0	14.65	3.24
UK[a]	2	$NaOH/Na_2SO_3$	Continuous	63	7.14	71.8	5.5	16.00	0.64

UK[a] Suspected degradation of UK hemp fibre

5 specimens were tested for each composite

Summary of Results for Injection Moulded Composites

Fibre Origin	Processing Method	Fibre Treatment	Fibre Length	Fibre Content (wt%)	MAPP Content (wt%)	I.M. Set-up	Max I.M. Temperature (°C)	Tensile Strength (MPa)	T.S. Std Dev (MPa)	Young's Modulus (GPa)	Y.M. Std Dev (GPa)
None	Extrusion and I.M.	None	-	0	0	1st	180	22.8	0.1	1.07	0.03
None	Extrusion and I.M.	None	-	0	1	1st	180	24.2	0.40	1.15	0.04
None	Extrusion and I.M.	None	-	0	2	1st	180	24.0	0.20	1.11	0.03
None	Extrusion and I.M.	None	-	0	4	1st	180	24.4	0.35	1.14	0.04
NZ	Extrusion and I.M.	NaOH	Normal	30	2	1st	180	36.7	0.7	2.93	0.10
NZ	Extrusion and I.M.	NaOH	Normal	40	2	1st	180	37.6	1.3	4.02	0.33
NZ	Extrusion and I.M.	NaOH	Normal	50	2	1st	180	35.6	0.4	5.93	0.78
UK	Extrusion and I.M.	Untreated	Normal	40	0	1st	145	31.5	0.8	4.88	0.45
UK	Extrusion and I.M.	Untreated	Normal	40	2	1st	145	37.7	1.2	4.20	0.33
UK	Extrusion and I.M.	Untreated	Normal	40	3	1st	145	38.6	1.2	3.98	0.18
UK	Extrusion and I.M.	Untreated	Normal	40	4	1st	145	39.0	1.3	3.97	0.32
UK	Extrusion and I.M.	Untreated	Normal	40	5	1st	145	38.9	2.9	4.30	0.37
UK	Extrusion and I.M.	NaOH	Normal	40	0	1st	180	29.1	0.9	5.07	0.39
UK	Extrusion and I.M.	NaOH	Normal	40	2	1st	180	37.5	0.8	3.87	0.15
UK	Extrusion and I.M.	NaOH	Normal	40	3	1st	180	38.9	1.2	3.85	0.34
UK	Extrusion and I.M.	NaOH	Normal	40	4	1st	180	41.3	1.1	4.11	0.26
UK	Extrusion and I.M.	NaOH	Normal	40	5	1st	180	40.9	1.7	4.36	0.23
UK	Extrusion and I.M.	NaOH	Normal	40	4	2nd	180	42.1	1.5	4.28	0.25
UK	Extrusion and I.M.	NaOH	Normal	40	5	2nd	180	40.6	1.1	4.32	0.19
UK	Extrusion and I.M.	$NaOH/Na_2SO_3$	Normal	40	0	1st	180	30.1	0.7	4.71	0.35
UK	Extrusion and I.M.	$NaOH/Na_2SO_3$	Normal	40	4	1st	180	50.5	1.1	5.31	0.29
UK[a]	Extrusion and I.M.	$NaOH/Na_2SO_3$	Short	40	4	1st	180	42.0	1.2	4.82	0.82
UK[a]	Extrusion and I.M.	$NaOH/Na_2SO_3$	Long	40	4	1st	180	41.0	1.8	4.99	0.67
UK[a]	Extrusion and I.M.	$NaOH/Na_2SO_3$	Normal	40	4	1st	180	42.2	1.2	4.60	0.35
UK[a]	Extrusion and I.M.	$NaOH/Na_2SO_3$	Normal	40	5	1st	180	42.5	2.1	4.79	0.53
UK[a]	Solution Mixed and I.M	$NaOH/Na_2SO_3$	Short	40	4	1st	180	43.1	2.5	4.99	0.72
UK[b]	Extrusion and I.M.	Untreated	Normal	40	3	1st	145	38.6	1.2	3.98	0.18
UK[b]	Extrusion and I.M.	Untreated	Normal	40	3	1st	150	37.4	1.9	4.12	0.65
UK[b]	Extrusion and I.M.	Untreated	Normal	40	3	1st	155	38.8	1.0	3.81	0.40
UK[b]	Extrusion and I.M.	Untreated	Normal	40	3	1st	160	38.6	1.3	3.92	0.22
UK[b]	Extrusion and I.M.	Untreated	Normal	40	3	1st	165	38.6	0.6	4.11	0.31
UK[b]	Extrusion and I.M.	Untreated	Normal	40	3	1st	170	37.0	1.7	3.92	0.13
UK[b]	Extrusion and I.M	NaOH	Normal	40	3	1st	155	38.7	0.5	3.62	0.19
UK[b]	Extrusion and I.M	NaOH	Normal	40	3	1st	160	38.3	0.3	4.04	0.38
UK[b]	Extrusion and I.M	NaOH	Normal	40	3	1st	165	39.2	1.0	3.92	0.62
UK[b]	Extrusion and I.M	NaOH	Normal	40	3	1st	170	39.7	0.9	3.90	0.20
UK[b]	Extrusion and I.M	NaOH	Normal	40	3	1st	175	40.8	1.3	3.91	0.44
UK[b]	Extrusion and I.M	NaOH	Normal	40	3	1st	180	38.9	1.2	3.85	0.34
UK[b]	Extrusion and I.M	NaOH	Normal	40	3	1st	185	39.9	0.8	4.19	0.26
UK[b]	Extrusion and I.M	NaOH	Normal	40	3	1st	190	39.9	0.5	4.13	0.18

UK[a] Suspected degradation of UK hemp fibre

UK[b] Only 5 specimens were tested

MAPP content is stated as a % of the total composite weight